Contents

Preface

The growing epidemic of metabolic syndrome which includes insulin resistance (IR), cardiovascular disease and obesity have made adipose tissue, an important subject of research and a target for therapeutic interventions. Adipocytes are one of the major cell types involved in the pathogenesis of metabolic syndrome. Recent advances in dissecting the cellular and molecular mechanisms involved in the regulation of adipogenesis and lipid metabolism indicate that, activation of endoplasmic reticulum (ER) stress plays a central role in regulating adipocyte function. Studies have shown that chronic activation of ER stress is closely linked to dysregulation of lipid metabolism in several metabolically important cells including hepatocytes, macrophages, β-cells, and adipocytes. The role of ER stress is a rapidly emerging field of interest in the pathogenesis of metabolic diseases and regulation of ER stress response may be a key approach for metabolic syndrome therapy. There is an increased demand for detailed studies in natural products, from the traditional knowledge database, for the treatment of metabolic syndrome. In the present study (-) hydroxycitric acid (HCA), a bioactive compound from *Garcinia cambogia* has been evaluated against chemically induced ER stress in 3T3-L1 adipocytes.

The work is divided into 7 chapters including summary and conclusion. Chapter 1 comprise a general introduction on metabolic syndrome, obesity, its 'prevalence and pathophysiology', role of adipocytes, linking adipocyte ER stress with oxidative stress, IR, inflammation and mitochondrial function. This chapter also shows light into the scope of the ER stress response in treating metabolic syndrome. Analytical methods used in the study are detailed in chapter 2 with specifications on the materials and techniques used. Chapter 3 deals with the induction of ER stress in 3T3-L1 adipocytes using tunicamycin. The effect of HCA on ER stress markers GRP78 and CHOP was determined. Effect of different concentrations of tunicamycin and HCA on cell viability and ROS production in 3T3-L1 adipocytes was evaluated.

The effect of ER stress on the innate antioxidant defense mechanism is illustrated in chapter 4. Protective effect of HCA on unfolded protein response pathway and antioxidant enzymes was also studied. The protein level and mRNA expression of UPR proteins, IRE1, PERK, ATF6, and the down stream effectors like PDI, ERO1, XBP1, peIF2α were determined. Chapter 5 links adipocyte ER stress to mitochondrial function. Since ER and mitochondria are connected physically and functionally, any stress on one may reflect on the other. The chapter deals with the effect of ER stress on mitochondrial function and the

protection by HCA. Various parameters determining mitochondrial function like mitochondrial membrane potential, transition pore opening, ETC complex, ATP content, oxygen consumption rate etc were studied.

In chapter 6 inflammatory responses and insulin sensitivity were studied in relation to ER stress. Secretion of inflammatory cytokines like TNF α, IL-6, IL1β, IL-10, and MCP-1 were quantified. In addition, effect of ER stress on endocrine function of adipocytes as well as the influence of HCA treatment was studied with respect to secretion of adiponectin, leptin and resistin. Expression of various intermediates of the inflammatory pathway and insulin signaling pathway and glucose transporters were quantified.

Chapter 7 describes the summary and conclusion of the study. The results of the study established the link between ER stress, oxidative stress, mitochondrial dysfunction, inflammation and IR. HCA ameliorated the deleterious effects of ER stress in 3T3-L1 adipocyte biology and proves a hopeful candidate molecule in the treatment and management of obesity related complications.

List of abbreviations

ABTS* : (2, 2'- Azino-di-(3-ethylbenzthiazoline sulphonate)

AMPK : Adenosine monophosphate-activated protein kinase

ARE : Antioxidant response element

ASK1 : Apoptosis signal-regulated kinase 1

ATCC : American type culture collection

ATF6 : Activating transcription factor 6

ATP : Adenosine triphosphate

BAT : Brown adipose tissue

BiP : Binding immunoglobulin protein

BMI : Body mass index

BSA : Bovine serum albumin

bZIP : Basic leucine zipper

CHOP : C/EBP homology protein

COX-I : Cytochrome c oxidase-1

CREBH : cAMP responsive element-binding protein, hepatocyte specific

DAB : γ,γ' diaminobenzidine

DCFHDA: 2, 7- dichlorodihydrofluorescein diacetate

DMEM : Dulbecco's modified Eagle's medium

DNPH : 2,4-dinitrophenylhydrazine

2-DG : 2-deoxy glucose

Drp1 : Dynamin-related protein 1

DsbA-L : Disulfide-bond A oxidoreductase-like protein

DTNB : 5,5'-dithiobis-2-(nitrobenzoic acid)

DTT : Dithiothreitol

EDTA : Ethylene diamine tetraacetic acid

EIA : Enzyme immunoassay

eIF2α : Eukaryotic initiation factor 2 alpha

ELISA : Enzyme linked immunosorbent assay

ER : Endoplasmic reticulum

ERAD : ER associated degradation

ERO1 : Endoplasmic oxidoreductin

FBS : Fetal bovine serum

FCS : Fetal calf serum

FFA : Free fatty acids

FITC : Fluorescein-isothiocyanate

GADD : Growth arrest and DNA damage inducible gene.

GLUT4 : Glucose transporter type 4

GRP78 : Glucose-regulated protein of 78 kDa

HBSS : Hank's balanced salt solution

HCA : (-) Hydroxycitric acid

HO-1 : Heme oxygenase-1

HSP70 : Heat shock protein 70

IFN-γ : Interferon γ

IL : Interleukin

iNOS : Inducible NO synthase

IP3R : Inositol 1,4,5-triphosphate receptor

IR : Insulin resistance

IRE-1α : Inositol-requiring protein 1

IRS-1 : Insulin receptor substrate-1

JNK : c-Jun N terminal kinase

LD : Low-density lipoprotein

MAM : Mitochondria-associated membrane

MAPK : Mitogen-activated protein kinase

MCP-1 : Monocyte chemoattractant protein

MFN-1 : Mitofusin 1

MPTP : Mitochondria permeability transition pore

mtDNA : Mitochondrial DNA

MTT : 3-(4,5-dimethylthiazol-2-yl)-2,5- diphenyl tetrazolium bromide

NADPH : Nicotinamide adenine dinucleotide phosphate

NBDG : 2-(7-Nitrobenz-2-oxa-1,3-diazol-4-yl) amino-2-deoxy-D-glucose

NBT : Nitroblue tetrazolium

NF-κβ : Nuclear factor-κβ

NO : Nitric oxide

Nox4 : NADPH oxidase 4

Nrf1 : Nuclear respiratory factor 1

Nrf2 : Nuclear factor erythroid 2-related factor-2

OMM : Outer mitochondrial membrane

OPA1 : Optic atrophy 1

OXPHOS: Oxidative phosphorylation

PAI-1 : Plasminogen activator inhibitor-1

PBA : Sodium phenyl butyrate/ 4-phenylbutyrate

PBS : Phosphate buffer saline

PDI : Protein disulphide isomerase

PERK : Double-stranded RNA-dependent protein kinase-like ER kinase

PGC-1α : Peroxisome proliferator-activated receptor-gamma coactivator α

PI3K : Phosphatidylinositol 3-kinase

PPAR : Peroxisome prolifarator activated receptor

PVDF : Polyvinylidene difluoride

q-RT PCR: Quantitative real time PCR

RIPA : Radioimmunoprecipitation

ROS : Reactive oxygen species

SERCA : Sarco-endoplasmic reticulum calcium ATPase

SOCS : Suppressor of cytokine signaling

T2DM	:	Type 2 diabetes
TBARS	:	Thiobarbituric acid reactive substances
TFAM	:	Transcription factor a, mitochondrial
TG	:	Triglyceride
TLR	:	Toll like receptor
TNB	:	5-thio-2-nitrobenzoic acid
TNF-α	:	Tumor necrosis factor-α
TRAF2	:	Tumour necrosis factor receptor-associated factor 2
TRAIL	:	Tumor necrosis factor-related apoptosis inducing ligand receptor
TUDCA	:	Taurodecahexanoic acid
UCP	:	Uncoupling Protein 1
UPR	:	Unfolded protein response
VDAC	:	Voltage-dependent anion channel
WAT	:	White adipose tissue
XBP1	:	X box binding protein 1
ΔΨM	:	Mitochondrial membrane potential

List of figures

List of tables

Chapter 1

Introduction

1.1 Endoplasmic Reticulum (ER) stress

Endoplasmic reticulum stress has been implicated in a variety of diseases including metabolic disease, neurodegenerative disease, inflammatory disease, and cancer (Hosoi and Ozawa, 2010; Ozcan and Tabas, 2012). ER stress response pathways are emerging as potential targets for intervention and treatment of human diseases. The ER is a dynamic organelle, with complex functions. A number of factors, like availability of oxygen or glucose, hyperthermia, acidosis, calcium levels, the redox milieu, energy levels (modulated by hypoxia and hypoglycemia), can influence and disturb the normal function of ER (Figure1.1)(Malhotra and Kaufman,2007). This impacts protein folding in the lumen of the ER and results in stress. Protein folding is a complex process that works by the interaction of chaperone proteins, foldases, and glycosylating enzymes, as well as appropriate calcium levels and an oxidizing environment.

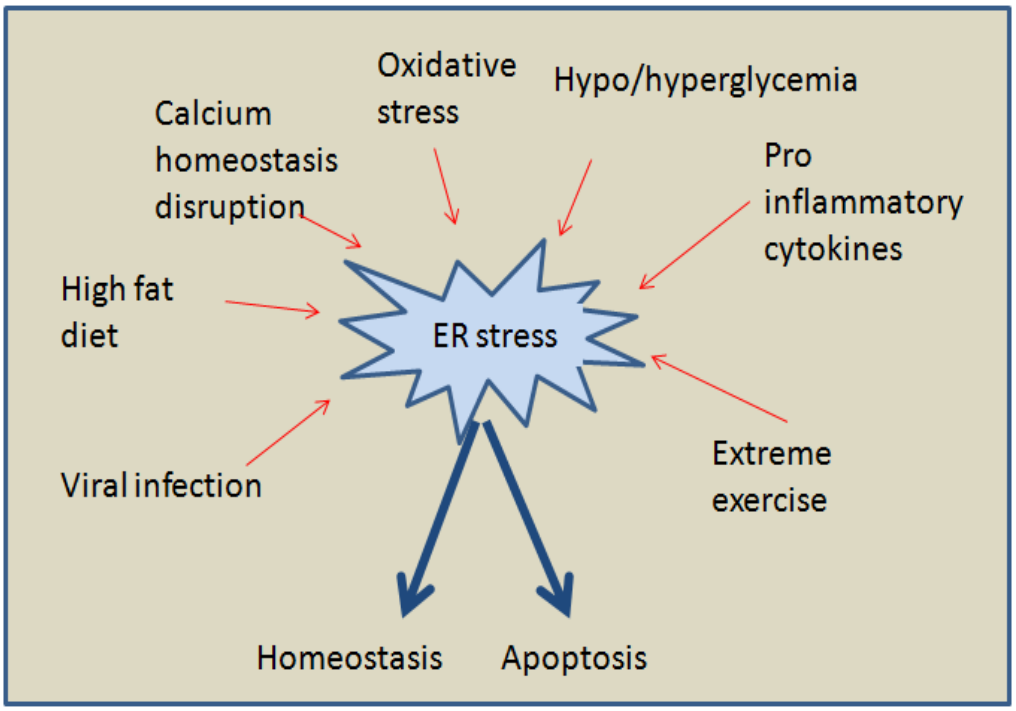

Figure 1.1 Factors involved in the induction of endoplasmic reticulum stress

Newly synthesized peptides from ribosomes attached to the ER membranes are released into the ER lumen, where chaperones and foldases aid in the proper posttranslational modification and folding of these peptides (Schroder and Kaufman, 2005). The properly

folded proteins then move to the Golgi complex for further modification, from where they are transported to their final destination. If the influx of misfolded or unfolded peptides exceeds the ER folding and/or processing capacity, ER stress arises. ER stress activates a cellular response process called the unfolded protein response (UPR). ER has the ability to sense any improper processing or misfolding within the ER lumen, so that any processing error may be rectified (Gregor et al, 2009).

1.1.1 ER structure and function

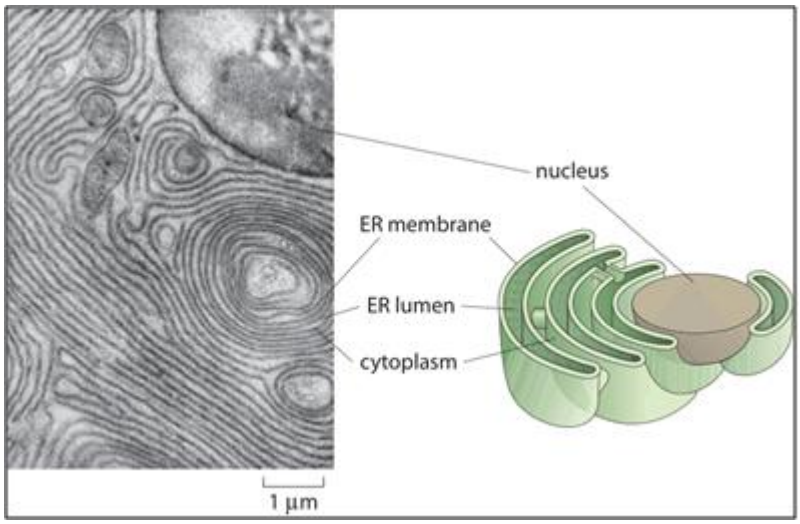

Figure 1.2 Endoplasmic reticulum structure (Fawcett et al, 1966).

The ER is a vital organelle present in all eukaryotic cells. It consists of interconnected, branching membranous tubules, vesicles and cisternae providing a distinct subcellular compartment with numerous functions (Figure 1.2). The rough ER contains ribosomes on its outer surface and plays a prominent role in protein synthesis and secretion. The smooth ER is deficient in associated ribosomes and is not largely involved in protein synthesis, but is central to fatty acids and phospholipids synthesis, lipid bilayer assembly, metabolism of carbohydrates and regulation of calcium homeostasis. In the liver, enzymes in the smooth ER are involved in the metabolism and detoxification of hydrophobic chemicals, such as drugs and carcinogens, and direct them for emission from the body. While some cells may have little smooth ER, all eukaryotic cells have conspicuous amounts of rough ER, as they are indispensable for the synthesis of plasma membrane proteins and proteins of the extracellular matrix. Rough ER is specifically abundant in secretory cells, such as antibody producing plasma cells, insulin secreting beta cells, or cells of milk producing glands, where ER occupies a large fraction of the cytosol. The sarcoplasmic reticulum is a specialized form

of the ER in muscle cells and function to sequester and release large amounts of calcium to effect muscle contractions and relaxation.

1.2 Adipocyte ER stress and obesity

Adipocytes are flooded with a continuous supply of high level of lipids during obesity, which leads to hypertrophy. An added burden is exerted on the metabolic machinery of adipocytes so as to meet the increasing demand, which in turn is translated into ER stress and oxidative stress in the mitochondria (Figure 1.3). This increased metabolic demand can be handled by ER stress up to the chaperones' capacity to deal with newly synthesised proteins. When this limit is surpassed, misfolded proteins accumulate within the lumen of the ER. This accumulation calls on the activation of a rescue response, UPR (Boden et al 2008; Gregor and Hotamisligil, 2007; Hotamisligil, 2010; Hummasti and Hotamisligil, 2010, Karalis et al, 2009). If ER stress is severe or prolonged, cell death may be induced. In general, caspase activation is involved in ER stress associated cell death (Hitomi et al, 2004; Nakagawa et al, 2000) but, caspase-independent necrosis and autophagy have also been reported (Ullman et al, 2008).

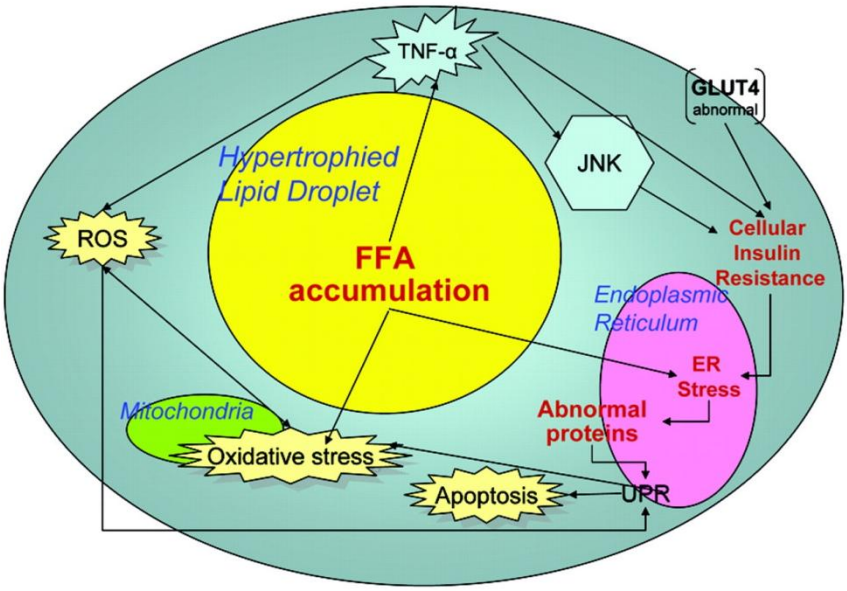

Figure 1.3 Adipocyte endoplasmic reticulum stress during obesity (Ferranti et al, 2008)

1.2.1 Obesity and metabolic syndrome

Obesity has been portrayed as a morbidity of epidemic proportions which predisposes as well as coexists with many other diseases. During obesity, excess of nutrients or a positive energy balance occurs. Adipocytes become hypertrophied which leads to hypoxia and

production of reactive oxygen species (ROS) within "obese" adipose tissue. Secretion of pro-inflammatory adipokines from adipose tissue increases hypertriglyceridemia and ectopic adiposity. These factors result in insulin insensitivity in tissues and ultimately insulin resistance (IR) leading to type 2 diabetes (T2DM). Proinflammatory adipokines also act as a chemo attractant to circulatory immune cells such as macrophages (Sell and Eckel, 2010; Suganami and Ogawa, 2010). Thus in obesity, adipose tissue becomes infiltrated with an increased number of macrophages and becomes inflamed. Obesity can exist in a person for many years and as such, a slow low level mediator of inflammation can arise for many years leading to stress on cellular mechanisms (Day, 2006; Nishimura et al, 2009; Wellen and Hotamisligil, 2005). Adipose tissue factors that interfere with insulin action and endothelial cell function are also identified to be the major contributors for cardiovascular diseases (Poirier et al, 2006).

1.2.2 Obesity

Prevalence of obesity all over the world has increased remarkably. Central obesity and IR have been acknowledged as important causative factors in the pathogenesis of metabolic syndrome (Anderson et al, 2001; Bonora et al, 1998; Nakamura et al, 1994; Nesto, 2003; Saad et al, 1991). The definitions of overweight and obesity are based on the body mass index (BMI), which is calculated as one's weight in kilograms divided by one's height in meters squared (kg/m2): a BMI of 18.5-24.9 denotes "normal weight", BMI $\geq$ 25 denotes "overweight", and BMI $\geq$ 30 denotes "obesity"(Flegal et al, 2007). Changes in lifestyle, like increased nutrient uptake and sedentary lifestyle may be the major contributors to the increased incidence of obesity and its related complications (Gross et al, 2004; Hu, 2003; Malik et al, 2010; Sacks et al, 2009). The worldwide epidemic of obesity has brought considerable attention to research aimed at understanding the biology of adipocytes and the events occurring in adipose tissue and in the bodies of obese individuals.

1.3 Adipose tissue/adipocytes

The main component of adipose tissue is adipocytes. It also contains other cell types, such as pre-adipocytes, mature adipocytes, vascular cells, nerves, macrophages and fibroblasts (Gesta et al, 2007). There are two types of adipose tissue which are distinct in histology as well as function: white adipose tissue (WAT) and brown adipose tissue (BAT) (Gesta et al, 2007). WAT is unilobular and are the storage facility for free fatty acids along with a number of other important endocrine functions regulating appetite and insulin

sensitivity through release of adipokines discovered over recent years. On the contrary, the main function of BAT is to generate heat for the organism through non-shivering effects of uncoupled oxidative metabolism, utilizing Uncoupling Protein 1 (UCP-1). Histologically, BAT is multilobular and contains an abundance of mitochondria, providing its brown coloration.

Obesity is a proinflammatory condition characterized by hypertrophy and hyperplasia of adipocytes. The adipocyte is obviously the cell, best studied in adipose biology with much work focused on adipocyte differentiation and triglyceride droplet formation (Figure 1.4). The chronic low-grade systemic inflammation associated with obesity, termed "metabolic inflammation," is regarded as a focal point in the pathogenesis of IR and T2D in humans and rodent animal models (Gregor and Hotamisligil, 2011; Hotamisligil, 2006; Ouchi et al, 2011; Shoelson et al, 2006). Though liver and muscle exhibit obesity-induced mild inflammatory responses, WAT is the key site mediating systemic inflammation (Odegaard and Chawla, 2013).

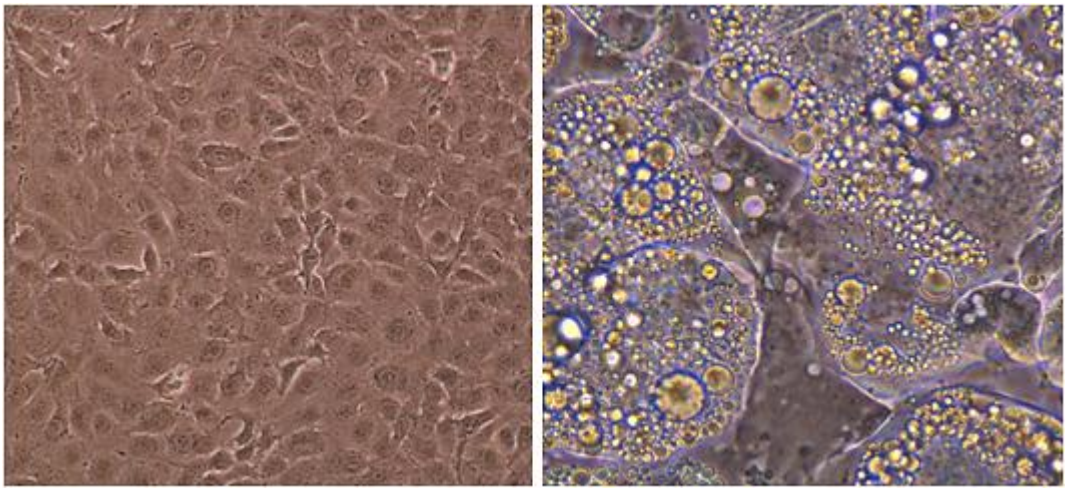

Figure 1.4 Phase contrast images of 3T3-L1 preadipocytes and differentiated lipid filled adipocytes

1.3.1 Adipose tissue function

Storage of excess energy in the form of triglycerides had been regarded as the function of adipose tissue for many years. During prolonged postprandial fasting, those triglycerides are broken down into free fatty acids and metabolised to produce adenosine triphosphate (ATP). The free fatty acids are secreted into the bloodstream to be metabolised by the liver. Another function of adipose tissue is that it acts as a shock absorber from external physical insults and a thermal insulator from cold. Adipose tissue secretes a number of proteins called adipokines, which include hormones and signaling molecules (Figure 1.5).

They exert their biological roles in an autocrine, paracrine, or systemic manner and influence several physiological processes related to energy, glucose metabolism, and immunity (Waki and Tontonoz, 2007). Adipokines show either proinflammatory or anti-inflammatory properties, thereby contributing to IR.

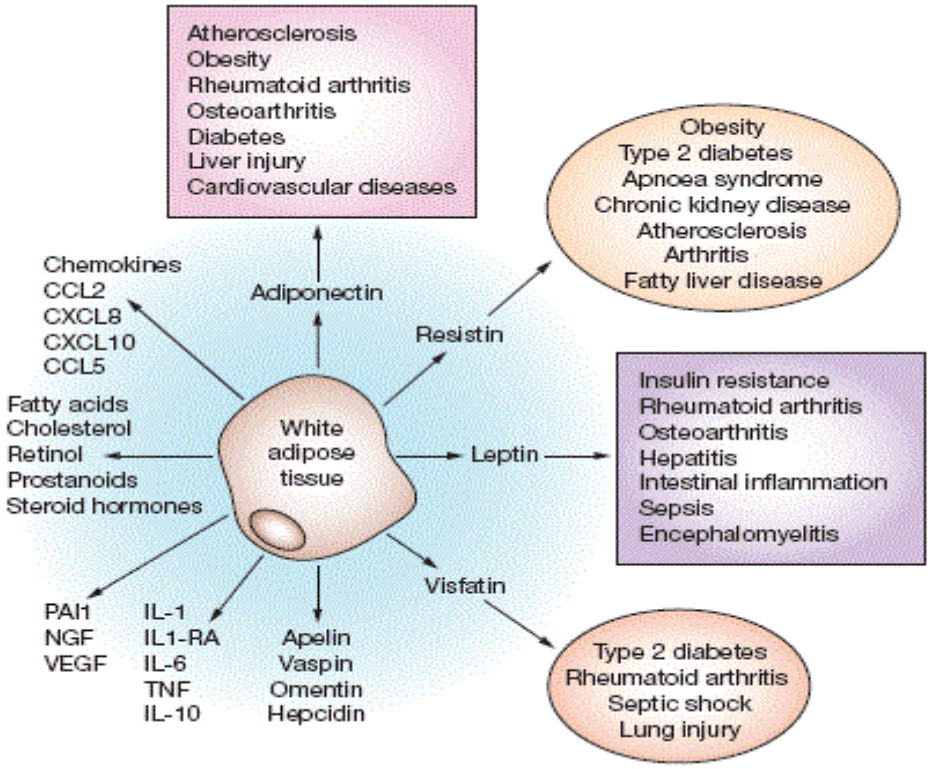

Figure 1.5 The multiple functions of white adipose tissue include the synthesis and secretion of adipokines, and the uptake, storage and synthesis of lipids. (Lago et al, 2007)

1.3.2 Adipokines

Adipokines are the bioactive peptides secreted by adipose tissue, which act locally and distally through autocrine, paracrine and endocrine effects. In obesity, alteration in the production and secretion of most adipokines affects multiple functions such as appetite and energy balance, immunity, insulin sensitivity, angiogenesis, blood pressure, lipid metabolism and haemostasis. Adipokines are integrated in a communication network with other tissues and organs such as the skeletal muscle, adrenal cortex, brain and sympathetic nervous. Dysregulation of adipokine expression is one of the key events in the pathogenesis of metabolic diseases.

Adiponectin is a 30 kDa protein produced and secreted exclusively by adipocytes (Nakano et al, 1996). It is present in serum as a trimer, hexamer or high molecular weight

isoform (Ouchi et al, 2003) and the concentration in human serum is ~10 μg/ml (Arita et al, 1999). A strong negative correlation between plasma adiponectin concentration and BMI in humans has been reported (Hu et al, 1996). Hypoadiponectinemia is associated with cardiovascular disease, hypertension, and metabolic syndrome (Ouchi et al, 2003). A decreased expression of the cytokine in obesity may promote IR. ER stress was reported to decrease the level of high molecular weight fractions as well as total adiponectin in human adipocytes. Adiponectin signaling targets adenosine monophosphate-activated protein kinase (AMPK), which is a negative regulator of mTOR. High levels of mTOR induce serine phosphorylation of insulin receptor substrate-1(IRS-1). When adiponectin levels are low, the IRS-1 is inhibited causing IR. Adiponectin also has direct anti-inflammatory and antiatherosclerotic effects (Kershaw et al, 2004; Ronti et al, 2006).

Leptin is a 16-kD adipocyte-derived cytokine, synthesized and secreted by adipocytes in response to changes in body fat. The secretion is directly proportional to adipose tissue mass and nutritional status, and this secretion is more from subcutaneous relative to visceral adipose tissue. Leptin reduces intracellular lipid levels in skeletal muscle, liver and pancreatic beta cells, thus promoting insulin sensitivity (Minokoshi and Kim, 2002). Caloric restriction and weight loss lowered the leptin levels. Some of the other important endocrine effects of leptin are regulation of immune function, hematopoiesis, angiogenesis, and bone development.

Resistin is a 10 kDa polypeptide secreted by preadipocytes and has been associated with IR. Apart from role in IR and diabetes, it plays regulatory role in a variety of biological processes: cardiovascular disease, non-alcoholic fatty liver disease, autoimmune disease, malignancy, asthma, inflammatory bowel disease and chronic kidney disease (Jamaluddin et al, 2012). ER stress has been found to reduce resistin mRNA expression in 3T3-L1 adipocytes in a time and dose-dependent manner, indicating that resistin is regulated by ER stress (Ronti et al, 2006).

TNF-α is a cytokine that links inflammation in adipocytes with obesity-induced IR. It is synthesized as a 26 kDa transmembrane protein, and the biologically active trimer is formed after the cleavage of transmembrane precursor by the TNF-α converting enzyme. TNF-α is expressed in adipose tissue and, importantly, overexpressed in obese mice. It inhibits insulin signaling by stimulating serine-phosphorylation of IRS-1, which reduces

tyrosine-phosphorylation of IRS-1 by insulin. Other proposed mechanisms are activation of a serine/threonine kinase IKKβ, leading to serine-phosphorylation of IRS-1, increased lipolysis leading to higher FFA levels, and suppression of adiponectin expression by TNF-α (Yuan et al, 2001).

Interleukin-6 (IL-6), a pleiotropic circulating cytokine, having multiple effects ranging from inflammation to host defence and tissue injury, circulates as a glycosylated protein and is secreted by many cell types, including immune cells, fibroblasts, endothelial cells, skeletal muscle and adipose tissue. Plasma concentrations correlate positively with human obesity and IR, and high IL-6 levels are predictive of T2DM and myocardial infarction. Weight loss significantly reduces IL-6 levels in adipose tissue and serum (Bastard et al, 2000; Mohamed-Ali and Pinkney, 1998).

Plasminogen activator inhibitor-1 (PAI-1) is a member of the serine protease inhibitor family that inactivates urokinase-type and tissue-type plasminogen activator and thereby inhibits fibrinolysis. PAI-1 is expressed in adipose tissue as well as in endothelial cells, liver, and platelets. Elevated cytokine levels increase the risk of atherothrombosis and promote the progression of vascular disease. High PAI-1 levels are also strongly associated with visceral fat mass. Expression of PAI-1 is induced by interleukin-1 (IL-1), TNF-α, transforming growth factor-beta (TGF-β), estrogen, thrombin, and insulin (Kershaw et al, 2004; Vaughan, 2005). A number of other cytokines like, IL-1, IL-10, MCP-1, IFN-γ visfatin, adipsin, angiotensinogen, aromatase and a lot more are also synthesised and secreted by adipocytes and plays significant roles in cellular functions

1.4 Unfolded protein response (UPR)

The UPR in mammalian cells is made up of three signalling branches which are initiated by three ER transmembrane sensors, inositol-requiring protein 1 (IRE-1α), double-stranded RNA-dependent protein kinase-like ER kinase (PERK), and activating transcription factor 6 (ATF6). Dissociation of the ER-resident chaperone, glucose-regulated protein of 78 kDa (GRP78), also known as BiP, from their luminal domains leads to the activation of these sensors (Hendershot, 2004). During ER stress conditions, GRP78 is recruited for the folding of proteins in the ER and is removed from IRE-1α, PERK, and ATF6, thus activating the UPR. Activation of the UPR pathways is usually used as an indicator of ER stress due to the technical difficulties in directly measuring compromised ER integrity or protein aggregates in

the ER (Lee and Glimcher, 2009). Figure 1.6 depicts an overview of mammalian UPR signalling pathways.

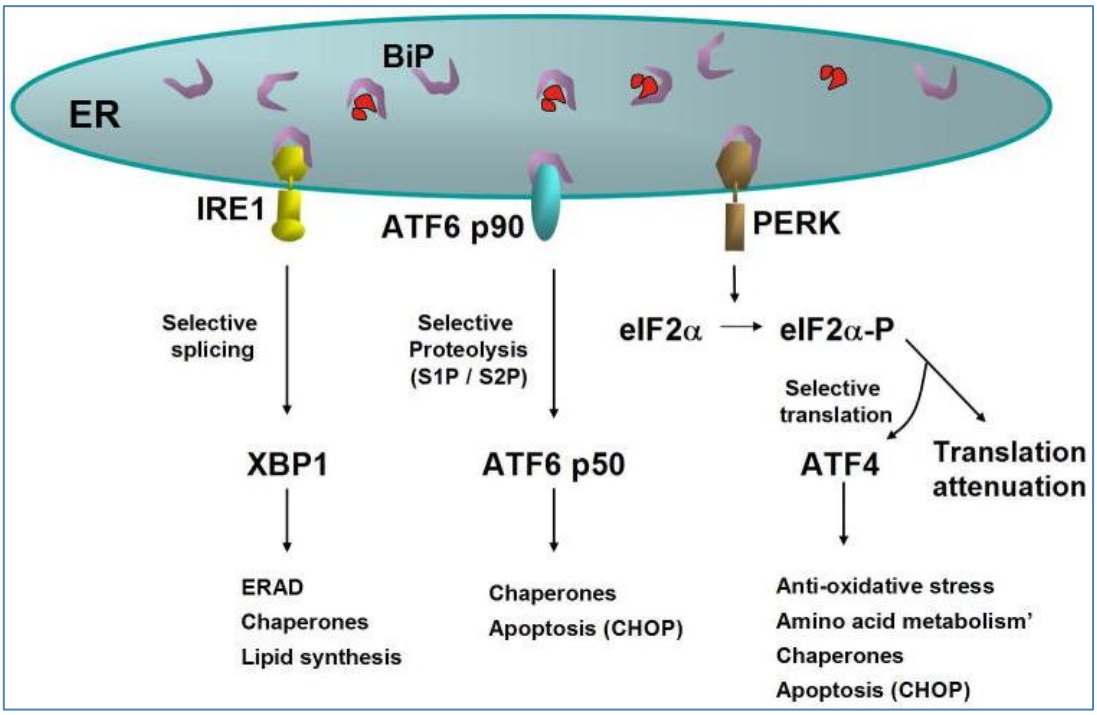

Figure 1.6 Unfolded protein response pathway (Gregor et al, 2007)

The primary objective of the UPR is to adapt to the changing environment, and restore normal ER function. When adaptation falls short, ER stress-initiated pathways activate NF-κB, a transcription factor that causes expression of genes encoding mediators of host defense. This occurs during excessive and/or prolonged ER stress when cell suicide is triggered, usually in the form of apoptosis. Apoptosis is a last resort of multicellular organisms to get rid of dysfunctional cells.

The activated UPR proteins initiate a cascade of events leading to

1. Attenuation of overall mRNA translation so the protein load in the ER is reduced
2. Increased transcription of chaperone proteins to meet the increased demand for protein folding
3. An increase in the induction of the ER associated degradation (ERAD) proteins
4. Finally, pro-apoptotic pathways are activated if all other mechanisms fail

Many studies have proposed ER stress as one potential route which links obesity to IR and T2DM. This study has ER stress as a focal point of investigation with the UPR as a

whole and its constituent components are used as explorative tool to examine the ER stress in linkage to IR, inflammation and mitochondrial dysfunction in adipocytes.

1.4.1 GRP78: the master regulator.

ER is resident for a number of proteins, of which the chaperone GRP78 stands out because of its key role as a master initiator of early ER stress response. In addition, it plays a vital component in calcium binding and protein processing function. As the name indicates, GRP78 initially has been characterized as a glucose-regulated protein, as limited availability of glucose in cell culture medium resulted in marked stimulation of GRP78 transcription and translation. And this provided initial clues to its activation during cellular stress conditions (Lee et al, 1981; Lee, 2001). Later, it was shown that a number of cellular and microenvironmental disturbances, as well as many pharmacological interventions, can increase GRP78 expression, along with aggravated ER stress. The significantly increased amount of GRP78 protein over baseline expression is an established indicator and marker for the presence of cellular ER stress (Healy et al, 2009; Luo and Lee et al, 2013; Zhang and Zhang et al, 2010).

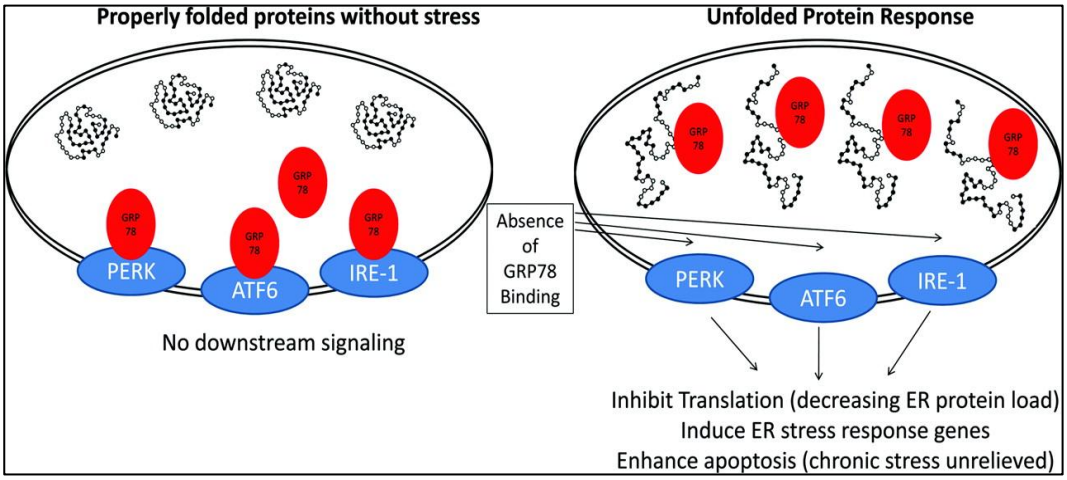

Figure 1.7 Endoplasmic reticulum stress and GRP78. In response to stress, proteins synthesized in the rough ER are refolded by resident molecular chaperones GRP78 (Willis et al, 2012)

GRP78 belongs to the heat shock protein 70 (HSP70) family of proteins, where many of its members have been identified as chaperones within the ER. It was also found to be present in the cytosol (Ni et al, 2009), in mitochondria (Sun et al, 2006), in the nucleus (Matsumoto et al, 2000), and at the cell surface of tumor cells (Arap et al, 2004; Liu et al, 2007; Misra et al, 2006; Shani et al, 2008; Zhang et al,2010). It has thus emerged that GRP78, as well as a few other traditional ER localized chaperones, can function beyond this compartment and are involved in processes not directly connected to posttranslational protein

processing (Ni et al, 2011; Zhang et al, 2010). In cells, during unstressed condition, GRP78 is bound to three different ER transmembrane proteins: (i) IRE-1α (Ron and Hubbard et al, 2008), (ii) PERK (Fels and Koumenis, 2006), and (iii) ATF6 (Sommer and Jarosch, 2002). Binding of GRP78 to the ER-luminal domains of these proteins keeps their activity suppressed and maintains them in an inactive state. During ER stress and associated accumulation of misfolded and unprocessed proteins, GRP78 is sequestered away from PERK, IRE-1α, and ATF6 to facilitate the folding of increased protein load. Consequently, dissociation from GRP78 causes the activation of all three of these transmembrane proteins, unfolding three distinct branches of the UPR (Figure 1.7) (Malhotra and Kaufman, 2007; Parmar and Schroder, 2012, Ron and Walter, 2007). As a result of these signaling events, expression of GRP78 is increased, which serves to provide the required additional chaperone capacity, and also eventually reassociate with PERK, IRE-1α, and ATF6 so that these signaling modules return to their inactive modes when homeostasis has been reestablished.

1.4.2 IRE-1α pathway

IRE-1α pathway is the most conserved signaling branch of the ER stress response (Kohno, 2010; Patil and Walter, 2001). The IRE-1α protein is a transmembrane protein weighing approximately 100 kDa and has two domains, serine/threonine kinase domain and an endoribonuclease domain. It is an enzyme with serine/ threonine protein kinase as well as endoribonuclease (RNase) activity in its cytosolic domain. On release of GRP78, IRE-1α is activated by homodimerization and autophosphorylation (Parmar and Schroder, 2012). Activated IRE-1α cleaves a 26-base fragment from the X box binding protein 1 (*Xbp1*) mRNA, resulting in spliced *Xbp1*s. Translation of transcription factors regulating the expression of genes involved in ERAD and protein folding, and the synthesis of phospholipids that are required for the ER biogenesis during ER stress are also activated (Ron and Hubbard et al, 2008; Shaffer et al, 2004). IRE-1α signaling and *Xbp1* splicing play significant role in secretory cells where the protein folding machinery is continuously engaged with an increased amount of nascent proteins (Iwakoshi et al, 2003). This branch of control operates as a key adaptive mechanism to match ER folding capacity with the demands of protein folding by increasing the ER chaperone expression (Braakman and Bulleid, 2011; Gorman et al, 2012). IRE-1α pathway also functions in activation of a signaling cascade required in controlling cell fate with regard to cell death. Activated IRE-1α leads to downstream activation of apoptosis signal-regulated kinase 1 (ASK1) and c-Jun N terminal

kinase (JNK) (Nishitoh, 2012; Urano et al, 2000). Sustained JNK activity during prolonged ER stress inhibits antiapoptotic proteins and activates proapoptotic proteins. Both these events together, lead to oligomerization of Bax and Bak, resulting in permeabilization of the outer mitochondrial membrane and execution of the intrinsic apoptotic process (Dhanasekaran and Reddy, 2008; Gorman et al, 2012; Kim et al, 2006).

1.4.3 ATF6 pathway

ATF6 protein regulates the second arm of the UPR. It is localized in ER transmembrane and contains a basic leucine zipper (bZIP) motif and transcription factor properties. Upon release from BiP in response to ER stress, is translocated to the Golgi apparatus for cleavage by resident proteins Site 1 Protease (S1P) and Site 2 Protease (S2P). The cleaved ATF6, also called ATF6f is released into the cytosol for entry into the nucleus and regulates gene expression. On translocation into the nucleus, ATF6 stimulates the expression of a multitude of genes involved in protein folding, secretion, and ERAD, thus assisting the cell's effort to deal with ER stress and accumulated misfolded/unfolded proteins (Healy et al, 2009; Yamamoto et al, 2007). GRP78 and GRP94, protein disulphide isomerase (PDI), XBP1, and C/EBP homology protein (CHOP) are some of the ATF6 regulated genes (Adachi et al, 2008; Parmar and Schroder, 2012; Yoshida et al, 2001).

1.4.4 PERK pathway

Mechanism of activation of PERK is similar to that of IRE-1α, as both possess a serine/threonine kinase domain sticking out into the cytoplasm. PERK is activated on dissociation of Bip. Activation of PERK involves homodimerization and autophosphorylation of the protein, which in turn phosphorylate eukaryotic initiation factor 2 alpha (eIF2α), one of its main substrate. Phosphorylation of eIF2α attenuates the overall protein synthesis; thereby protein influx into the ER is reduced. This reduces the protein load for ER chaperones (Harding et al, 2000). At the same time, preferential translation of a small number of mRNAs, including activating transcription factor 4 (ATF4), a transcription factor that stimulates a set of genes involved in recovery and adaptation also occurs (Fels and Koumenis, 2006). CHOP, a key transcription factor that is important in initiating the apoptotic program during excessive ER stress is regulated by ATF4 (Nishitoh, 2012). Nuclear factor-erythroid 2-related factor 2 (Nrf2) is another substrate phosphorylated by PERK. When activated, this basic leucine zipper transcription factor translocates to the nucleus where it activates genes encoding antioxidant proteins and detoxifying enzymes (Cullinan and Diehl,

2004). As ER stress involves perturbations in redox homeostasis due to the increased accumulation of ROS, Nrf2 might play critical role in adapting (Cullinan and Diehl, 2006). Nrf2 deficient cells were observed to greatly increase the cell death following exposure to ER stress.

1.4.5 Pro-apoptotic pathway

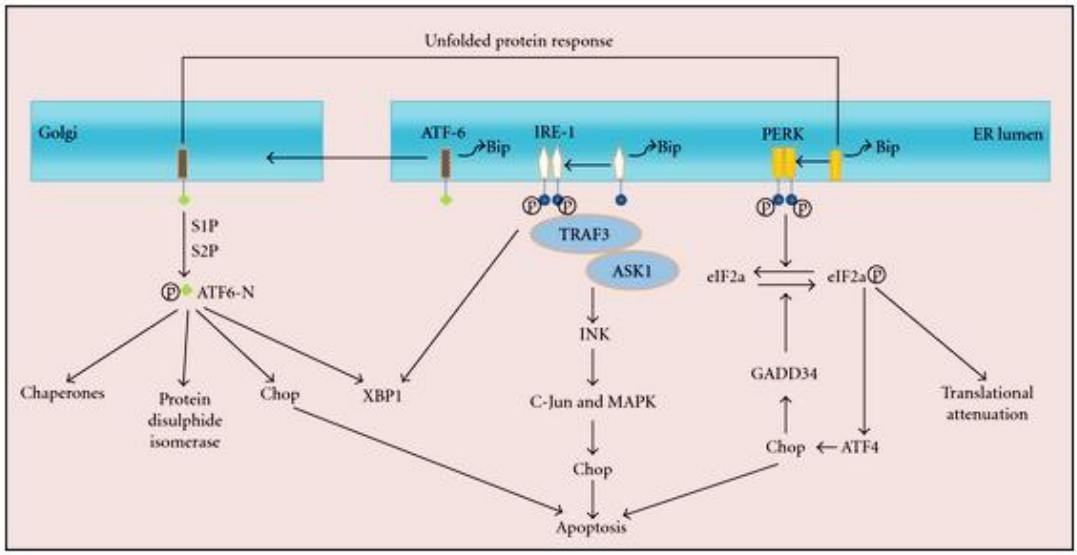

Figure 1.8 Mechanism of endoplasmic reticulum stress mediated apoptosis pathway. ER stress activated PERK, IRE and ATF6. These signals are transmitted by XBP-1, ATF4 and p50ATF6, and lead to induction of CHOP. IRE also activates JNK. Caspase 12 is activated directly in response to ER stress (Hu et al, 2012)

UPR primarily functions to relieve the ER from its protein overload and consequent stress firstly by increasing the expression of the ER chaperone and ER biogenesis proteins along with attenuation of the translation of global proteins. If the mission to restore ER functional integrity through those adaptive processes becomes unsuccessful, apoptosis is induced as a last resort option. All the three UPR pathways play a role in initiating the apoptotic process, though some are more prominent than others. PERK pathway is known to be the most prominent and direct route which triggers apoptosis. The activation of PERK has an inhibitory effect on eIF2α which consequently reduces global protein translation. Inactivated eIF2α also results in increased preferential translation of ATF4, which targets *Chop* gene, also called GADD153: growth arrest and DNA damage inducible gene. *Chop* gene promoter has binding sites for both ATF6f and XBP-1s. Hence ATF6 as well as IRE-1α can trigger apoptosis through this pathway. IRE-1α has yet another distinct apoptosis-inducing pathway. The cytoplasmic portion of IRE-1α binds to Tumour necrosis factor

receptor-associated factor 2 (TRAF2), an adaptor protein, through its protein kinase activity, forming a unit which then binds to form a complex with ASK1. This complex, IRE-1α – TRAF2 – ASK1, phosphorylates and activates JNK protein which has a pro-apoptotic function (Figure 1.8) (Hummasti and Hotamisligil, 2010; Marciniak and Ron, 2006; Ron and Walter, 2007; Yoshida, 2007).

The expression levels of CHOP are kept very low in unstressed cells. However, during acute ER stress, CHOP expression is robustly stimulated through IRE-1α and PERK-mediated signaling and the activities of ATF4 and ATF6 transcription factors. The full proapoptotic effect of CHOP appears only when ER stress cannot be suppressed by the efforts of the prosurvival module of the response system, and the misfolded protein levels remain high. CHOP activates a transcriptional pathway that triggers a pro-apoptotic program which includes expression of proapoptotic Bim and repression of antiapoptotic Bcl-2 (McCullough et al, 2001; Puthalakath et al, 2007). This mechanism is similar to the pro- apoptotic effects of JNK (Kim et al, 2006; Malhi and Kaufman, 2011; Nishitoh, 2012). CHOP also induces death receptor 5 (DR5), which additionally sensitizes cells to apoptotic stimulation by a number of conditions that cause ER stress (Yamaguchi and Wang, 2004). Growth arrest and DNA damage inducible protein 34 (GADD34), a regulatory subunit of protein phosphatase type 1 (PP1) is yet another target gene of CHOP. Activation of GADD34 expression results in PP1 activation and dephosphorylation of eIF2α, leading to the recommencement of general translation and normal functioning (Kojima et al, 2013; Novoa et al, 2001). While persistently increased CHOP expression triggers strong pro-apoptotic signaling, its initial effect on GADD34 might lead to the restoration of homeostasis. The stipulations are that the renewed supply of client proteins to the ER, if taking place too early, that is, under conditions where ER stress is not yet completely resolved, can trigger the ROS production, with deadly consequences for cell survival (Malhi and Kaufman, 2011). Whatever the case may be, the dissolution of ER stress entails mandatory inhibition of CHOP levels as a prerequisite for return to homeostasis (Rutkowski et al, 2006).

1.5 Involvement of oxidative stress in ER stress

1.5.1 Understanding of ROS

Cells contain basal level of ROS for signaling and normal physiological functioning. On the contrary, ROS levels are elevated significantly on exposure to toxic agents such as irradiation and environmental pollutants or during enzymatic reactions (e.g, mitochondrial

respiratory chain reactions, arachidonic acid pathway, cytochrome P450 family and those involving glucose oxidase, amino acid oxidase, xanthine oxidase, NADP/NADPH oxidase or NO synthases) (Malhotra and Kaufman, 2007; Perjes et al, 2012). The mitochondrial inner membrane potential determines the rate of electron transport chain, which leads to the production of membrane-impermeable superoxide anion. The superoxide produced is converted to hydrogen peroxide (H_2O_2) by mitochondrial dismutase and diffuses out of the mitochondria into the cytoplasm. Highly reactive hydroxyl radical ($OH^{\bullet}$) are generated from H_2O_2 through the Fenton reaction in the presence of iron (Murphy, 2009). In addition, the superoxide anion radical ($O2^{-\bullet}$) generates other toxic metabolites such as peroxynitrite ($ONOO^{-}$), hypochlorous acid (HOCl), and singlet oxygen ($^1O_2$) (Sanz et al, 2012). Under basal physiological conditions, endogenous antioxidant defense mechanisms which consists of enzymatic (e.g, superoxide dismutase, glutathione peroxidase, catalase, and thioredoxin reductase) and non-enzymatic (e.g, vitamins) antioxidant systems prevent ROS accumulation (Murphy, 2009; Sanz et al, 2012). In addition, number of redox systems like NAD+/NADH, NADP+/NADPH, and oxidized glutathione/reduced glutathione (GSSG/GSH) are involved in regulating redox homeostasis (Malhotra and Kaufman, 2007).

1.5.2 Oxidative protein folding in ER

ER is the site for protein synthesis, proper protein folding and formation of disulfide bonds. The redox status within the lumen of the ER influences the protein folding and disulfide formation. The lumen of the ER has a highly oxidizing environment, in contrast to the cytosol with a high ratio of GSSG/GSH. The oxidizing environment in the ER lumen is known to facilitate disulfide bond formation. Additionally, the greater oxidizing environment of the ER inhibits the aggregation or accumulation of unfolded proteins in the ER lumen because of its preferred oxidation state and abundant ER-resident proteins like protein disulfide isomerase (Van der Vlies et al, 2003). Before the properly folded proteins are secreted from the ER lumen, these proteins undergo compulsory disulfide bond formation for stability and maturation. Alterations in the disulfide bond formation or mispairing of cysteine residues causes protein misfolding or inability of the protein to attain its proper configuration (Lisa et al, 2012; Sideraki and Gilbert, 2000). GSH plays a major role in preventing non-native disulfide bond formation or the generation of misfolded proteins. There are many other pathways that cells use to maintain native protein structure. A number of folding catalysts present in the ER lumen, which regulate redox conditions, may facilitate the formation and isomerization of disulfide bonds (Sideraki and Gilbert, 2000). Oxidative protein folding is

catalyzed by a family of ER oxidoreductases including PDI, endoplasmic reticulum protein p72 (ERp72), ERp61, ERp57, ERp44, ERp29, and PDI-P5 (Malhotra and Kaufman, 2007). These folding enzymes help proteins form correct disulfide bonds by oxidizing cysteine residues of nascent proteins. Reduced folding enzymes are reoxidized by endoplasmic reticulum oxidoreductin (ERO1), the enzyme which uses molecular oxygen as a terminal electron acceptor (Gross et al, 2004). Research has shown a strong crosstalk between ROS production and the ER stress response.

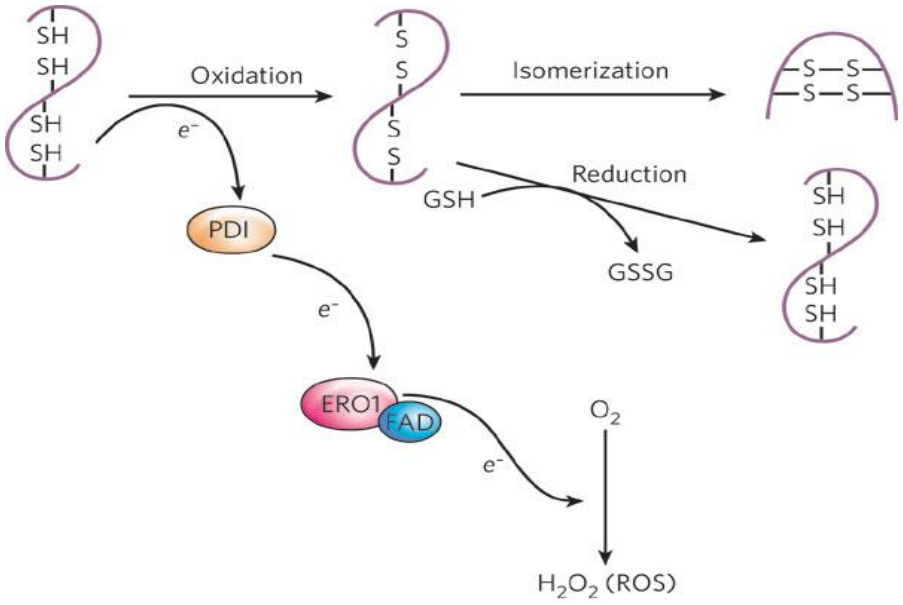

Figure 1.9 The formation of disulphide bonds in proteins in the endoplasmic reticulum is driven by the enzymes PDI and ERO1 (Zhang et al, 2008).

Alteration in the functions of PERK and ATF4 causes redox imbalance in cells. But these proteins are also responsible for the elimination of ROS through transcriptional regulation. Disulfide-bond formation involving ERO1 contributes significantly to the total production of ROS in the cell (Cullinan and Diehl, 2004; Harding et al, 2003). Overexpression of ERO1 protein alters the redox state of PDI towards the oxidized form, which also influences oxidation of PDI substrates. During disulfide bond formation, electrons pass several thiol-disulfide exchange reactions, through the thiols of the substrates, PDI and ERO1 before reaching the molecular oxygen. Superoxide anion radicals which are formed as a result of incomplete reduction of oxygen can be transformed to H_2O_2 or converted to other ROS (Figure 1.9). ER stress-associated oxido/reduction environment show associations with ER stress associated ROS.

1.5.2.1 ER associated ROS production under ER Stress

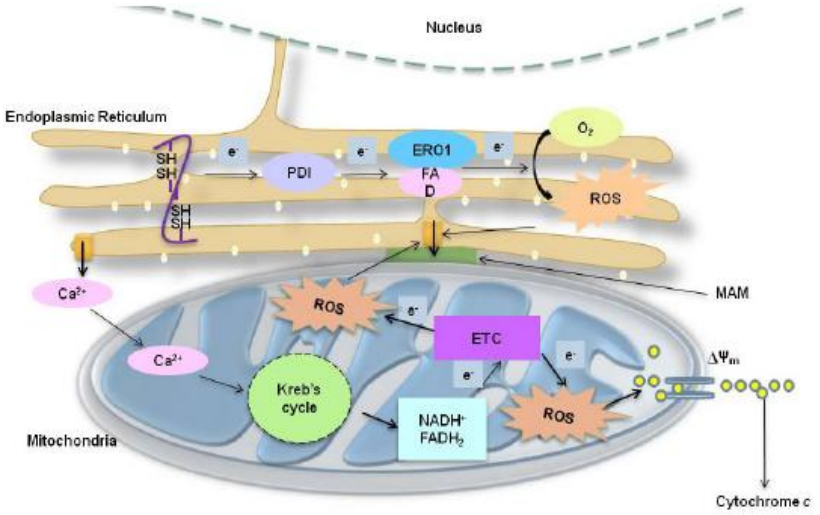

Figure 1.10 Protein misfolding and oxidative stress create a vicious cycle along with reactive oxygen species production in mitochondria leading to endoplasmic reticulum stress and cell death (Bhandary et al, 2012)

Two mechanisms have been suggested for generation of ROS during disulfide bond formation. ROS can be formed as a byproduct during electron transfer from protein thiol to molecular oxygen by ERO1 and PDI. Alternatively, ROS is produced during protein misfolding due to the depletion of GSH (Santos et al, 2009; Tu and Weissman, 2002). The GSH are utilized so that thiols involved in non-native disulfide bonds would return to their reduced form and they may again interact with ERO1/PDI to be reoxidized. This would create a futile cycle of disulfide bond formation and breakage, in which each cycle would generate more ROS and consume GSH. As a result, it is expected that proteins with multiple disulfide bonds are more prone to generating oxidative stress. ROS can also be generated by accumulated unfolded proteins independent of the formation of disulfide bonds. Accordingly, accumulation of unfolded proteins in the ER leads to Ca^{2+} leakage into the cytosol, increasing ROS production in the mitochondria (Malhotra and Kaufman, 2007). As protein folding and refolding in the ER lumen are highly energy-dependent processes, ATP depletion following the protein misfolding may accelerate mitochondrial oxidative phosphorylation to increase ATP and ROS production (Figure 1.10). NADPH oxidase 4 (Nox4), one of the NADPH oxidase isoforms, is also shown as a possible ROS source during ER stress (Pedruzzi et al, 2004; Radermacher et al, 2013).

1.5.3 Mitochondria-associated ROS production under ER stress

The mitochondrial oxidative phosphorylation and electron transport system have significant participation in mitochondrial ROS generation. Studies have also indicated that ER stress events are also associated with the mitochondrial ROS production mechanisms within cells.

1.5.3.1 ER stress induced mitochondrial ROS: role of electron transport chain

During sustained ER stress the mitochondria contribute significantly to lethal levels of ROS production. Though ROS generation is initiated by the ER stress, later affects the mitochondrial electron transfer system, and amplifies mitochondrial ROS production especially during severe/sustained ER stress. In mitochondria ROS may be originating from leaky electrons from the electron transfer system. This ROS may in turn enhance the ER stress response further, thus amplifying mitochondrial ROS accumulation by a feedback pathway (Yoon et al, 2011). During early phase of ER stress, UPR-induced ROS accumulation was significantly decreased by interfering with the mitochondrial respiration (Bravo et al, 2011).

1.5.3.2 Calcium related ROS generation in ER stress

Alteration in Ca^{2+} regulation is another factor (Malhotra and Kaufman, 2007; Bravo et al, 2011) affecting mitochondrial membrane potential ($\Delta\Psi M$), ATP depletion and ROS formation (Radermacher et al, 2012). Enhanced ROS levels set off a Ca^{2+} influx from the extracellular environment through membrane-linked channels or from the ER through the ER-localized channels, respectively into the cytoplasm. An elevated Ca^{2+} concentration in the cytoplasm promotes Ca^{2+} influx into the nuclei and mitochondria (Murphy, 2009). Mitochondrial Ca^{2+} loading alters mitochondrial metabolism and subsequently increase ROS production. The increased mitochondrial ROS level triggers a series of events by which oxidative stress add to the probability of Ca^{2+} release from ER. The very close proximity between ER and mitochondria leads to the accumulation of Ca^{2+} in the mitochondria (Moserova and Kralova, 2012).

Depletion of GSH also causes ROS to be generated by the mitochondria, leading to cell death (Chen et al, 2011; Lee et al, 2011). Besides GSH, pyroredoxin IV enzymes present in the ER lumen can also nullify the H_2PO_2 formed during disulfide bond formation (Tavender and Bulleid, 2010). Similar to GSH, this enzyme also function in regulating oxido/reduction. Hence, maintaining the oxido/reduction mechanism may play a regulatory

role in the production of ER stress-associated ROS. The specific expression of inducible genes, such as Lon protease, and NIX are also involved in ER stress induced mitochondrial ROS production. Lon proteases protect mitochondria by interfering with cytochrome c oxidase complex assembly/degradation. NIX is a Bcl-2 family protein that regulates ER Ca^{2+} and ΔΨM and opening of the mitochondrial permeability transition pore (MPTP) (Diwan et al, 2009; Chen et al, 2010).

1.6 Interaction between mitochondria and the endoplasmic reticulum

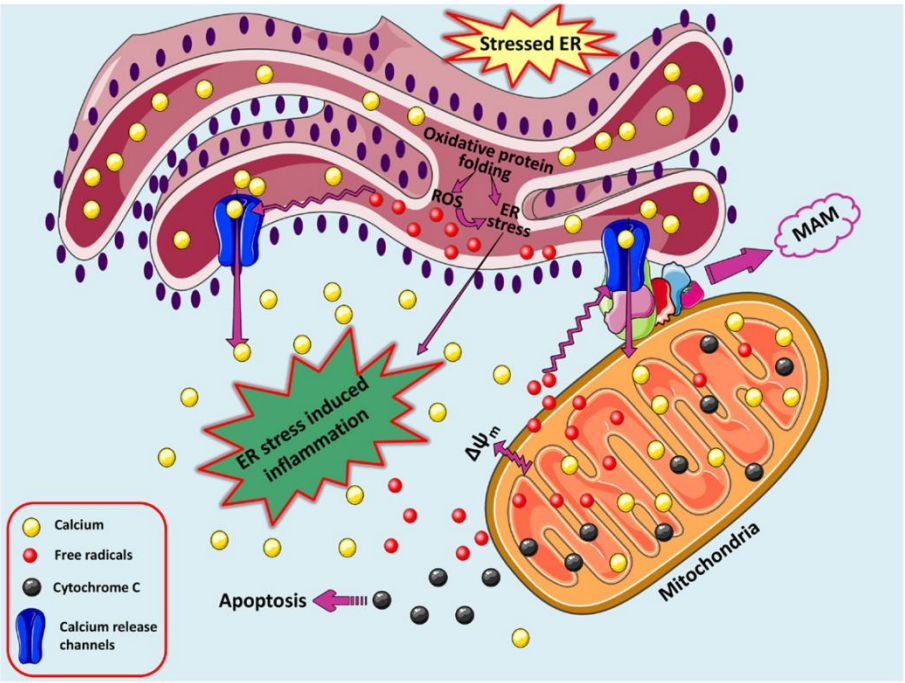

Figure 1.11 Structural and functional interaction between endoplasmic reticulum and mitochondria (Chaudhari et al, 2014).

Mitochondria are cell organelles with vital role in cellular bioenergetics. It converts energy from nutrients into ATP via tricarboxylic acid (TCA) cycle and oxidative phosphorylation (OXPHOS). In addition to supplying cellular energy, mitochondria are involved in several cellular stresses and human diseases (Lane, 2006). Mitochondria have an important role in the pathophysiology of obesity. The mitochondria of obese individuals are different from those of nonobese. Alterations in mitochondrial morphology, impaired mitochondrial bioenergetics, increased mitochondrial lipid peroxides, decreased ATP content, and other mitochondrial dysfunctions increase the risks of developing metabolic complications associated with obesity (Grattagliano et al, 2012; Rong et al, 2007).

1.6.1 Structural communication between mitochondria and the ER

Mitochondria and the ER are found to have structural communication with each other. This was proven by cosedimentation of ER particles with mitochondria, as well as electron microscopic observation of a close physical apposition between mitochondria and the ER (Pickett et al, 1980; Shore and Tata, 1977). High-resolution three-dimensional images showing an interaction between mitochondria and the ER have been obtained (Rizzuto et al, 1998). A recent study using electron tomography has shown that the outer mitochondrial membrane (OMM) and the ER are joined by tethers, enabling ER proteins to associate directly with proteins and lipids of the OMM (Csordás et al, 2006). The structural membrane that bridges between mitochondria and the ER is called the mitochondria-associated membrane (MAM) (Figure 1.11) (Vance, 1990). The MAM have essential roles in several physiological functions, like lipid transport, Ca^{2+} signaling, and apoptosis (Hayashi et al, 2009). Numerous mitochondrial or ER-bound proteins are vital for maintaining structural communication between the two organelles at the MAM (Hayashi et al, 2009; Simmen et al, 2010). Communication between the organelles is specifically modulated by a family of chaperone proteins. The molecular chaperone GRP75 connects the voltage-dependent anion channel (VDAC) to the inositol 1,4,5-triphosphate receptor (IP_{3R}) (Szabadkai et al, 2006). Another protein that regulates interaction between mitochondria and the ER is phospho furin acidic cluster sorting protein 2 (PACS-2), which integrates ER-mitochondrial communication and apoptosis signaling (Simmen et al, 2005). More recently, Sigma-1 receptors have been shown to be present at the MAM of the ER, where they form complexes with Bip (Hayashi and Su, 2007). Sigma-1 receptors dissociate from Bip and bind to type-3 IP_{3Rs} during ER Ca^{2+} depletion so that, type-3 IP3Rs are not degraded by proteasomes. This Ca^{2+} depletion induces a prolonged Ca^{2+} signaling event from the ER to the mitochondria, via IP_{3Rs}. Together, the data indicate that Sigma-1 receptors are involved in maintaining normal Ca^{2+} signaling from the ER to mitochondria.

1.6.1.1 Mitochondrial biogenesis

Mitochondrial biogenesis can be defined as growth and division of pre-existing mitochondria. This process involves the coordinated action of both nuclear and mitochondrial encoded genomes. Peroxisome proliferator-activated receptor-gamma coactivator (PGC) - 1α is a central regulator of mitochondrial biogenesis. PGC-1α acts as co-transcriptional regulatory factor activating different transcription factors, including Nuclear respiratory factor 1(Nrf1) and nuclear factor erythroid 2-related factor-2 (Nrf2), which promote the expression of

transcription factor a, mitochondrial (TFAM). Nrf1 and Nrf2 are important contributors to the sequence of events leading to the increase in transcription of key mitochondrial enzymes, and they have been shown to interact with TFAM, which drives the transcription and replication of mtDNA (Figure 1.12) (Virbasius and Carpulla, 1994). Decreased expression of markers of mitochondrial biogenesis and metabolism were found in overweight and obese insulin resistant subjects (Heilbronn et al, 2007). Studies also reported that transgenic as well as high fat diet obese mice had less mitochondrial density compared to lean control (Zhang et al, 2010).

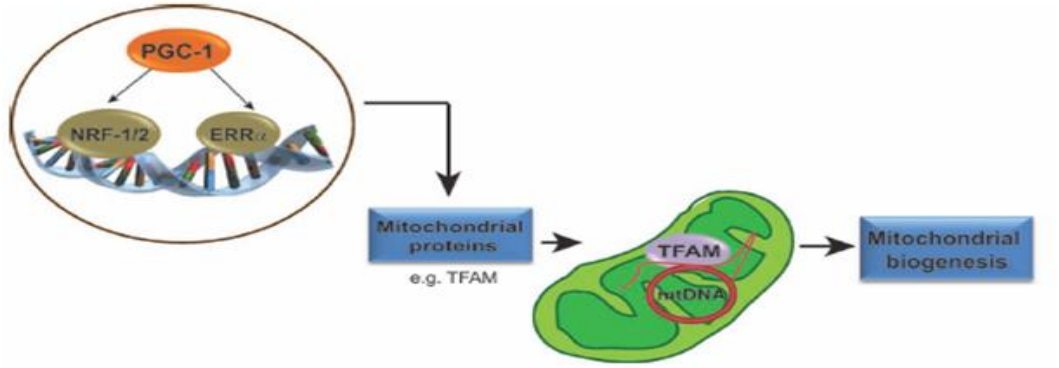

Figure 1.12 Regulation of mitochondrial biogenesis (Dillon et al, 2012)

1.6.1.2 Mitochondrial dynamics

Structural communication between mitochondria and the ER is also regulated by fission and fusion of mitochondria. Fission and fusion are modulated by a family of mitochondrion-shaping proteins including dynamin-related protein 1 (Drp1), Optic atrophy 1 (OPA1), mitofusin 1(Mfn-1), and mitofusin 2(Mfn-2) (Westermann, 2010). Mfn-2 is a mitochondrial transmembrane GTPase that regulates mitochondrial fusion and this protein is abundant at MAMs (de Brito and Scorrano, 2008). Mfn-2 tethers the ER to mitochondria via formation of both homotypic and heterotypic complexes. The tethering effect of Mfn-2 appears to play a role in the control of Ca^{2+} flow between mitochondria and the ER (de Brito and Scorrano, 2008; Mozdy and Shaw, 2003). OPA1 is a dynamin related GTPase associated with the mitochondrial inner membrane or intermembrane space. Outer membrane fusion depends on the mitofusins Mfn1 and Mfn2. Inner membrane fusion depends on the OPA1 depletion. The central player appears to be Drp1. Drp1 assembles on mitochondrial tubules and mediates constriction and scission. Much of Drp1 resides in the cytosol, and therefore a second class of mitochondria residing proteins which includes fission 1 (Fis1), which efficiently recruits DRP1 for fission (Figure 1.13). Mitochondrial fusion and fission result in

content exchange between mitochondria. These exchange events keep the mitochondrial population homogeneous and functional. Mitochondrial dynamics is involved in multiple mitochondrial functions, including mtDNA stability, respiratory function, apoptosis, response to cellular stress, and mitochondrial degradation (Chan, 2012).

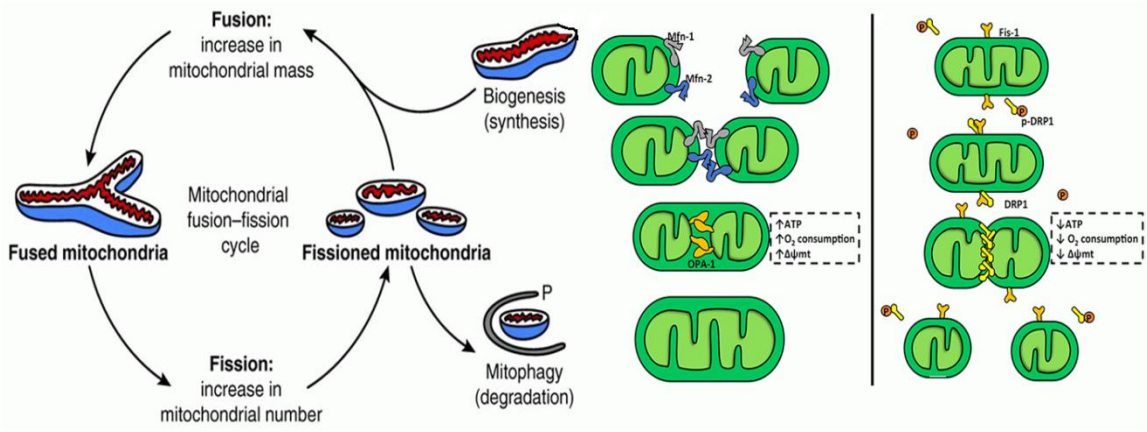

Figure 1.13 Possible relationship between mitochondrial fusion, fission, biogenesis and degradation (Chiong et al, 2014, Zeo et al, 2010).

1.6.2 Functional communication between mitochondria and the ER

1.6.2.1 Role of ER stress in induction of mitochondrial dysfunction

Mitochondrial dysfunction and ER stress have each been recognized to play crucial roles in the pathogenesis of metabolic syndrome. Accumulating evidence has shown that ER stress induces mitochondrial dysfunction, thereby leading to disturbances in various physiological responses within cells (Csordás and Hajnóczky, 2009; Giorgi et al, 2009). Regulation of Ca^{2+} signaling and Ca^{2+}-dependent cellular processes such as apoptosis are facilitated through the interactions between mitochondria and the ER (Pinton et al, 2008; Szabadkai and Duchen, 2008). Severe or prolonged ER stress leads to release of Ca^{2+} from the ER lumen at the MAM. On the contrary, such stress causes increased Ca^{2+} uptake into the mitochondrial matrix. An imbalance between mitochondrial Ca^{2+} load and the buffering capacity of the matrix is generated by elevated Ca^{2+} uptake, and such imbalance ultimately leads to a prolonged episode of massive mitochondrial Ca^{2+} accumulation. Persistent Ca^{2+} accumulation triggers opening of the MPTP resulting in swelling of the organelle, rupture of the OMM, and release of proapoptotic proteins into the cytosol (Figure 1.14)(Deniaud et al, 2008).

ROS have been identified as local messengers between the ER and mitochondria (Csordás and Hajnóczky, 2009). ER and mitochondria form the sites for many ROS sources as well as targets (Feissner et al, 2009; Malhotra and Kaufman, 2007). ROS are produced by ERO1 during disulfide bond formation and previous studies have shown that ER stress can activate ERO1 (Harding et al, 2003; Marciniak et al, 2004). Therefore, conditions that trigger such stress may lead to excessive production of ROS in the ER. High ROS levels can inactivate the sarco-endoplasmic reticulum Ca^{2+}ATPase (SERCA) and activate IP_3R via oxidation (Adachi et al, 2004; Li et al, 2009). Modulation of Ca^{2+} channel activity by ROS increases the level of Ca^{2+} on the cytosolic face of the ER and also promotes Ca^{2+} uptake into the mitochondrial matrix. Hence, ROS production mediated by ERO1 presents an additional mechanism by which ER stress can induce mitochondrial dysfunction.

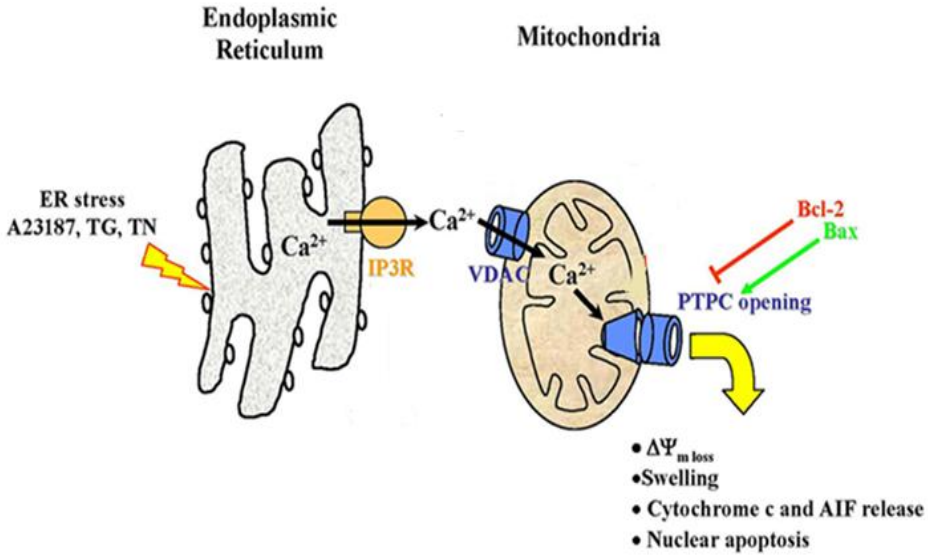

Figure 1.14 Ca^{2+} signaling between mitochondria and the endoplasmic reticulum regulates Ca^{2+}-dependent cellular processes such as apoptosis (Sharaf et al, 2008).

1.6.2.2 Correlation between ER stress induced Ca^{2+} and ROS at mitochondria

Both ER stress and oxidative stress increase the release of Ca^{2+} from the ER lumen through ROS production (Malhotra and Kaufman, 2007). Ca^{2+} can be both a physiological and a pathological effecter of the mitochondria, so that increases of Ca^{2+} in the mitochondria may alter mitochondrial functions (Gorlach et al, 2006). The elevated Ca^{2+} stimulates the tricarboxylic acid cycle and mitochondrial oxidative phosphorylation, increasing ROS output by stimulating the mitochondria to work faster thus consuming more O_2 in the process. In addition, nitric oxide synthase is stimulated by Ca^{2+} to generate NO, inhibiting complex IV

activity, which then enhances ROS generation at Qo site in complex III (Meares et al, 2011; Murphy, 2009, Xu et al, 2004). This signaling axis operates within a physiological concentration of NO. NO, together with high Ca^{2+}, can inhibit mitochondrial complex I, resulting in the release of cytochrome c. This is by inducing the opening of MPTP and blocking the respiratory chain at complex III, thereby increasing the production of ROS (Jekabsone et al, 2003). On the other hand, Ca^{2+} may perturb the mitochondrial antioxidant status. Mitochondrial GSH is released very early in Ca^{2+} induced MPTP opening, suggesting that a higher amount of Ca^{2+} exposed mitochondria may generate more ROS because of diminished GSH levels.

1.7 ER Stress and inflammation

Obesity is associated with inflammation of adipose tissue playing a key role in the development of IR. This is evident by the increased levels of inflammatory markers such as TNF-α, IL-6, MCP-1, and IL-8, altered levels of adipokines including adiponectin and leptin and increased C reactive protein and osteopontin.

1.7.1 The UPR and inflammation

ER stress and UPR pathways are found to be linked to many major inflammatory and stress signaling networks, including the activation of the JNK-AP1 and NF-κB-IKK pathways (Deng et al, 2004; Hu et al, 2006), as well as production of ROS and nitric oxide (Cullinan and Diehl, 2006; Gotoh and Mori, 2006). The activation of these pathways leads to production of pro-inflammatory adipokines, creating an additional burden on ER internally and externally. Internally, ER has to deal with an increasing demand for synthesis of pro-inflammatory adipokines. Externally, the proinflammatory adipokines successfully synthesised and secreted would exert their pro-inflammatory effects at autocrine and paracrine level, thus creating a feedback cycle. All the three ER stress related transmembrane proteins contribute in this process. IRE-1α activates JNK and NF-κB through TRAF2 and ASK1 (Urano et al, 2000). PERK phosphorylates eiF2α and activates both JNK and IKK (Deng et al, 2004, Hu et al, 2006, Shoelson et al, 2006) while ATF6 also activates nuclear factor κB (NF-kB) (Yamazaki et al, 2009). Finally, ER stress activates cAMP responsive element-binding protein, hepatocyte specific (CREBH), which together with NF-kB augment transcription of genes taking part in inflammation (Vecchi et al, 2009). Another immunomodulator transcription factor upregulated by the UPR is AP-1, which activates the tumor necrosis factor-alpha (TNFα), keratinocyte growth factor (KGF), interleukin (IL)-8,

granulocyte macrophage colony-stimulating factor (GM-CSF) and also some cytokine receptors. AP-1 is activated by IRE-1α (Figure 1.15).

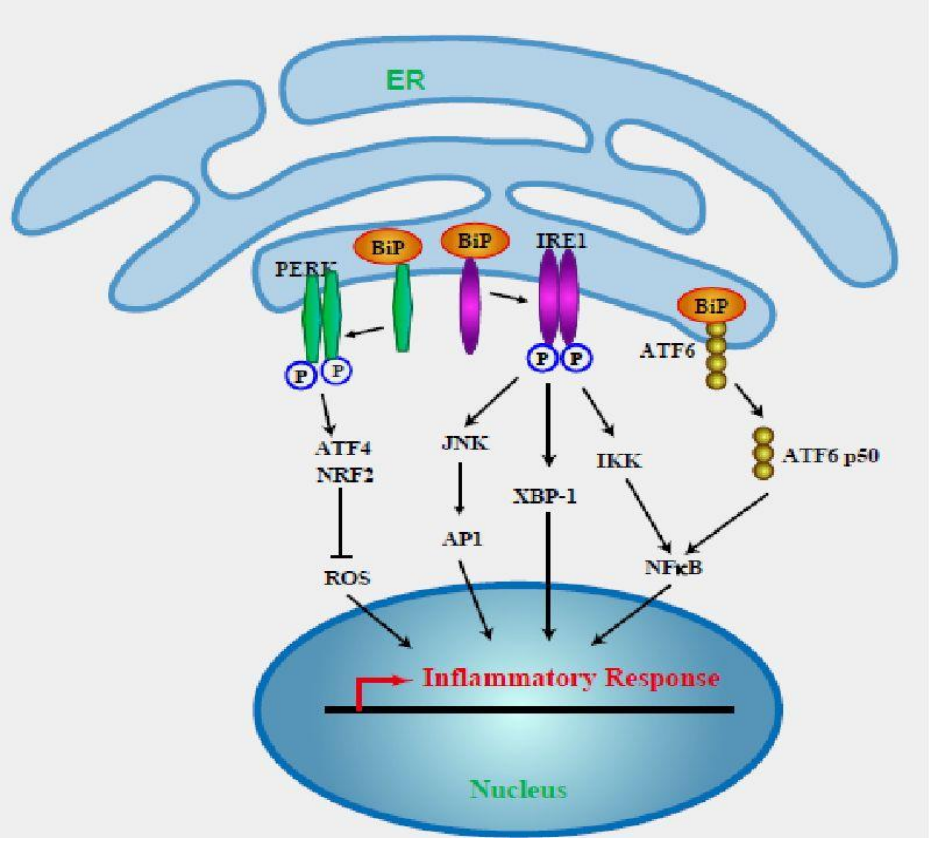

Figure 1.15 Unfolded protein response mediated inflammation (Zhong et al, 2014)

PERK plays a unique role in linking nutrients and ER stress to inflammation and metabolic regulation (Nakamura et al, 2010). It is strikingly activated by lipids and during obesity and plays a critical role in the activation of JNK and the inflammatory response. PERK also directly interferes with insulin action by interacting with IRS-1 and thus help in the assembly of a metabolically activated inflammatory complex called the metabolic inflammasome or metaflammasome, which integrates insulin action, pathogen responses, and translational control with nutrient sensing and ER stress. Formation of a metaflammasome and its activation by nutrients and ER stress explains the functional overlap between multiple signaling pathways, such as JNK, IKK, and others, in modulating metabolism.

The relationship between ER stress and inflammation is possibly not one-sided. Inflammatory mediators and activation of cellular stress pathways, such as the JNK and IKK pathways, may have a negative impact on ER function too. Studies provide evidence that both ER stress and inflammation can activate each other and inhibit normal cellular metabolism (Zhang et al, 2008).

1.7.1.1 NF-κB and JNK pathway

The IKKβ/NF-κB pathway is one of the principal inflammation signaling pathways. The IkB families of protein regulate the activation of NF-kB whose entry into nucleus can initiate inflammation. IkB controls NF- kB by sequestering NF-kB in the cytoplasm. IkB in turn can be degraded by IkB Kinase (IKK) which then causes the NF-kB dimers to enter nucleus and trigger inflammation. Therefore a decreased level of IkB (due to increased IKK activity) provides a pathway by which ER stress induce inflammation. The serine kinase IKK has three major isoforms including IKKα (IKK1), IKKβ (IKK2) and IKKγ, of which IKKβ is involved in NF-kB activation. During obesity, a number of intracellular signals, like ROS, ER stress, DAG, and ceramide activate IKKβ. IKKβ is also activated by the extracellular stimuli such as TNF-α, IL-1, fatty acids, and hypoxia (Ye and Keller, 2010). In the classical pathway, NFκB activation is mediated by IKKβ induced phosphorylation and proteasome-mediated degradation of IkBα (Karin and Ben-Neriah, 2010). It leads to transcription of inflammatory cytokines TNFα, IL-1β, IL-6, MCP-1, etc. In the alternative pathway, activation of NFκB involves IKKα (Ye, 2009). This type of NFκB activation in adipocytes and macrophages contributes to chronic inflammation in the adipose tissue of obese individuals.

The JNK belongs to a family of mitogen-activated kinases (MAPKs), together with extracellular regulated kinases (ERKs) and p38. The JNK subgroup of MAPKs is encoded by three loci, Jnk1 and Jnk2 are located ubiquitously, and Jnk3 is expressed primarily in heart, testis, and brain (Maeda, 2010). JNK- AP1 pathways are activated during metabolic dysregulation by TNF-α, IL-1, TLR, or free fatty acids, intracellular stresses including ROS and ER stress, ceramides, and various PKC isoforms.

1.8 ER stress and insulin resistance(IR)

Ozcan and colleagues first showed that ER stress in adipose tissue of obese mice and proposed it as a risk factor for IR (Ozcan et al, 2004). Since then, studies have shown that any stress inducing conditions like obesity is clearly associated with ER stress and apoptosis of beta-cells, hepatocytes and adipocytes which eventually leads to metabolic derangements, especially with IR (Boden et al, 2008; Gregor and Hotamisligil, 2007; Hotamisligil, 2010; Hummasti and Hotamisligil, 2010; Karalis et al, 2009; Nakatani et al, 2005; Ozcan et al, 2006).

1.8.1 IR

IR is denoted as the impaired sensitivity of target organs, like adipose tissue, the liver and muscle, to insulin. Insulin regulates glucose uptake in the liver and muscle. Insulin is also the key regulator of circulating FFA concentrations. In adipose tissue, insulin lowers lipolysis and thereby reduces FFA efflux from adipocytes, in skeletal muscle, insulin mainly induces glucose uptake by stimulating the translocation of glucose transporter type 4 (GLUT4) to the plasma membrane. In the liver, insulin inhibits gluconeogenesis by reducing the activity of key enzymes. Consequently IR increases the circulating FFA concentrations, leading to ectopic fat deposition that slow down insulin mediated glucose uptake in skeletal muscle and increases glucose generation in the liver (Samuel and Shulman, 2012). A combination of IR and abnormalities in insulin secretion is the cause of T2DM.

1.8.2 IR at the molecular level

In normal conditions, insulin works through a set of complex signaling cascades. Insulin receptor mediated tyrosine phosphorylation of insulin receptor substrates (IRSs) induces the activation of at least two major pathways: The phosphatidylinositol 3-kinase (PI3K)-AKT and MAPK pathways. The PI3K-AKT pathway primarily influences the effect of insulin on glucose uptake and the suppression of gluconeogenesis, whereas the MAPK pathway modulates gene expression and interacts with the PI3K-AKT pathway to regulate cell growth and differentiation. Serine phosphorylation of IRSs at specific serine residues inhibits insulin signaling. IκB kinase-β (IKK-β), JNK 1 and MAPKs are some of the serine kinases that phosphorylate IRS-1, inactivating its insulin signaling activity.

These serine kinases are also mediators of inflammatory signaling pathways, indicating that an inhibitory crosstalk exists between inflammatory and insulin signaling at a molecular level. The association between cytokine signaling and the inhibition of insulin signaling is also demonstrated by the presence of molecular mediators, including suppressor of cytokine signaling (SOCS) 1 and 3 and nitric oxide (NO). IL-6 induces the activation of SOCS proteins during inflammation, causing the ubiquitinylation and degradation of IRS proteins. Endogenous NO production by inducible NO synthase (iNOS), under the action of numerous inflammatory cytokines, can limit IRS-1 and iNOS activity, resulting in reduced AKT activity, which is a key mediator of IRS signaling (Zeyda and Stulnig, 2009).

1.8.3 Impact of IRE-1α-JNK-IRS-1 signaling pathway in IR

ER stress in adipocytes is linked to insulin signaling through the activation of IRE-1α. ER stress increases serine (Ser) phosphorylation and decrease of tyrosine (Tyr) phosphorylation of IRS-1, which causes inactivation of signal transduction thus leading to IR. Both IRE-1α and PERK can activate JNK and activated JNK phosphorylates IRS-1 at Ser307. PERK can also inhibit insulin signaling by directly phosphorylating IRS-1 on serine 307(Spiegelman, 1998). The inflammatory cytokines secreted from adipocytes and macrophages during inflammation can also stimulate JNK pathways (Samuel and Shulman, 2012). In addition, inflammatory cytokines hampers insulin signaling by interfering with IRS-1 insulin receptor interaction and promoting IRS-1 degradation (Figure 1.16) (Zeyda and Stulnig, 2009).

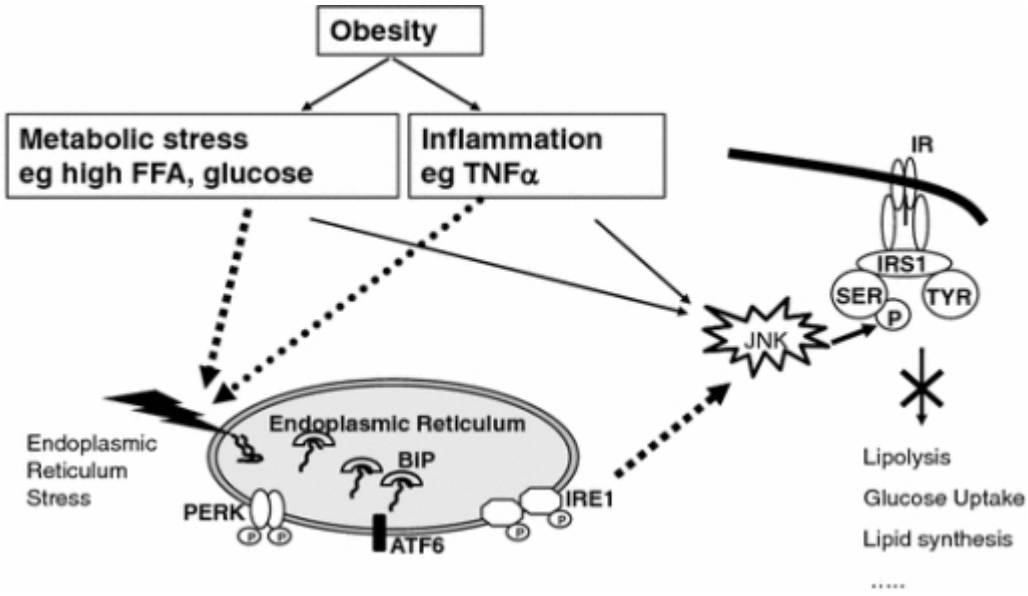

Figure 1.16 Role of endoplasmic reticulum stress in obesity related insulin resistnce (van der Kallen, 2009)

1.8.4 Adipokines in IR

Several studies have shown that insulin resistant states are not only associated with increased lipolysis and adipose ER stress but also altered adipokines production. In obesity, there is derangement in leptin and adiponectin secretion and an increase of IL-6 secretion (Kars et al, 2010). Decreased expression of adiponectin favors IR in obesity (Gual et al, 2005; Itani et al, 2002; Yuan et al, 2001). ER stress caused decreased levels of adiponectin in human adipocytes and was shown to alter insulin sensitivity and other metabolic syndromes (Arkan et al, 2005; Hirosumi et al, 2002). Adiponectin signaling targets AMPK, which is a negative regulator of mTOR and high level of mTOR causes serine phosphorylation of IRS-1. Resistin

(Zhang and Kaufman, 2008) also has been found to be associated with IR. The role of resistin in the IR needs further clarification as it showed positive correlation with the IR in some studies (Nakamura et al, 2010), while other studies showed no correlation (Boden and Merali, 2011; Kyriakis and Avruch, 2001; Shoelson et al, 2006). TNF-α also activates several IR-related pathways, including IKK-β and SOCS3, in cultured murine adipocytes (Hotamisligil et al, 1996; Shi et al, 2004). TNF-α interferes with insulin sensitivity by modifying the expression of IRS-1, GLUT4, adiponectin and PPAR-α (Jager et al, 2007; Ruan et al, 2003).

1.9 Targeting ER stress in metabolic disease

Given that, ER stress contributes significantly to the pathogenesis of multiple metabolic diseases, protein folding and UPR signaling have been targeted as a therapeutic approach for pharmacological intervention. A number of strategies have been tested in cell culture, animal models and clinical studies. Chemical chaperones are small molecules that prevent protein misfolding by stabilizing folding intermediates and preventing aggregation in the cell. Such compounds usually functions nonspecific to the folding substrate. Certainly, there are some chaperones which are protein specific. A second type of small molecules increase ER protein folding capacity and inhibit proapoptotic ER stress signaling by targeting specific UPR components, including ER stress sensors and transcription factors. The third type reinforces the function of the proteostasis network by improving the microenvironment for ER protein folding, for example, orchestrating ER Ca^{2+} flux and signaling. The last type of compounds alleviates ER stress and boosts protein folding capacity by aiming ER stress associated intracellular signaling pathways involved, like oxidative stress, inflammation and autophagy.

The emergence of compounds that target specific UPR signaling components, such as ATF6, IRE-1α, spliced XBP1 and the proteasomes, might provide promising therapeutics for the treatment of human metabolic diseases (Engin and Hotamisligil, 2010; Minamino et al, 2010). Chemical chaperones such as sodium phenylbutyrate (PBA), reduce ER stress and restore glucose homeostasis in a mouse model of T2DM (Ozcan et al, 2006). The ER modifications by chemical chaperones in macrophages and adipocytes have therapeutic efficacy against atherosclerosis in mouse models (Erbay et al, 2009). Some clinically approved pharmacological agents used in clinical settings affect the UPR pathways. The lipid-lowering compound provastatin ameliorates ER stress in cultured neonatal rat cardiomyocytes and in pressure overloaded hearts, and the antidiabetic agent pioglitazone represses hepatic ER stress and reduce IR (Zhao et al, 2008; Yoshiuchi et al, 2009).

1.10 ER stress and phytochemicals

The use of herbal medicines is on continuous rise for management of lifestyle related metabolic disorders. These preparations are being used both as medicine and also as food supplements. Most of these preparations possess antioxidant and anti-inflammatory property, due to the high polyphenolic content. So it would be logical to explore plant extracts and also pure phytochemicals on management of ER stress. This part has not been fully exploited for novel drug development, but it has a great potential. During the past few years many studies have tried to identify natural compounds which are able to interfere with or inhibit the UPR. ER stress induces the upregulation of Tumor necrosis factor-related apoptosis inducing ligand (TRAIL) receptor and opening new horizons for cancer therapeutic research. Hence, a large number of phytochemicals have been identified to be promoting ER stress and inducing cell death. Potential benefits of phytochemicals and polyphenols in reducing the elevated oxidative and lipid-mediated ER stress has also been studied (Chuang and McIntosh, 2011; Zingg et al, 2013). Vaticanol B, a resveratrol derivative, inhibits inflammation and improves the ER environment by reducing the ER protein load and by maintaining the ER membrane integrity (Tabata et al, 2007). Grape seed proanthocyanidin extracts were found to alleviate oxidative stress and ER stress in the skeletal muscle during T2DM (Ding et al, 2013). The phytoalexins glyceollins enhances insulinotropic actions in enteroendocrine cells and normalizes glucose homeostasis by reducing ER stress (Park et al, 2010). Quercetin protects macrophages from oxidized low-density lipoprotein (LDL)-induced apoptosis by interfering with the ER stress-CHOP signaling pathway (Yao et al, 2012). In the present study we analysed the protective effect of (-) hydroxycitric acid (HCA), against ER stress induced dysfunctions.

1.11 (-)-Hydroxycitric Acid

HCA is an organic acid derivative from the fruit rinds of certain species of *Garcinia*, which include *G. cambogia*, *G. indica*, and *G. atroviridis*. *G. cambogia* is a medium or large -sized tree with a rounded crown and horizontal or drooping branches, its leaves are dark green and shiny, elliptic obovate, 2-5 inch long and 1-3 inch broad, its fruits are ovoid, 2 inch diameter, yellow when ripe with six to eight grooves, and the fruits have six to eight seeds surrounded by a succulent aril (Figure 1.17A). The tree is found commonly in the evergreen forests of Western Ghats, from Konkan southward to Travancore, and in the Shola forests of Nilgiris up to an altitude of 6000 ft. It flowers during the hot season, and fruits ripen during the rainy season.

A

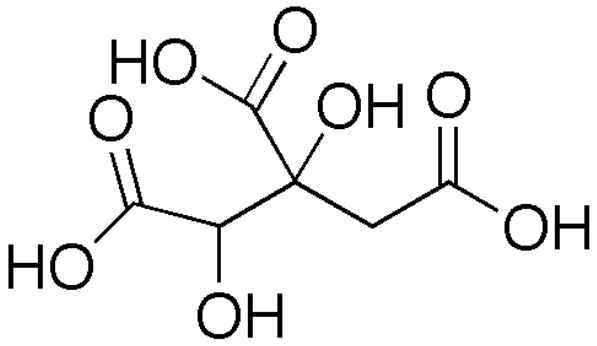

B

Figure 1.17 A. Structure of HCA B. Fruits of *Garcinia cambogia*

The fruits of *G. cambogia* are too acidic to be eaten raw. They are valued for their dried rinds, which are used as a condiment for flavoring curries in place of tamarind or lemon. The dried fruit rinds of *G. cambogia* are used along with salt in the curing of fish (Jena et al, 2002). A myriad of health effects have been attributed to *G. cambogia*, like antiobesity (Ohia et al, 2002; Preuss et al, 2004; Roy et al, 2003), antiulcerogenic (Mahendran et al, 2002), antioxidative (Asghar et al, 2007), antidiabetes (Wielinga et al, 2005), antimicrobial (Negi and Jayaprakasha, 2004), antifungal (Mackeen et al, 2002), anti-inflammatory (Reis et al, 2009), and anticancer effects (Prasad et al, 2009). In particular, the antiobesity effects of *Garcinia* or more specifically of its HCA content have been elucidated with clarity over the last few decades. Besides its efficacy in the reduction of body weight and food intake, HCA has been proven to be beneficial in ameliorating obesity-related complications such as inflammation, oxidative stress, and IR (Wielinga et al, 2005). The results obtained from several studies supported the positive effects of HCA administration alone or in combination with other ingredients on body weight loss, reduced food intake, increased fat oxidation, or energy expenditure (Ohia et al, 2002; Preuss et al, 2004; Roy et al, 2003) while some studies did not (Heymsfield et al, 1998; Kovacs et al, 2001; Kriketo et al, 1999).

HCA is a derivative of citric acid (Figure 1.17A) present in the pericarp of the fruits of *Garcinia cambogia* up to 30% by weight. Commercially available *Garcinia cambogia* extracts are prepared from the fruit rinds and contain 50% HCA (Jena et al, 2002; Mattes and Bormann, 2000). Among the components of the *Garcinia cambogia* extract, HCA exists as a free acid and as hydroxycitric acid lactone forms which are more stable. The free acid form is considered to be biologically active. For consumer products, the free acid is often stabilized by forming salts of HCA (Majeed et al, 1998).

Anti- obesity property of HCA is attributed to its effect of being a potent inhibitor of ATP citrate lyase, which catalyzes the extramitochondrial cleavage of citrate to oxaloacetate and acetyl-CoA, limiting the availability of acetyl CoA units required for fatty acid synthesis. Supplementation with HCA constitutes a novel means of reducing inflammation and is useful for preventing, treating and ameliorating conditions involving inflammation (US patent No WO2005002565 A1, 2005)

1.12 Scope of the study

Recent findings in biochemistry, cell biology and animal physiology demonstrate that protein misfolding in the ER and UPR signaling plays critical roles in the pathogenesis of metabolic diseases, including obesity, T2DM, nonalcoholic fatty liver disease (NAFLD) and atherosclerosis. The physiological significance demonstrated for ER protein folding homeostasis in metabolic disorders provides unique opportunities for scientists and physicians to intervene towards treating these diseases. To date, preclinical and clinical studies demonstrate the therapeutic potential of a wide range of small molecular modulators and regulators of ER stress and the UPR for treatment of metabolic syndrome. Among these compounds, chemical chaperones have shown efficacy in animal and clinical studies, while other molecules, including the regulators of IRE-1αa and BiP, still need extensive preclinical investigation. The emergence of small molecules that target specific UPR pathways will provide more options toward this goal. Despite all the recent progress, it is still necessary to elucidate the diverse biological functions of UPR components in different cells/ tissues in response to various metabolic stresses, and to understand how the UPR interacts with other cell signaling pathways, including oxidative stress, inflammation, autophagy and mitochondrial function under pathophysiological conditions. As UPR signaling may be preferentially activated in ER-stressed cells, targeting selective UPR components might provide some specificity toward those ER-stressed cells. Given the multifunctional nature of UPR signaling in different cell types, rational design and dosing of drugs will be critical for

success. More mechanistic and physiological studies are still needed to elucidate the efficacy and safety of these pharmacological interventions.

1.13 Objectives of the study

- To investigate the effect of ER stress on the physiological functions of 3T3-L1 adipocytes, emphasizing on, oxidative stress and ER stress and also evaluate the protective effect of (-) hydroxycitric acid on ER stress induced alterations.
- To evaluate the effect of ER stress on adipocyte mitochondrial function, biogenesis and structural dynamics, and possible protection with (-) hydroxycitric acid.
- To study the crosstalk between ER stress induced inflammation and IR, and, also the secretion of adipokines in 3T3-L1 adipocytes and possible reversal with (-) hydroxycitric acid.

Chapter 2

Materials and methods

2.1 Materials

2.1.1 Chemicals

(-) Hydroxycitric acid calcium salt (HCA) was purchased from Natural Remedies (Bangalore, India). 3- isobutyl-1-methylxanthine (IBMX), dexamethasone (DEX), insulin, 2, 7- dichlorodihydrofluorescein diacetate (DCFH-DA), ethylene diamine tetraacetic acid (EDTA), 3-(4,5-dimethylthiazol-2-yl)-2,5- diphenyl tetrazolium bromide (MTT), dimethyl sulfoxide (DMSO), bovine serum albumin (BSA), γ,γ' diaminobenzidine (DAB), sodium azide (NaN_3), sodium citrate, Tween- 20, phenyl methyl sulphonyl fluoride (PMSF), glucose-6-phosphate dehydrogenase, biliverdin reductase, hemin, radioimmunoprecipitation (RIPA) buffer, TRIzol and protease inhibitor cocktail, Hank's balanced salt solution (HBSS) were purchased from Sigma Aldrich (St. Louis, Mo, USA). 4-phenylbutyrate (PBA), trichloroacetic acid (TCA), dipotassium hydrogen phosphate (K_2HPO_4), potassium dihydrogen phosphate (KH_2PO_4), potassium phosphate (K_2PO_4), sodium pyrophosphate, methanol, hydrogen peroxide (H_2O_2), phenazine methosulphate (PMS), nitroblue tetrazolium (NBT), 5,5'-dithiobis-2-nitrobenzoic acid (DTNB), glacial acetic acid, n-butanol, nicotinamide adenine dinucleotide phosphate (NADPH), sucrose, glycine, methanol, hydrogen peroxide (H_2O_2) and triton-x 100 were purchased from Merck specialities Pvt. Ltd. USA. Fetal bovine serum (FBS), fetal calf serum (FCS), penicillin streptomycin antibiotics, Dulbecco's modified Eagle's medium (DMEM), Krebs' ringer phosphate buffer and trypsin-EDTA were purchased from Himedia Pvt Ltd (Himedia Pvt. Ltd, India). 2-(7-nitrobenz-2-oxa-1,3-diazol-4-yl) amino-2-deoxy-D-glucose (2-NBDG) was from Invitrogen (Carlsbad, CA, USA). Tris hydroxymethyl aminomethane hydrochloride (Tris HCl) and paraformaldehyde was purchased from Sisco research laboratory, Mumbai, India. Fura 2 AM, Mitotracker Deep Red FM, calcein AM and MitoSOX™ red were purchased from Molecular probes, Life technologies, USA. TRIzol was from Biochem Life Science, India. All other chemicals used were of analytical grade.

2.1.2 Assay kits

Protein carbonyl, total antioxidant, reduced glutathione (GSH), aconitase, O_2 consumption, Ca^{2+} content, triglyceride (TG), nuclear extraction kit and nuclear factor-κβ (NF-κβ) expression cell based assay kits, Nrf2 transcription factor assay kit, glycerol cell based assay kit were from Cayman Chemicals, USA. JC-1 mitochondria staining kit was from Sigma-Aldrich, (St. Louis, MO, USA). 2-deoxy glucose (2-DG) uptake colorimetric assay and mitochondrial biogenesis assay kit were from Abcam (Abcam, Cambridge, MA, USA). Adiponectin enzyme immunoassay (EIA) kit was from SPI Bio (SPI Bio, Bertin Pharma, France). Leptin ELISA kit was from Merck (Merck Millipore, USA). BCA protein assay kit was from Pierce (Rockford, IL USA). Cytochrome oxidase kit, lactate assay kits were from Sigma Aldrich chemicals (USA). ATP determination kit was from Molecular Probes Inc, Eugene, USA. Interleukin-6 (IL-6), interleukin-2 (IL-2), interleukin-10 (IL-10), monocyte chemattractant protein (MCP-1), interferon-gamma (IFN-γ) and IL-1β assay kits were from BD Biosciences, USA. Primers for PCR were from Hysel India Pvt Ltd, India. Superscript III 1st strand synthesis system kit was from Life technologies, Bangalore, India. Primary antibodies for western blotting, horseradish peroxidase (HRP) conjugated secondary antibodies and fluorescein-isothiocyanate (FITC) conjugated secondary antibodies were from Santa Cruz, USA.

2.2 Cell culture

3T3-L1 preadipocytes (ATCC, VA, USA) were cultured in complete growth medium [high-glucose (4.5g/l) DMEM supplemented with 10% FBS and 100 units/ml penicillin streptomycin] in a humidified incubator with 5% CO_2 at 37°C. Cells were passaged regularly and subcultured at 70% confluence before the experiments.

2.2.1 Differentiation of 3T3-L1 pre-adipocytes and ER stress induction

3T3-L1 preadipocytes were seeded in cell culture plates. Two days post confluence; the cells were differentiated with standard cocktail consisting of growth medium with 0.5 mM dexamethasone, 1 µg/ml bovine insulin, and 0.25 mM isobutyl-1-methylxanthine (Sigma, St Louis, MO, USA,). After 48 hours, differentiation medium was replaced with complete growth medium, containing 1 µg/ml bovine insulin. The cells were further maintained in insulin containing growth medium till used for experiments on day 9, after induction of differentiation. Mature adipocytes were incubated with tunicamycin (2 µg/ml) for 18 hours to induce ER stress. ER stress was induced in presence or absence of HCA at 5,

10, 20 μM concentrations to study the protective effect. PBA (1 mM) was used as a positive control.

2.3 Evaluation of cell viability

Cell viability was determined by MTT assay. Cells in exponential growth phase were plated at 5×10^4 cells per well in 24-well plate. Then, cells were exposed to various concentrations (5, 10, 20, 50 and 100 μM) of HCA, for 24 hours and were subjected to MTT assay. MTT solution (0.5 mg/ml) was added to each well and incubated for 4 hours at 37 ^{o}C. MTT was reduced to insoluble formazan crystals by mitochondrial succinate dehydrogenase. The formazan crystals thus formed were dissolved in DMSO and the absorbance was read after 45 minutes in a microplate reader (Biotek Synergy 4, US) at 570 nm and percentage of viable cells were calculated.

2.4 Determination of intracellular ROS generation

Intracellular ROS generation was assessed using H2-DCFDA, as described previously (Wang et al, 1999). Cells were washed twice in Kreb's Ringer buffer (KRB) and incubated in prewarmed KRB containing 5 μM DCFDA at 37°C. After 20 minutes, the cells were washed twice with KRB, and fluorescence was immediately measured in a plate reader, and the images were captured using spinning disk fluorescent microscope (BD Pathway, BD Biosciences, USA). The fluorescence intensity was reflected as intracellular ROS level.

2.5 Estimation of glutathione level

GSH activity was assayed spectrophotometrically according to manufacturer's instruction (Cayman, USA). Sulfhydryl group of GSH reacts with DTNB and produces a yellow coloured 5-thio-2-nitrobenzoic acid (TNB). The mixed disulfide that is concomitantly produced during this reaction is reduced by glutathione reductase to recycle the GSH and produce more TNB. The rate of TNB production is directly proportional to this recycling reaction which in turn is directly proportional to the concentration of GSH in the sample. The absorbance of TNB was noted at 407 nm. For assay, the cells after treatments were collected and centrifuged (2,000×g) for 10 minutes at 4 °C. The cell pellets were homogenised in 2 ml of cold buffer and was centrifuged at 10,000×g for 15 minutes at 4 °C. The supernatant was deproteinized. 50 μl of standard and sample were added to the designated wells and covered with the plate cover. 150 μl of the assay cocktail mixture containing PBS, reconstituted cofactor mixture, reconstituted enzyme mixture, water and reconstituted DTNB was added to

each well containing sample and standard and incubated in dark on a shaker. The absorbance was measured at 407 nm at 5 minute intervals for 30 minutes.

2.6 Preparation of cell lysate for antioxidant enzymes

The cells were washed in ice cold PBS and harvested in PBS. The harvested cells were homogenised in 20 mM Tris/ HCl buffer (pH 7.5) containing 0.2% triton-X 100 and 0.5 mM PMSF and sonicated for 30 seconds in ice. Cell lysate was centrifuged at 3000 rpm for 15 minutes at 4^{o}C. Supernatant was collected, aliquoted for storage

2.7 Estimation of glutathione reductase activity

The assay system contained 0.1 M phosphate buffer, 15 mM EDTA, 65.3 mM oxidized glutathione, and 0.1 ml of sample, and the volume was made up to 2 ml using distilled water. The tubes were incubated for 3 minutes and 0.1 ml of 9.6 mM NADPH was added. The absorbance was read at 340 nm in a spectrophotometer (Tecan, Switzerland). Controls were set up that contained water instead of oxidized glutathione. The enzyme activity was expressed as mmoles of NADPH oxidized/mg protein (David and Richard, 1983).

2.8 Estimation of glutathione peroxidase (GPx) activity

Glutathione peroxidase activity was quantified as follows: to 0.2 ml of the Tris buffer (0.4 M), 0.2 ml of EDTA (0.4 mM), 0.1 ml of sodium azide (10 mM), and 0.5 ml of cell lysate were added and mixed, to this, 0.2 ml of GSH was added, followed by H_2O_2. The reaction was stopped after 10 minutes by adding 0.5 ml of 10% TCA. The obtained product was centrifuged and the supernatant was read at 412 nm (Gunzler et al, 1974).

2.9 Estimation of total antioxidant level

Total antioxidant activity of the samples was assayed as per Cayman kit protocol. This assay was based on the ability of antioxidants in the sample to inhibit the oxidation of ABTS* (2, 2'- azino-di-(3-ethylbenzthiazoline sulphonate)) to reduced ABTS**$^{+}$ by metmyoglobin. The amount of ABTS**$^{+}$ produced was monitored by measuring the absorbance at 405 nm. For performing the assay, treated cells were collected by centrifugation (2000×g) for 10 minutes at 4°C. The pellets were sonicated and centrifuged at 10,000×g for 15 minutes at 4 °C. 10 µl of the sample was added into plate wells. 10 µl of metmyoglobin and 150 µl of chromogen were added and the reaction was initiated by adding

H_2O_2. The plate was incubated for 5 minutes at room temperature and then absorbance was read at 405 nm.

2.10 Estimation of catalase activity

Catalase activity was assayed according to the method of Cohen et al. (Cohen et al, 1970) and expressed as µM of H_2O_2 decomposed per minute at 25 °C. The protein concentration was measured using BCA kit from Pierce. The sample was added into a 3 ml of reaction mixture containing 50 mM potassium phosphate and 0.036% (w/w) H_2O_2. It was mixed well immediately by inversion. The decrease in absorbance for ~180 seconds was recorded. The disappearance of H_2O_2 activity was spectrophotometrically assayed at 240 nm.

2.11 Estimation of total SOD, Mn- SOD, Cu-Zn SOD activity

SOD was assayed by the method of Kakkar et al (Kakkar et al, 1984). The assay mixture contained 1.2 ml of sodium pyrophosphate buffer (pH 8.3, 0.52 M), 0.1 ml of 186 µM PMS, 0.3 ml of 300 µM NBT, and 0.2 ml of 780 µM NADH and finally made up into a volume of 3 ml with addition of distilled water. The reaction was started by the addition of NADH. After incubation at 30 °C for 90 seconds the reaction was stopped by the addition of glacial acetic acid. The reaction mixture was stirred vigorously and shaken with 4 ml of n-butanol. The mixture was allowed to stand for 10 minutes and then centrifuged and the butanol layer was removed. The colour intensity of the chromogen NBT diformazan in butanol was measured at 560 nm using a multimode plate reader. Cu-Zn SODs (Hodgson and Fridovich, 1975) were inhibited by adding 5 mM H_2O_2 to quantify Mn SOD activity. The difference between the total activity and Mn SOD activity gave CuZn SOD activity (Nandi and Chatterjee, 1988).

2.12 Estimation of protein carbonyl content

The protein carbonyl content in cell lysate was estimated using assay kit from Cayman Chemical Company as per the manufacturer's instructions. The kit utilizes the reaction between 2,4-dinitrophenylhydrazine (DNPH) and protein carbonyls in the cell lysate. DNPH reacts with protein carbonyls, to form a schiff base producing the corresponding hydrazone, which can be analyzed spectrophotometrically. 200 µl of cell lysate was mixed with 800 µl of DNPH, mixed and kept at room temperature in dark for 1 hour, vortexing the tube every 15 minutes. Then, 1 ml of 20% TCA was added to each tube vortexed and incubated in ice for 5 minutes. The tubes were centrifuged at 10,000 x g for 10 minutes at

4^0C, the supernatant was discarded and the pellet was washed two times in 1 ml of 1:1 mixture of ethanol/ethyl acetate mixture. The tubes were centrifuged at 10,000 x g for 10 minutes at 4^0 C. After final wash, the pellet was dissolved in 500 µl of guanidine hydrochloride by vortexing and the supernatant was read at 385 nm.

2.13 Estimation of lipid peroxidation

The estimation of thiobarbituric acid reactive substances (TBARS) method was used to determine lipid peroxidation products as described previously (Choi et al, 2007). After treatments, cells were washed twice with PBS and lysed in SDS solution. To the 200 µl of cell lysates, 50 µl of BHT were added to prevent sporadic lipid peroxidation during heating. 1.5 ml of 0.5M HCl, 1.5 ml of 20 mM TBA solution and 250 µl of distilled water were added. The reaction mixture was mixed well and heated for 30 minutes in a boiling water bath. After cooling for 20 minutes, 2 ml of n-butanol was added. The mixture was mixed vigorously and centrifuged at 3000 rpm for 15 minutes. The fluorescence of the organic layer was measured at excitation 515 nm and emission 555 nm and the TBARS were calculated using 1, 1, 3, 3-tetramethoxypropane as standard.

2.14 Nrf2 transcription factor translocation assay

Nrf2 transcription factor assay and nuclear extraction was done using Nrf2 assay kit and nuclear extraction kit from Cayman. Nrf2 contained in nuclear extract and cytosolic fraction samples were bound specifically to the double stranded DNA (dsDNA) sequence containing the Nrf2 response element immobilized in 96 well plate. Specific Nrf2 antibody and a secondary antibody conjugated to HRP were used for the detection of protein content. The absorbance was read at 450 nm.

2.15 Indirect immunofluorescence

3T3-L1 cells were seeded in clear bottom black well plates and treated as described earlier. Cells were washed twice with PBS, and then fixed and permeabilized with 4% formaldehyde and 0.05% triton X-100 in PBS for 10 minutes. After washing with PBS, cells were blocked with 1% bovine serum albumin and incubated with anti-CHOP or anti-GRP78 (Bip) antibodies as primary antibody for 1 hour. Following incubation, cells were washed three times with PBS, and then incubated for an additional hour with secondary antibody (1:200) conjugated with FITC. Cells were washed three times with PBS and imaged using spinning disc microscope (Irie et al, 2000).

2.16 Estimation of heme oxygenase-1(HO-1) activity

The HO-1 activity assay was carried out according to the method reported by Foresti et al. with slight modifications (Foresti et al, 1997). Briefly, cells were washed and gently scraped in cold PBS. The cell pellet obtained was homogenised and centrifuged. The supernatant was added to a reaction mixture containing biliverdin reductase (0.2 U), 100 mM potassium phosphate buffer (pH 7.4), containing 2 mM $MgCl_2$, 10 µM hemin, 2 mM glucose-6-phosphate, 0.2 unit of glucose-6-phosphate dehydrogenase, and 0.8 mM NADPH. The reaction mixture was incubated in the dark at 37°C for 1 hour and terminated by the addition of 1 ml of chloroform. After vigorous vortexing and centrifugation, the extracted bilirubin in the chloroform layer was measured by the difference in absorbance between 464 and 530 nm (ϵ = 40 mM^{-1} cm^{-1}).

2.17 Detection of mitochondrial superoxide generation

Mitochondrial superoxide production in the cells was determined using fluorescent dye, mitoSOX™. This dye selectively detects $O_2^{\bullet -}$ in the mitochondria of live cells. The cells were seeded in 96-well black clear bottom plates at a density of 5×10^3 cells per well. The cells were incubated with 5 mM mitoSOX™ in HBSS. After incubation for 20 minutes, the cells were imaged by exciting the dye at 514 nm as described earlier (Mukhopadhyay et al, 2007).

2.18 Determination of aconitase activity

Activity of aconitase was assayed in the cell lysate using kits from Cayman chemicals. This assay utilizes the coupled enzymatic reactions of citrate to isocitrate by aconitase and isocitrate to α-ketoglutarate by isocitrate dehydrogenase. The assay is based on the measurement of formation of NADPH from $NADP^+$. NADPH reacts with the fluorescent substrate to yield a highly fluorescent product. The fluorescent product was sensed with an excitation wavelength of 535 nm and an emission wavelength of 590 nm. The rate of NADPH was proportional to aconitase activity. 10 µl of 1X assay buffer, 50 µl of $NADP^+$ reagent, 50 µl of isocitric dehydrogenase, 10 µl of reconstituted enzyme mixture and 10 µl of reconstituted fluorometric detector were added to 50 µl of sample. The reaction was initiated by adding 50 µl of diluted substrate solution and the fluorescence was read once every minute for 30 minutes at 37 °C.

2.19 Determination of mitochondrial mass

Relative mitochondrial mass was assessed using MitoTracker Deep Red FM (Molecular Probes, Invitrogen). MitoTracker is a fluorescent dye that enters into the mitochondrial matrix independent of the membrane potential and forms covalent bonds with free thiol groups of cysteine residues of mitochondrial proteins. Fluorescence intensity was related to mitochondrial number. MitoTracker (5 µM) was added to each well and incubated for 30 minutes, after which cells were rinsed using PBS and imaged using confocal microscope. Fluorescence intensity was also measured in a multiplate reader using excitation and emission wavelengths of 644 nm and 665 nm, respectively (Sharon et al, 2007).

2.20 Detection of alteration in mitochondrial membrane potential

The cells were seeded in 96-well black clear bottom plate in 200 µl of culture medium and subjected to treatments. The experiment was done as per the manufacturer's protocol (JC-1 mitochondria staining kit, Sigma). The cells were stained with JC-1 stain for 20 minutes at 37 °C and washed with growth medium. The shift of fluorescence was visualized under spinning disk microscope and fluorescence intensity was measured in multiwell plate reader. In normal cells, the JC-1 dye concentrates in the mitochondrial matrix, where it forms red fluorescent aggregates because of the electrochemical potential gradient. Dissipation of $\Delta\Psi M$ prevents the accumulation of JC-1 in the mitochondria, leading to a shift from red (J-aggregates) to green fluorescence (JC-1 monomers) (Javadov et al, 2006). For JC-1 monomers, the fluorimeter was set at 490 nm excitation and 530 nm emission wavelengths and for J- aggregates, the fluorimeter was set at 525 nm excitation and 590 nm emission wavelengths. Valinomycin (1 µg/ml) was used as positive control for the measurement of dissipation of mitochondrial membrane potential.

2.21 Determination of mitochondrial permeability transition pore integrity

Integrity of MPTP was detected by treating the cells with 0.25 µM calcein-AM in the presence of 8 mM cobalt chloride for 30 minutes to quench cytosolic and nuclear calcein loading. The calcein fluorescence is compartmentalized within mitochondria until MPTP opening permits the entry of cobalt into mitochondria, which results in the quenching of calcein fluorescence in the mitochondrial matrix (Petronilli et al, 1999). Cells were imaged using spinning disc facility at 488 nm excitation and 525 nm emission.

2.22 Detection of intracellular calcium overload

Calcium overload was detected by staining the cells with Fura-2AM (Robinson et al, 2004). The cells were seeded in 96-well black clear bottom plate in 200 µl of culture medium and subjected to experimental treatments. After treatments, cells were stained with Fura-2AM (5 µM) and incubated at 37°C for 30 minutes. After incubation, cells were washed three times with HBSS and the images were visualized using BD PathwayTM Bioimager System (BD Biosciences). The dye was excited at 340/380 nm and the emission range was 510 nm.

2.23 Quantification of intracellular calcium

The total calcium content in the cell lysate was quantified as per the Cayman kit protocol. Cells were seeded at 5 $X10^6$ cells per well. The assay utilizes an optimized o-cresolphthalein-calcium reaction in which a vivid purple complex is formed in the presence of calcium that absorbs between 560 nm and 590 nm. The intensity of the colour is directly proportional to the concentration of calcium in the sample. In brief, supernatant from cell lysate was prepared by homogenization and centrifugation in ice cold buffer (10000xg for 15 minutes at 4^oC). 200 µl of working detection reagent was added to 10 µl of sample, gently shaken and incubated for 5 minutes. The resulting color was read spectrophotometrically.

2.24 Determination of oxygen consumption rate

Oxygen consumption rate was assayed using Cayman's cell based oxygen consumption rate assay kit. Antimycin A was used as standard inhibitor. Cayman's oxygen consumption rate assay kit utilizes a phosphorescent oxygen probe to measure oxygen consumption rate. The phosphorescence of MitoXpress-Xtra, the phosphorescent oxygen probe, is quenched by oxygen and the phosphorescent signal is inversely proportional to the amount of oxygen present. After respective treatments, the culture medium was removed and replaced with fresh medium. 10 µl MitoXpress® -Xtra solution was added to all the wells except blank wells and then 100 µl of HS mineral oil over each well. The fluorescence was read at excitation, 380 nm and emission, 650 nm kinetically for 150 minutes.

2.25 Estimation of ATP content

ATP in cell lysates was quantified using ATP determination kit (Molecular Probes®, Life Technologies, USA). It is a bioluminescence assay for quantitative determination of ATP with recombinant firefly luciferase and its substrate D-luciferin. The assay is based on requirement of ATP for luciferase to produce light (emission maximum 560 nm at pH 7.8).

The reaction mixture consisting of 8.9 ml of distilled water, 0.5 ml of 20X reaction buffer, 0.1 ml of 0.1 M DTT, 0.5 ml of 10 mM D-luciferin, 2.5 µl of firefly luciferase (5 mg/ml stock solution) and 100 µl of sample was mixed gently and the luminescence was read at 560 nm.

2.26 Detection of activities of mitochondrial enzyme complexes

Complex I-mediated electron transfer (NADH dehydrogenase) was studied using NADH as the substrate and menadione as electron acceptor. The reaction mixture containing 200 mM menadione and 150 mM NADH was prepared in phosphate buffer (0.1 M, pH 8.0). 100 µg mitochondria was added, mixed immediately and observed quickly for change in the absorbance (ΔOD) at 340 nm for 8 minutes (Paul et al, 2008).

Complex II mediated activity (succinate dehydrogenase) was measured spectrophotometrically at 600 nm using DCPIP as an artificial electron acceptor and succinate as substrate. The extent of decrease of absorbance (ΔOD) was considered as the measure of the electron transfer activity of complex II (Paul et al, 2008). The reaction mixture was prepared in 0.1 M phosphate buffer (pH 7.4) containing 10 mM EDTA, 50 mM DCPIP, 20 mM succinate and mitochondria (50 µg). The change in absorbance was read immediately for 8 minutes at 30 °C.

Complex III (decylubiquinol cytochrome c oxidoreductase) activity was assessed in assay buffer containing 50 mM Tris-HCl, 4 mM NaN_3, 0.1 mg/ml of BSA, and 0.05% (vol/vol) Tween 20. The reaction was started by addition of 0.25 mM decylubiquinol and 0.0625 mM cytochrome *c*. Reduction of cytochrome c with decylubiquinol was determined at 550 nm. Antimycin was used as a negative control (Luo et al, 2008).

Complex IV activity of mitochondria was assayed using cytochrome oxidase kits from Sigma Aldrich chemicals (USA) as per manufacturer's instructions. Briefly, 950 µl of 1X assay buffer was added to a cuvette and then 10 µg of mitochondrial suspension was added and brought the reaction volume to 1.05 ml with 1X enzyme dilution buffer. The reaction was initiated by the addition of 50 µl of ferrocytochrome c substrate solution. Absorbance was read at 550 nm per minute. The activity of the sample was expressed as U/ml.

2.27 Determination of mitochondrial biogenesis

Mitochondrial biogenesis was analysed with MitoBiogenesis™ In-Cell ELISA Kit (ABCAM, MA, USA) according to manufacturer's protocol. In brief, the cells after treatment were fixed with 4% paraformaldehyde. Cells were then washed with PBS and followed by

the addition of 100 µl of freshly prepared 0.5% acetic acid for 5 minutes to block endogenous alkaline phosphatase activity. Cells were washed again with PBS and permeabilized with 0.1% triton X-100 for 30 minutes and followed by the addition of 200 µl of 1X Blocking Solution for 2 hours. These cells were then incubated with primary antibodies specifically against mtDNA encoded COX-I (subunit I of Complex IV, cytochrome c oxidase-1), and nuclear-DNA encoded SDH-A (a subunit of complex II, succinate dehydrogenase) proteins overnight at 4ºC. Cells were washed with a washing buffer and incubated with alkaline phosphatase (AP) for SDH-A and HRP for COX-I secondary antibodies for 1 hour. After thorough washing, AP Substrate was added and colour development was measured at 405 nm for SDH-A. Then the wells were emptied and added HRP substrate. The colour developed was measured at 600 nm for COX-I. COX-I signal and SDH-A signal were then plotted independently for analysing the data.

2.28 Estimation of adiponectin secretion

Adiponectin was estimated in the conditioned medium using a mouse adiponectin enzyme immunoassay (EIA) kit (SPI Bio, Bertin Pharma, France). Conditioned media was collected and added to wells coated with a monoclonal antibody specific of mouse adiponectin. After 1 hour incubation, the wells were washed and polyclonal anti-mouse adiponectin antibody conjugated with biotin was added and incubated for 1 hour. After washing, streptavidin-horseradish peroxidase tracer was added and incubated for 30 minutes. The concentration of the adiponectin was then determined by measuring the enzymatic activity of the HRP using the hydrogen peroxide/TMB solution. The absorbance was measured at a wavelength of 450 nm using a multimode reader (Biotek Synergy 4, USA).

2.29 Estimation of leptin secretion

The amount of leptin in the conditioned media was quantified using leptin ELISA kit (Merck Millipore, USA). This assay is a sandwich ELISA based method. Leptin in the conditioned media was bound by a pre-titered antiserum and the resulting complexes were immobilized in the wells of the microtiter plate. After washing, purified biotinylated detection antibody was added to the immobilized leptin. HRP enzyme solution was added to the immobilized biotinylated antibodies. The concentration of leptin was determined by measuring the enzymatic activity of the HRP using the H_2O_2/TMB solution. Absorbance was read at 450 nm and 590 nm within 5 minutess.

2.30 Quantification of inflammatory cytokines

Inflammatory cytokines TNF-α, IL-6, IL-2, IL-1β, IL-10, MCP-1 and IFN-γ in culture media were quantified using ELISA kits from BD Biosciences. For performing these assays, 100 µl of diluted capture antibody was added to the wells and incubated overnight at 4 °C. After incubation the supernatant was aspirated and the wells were washed 3 times with 300 µl of wash buffer. 200 µl of blocking buffer were added to all wells and were incubated for 1 hour at room temperature. After incubation the wells were washed 3 times. 100 µl of samples were added to the wells and incubated for 2 hours at room temperature and the washing step was repeated. 100 µl of working detector were added to all the wells and incubated for 1 hour at room temperature and repeated the washing step with wash buffer. 100 µl of substrate solution was added and incubated for 30 minutes in dark. 50 µl of stop solution was added and the absorbance was read at 450 nm. This procedure was common for MCP-1, IL-6, IL-2, IL-10, IL-1β and IFN-γ. For TNF-α ELISA, the wells were washed with 300 µl of wash buffer and after that 50 µl of samples were added to the wells. The plates were incubated for 2 hours at room temperature with shaking at 200 rpm. The contents of the plate were discarded and the plates were washed with 1X wash buffer. 100 µl of TNF-α detection antibody was added to the wells and incubated the plates for 1 hour at room temperature. Again the plates were washed with wash buffer. After washing 100 µl of avidin-HRP A solution was added and incubated for 30 minutes at room temperature. The contents of the plate were discarded and again washing step was repeated. 100 µl of substrate solutions were added to the wells and incubated in dark for 15 minutes. 100 µl of stop solution was added and the absorbance was read at 450 nm.

2.31 Detection of NF-kB (p65) translocation

NF-kB (p65) transcription factor assay is a non-radioactive sensitive method for detecting specific transcription factor DNA binding activity in nuclear extracts. NF-kB contained in the nuclear extract, binds specifically to the NF-kB response element. After respective treatments the cells were collected by centrifugation and using Cayman's nuclear extraction kit, nuclear proteins were isolated. NF-kB (p65) level in the cytosolic and nuclear extract were detected. 10 µl of samples containing NF-kB were added to the wells and incubated overnight at 4 °C. All the wells were washed with 200 µl 1X wash buffer. 100 µl of NF-kB (p65) primary antibody was added to all the wells except blank and incubated for 1 hour at room temperature. The washing step was repeated with 1X wash buffer and to all the

wells except blank 100 µl of diluted goat anti-rabbit secondary antibody was added and incubated for 1 hour at room temperature. After incubation it was again washed with 1X wash buffer. 100 µl of developing solution was added and incubated for 30 minutes with gentle agitation. 100 µl of stop solution was added to all the wells and the absorbance was read at 450 nm.

2.32 Estimation of nitrite levels

After treatment, 100µl of Griess reagent was immediately added per 100µl of sample volume. The sample/reagent mixture and blank was allowed to develop in the dark for 30 minutes. The absorbance was measured at 548 nm using multiwell plate spectrophotometer.

2.33 Estimation of glucose uptake

Fully differentiated 3T3-L1 adipocytes were treated as earlier. Cells were stimulated with 1 µg/ml of insulin for 10 minutes. Culture medium was removed from each well and replaced with fresh culture medium containing 10 µM fluorescent 2-NBDG (Molecular Probes-Invitrogen, USA), and incubated for 30 minutes. The cells were then washed twice with cold PBS and the fluorescence intensity of 2-NBDG in the cells was recorded using a FACS Aria II flow cytometer (BD Biosciences, USA)

2.34 Estimation of lactate

The concentration of lactate in the conditioned media was quantified using lactate assay kit (Sigma Aldrich, USA) according to the manufacturer's protocol. In this assay, lactate concentration is determined by an enzymatic reaction, which results in a colored product, proportional to the amount of lactate present. In this assay, lactate dehydrogenase catalyzes the oxidation of lactate to pyruvate, along with the concomitant reduction of NAD^+ to NADH. NADH reacts with the fluorescent substrate to yield a highly fluorescent product. The fluorescent product was then analysed with an excitation wavelength of 530-540 nm and an emission wavelength of 585-595 nm.

2.35 Estimation of triglyceride content

Triglyceride content in the samples was quantified using Cayman's triglyceride assay kit. The reaction was initiated by adding 150 µl of the enzyme buffer solution to the sample and shaken. The plate was incubated for 15 minutes and absorbance was read at 530 -550 nm. The kit utilizes the action of the enzyme, lipases, which cause the enzymatic hydrolysis of triglyceride to glycerol and fatty acid. The glycerol formed is phosphorylated by glycerol

kinase to form glycerol-3-phosphate, which is then oxidized to dihydroxy acetone phosphate and hydrogen peroxide by glycerol phosphate oxidase. The H_2O_2 formed is coupled with 4-aminoantipyrine and N-ethyl- N-(3-sulfopropyl)-m-anisidine (ESPA), in a redox coupled reaction by peroxidase, producing a brilliant purple colour, whose intensity is proportional to the amount of triglyceride in the sample. The intensity of the colour formed was measured at 540 nm on a multimode reader (Biotek Synergy 4, USA).

2.36 Determination of lipid droplet content

3T3-L1 cells were seeded in clear bottom black well plates and treated as described earlier. The supernatant was removed and washed with 200 µl of PBS. 0.5 ml of Nile red was added and incubated for 10 minutes at room temperature. Cells were imaged using spinning disc microscope.

2.37 Estimation of glycerol release

Glycerol release was quantified using glycerol cell based assay kit from Cayman. 100 µl of free glycerol assay reagent was added to 25 µl of cell culture supernatant and incubated for 15 minutes at room temperature. The assay employs a coupled enzymatic reaction system that yields a brilliant purple product with an absorbance of maximum at 540 nm

2.38 Quantitative real time-PCR

Cellular mRNA expression of the genes was quantified using RT-PCR. Total RNA was isolated from cells using TRIzol (Biochem Life Science, India). Subsequently, superscript III 1st strand synthesis system (Life technologies, Bangalore, India) kit was utilised for the reverse transcription (RT) of the samples. The samples were incubated in a Bio-rad CFX96™ Real-Time system at 25 °C for 10 minutes, 50 °C for 50 minutes, 85 °C for 5 minutes and then at 4 °C for 5 minutes. The specific PCR primers were synthesized based on nucleotides. β Actin mRNA was used as an internal reference. The amplification included the following reaction stages: stage I (initial denaturation), which involved an incubation at 95 °C for 10 minutes, stage II (39 cycles of PCR amplification), which involved 39 cycles of incubation at 95 °C for 15 s, 30 s annealing at appropriate primer temperature, and 72 °C for 10 s, and stage III (melting curve analysis), which involved an incubation at 72 °C for 5 minutes followed by an incubation at 16 °C for 10 minutes. The primers for various genes were designed using the Primer 3, a free online tool to design and analyze primers for PCR and real time PCR experiments and synthesised by Hysel India Pvt Ltd. In particular, the following specific primers were synthesized (table 2.1). Based on the amplification results,

the comparative CT method (ΔΔCT) was used to calculate the relative multiple of the starting copy number that existed in the template from each experimental group. The normalized gene expression was calculated.

Fold change = 2^ (-Δ (ΔCT))

where ΔCT = CT(target) - CT (β Actin) and ΔΔCT = ΔCT(stimulated- ΔCT (control) CT(threshold cycle) is the intersection between an amplification curve and a threshold line.

Grp78	Forward	5'-CCACTTCATCTTACCATTTA-3'
	Reverse	5'-ATCTGCATCTGAGTTTAATC-3'
Chop	Forward	5'-GTCCAGCTGGGAGCTGGAAG-3'
	Reverse	3'-GTCCAGCTGGGAGCTGGAAG-3'
Tfam	Forward	5'-GGAATGTGGAGCGTCCTAAAA-3'
	Reverse	5'-TGCTGGAAAAACACTTCGGAATA-3'
Pgc1a	Forward	5'-CGGAAATCATATCCAACCAG-3'
	Reverse	5'-TGAGGACCGCTAGCAAGTTTG-3'
Nrf1	Forward	5'-TGGTCCAGAGAGTGCTTGTG-3'
	Reverse	5'-TTCCTGGGAAGGGAGAAGAT-3'
Mt dna	Forward	5'-CCACTTCATCTTACCATTTA-3'
	Reverse	5'-ATCTGCATCTGAGTTTAATC-3'
Cyt B	Forward	5'-TTTTATCTGCATCTGAGTTTAATCCTG-3'
	Reverse	5'-CCACTTCATCTTACCATTTATTATCGC-3'
Adiponectin	Forward	5'-GTTGCAAGCTCTCCTGTTCC-3'
	Reverse	5'-CTTGCCAGTGCTGTTGTCAT-3'
Resistin	Forward	5'-TCATTTCCCCTCCTTTTCCTTT-3'
	Reverse	5'-TGGGACACAGTGGCATGCT-3'
Tlr4	Forward	5'-CGCCCTTTAAGCTGTGTCTC-3'
	Reverse	5'-CAAAGAGCCTGAAGTGGGAG-3'
Glut-1	Forward	5'-AGGCTTGCTTGTAGAGTGAC-3'
	Reverse	5'- TAAGGATGCCAACGACGATTC-3'
Glut-4	Forward	5'-CAACGTGGCTGGGTAGGC-3'
	Reverse	5'-ACACATCAGCCCAGCCGGT-3'
Ppar-γ2	Forward	5'-GCTGTTATGGGTGAAACTCTG-3'

	Reverse	5’-ATAAGGTGGAGATGCAGGTTC-3’
β Actin	Forward	5’-AGTACCCCATTGAACGC-3’
	Reverse	5’- TGTCAGCAATGCCTGGGTAC-3’
Xbp1	Forward	5’-ACACGCTTGGGAATGGACAC-3’
	Reverse	5’-CCATGGGAAGATGTTCTGGG-3’
Pdi	Forward	5’-CAAGATCAAGCCCCACCTGAT-3’
	Reverse	5’-AGTTCGCCCCAACCAGTACTT-3’
IRS-1	Forward	5’-CTTCTGTCAGGTGTCCATCC-3’
	Reverse	5’-CTCTGCAGCAATGCCTGTTC-3’
Irs2	Forward	5’-GGCCTCTGTGGAAAATGTCTC-3’
	Reverse	5’-CTGTGGCTTCCTTCAAGTGAT-3’

Table 2.1 List of primers

2.39 Western blotting

Cells were seeded in a T25 flask containing 5 ml of DMEM medium and treatments were carried out. At the end of the treatments, the cells were harvested and lysed with ice-cold cell lysis solution (RIPA buffer containing a protease inhibitor cocktail) and the homogenate was centrifuged at 10,000×g for 15 minutes at 4 °C. Total protein in the supernatant was quantified using a BCA protein assay kit (Pierce, Rockford, IL USA). Total protein (40 μg) from each sample was separated by 10% SDS-PAGE at 55 V. The protein in the gel was transferred into polyvinylidene difluoride (PVDF) membrane using Trans-Blot Turbo™ (Bio-Rad). The membrane was blocked with BSA in TBST (Tris buffered saline-tween 20) for 1 hour at room temperature, and then incubated with the specific primary antibodies with gentle agitation at 4 °C overnight. The incubation was followed by 3 times wash with TBST for 10 minutes in a shaker, followed by HRP-conjugated secondary antibodies (1:1000) in 0.25% BSA in TBST for 60 minutes at room temperature with continuous shaking. After three washes with TBST, the membranes were developed using DAB tablets (Sigma Aldrich, St Louis, MO, USA) and the relative intensity of bands were quantified using Bio-Rad Quantity One version 4.5 software in a Bio-Rad gel doc. The quantity of protein in cell lysate was normalized with the content of β Actin.

Primary antibodies used were:

GRP78, CHOP, PERK, IRE1α, ATF6, p eIF2A, PDI, ERO1α, HO-1, OPA-1, MFN2, DRP-1, FIS-1, Adiponectin, GLUT-1, GLUT4, JNK, pJNK, pIRS-1(SER-307), IRS2, PPARγ, P13K, PTP1B, p AKT

2.40 Statistical data analysis

Results are expressed as means ± standard deviations (n = 6). Data were analyzed using one-way ANOVA and the significance of differences between means was calculated by Duncan's multiple range tests using SPSS for Windows standard version 7.5.1 (SPSS, Inc.). $P \leq 0.05$ was considered significant.

Chapter 3

Induction of ER stress in 3T3-L1 adipocytes and possible protection with HCA

3.1 Introduction

In obese individuals, adipose tissue undergoes several types of stress, like inflammation, hypoxia, oxidative stress, ER stress, metabolic stress etc. This is caused by the excess of nutrients, and mechanical stress from hypertrophy which ensues during obesity (Gregor and Hotamisligil, 2007; Ozcan et al, 2004; Rudich et al, 2007). ER stress in obese adipose tissue may be resulting from the nutrient overload, increased demand for protein synthesis, or local glucose deprivation in the setting of IR and decreased adipose tissue vascularization (Gregor and Hotamisligil, 2007). Unresolved ER stress may be a key factor in the dysregulated adipose tissue function, where insulin sensitivity is diminished and irregular adipokine secretion occurs (Gregor and Hotamisligil, 2007).

Numerous genetic and environmental factors lead to the accumulation of unfolded proteins in the ER lumen, triggering ER stress. Excessive or prolonged ER stress ultimately leads to apoptotic cell death. Cells try to alleviate ER stress, by an innate system known as the UPR (Kaufman, 2002; Ron, 2002; Schröder and Kaufman, 2005). The UPR acts through three major pathways, PERK, IRE1 and ATF6. These proteins transmit signals from the ER to the cytoplasm or nucleus, and activate three pathways: i) suppression of protein translation to avoid the generation of more unfolded proteins (Harding et al, 2000), ii) induction of genes encoding ER molecular chaperones to facilitate protein folding, (Li et al, 2000; Yoshida et al, 1998), and iii) activation of ER-associated degradation to reduce unfolded protein accumulation in the ER (Ng et al, 2000; Travers et al, 2000). When all these strategies fail and the cells are unable to maintain ER homeostasis, the cells are directed to apoptosis (Nakagawa et al, 2000; Urano et al, 2000).

BiP and CHOP are two of the best studied genes transcriptionally induced by ER stress, and robust protocols are available to quantify their mRNA levels (Hiramatsu et al, 2011). BiP is an ER-localized HSP70-class chaperone that participates in protein folding in the ER and bind to misfolded ER proteins for further quality control(Bukau et al, 2006; Chang et al, 2007; Mayer and Bukau et al, 2005). CHOP is a transcription factor that

promotes apoptosis in response to uncontrolled ER stress (Tabas and Ron, 2011; Zinszner, 1998). Upon heterodimerization, CHOP is transported to the nucleus and induces ER stress mediated apoptosis. Elevated *Chop* mRNA levels have been identified in diseases associated with ER stress.

Recent preclinical and clinical studies show that pharmacological modulators of ER stress have therapeutic potential as novel treatments of metabolic disorders, including obesity, fatty liver disease and atherosclerosis (Cao and Kaufman, 2013; Pagliassotti, 2012). The present study attempted to investigate whether HCA inhibited the induction of UPR signaling components in the ER stressor, tunicamycin exposed 3T3-L1 adipocytes. This study examined ER stress markers and HCA cytoprotection from ER stress in lipid-laden adipocytes.

HCA is a derivative of citric acid and is found in plant species such as *Garcinia cambogia, Garcinia indica,* and *Garcinia atroviridis* (Roongpisuthipong et al, 2007). It is commonly marketed as a weight loss supplement either alone or in combination with other supplements (Downs et al, 2005; Roongpisuthipong et al, 2007,) and is reported with multiple health benefits.

3.2 Methods

Cell culture and treatments were same as described in Chapter 2. Experimental groups were

B - Control
T - Tunicamycin treated groups
H1 - Tunicamycin + HCA 5 µM
H2 - Tunicamycin + HCA 10 µM
H3 - Tunicamycin + HCA 20 µM
P - Tunicamycin + PBA 1 mM

Initially experiments were conducted to rule out the cytotoxicity of HCA by incubating cell with various concentrations of HCA. Following experiments were conducted to assess the cytotoxicity and confirm the induction of ER stress through western blot, RT PCR and ROS generation. Detailed procedures of all the experiments are given in Chapter 2

- MTT assay for HCA and tunicamycin
- ROS generation by HCA and tunicamycin using DCFDA

- Immunofluorescence imaging of GRP78 and CHOP
- Western blot analysis of GRP78 and CHOP
- mRNA quantification of *Grp78* and *Chop*

3.3 Results

3.3.1 Cytotoxicity of HCA

Cytotoxic effect of HCA was evaluated using MTT assay. 3T3-L1 adipocytes were treated with different concentrations of HCA for 24 hours. The compound did not cause any toxicity to 3T3-L1 cells up to 100 µM (Figure 3.1).

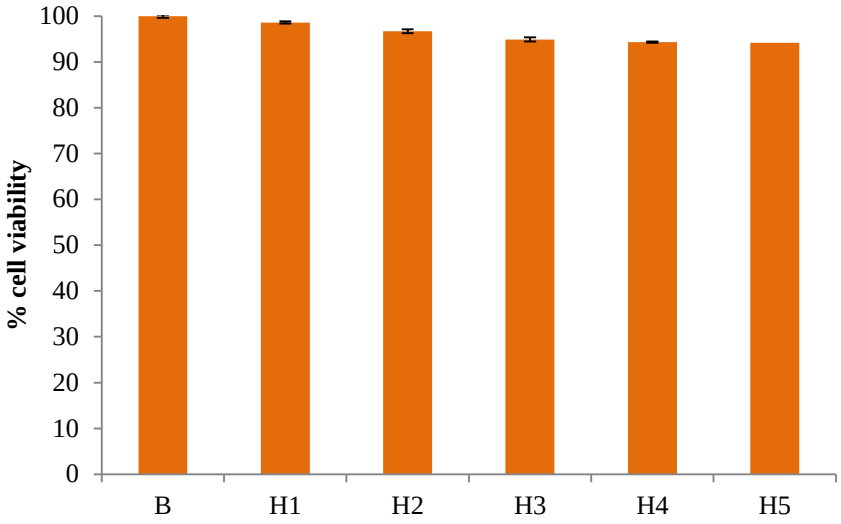

Figure 3.1 MTT assay of 3T3-L1 adipocytes with different concentrations of (-) hydroxycitric acid. (B) control (H1) 5 µM (-) hydroxycitric acid, (H2) 10 µM (-) hydroxycitric acid, (H3) 20 µM (-) hydroxycitric acid, (H4) 50 µM (-) hydroxycitric acid , (H5) 100 µM (-) hydroxycitric acid. Values are means ± SD (n = 6) represented by vertical bars.

3.3.2 Effect of HCA on ROS production

Oxidative stress, if any with HCA was checked to confirm the safety of HCA (5, 10, 20, 50, 100 µM). HCA treatment at concentrations up to 50 µM showed no ROS production at all. But 100 µM of HCA produced significant amount of ROS compared to the control (Figure 3.2).

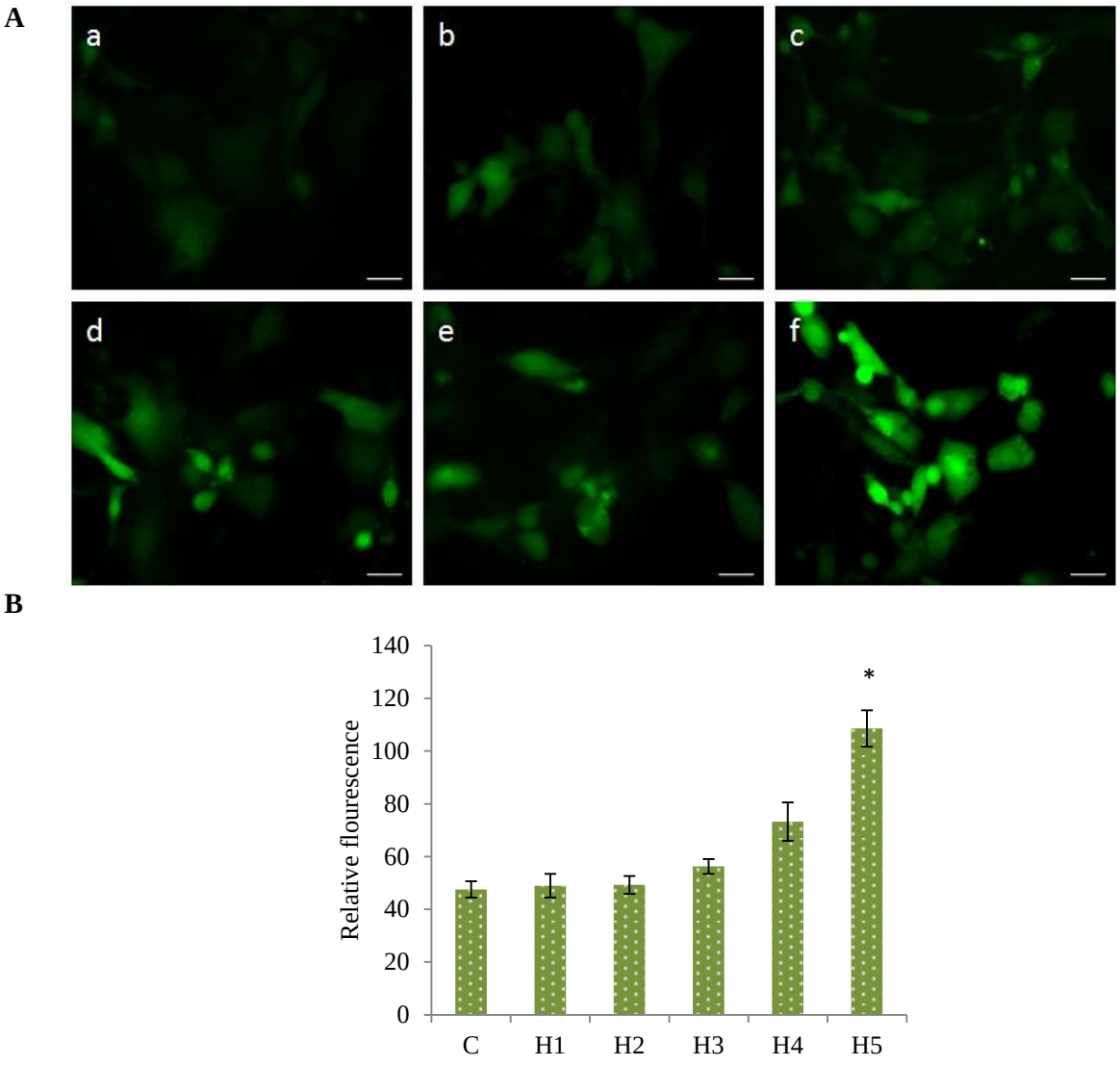

Figure 3.2 Reactive oxygen species production by (-) hydroxycitric acid at various concentrations in 3T3-L1 adipocytes. A. The representative images of reactive oygen species generation in 3T3-L1 cells stained with DCFDA. (a) control (b) 5 µM (-) hydroxycitric acid, (c) 10 µM (-) hydroxycitric acid, (d) 20 µM (-) hydroxycitric acid, (e) 50 µM (-) hydroxycitric acid, (f) 100 µM (-) hydroxycitric acid. Scale bar corresponds to 100 µm. B. ROS production as shown by fluorimetric analysis. (C) control (H1) 5 µM (-) hydroxycitric acid, (H2) 10 µM (-) hydroxycitric acid, (H3) 20 µM (-) hydroxycitric acid, (H4) 50 µM (-) hydroxycitric acid, (H5) 100 µM (-) hydroxycitric acid. Values are means, with standard deviations represented by vertical bars (n = 6).* Mean values are significantly different from the control cells $P \leq 0.05$.

3.3.3 Effect of tunicamycin on ROS production

ROS generation by different concentrations of tunicamycin (1, 2, 3, 4, and 5 µM for 18 hours) was studied using DCFDA. The control cells showed very low fluorescence, while treatment with tunicamycin for 18 hours increased ROS production in the cultured adipocytes in a dose dependent manner (Figure 3.3). Fluorimetric analysis also showed significant increase (3.63, 6.84, 9.50, 11.28, 12.73 fold respectively) in ROS production during tunicamycin treatment. Based on this result 2 µM of tunicamycin was used to induce ER stress in all the experients in the thesis.

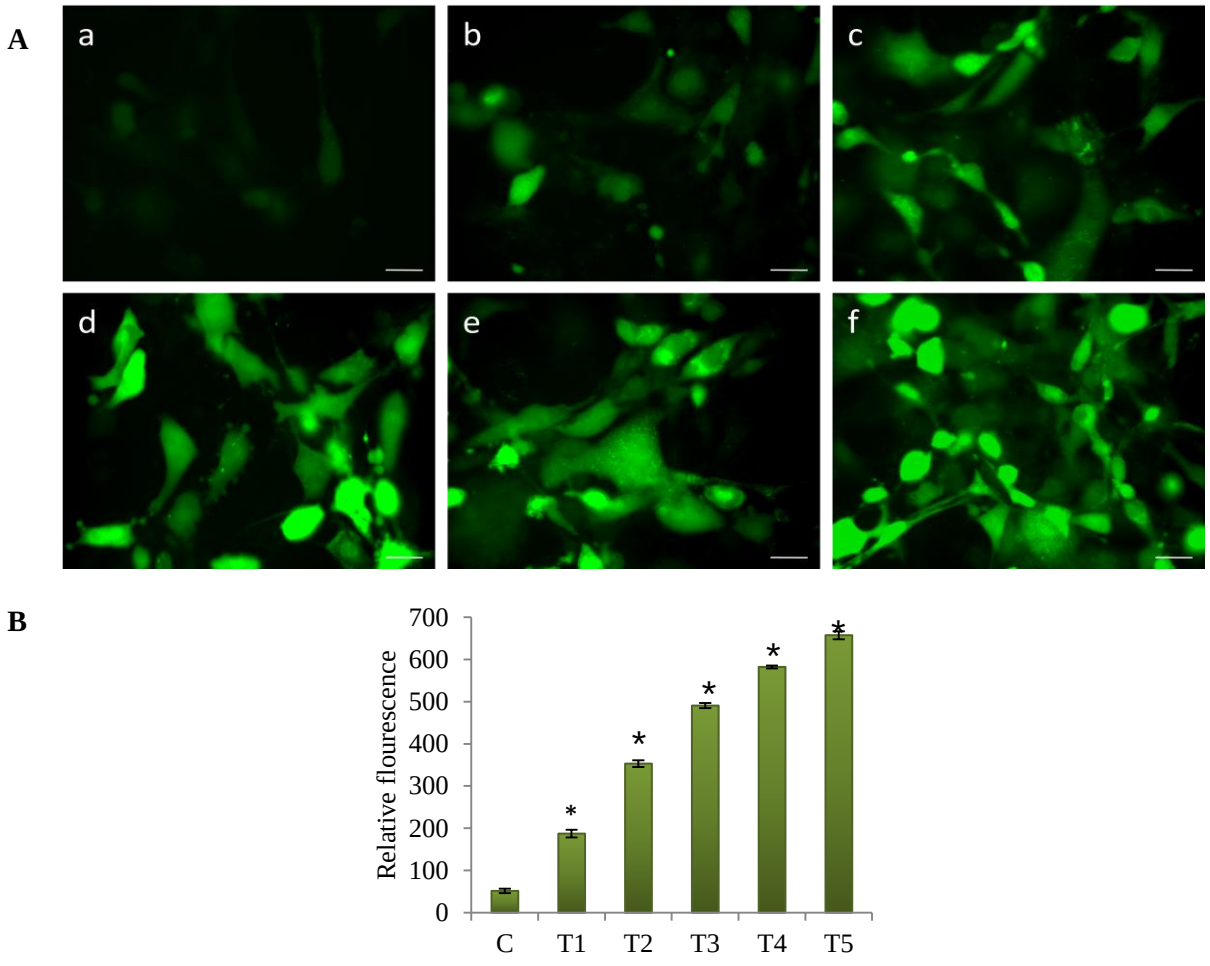

Figure 3.3 Reactive oxygen species production by different concentrations of tunicamycin in 3T3-L1 adipocytes. A. The representative images of ROS induced fluorescence in 3T3-L1 adipocytes treated with different concentrations of tunicamycin for 18 hours, (a) control, (b) 1 µM tunicamycin, (c) 2 µM tunicamycin, (d) 3 µM tunicamycin, (e) 4 µM tunicamycin, (f) 5 µM tunicamycin. Scale bar corresponds to 100 µm. B. ROS production according to fluorometric analysis, (C) control, (T1) 1 µM tunicamycin, (T2) 2 µM tunicamycin, (T3) 3 µM tunicamycin, (T4) 4 µM tunicamycin, (T5) 5 µM tunicamycin. Values expressed as means ± SD (n = 6), represented by vertical bars.* indicates values are significantly different from the control cells and significance accepted at $P \leq 0.05$.

3.3.4 Effect of tunicamycin treatment on the morphology of 3T3-L1 adipocytes

Changes in the morphology of 3T3-L1 adipocytes during treatment with tunicamycin were monitored by imaging with phase contrast microscopy. Mature adipocytes were characterized by the presence of lipid droplets inside the cells. Treatment with tunicamycin at 1, 2 and 3 µM concentrations for 18 hours reduced the lipid content in the cells. 3 µM concentration of tunicamycin induced cell death in adipocytes while at 5 µM, almost all the cells were dead indicating severe toxicity (Figure 3.4).

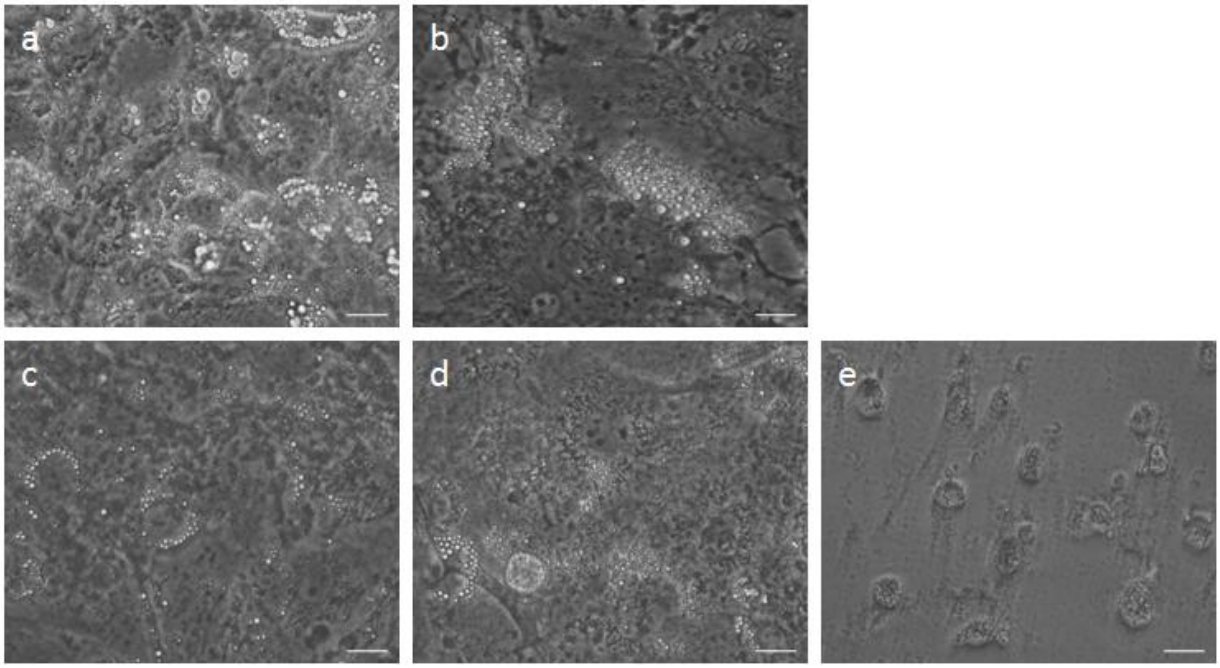

Figure 3.4 Changes in the morphology of 3T3-L1 adipocytes on treatment with tunicamycin at different concentrations. The representative images of 3T3-L1 adipocytes treated with different concentrations of tunicamycin for 18 hours. (a) control, (b) 1 µM tunicamycin, (c) 2 µM tunicamycin, (d) 3 µM tunicamycin, (e) 5 µM tunicamycin. Scale bar corresponds to 100µm.

3.3.5 Cytoprotective effect of HCA in tunicamycin treated cells

The effect of HCA on tunicamycin-induced cell death was also determined. 3T3-L1 adipocytes were treated with 2 µM of tunicamycin for 18 hours along with different concentrations of HCA (5, 10, 20 µM). There was a decrease of 5.22% in cell viability on treatment with tunicamycin alone, but co treatment with HCA reduced the cell death due to tunicamycin significantly (Figure 3.5). PBA (1 mM) also reduced the cell death induced by tunicamycin.

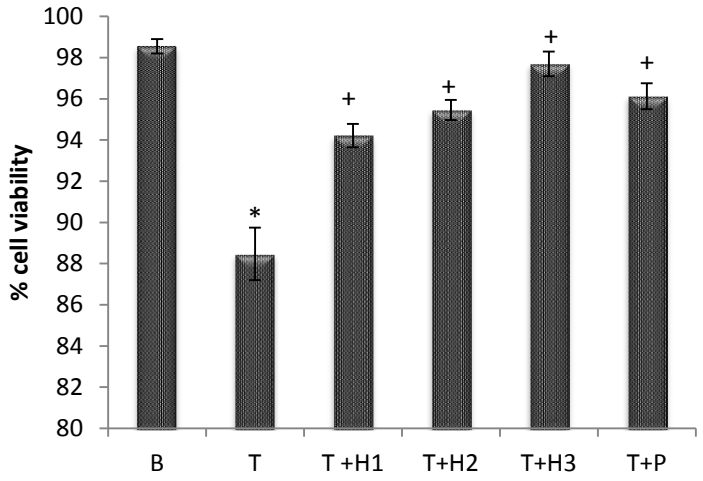

Figure 3.5 MTT assay of 3T3-L1 cells treated with tunicamycin and tunicamycin along with different concentrations of (-) hydroxycitric acid. (B) Control, (T) tunicamycin, (T+H1) tunicamycin + 5 µM (-) hydroxycitric acid, (T+H2) tunicamycin + 10 µM (-) hydroxycitric acid, (T+H3) tunicamycin + 20 µM (-) hydroxycitric acid, (T+P) tunicamycin + 1 mM sodium phenyl butyrate. Values expressed as means with standard deviation (n = 6), represented by vertical bars.* indicates values are significantly different from the control cells and significance accepted at $P \leq 0.05$.

3.3.6 Effect of HCA on expression of GRP78

To determine the activation of ER stress protein response in 3T3-L1 adipocytes on treatment with 2 µM of tunicamycin for 18 hours, we assessed protein levels and mRNA levels of the ER stress response marker, GRP78/BiP in the cells (Figure 3.6). BiP levels were significantly increased (7.1 fold) in the tunicamycin treated group compared with the control group ($P < 0.05$). mRNA expression was also significantly increased (3.37 fold) in tunicamycin treated group. This study also investigated whether HCA was able to inhibit the induction of UPR response and thus alleviate adipocyte ER stress. HCA at concentrations 5, 10, 20 µM and 1 mM PBA suppressed the induction of GRP78 at protein level (1.11, 1.25, 2.95 and 4.55 fold respectively) and mRNA (1.12, 1.15, 1.72 and 2.83 fold respectively) level.

A

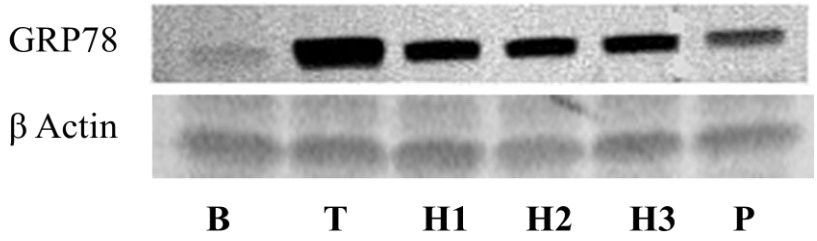

B

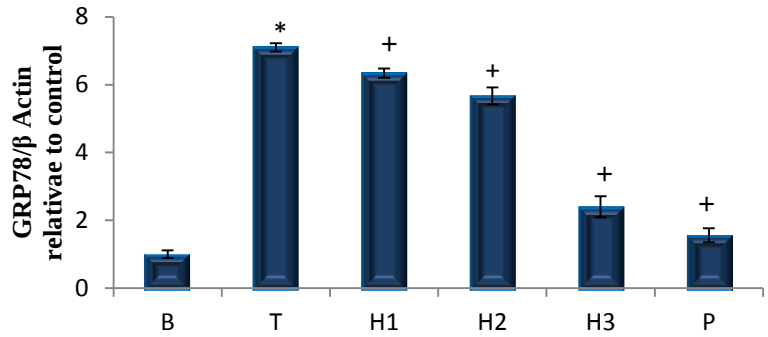

C

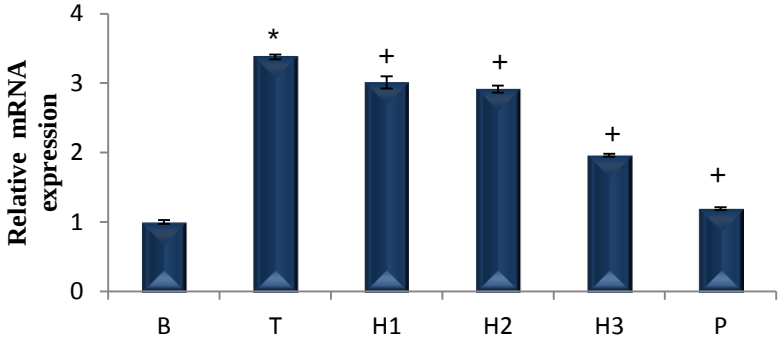

Figure 3.6 Protein and mRNA level expression of GRP78 in 3T3-L1 adipocytes treated with tunicamycin alone and tunicamycin with (-) hydroxycitric acid. A. Representative western blot of GRP78. B. Densitometric quantification of GRP78 protein level normalised to β Actin. C. Relative mRNA expression normalised to β Actin. (B) control, (T) tunicamycin, (H1) tunicamycin + 5 µM (-) hydroxycitric acid, (H2) tunicamycin + 10 µM (-) hydroxycitric acid, (H3) tunicamycin + 20 µM (-) hydroxycitric acid, (P) tunicamycin + 1 mM sodium phenyl butyrate. Values expressed as means ± SD (n = 6), represented by vertical bars.* indicates values are significantly different from the control cells and + indicates values are significantly different from theendoplasmic reticulum stressed group, significance accepted at $P \leq 0.05$.

To confirm our findings obtained by immunoblotting we performed immunofluorescent confocal microscopy for GRP78. The results supported the earlier findings (Figure 3. 7).

A

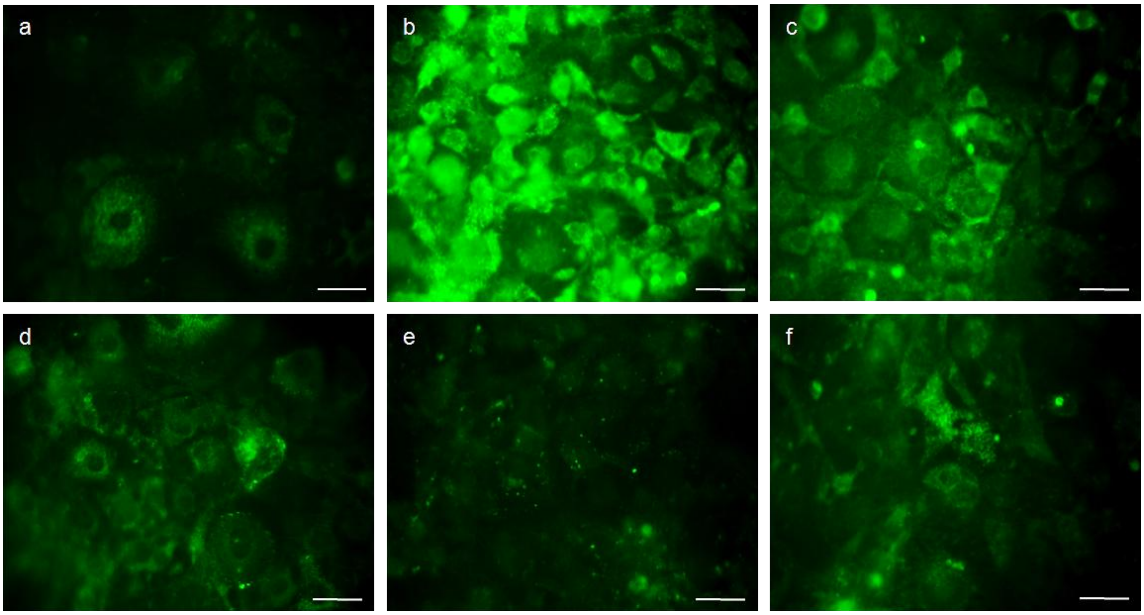

B

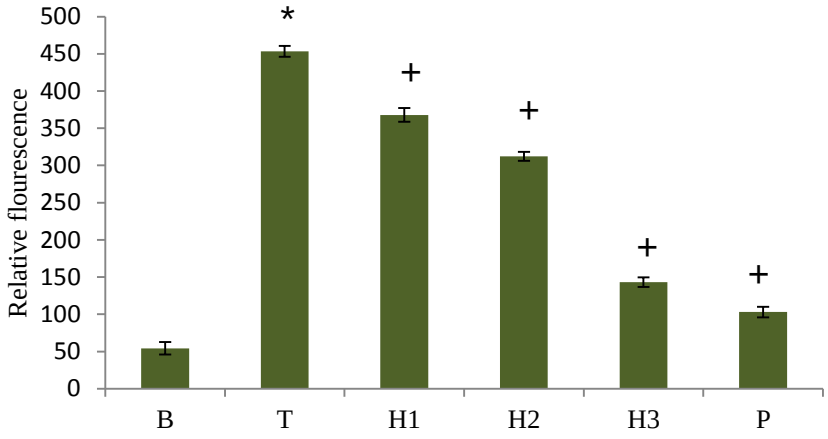

Figure 3.7 Expression of GRP78 in 3T3-L1 adipocytes on treatment with tunicamycin alone and tunicamycin along with (-) hydroxycitric acid. A. Representative images of GRP78 immunofluorescence in 3T3-L1 cells treated with tunicamycin and different concentrations of (-) hydroxycitric acid for 18 hours. (a) control, (b) tunicamycin treated, (c) tunicamycin + 5 µM (-) hydroxycitric acid, (d) tunicamycin + 10 µM (-) hydroxycitric acid, (e) tunicamycin + 20 µM (-) hydroxycitric acid, (f) tunicamycin + 1 mM sodium phenyl butyrate. Scale bar corresponds to 100 µm. B. Relative fluorescence shown by fluorimetric analysis. (B) control, (T) tunicamycin, (H1) tunicamycin + 5 µM (-) hydroxycitric acid, (H2) tunicamycin + 10 µM (-) hydroxycitric acid, (H3) tunicamycin + 20 µM (-) hydroxycitric acid, (P) tunicamycin + 1 mM sodium phenyl butyrate. Values expressed as means ± SD (n = 6), represented by vertical bars.* indicates values are significantly different from the control cells and + indicates values are significantly different from theendoplasmic reticulum stressed group, significance accepted at $P \leq 0.05$.

3.3.7 Effect of HCA on expression of CHOP

In order to verify and confirm the induction of chronic/prolonged ER stress, we examined the effect of tunicamycin administration on CHOP expression by using immunofluorescence microscopy. Treatment with 2 µM tunicamycin resulted in increased (7.34 fold) fluorescence signals, indicating that CHOP expression was induced by ER stress (Figure. 3.8). Furthermore, we analyzed ER stress marker protein by immunoblotting. We also analysed theeffect of HCA. HCA treatment with different concentrations (5, 10, 20 µM) significantly reduced the expression of CHOP in ER stressed cells. PBA (1 mM) was used as a positive control in this study. Immunofluorescence signals were reduced by 1.47, 1.92, 3.68 and 5.30 fold respectively. Western blot analysis showed 8.4 fold increase in protein expression in ER stress, while HCA treatment made a significant lowering in expression (1.39, 1.64, 2.67, 4.15 fold respectively). These results paralleled the findings from the mRNA analysis, i.e; chronic ER stress was induced by tunicamycin treatment and amelioration with HCA in a dose dependent manner. PBA was effective against ER stress induced by tunicamycin (Figure 3.9).

A

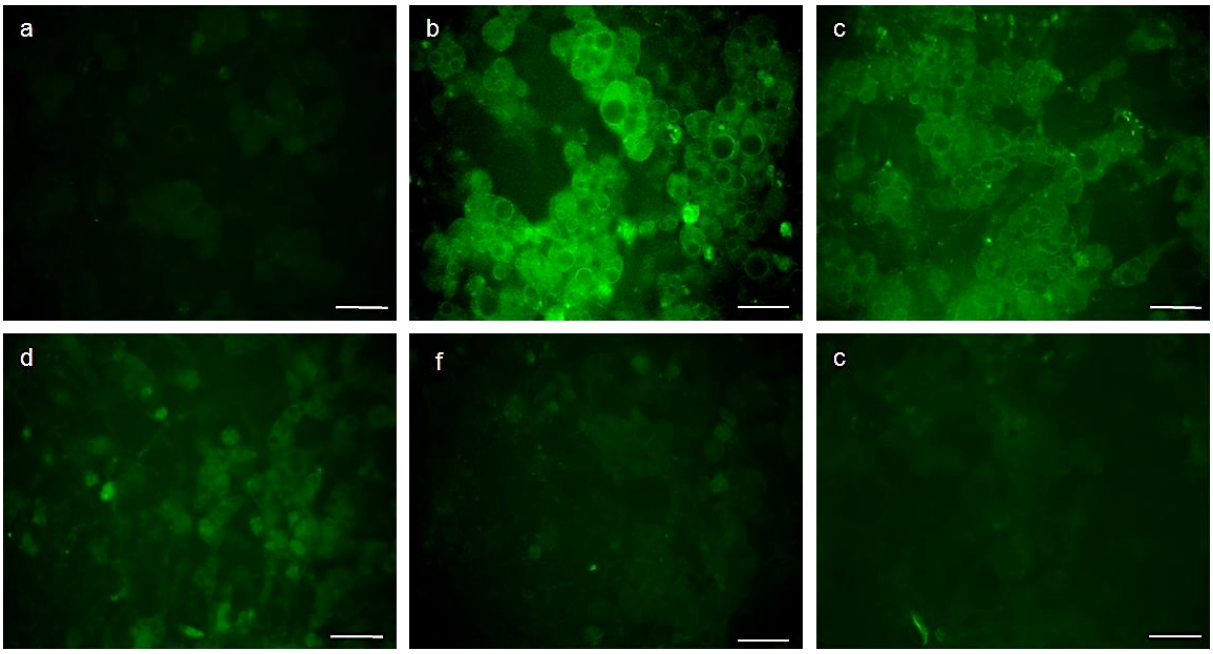

B

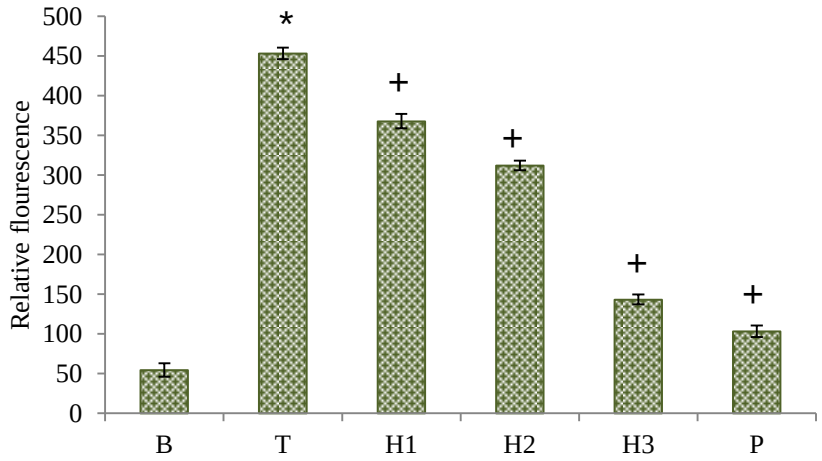

Figure 3.8 Expression of CHOP in 3T3-L1 adipocytes on treatment with tunicamycin alone and tunicamycin along with (-) hydroxycitric acid. A. Representative images of CHOP immunofluorescence in 3T3-L1 cells treated with tunicamycin and different concentrations of (-) hydroxycitric acid for 18 hours. (a) control, (b) tunicamycin treated, (c) tunicamycin + 5 µM (-) hydroxycitric acid, (d) tunicamycin + 10 µM (-) hydroxycitric acid, (e) tunicamycin + 20 µM (-) hydroxycitric acid, (f) tunicamycin + 1 mM sodium phenyl butyrate. Scale bar corresponds to 100 µm. B. Relative fluorescence shown by fluorimetric analysis. (B) control, (T) tunicamycin, (H1) tunicamycin + 5 µM (-) hydroxycitric acid, (H2) tunicamycin + 10 µM (-) hydroxycitric acid, (H3) tunicamycin + 20 µM (-) hydroxycitric acid, (P) tunicamycin + 1 mM sodium phenyl butyrate. Values expressed as means ± SD (n = 6), represented by vertical bars.* indicates values are significantly different from the control cells and + indicates values are significantly different from the endoplasmic reticulum stressed group, significance accepted at $P \leq 0.05$.

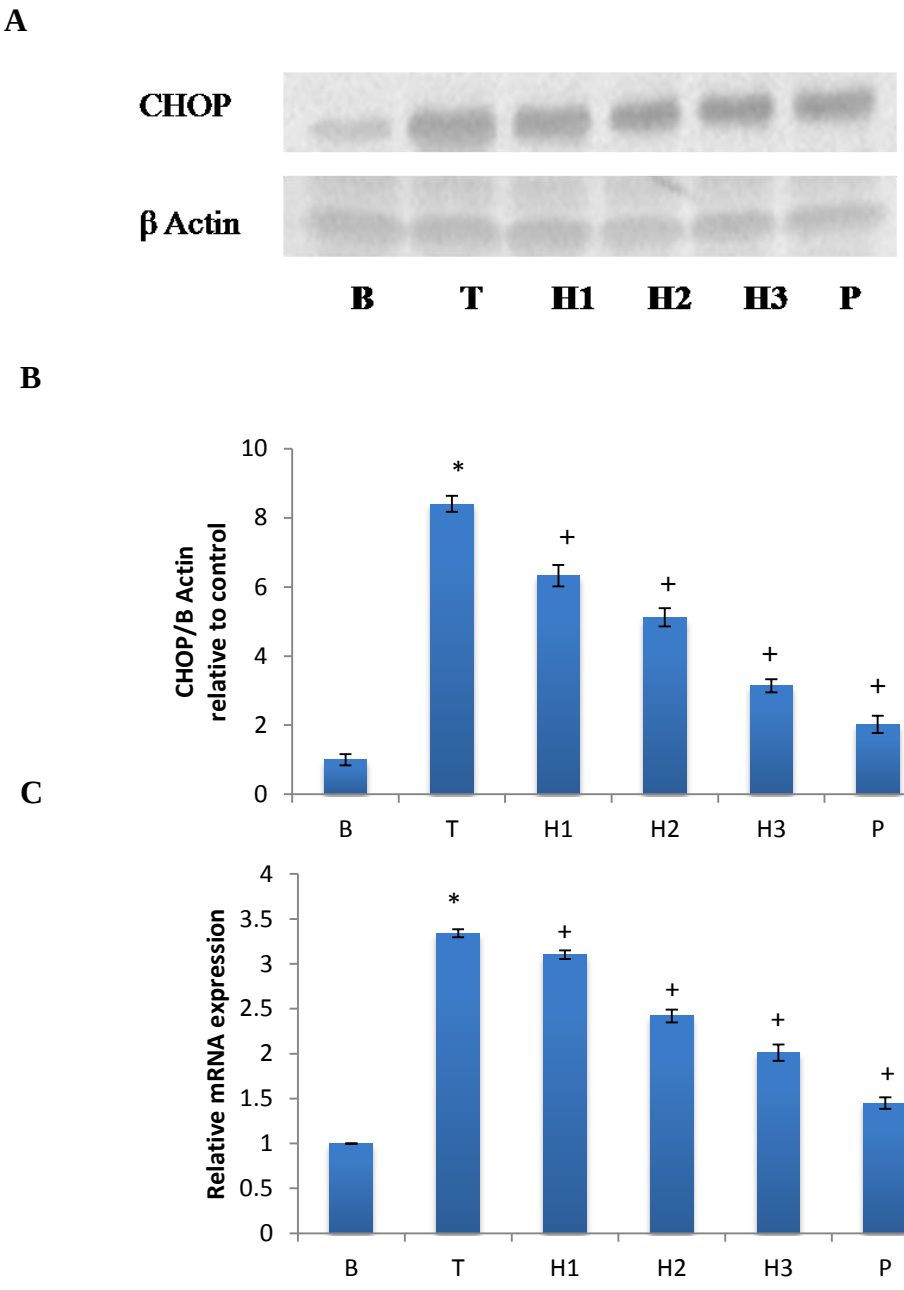

Figure 3.9 Protein and mRNA level expression of CHOP in 3T3-L1 adipocytes treated with tunicamycin alone and tunicamycin with (-) hydroxycitric acid. A. Representative western blot of CHOP. B. Densitometric quantification of CHOP protein level normalised to β Actin. C. Relative mRNA expression normalised to β Actin. (B) control, (T) tunicamycin, (H1) tunicamycin + 5 µM (-) hydroxycitric acid, (H2) tunicamycin + 10 µM (-) hydroxycitric acid, (H3) tunicamycin + 20 µM (-) hydroxycitric acid, (P) tunicamycin + 1 mM sodium phenyl butyrate. Values expressed as means ± SD (n = 6), represented by vertical bars.* indicates values are significantly different from the control cells and + indicates values are significantly different from the endoplasmic reticulum stressed group, significance accepted at $P \leq 0.05$.

3.4 Discussion

Obesity is a major risk factor in the development of metabolic diseases which include IR and T2DM as well as lipid metabolism disorders, hypertension, arteriosclerosis, and ischemic heart disease. Although the worldwide prevalence of obesity has amplified, current pharmacotherapeutic options for treating obesity and metabolic diseases remains inadequate and in vain. Therefore, understanding the molecular mechanisms in the development of obesity related complications is necessary. ER stress and its stress responses in adipose tissue have been recognized as a key factor in aggravating obesity related problems. Hence, ER stress is a potential therapeutic target for the treatment for obesity.

In the present study, the effect of tunicamycin and hydroxycitric acid on the viability of 3T3-L1 adipocytes was determined. It was shown that tunicamycin induced ER stress in 3T3-L1 adipocytes and treatment with HCA reduced the level of ER stress markers Bip and CHOP. We used DCFDA to quantify the oxidative stress produced by tunicamycin and HCA to confirm the concentration of both that can be used for the study. Oxidative stress is a marker for any toxic effects produced in the cells. Tunicamycin is reported to induce ROS production in cells leading to apoptosis and cell death (Lim et al, 2015; Lee et al, 2007)

Increasing number of evidences support the fact that targeting ER stress could be an attractive strategy for the treatment of metabolic diseases. Here we show that tunicamycin induced ER stress in 3T3-L1 adipocytes with 2 µM for 18 hours of exposure and HCA reduced the level of ER stress markers like Bip and CHOP significantly. BiP mRNA levels were rapidly upregulated in mammalian cells when confronted with ER stress (Kozutsumi et al, 1988; Yoshida et al, 1998). Elevated BiP mRNA levels are a sensitive indicator of ER stress and have been reported in diseases linked to ER stress (Lindholm et al, 2006; Mulhern et al, 2006; Tsang et al, 2007). BiP facilitates cells to deal with ER stress, partly, by lowering the levels of misfolded intermediates in the ER (Pincus et al, 2010). The expression levels of CHOP (Fornace Jr, 1989; Price and Calderwood, 1992) are kept very low in normal cells. During acute ER stress condition, CHOP expression is upregulated through IRE1-α and PERK-mediated signaling and the activities of ATF4 and ATF6 transcription factors. The full proapoptotic effect of CHOP emerges only when ER stress cannot be suppressed by the efforts of the survival mechanism, and the levels of misfolded proteins remain high. CHOP activates a transcriptional profile that facilitates a pro-apoptotic program. It includes expression of proapoptotic Bim and repression of antiapoptotic Bcl-2 (McCullough et al,

2001; Puthalakath et al, 2007). In fact, the presence of conspicuous amounts of CHOP protein represents a marker for the acute phase of the activated ER stress response. Prolonged, high-level expression of CHOP denotes that the ER stress response system has exceeded the limits of its protective capacity and that it has switched to its pro-apoptotic module in spite of the continued presence of elevated GRP78 (Nishitoh, 2012; Rutkowski et al, 2006). During moderately intense short-term stress, or while the cell is adapting to longer-lasting chronic stress, pro-survival module leads to suppression of CHOP expression. This is by reassociation of GRP78 with the primary UPR sensors, PERK, IRE1, and ATF6 and inactivation of the downstream ER transmembrane signaling components (Boyce and Yuan, 2006; Rutkowski et al, 2006; Suzuki et al, 2007).

Tunicamycin is an inhibitor of the UDP-N-acetylglucosamine-dolichol phosphate N-acetylglucosamine-1-phosphate transferase (GPT), which catalyses the initial step of glycoprotein biosynthesis in the ER. Thus, treatment with tunicamycin causes accumulation of unfolded glycoproteins in the ER, leading to ER stress. A number of chemicals have been identified to induce ER stress and activate the UPR in tissue culture system including tunicamycin, thapsigargin, brefeldin A, dithiothreitol (DTT), and MG132. The concentration and duration of treatment in which ER stress is induced by these compounds should be determined for each particular system. Typically only a few hours are needed to induce ER stress and long exposures often induce ER stress-mediated cell death.

Within cells, tunicamycin inhibits *N*-linked glycosylation of proteins and lipids by binding to the enzyme *N*-acetylglucosamine-1-phosphate transferase and prevents the incorporation of *N*-acetylglucosamine into lipids and proteins (Keller et al, 1979; Takatsuki and Tamura, 1971). When cells take up glucose, a small fraction (2–3%) is metabolized in the hexosamine biosynthesis pathway and *N*-acetylglucosamine is formed which act as precursors for glycosylation of proteins and lipids (Marshall et al, 1991). Ong and Kern reported that, in adipose tissue, glucose deprivation inhibited glycosylation and GRP78 was up-regulated (Ong and Kern, 1989). This is comparable with the effect produced by tunicamycin.

HCA is a citric acid derivative and is the principal compound found in *Garcinia* fruit. Numerous in *vitro* and *in vivo* studies have reported that HCA suppresses the *de novo* fatty acid synthesis and lipogenesis. Some authors have suggested that weight loss may be by competitive inhibition of the enzyme adenosine triphosphatase-citrate-lyase (Hayamizu et al,

2003; Mattes and Borman, 2000; Preuss et al, 2004; Roongpisuthipong et al, 2007). HCA has also been reported to increase the release or availability of serotonin in the brain, thereby leading to appetite suppression (Toromanyan et al, 2007). Other postulated weight loss mechanisms include inhibition of pancreatic alpha amylase and intestinal alpha glucosidase, thereby leading to a reduction in carbohydrate metabolism (Yamada et al, 2007). Pharmaceutical compositions containing HCA are found useful for reducing inflammation and regulating inflammatory responses and processes. In our study HCA was observed to reduce the level of ER stress markers GRP78 and CHOP. Under tunicamycin induced ER stress condition, GRP78 levels were reduced by phytochemicals like genistein, epigallocatechin gallate, and salicylic acid (Deng et al, 2001; Ermakova et al, 2006; Zhou and Lee, 1998). Alleviation of ER stress has been reported to improve the symptoms of obesity (Kawasaki et al, 2012). A number of phytochemicals were found to reduce ER stress and reduce the protein load, though by different mechanisms (Ding et al, 2013; Park et al, 2010; Tabata et al, 2007; Yao et al, 2012).

ER stress and its stress response (UPR) offer novel drug targets for obesity. However, ER stress has various physiologic roles, including escape from apoptosis in cells with unfolded protein in the ER (Nakagawa et al, 2000, Urano et al, 2000), regulation of secretory cell differentiation or maturation (Asada et al, 2012; Basseri et al, 2009; Kondo et al, 2011; Murakami et al, 2009) and maintenance of cellular homeostasis (Rutkowski et al, 2010). Consequently, complete elimination of ER stress by agents that prevent ER stress could cause disadvantage for living cells and biological regulation. To develop the agents targeting ER stress in clinical, further studies are needed to characterize the functional changes in cells dependent on ER stress.

In brief, tunicamycin induced ER stress in 3T3-L1 adipocytes as indicated by increased expression of GRP78 and CHOP. The presence of CHOP indicated a severe or prolonged ER stress. HCA when co-treated with tunicamycin reduced the severity of the ER stress. The present study shows light to the possibility that inhibition of ER stress may be an effective approach to reduce the risk of obesity and its complications.

Chapter 4

HCA improves the alterations in UPR and antioxidant status in 3T3-L1 adipocytes during ER stress

4.1 Introduction

The endoplasmic reticulum plays a central role in multiple cellular processes, including the folding of membrane and secretory proteins (Pagliassotti, 2012). Various cellular stresses can disturb ER homeostasis and lead to the accumulation of unfolded proteins within the ER lumen. This activates an adaptive pathway called UPR that aims to restore ER function (Kaufman, 2002). The UPR is initiated by activation of three ER transmembrane proteins: PERK, ATF6, and IRE1. On activation, these proteins communicate to the nucleus to control the transcription of genes involved in protein folding and processing, to increase the ER protein folding capacity, ERAD and autophagy components to reduce the ER workload, and cell survival and death factors. The fate of the cell is determined depending on the ER stress condition (Zhang and Kaufman, 2006). UPR activation levels could ideally be established by measuring IRE1α and PERK phosphorylation, and ATF6α cleavage.

All the 3 pathways of UPR, IRE1α, PERK and ATF6α are engaged in regulating transcription during ER stress. IRE1α directly modulates the splicing of XBP1 mRNA which regulates chaperones, folding catalysts and ERAD components. PERK phosphorylates eIF2α to reduce mRNA translation, though, preferentially favors translation of some mRNAs such as the transcription factor ATF4. Translational attenuation is an early UPR response to reduce the ER protein workload. ATF4 are involved in the regulation of genes related to antioxidative stress, amino acid biosynthesis, protein folding and degradation, and apoptosis. CHOP is a bZIP transcription factor, regulating apoptosis related genes. Upon ER activation, ATF6α transits to the Golgi where it is cleaved by site 1 (S1) and site 2 (S2) proteases, generating an activated b-ZIP factor (Ye et al, 2000). This processed form of ATF6α translocates to the nucleus and activates genes involved in protein folding, processing, and degradation (Haze et al, 1999; Yoshida et al, 2001).

Oxidative stress and ROS generation are not just consequences of ER stress induction but they are vital components of ER stress. Cellular events such as protein oxidation and protein folding are closely connected with the production of ROS (Higa and Chevet, 2012). PDI, ERO1, the protein folding enzymes and NADPH oxidase complexes (especially the Nox4) are the major enzymes involved in ER ROS production. In addition, ROS is generated by mitochondrial electron transport enzymes (Santos et al, 2009). In this study, we discuss the activation of UPR signaling proteins, ER stress-associated ROS and related alterations in the innate antioxidant status in the 3T3-L1 adipocytes.

4.2 Methods

Cell culture and treatments were same as described in Chapter 2. Experimental groups were

B - Control

T - Tunicamycin treated groups

H1 - Tunicamycin + HCA 5 µM

H2 - Tunicamycin + HCA 10 µM

H3 - Tunicamycin + HCA 20 µM

P - Tunicamycin + PBA 1 mM

Following parameters were assessed to determine the effect of HCA on alterations in UPR signaling proteins in 3T3-L1 adipocytes during tunicamycin induced ER stress. Antioxidant status was also studied, with respect to antioxidant enzymes and oxidation products. Detailed procedures of all the experiments are given in Chapter 2.

- Effect of HCA on protein level and mRNA level expression UPR master sensors, PERK, IRE1α, ATF6
- Effect of HCA on expression and response of UPR downstream markers
- Intracellular ROS generation determined by DCFDA incorporation
- Effect of HCA on HO-1 enzyme activity and protein expression in ER stress
- Effect of HCA on Nrf2 translocation during ER stress
- Effect of HCA on endogenous antioxidant status during ER stress

4.3 Results

4.3.1 Effect of HCA on UPR master sensors PERK, IRE1α, ATF6

Expression of the proximal UPR stress sensors and the effect of HCA on their expression are shown in Figure 4.1. Expression of IRE1 was significantly greater (6.67 fold, $P \leq 0.05$) in ER stress compared to normal adipocytes, while treatment with HCA at different concentrations, and PBA lowered the level significantly (1.07, 1.39, 2.07, 2.29 fold respectively, $P \leq 0.05$). ER stressed cells, also showed greater activation of PERK, as indicated by the increased (8.43 fold) expression of the protein ($P \leq 0.05$). HCA reduced (1.15, 1.85, 3.79 fold respectively) the PERK levels significantly in dose dependent manner ($P \leq 0.05$). PBA reduced PERK levels by 2.70 fold ($P \leq 0.05$). ATF6 was also increased (3.67 fold) in ER stressed adipocytes compared with control ($P \leq 0.05$). There was significant lowering of ATF6 expression in 3T3-L1 adipocytes treated with different concentrations of HCA and PBA (1.17, 1.38, 2.49 and 2.95 fold respectively, $P \leq 0.05$).

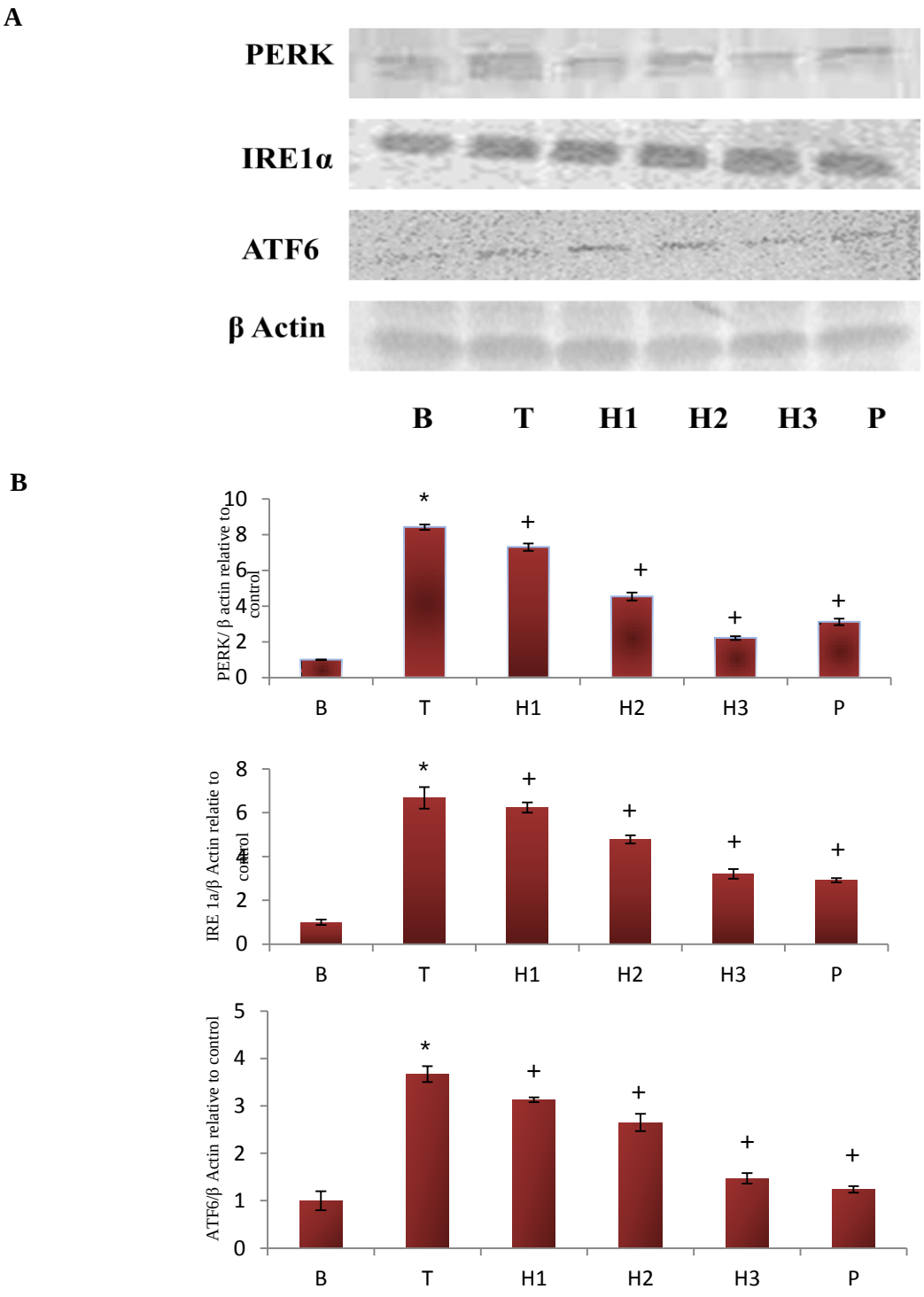

Figure 4.1 Effect of (-) hydroxycitric acid on unfolded protein response master sensors in 3T3-L1 adipocytes during endoplasmic reticulum stress. A. Representative immunoblots of PERK, IRE1α, ATF6. B. Densitometric quantification of protein level normalised to β Actin. (B) control, (T) tunicamycin, (H1) tunicamycin + 5 µM (-) hydroxycitric acid, (H2) tunicamycin + 10 µM (-) hydroxycitric acid (H3) tunicamycin + 20 µM (-) hydroxycitric acid, (P) tunicamycin + 1 mM sodium phenyl butyrate. Values expressed as means ± SD (n = 6), represented by vertical bars.* indicates values are significantly different from the control cells and + indicates values are significantly different from the endoplasmic reticulum stressed group, significance accepted at $P \leq 0.05$.

4.3.2 Study of UPR downstream markers and response

4.3.2.1 Effect of HCA on expression of p-eIF2α during ER stress

Measuring eIF2α phosphorylation levels by immunoblot method using anti-phopho-eIF2α specific antibody (Cell Signaling, Danvers, MA) indirectly reflects PERK activation. Increased phosphorylation of eIF2α was detected (5.62 fold, $P \leq 0.05$) in ER stress induced cells, but various concentrations of HCA as well as PBA (1 mM) treatment significantly reduced (1.24, 1.65, 2.40 and 2.65 fold respectively, $P \leq 0.05$) the phosphorylation. The effect of HCA was dose dependent (Figure 4.2).

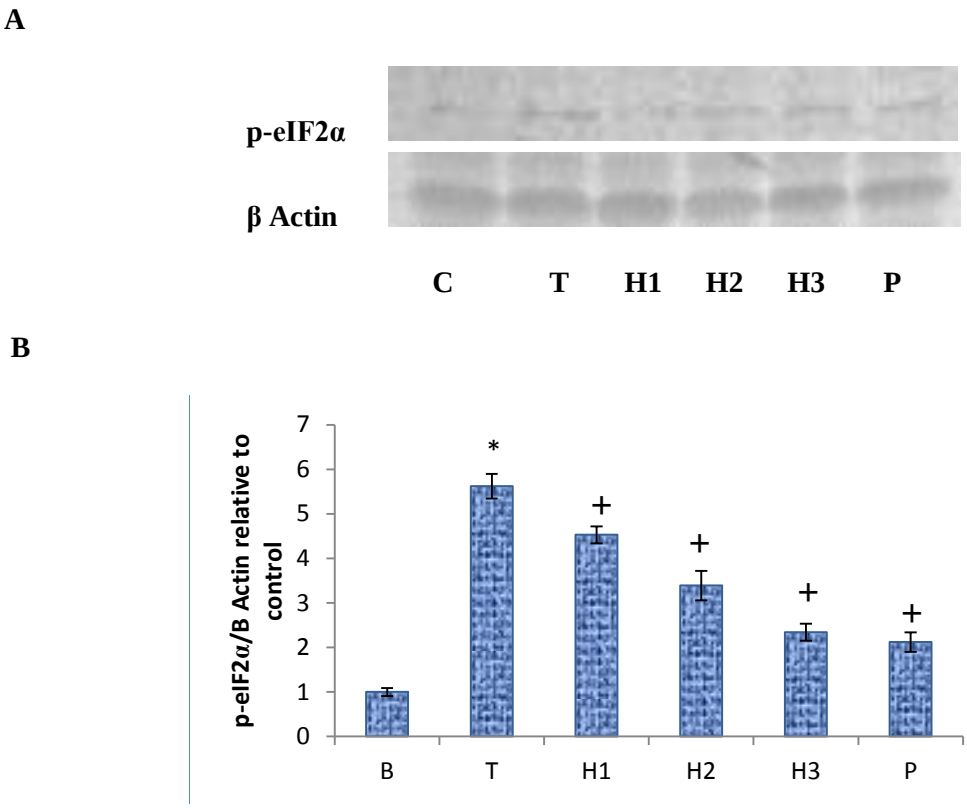

Figure 4.2 Effect of (-) hydroxycitric acid on phosphorylation of eIF2α in 3T3-L1 adipocytes during endoplasmic reticulum stress. A. Representative immunoblot of peIF2α. B. Densitometric quantification of protein level normalised to β Actin. (B) control, (T) tunicamycin, (H1) tunicamycin + 5 µM (-) hydroxycitric acid, (H2) tunicamycin + 10 µM (-) hydroxycitric acid (H3) tunicamycin + 20 µM (-) hydroxycitric acid, (P) tunicamycin + 1 mM sodium phenyl butyrate. Values expressed as means ± SD (n = 6), represented by vertical bars.* indicates values are significantly different from the control cells and + indicates values are significantly different from the endoplasmic reticulum stressed group, significance accepted at $P \leq 0.05$.

4.3.2.2 Effect of HCA on relative mRNA expression of *Xbp-1*

Xbp1 mRNA is induced by ATF6 and spliced by IRE1 in response to ER stress, resulting in production of a highly active transcription factor that can activate the mammalian UPR (Yoshida et al, 2001). mRNA expression of *Xbp1* was significantly increased by

induction of ER stress in 3T3-L1 adipocytes. HCA at concentrations of 5, 10, 20 µM and PBA (1 mM) reduced the mRNA expression of *Xbp1* significantly (Figure 4.3).

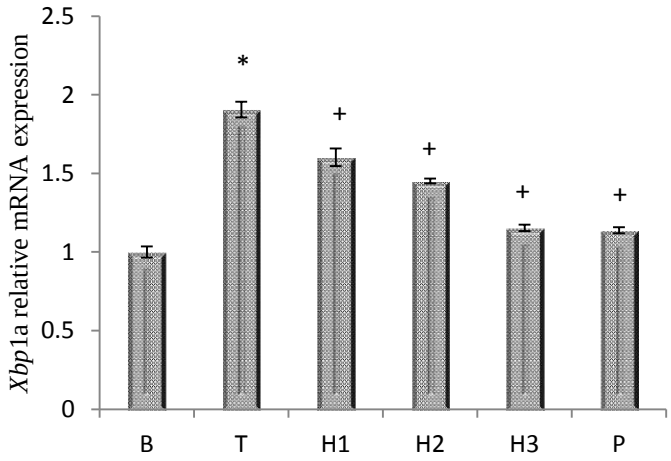

Figure 4.3 Effect of (-) hydroxycitric acid on expression of *Xbp1* in 3T3-L1 adipocytes during endoplasmic reticulum stress. Quantification of mRNA level normalised to β Actin. (B) control, (T) tunicamycin, (H1) tunicamycin + 5 µM (-) hydroxycitric acid, (H2) tunicamycin + 10 µM (-) hydroxycitric acid (H3) tunicamycin + 20 µM (-) hydroxycitric acid, (P) tunicamycin + 1 mM sodium phenyl butyrate. Values expressed as means ± SD (n = 6), represented by vertical bars.* indicates values are significantly different from the control cells and + indicates values are significantly different from the endoplasmic reticulum stressed group, significance accepted at $P \leq 0.05$.

4.3.2.3 Effect of HCA on expression of ERO 1α and PDI

The expression levels of PDI and ERO 1α were quantified using immunoblot analysis (Figure 4.4 A). The level of PDI was found to be increased significantly (7.89 fold, $P \leq 0.05$) in correlation with the increased ROS production. HCA treatment at 5, 10 and 20 µM concentrations reduced significantly (1.26, 1.54, 2.83 fold, $P \leq 0.05$) the PDI expression compared to ER group. The reduction was comparable with that of the positive control, PBA (3.22 fold) (Figure 4.4B). The mRNA expression of *Pdi* was also analysed (Figure 4.4C) and found increased during ER stress. Here also both HCA and PBA significantly reduced the level of *Pdi*. ERO 1α expression was also seen by western blotting. The protein levels were elevated significantly (5.21 fold, $P \leq 0.05$) by ER stress while treatment with HCA and PBA lowered the expression by 1.19, 1.48, 2.17 and 2.33 fold respectively ($P \leq 0.05$, Figure 4.4B).

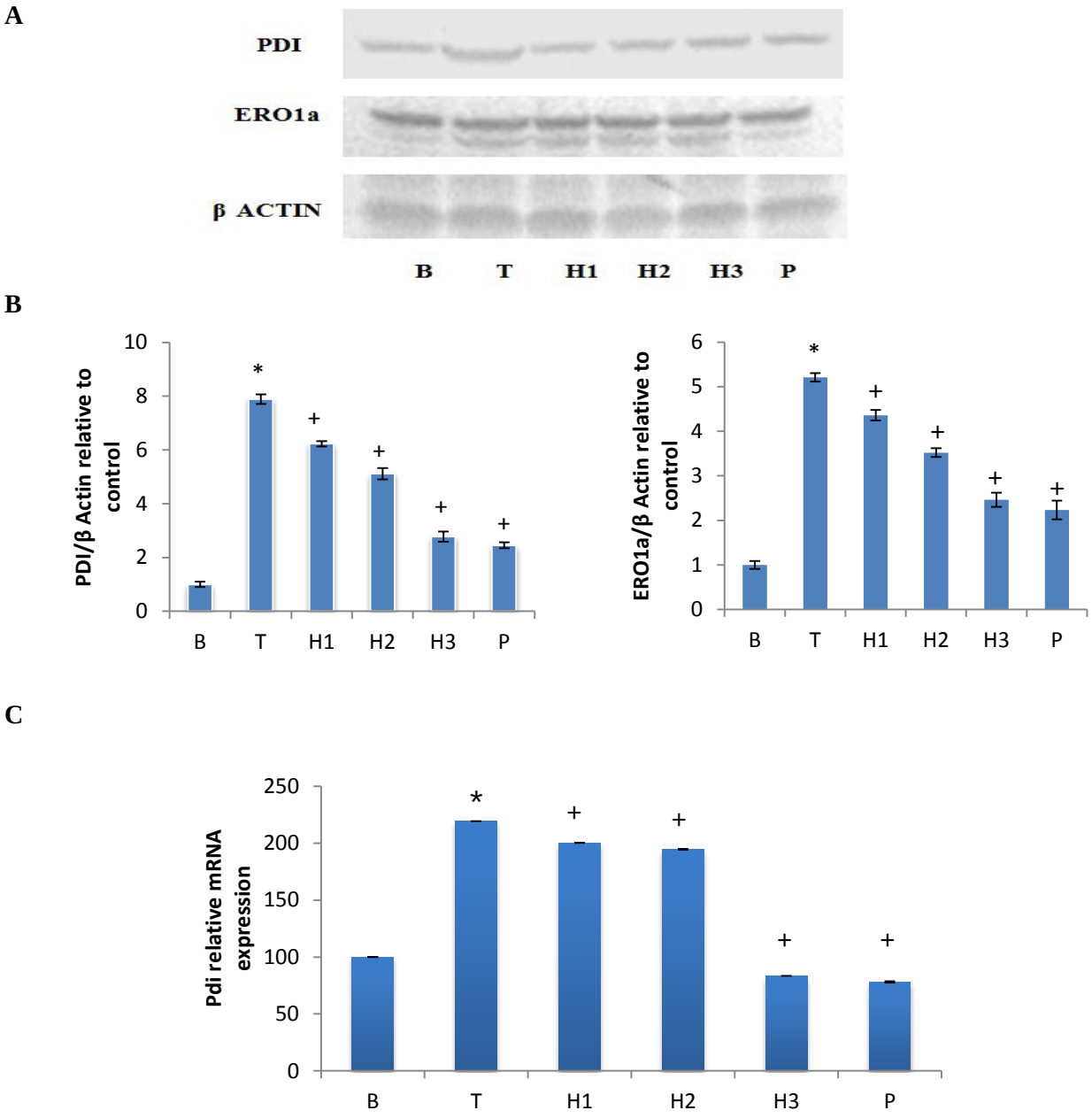

Figure 4.4 Effect of (-) hydroxycitric acid on expression of PDI and ERO1α in 3T3-L1 adipocytes during endoplasmic reticulum stress. A. Representative images of immunoblot analysis. B. Densitometric quantification of ERO1 and PDI protein level normalised to β Actin. C. Quantification of *Pdi* mRNA level normalised to β Actin. (B) control, (T) tunicamycin, (H1) tunicamycin + 5 µM (-) hydroxycitric acid, (H2) tunicamycin + 10 µM (-) hydroxycitric acid (H3) tunicamycin + 20 µM (-) hydroxycitric acid, (P) tunicamycin + 1 mM sodium phenyl butyrate. Values expressed as means ± SD (n = 6), represented by vertical bars.* indicates values are significantly different from the control cells and + indicates values are significantly different from the endoplasmic reticulum stressed group, significance accepted at $P \leq 0.05$.

4.3.3 Intracellular ROS generation determined by DCFDA incorporation

ER stress caused significant ROS generation in 3T3-L1 adipocytes compared to the control cells. The different concentrations of HCA dose dependently reduced the ROS

generation during ER stress. PBA, which was used as positive control also reduced ROS production. The amount of ROS was quantified using DCFDA with bioimaging (Figure 4.5) and cytometry (Figure 4.6). There was 7.2 fold increases in the ROS during ER stress ($P \leq 0.05$). Addition of HCA along with tunicamycin reduced the level of ROS significantly ($P \leq 0.05$) by about 1.4, 1.8 and 3.2 fold respectively.

A

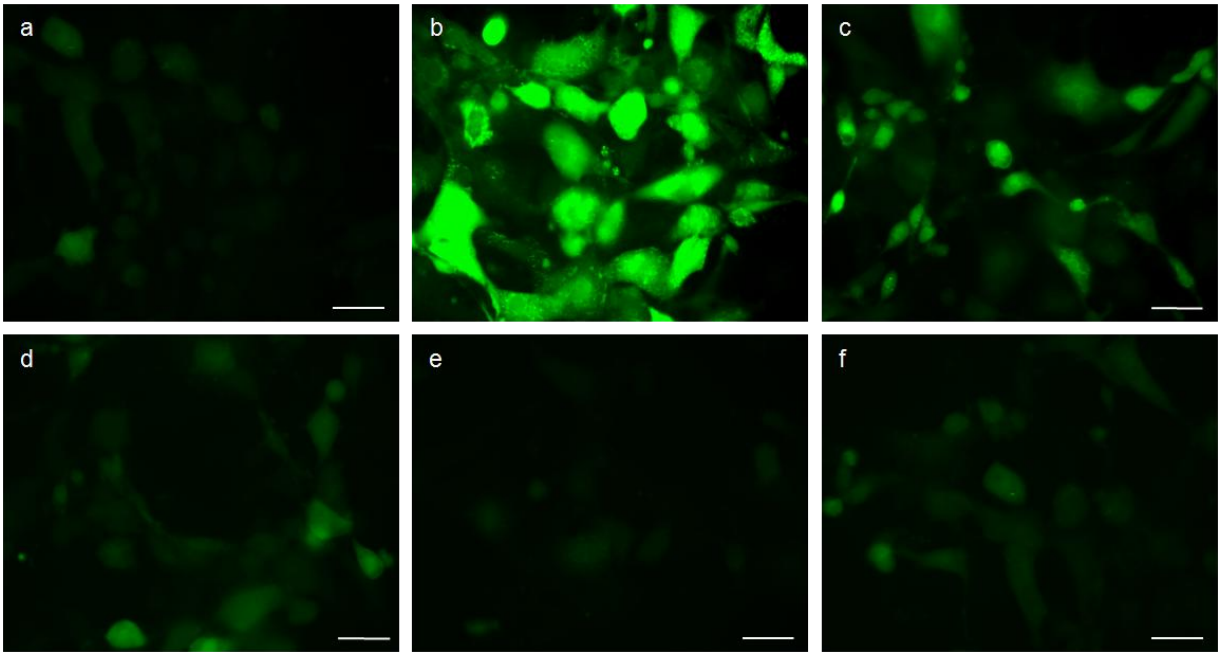

B

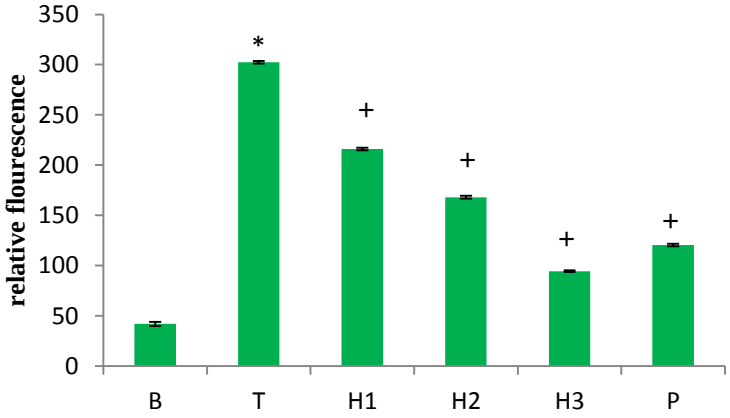

Figure 4.5 Reactive oxygen species generation in 3T3-L1 adipocytes on treatment with tunicamycin. A. Representative images of DCFDA fluorescence in 3T3-L1 cells treated with tunicamycin and different concentrations of hydroxycitric acid for 18 hours. (a) control, (b) tunicamycin treated, (c) tunicamycin + 5 µM (-) hydroxycitric acid, (d) tunicamycin + 10 µM (-) hydroxycitric acid, (e) tunicamycin + 20 µM (-) hydroxycitric acid, (f) tunicamycin + 1 mM sodium phenyl butyrate. Scale bar corresponds to 100 µm. B. Relative fluorescence shown by fluorimetric analysis. (B) control, (T) tunicamycin, (H1) tunicamycin + 5 µM (-) hydroxycitric acid, (H2) tunicamycin + 10 µM (-) hydroxycitric acid (H3) tunicamycin + 20 µM (-) hydroxycitric acid, (P) tunicamycin + 1 mM sodium phenyl butyrate. Values expressed as means ± SD (n = 6), represented by vertical bars.* indicates values are significantly different from the control cells and + indicates values are significantly different from the endoplasmic reticulum stressed group, significance accepted at $P \leq 0.05$.

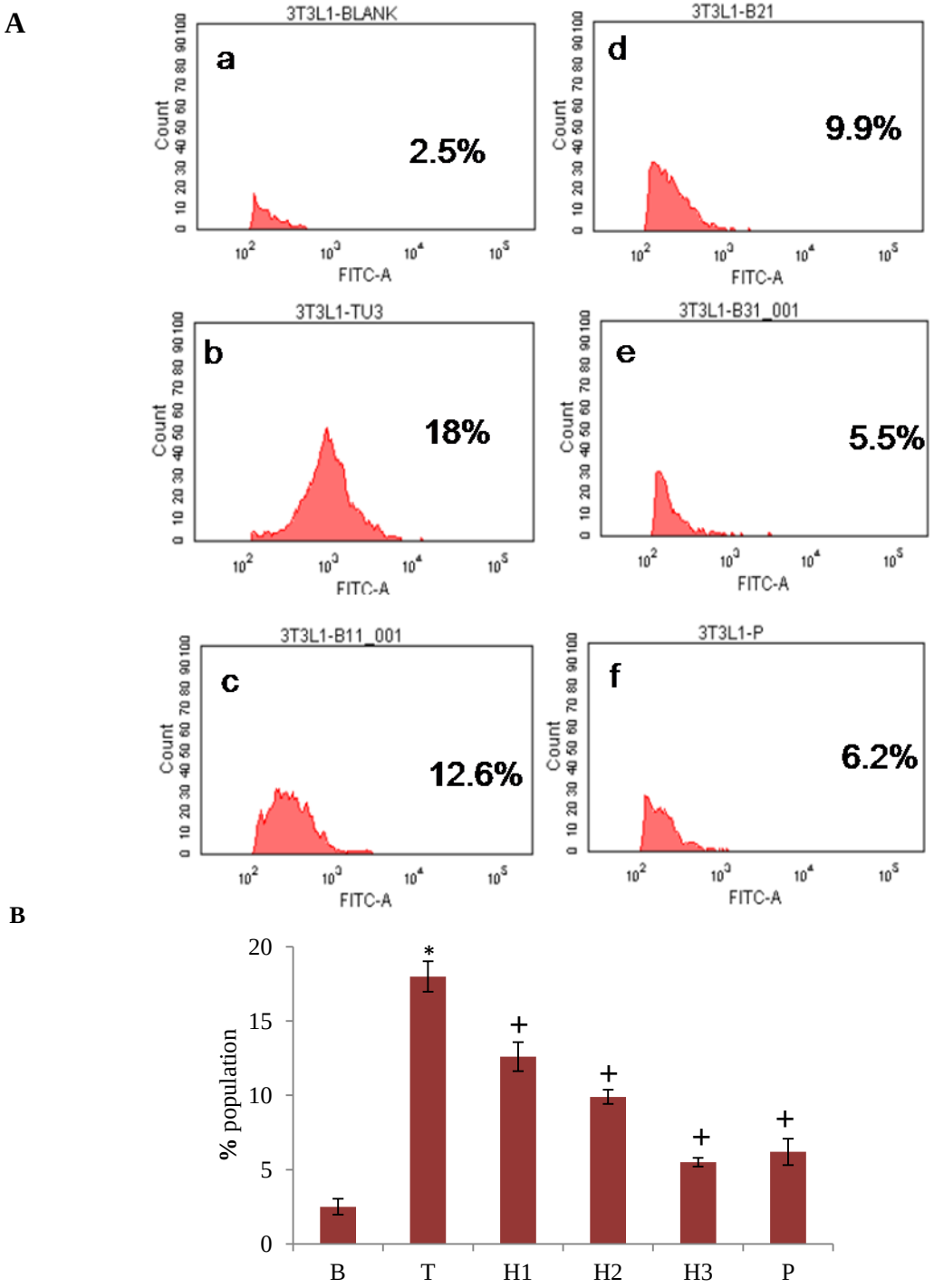

Figure 4.6 Intracellular reactive oxygen species generation determined by flow cytometry. A.The representative histograms of reactive oxygen species induced fluorescence by flow cytometry (a) control, (b) tunicamycin treated, (c) tunicamycin + 5 µM (-) hydroxycitric acid, (d) tunicamycin + 10 µM (-) hydroxycitric acid, (e) tunicamycin + 20 µM (-) hydroxycitric acid, (f) tunicamycin + 1 mM sodium phenyl butyrate. B. Relative fluorescence shown by fluorimetric analysis. (B) control, (T) tunicamycin, (H1) tunicamycin + 5 µM (-) hydroxycitric acid, (H2) tunicamycin + 10 µM (-) hydroxycitric acid (H3) tunicamycin + 20 µM (-) hydroxycitric acid, (P) tunicamycin + 1 mM sodium phenyl butyrate. Values expressed as means ± SD (n = 6), represented by vertical bars.* indicates values are significantly different from the control cells and + indicates values are significantly different from the endoplasmic reticulum stressed group, significance accepted at $P \leq 0.05$.

4.3.4 Effect of HCA on HO-1 enzyme activity and protein expression in ER stress

Enzyme activity of HO-1, which is a downstream molecule of Nrf2, was analysed (Figure 4.7). Activity of HO-1 were significantly ($P \leq 0.05$) increased (8.16 fold) in ER stress induced group, indicating increased oxidative stress. The treatment with HCA (5, 10 and 20 µM) and PBA (1 mM) reduced the HO-1 activity to significant levels (2.10, 2.98, 5.05 and 5.40 fold respectively). The results were supported by protein level expression studies.

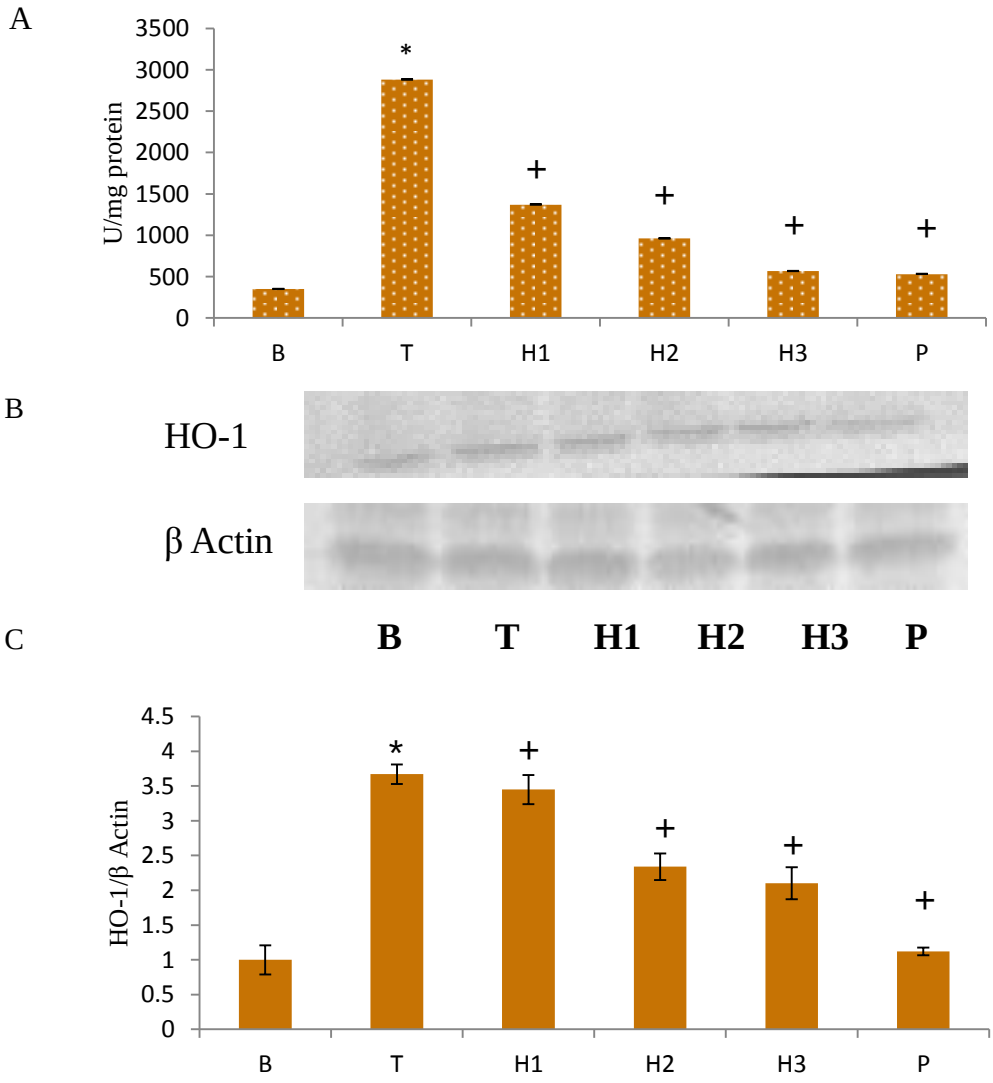

Figure 4.7 Hemeoxygenase-1 enzyme activity and protein expression in 3T3-L1 adipocytes during endoplasmic reticulum stress. A. HO-1 enzyme activity. B. Representative immunoblot of HO-1. C. Densitometric quantification of HO-1. (B) control, (T) tunicamycin, (H1) tunicamycin + 5 µM (-) hydroxycitric acid, (H2) tunicamycin + 10 µM (-) hydroxycitric acid (H3) tunicamycin + 20 µM (-) hydroxycitric acid, (P) tunicamycin + 1 mM sodium phenyl butyrate. Values expressed as means ± SD (n = 6), represented by vertical bars.* indicates values are significantly different from the control cells and + indicates values are significantly different from the endoplasmic reticulum stressed group, significance accepted at $P \leq 0.05$.

4.3.5 Effect of HCA on Nrf2 translocation

In response to oxidative stress, Nrf2 is translocated to the nucleus, where it binds to ARE sequences resulting in transcriptional activation of antioxidant genes, such as HO-1. Here we investigated the effect of ER stress on expression of Nrf2 (Figure 4.8). The analysis of Nrf2 in nuclear and cytosolic fraction of ER stress induced cells, showed an increased protein level expression of Nrf2 in nuclear fraction (2.21 fold, $P \leq 0.05$) compared to control. But, in normal cells cytosolic expression of Nrf2 was significantly higher, relative to nuclear fraction. This clearly shows the nuclear translocation of Nrf2 during ER stress. HCA (5, 10 and 20 µM) and PBA (1 mM) treated cells showed reduced (1.10, 1.23, 1.69 and 1.80 fold respectively) levels of Nrf2 in the nuclear extracts indicating a reduced stress generation in these groups.

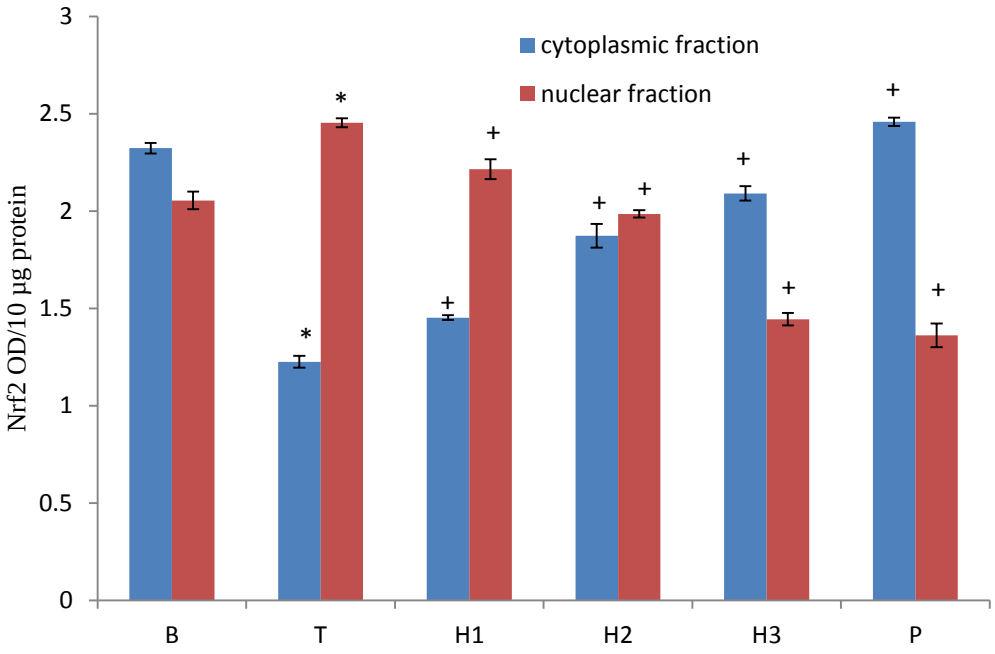

Figure 4.8 Nuclear translocation of Nrf2 in 3T3-L1 adipocytes during endoplasmic reticulum stress. (B) control, (T) tunicamycin, (H1) tunicamycin + 5 µM (-) hydroxycitric acid, (H2) tunicamycin + 10 µM (-) hydroxycitric acid (H3) tunicamycin + 20 µM (-) hydroxycitric acid, (P) tunicamycin + 1 mM sodium phenyl butyrate. Values expressed as means ± SD (n = 6), represented by vertical bars.* indicates values are significantly different from the control cells and + indicates values are significantly different from the endoplasmic reticulum stressed group, significance accepted at $P \leq 0.05$.

4.3.6 Effect of HCA on endogenous antioxidant status

Evaluation of endogenous antioxidant status during ER stress provides an indication of oxidative damage. For this, we measured the activities of various innate antioxidant enzymes like catalase, SOD, GPx, GR, and total antioxidant activity in all experimental groups. Concentrations of TBARS, protein carbonyls and GSH were also quantified. ER

stress was found to inhibit both SOD (1.38 fold) and catalase activity (2.11 fold) significantly ($P \leq 0.05$, Table 4.1) in 3T3-L1 adipocytes compared to normal cells. Treatment with different concentrations (5, 10, and 20 µM) of HCA restored ($P \leq 0.05$) SOD (1.06, 1.13, 1.28 fold respectively) and catalase activity (1.20, 1.39, 1.94 fold respectively, Table 4.1). Similarly the activities of antioxidant enzymes GPx and GR were reduced in tunicamycin treated cell (2.38, 1.27 fold respectively, $P \leq 0.05$) when compared with normal cells. The treatment with different doses of HCA significantly improved ($P \leq 0.05$) GPx (1.47, 2.16, 2.39 fold) and GR (1.02, 1.11, 1.20 fold) activities in a dose dependant manner (Table 4.1). PBA treatment also improved enzyme activities. There was a significant ($P \leq 0.05$) depletion of total antioxidant activity (4.78) fold in ER stress group compared with normal cells and the activity were restored to almost normal level by treatment with HCA in a dose dependent manner(1.79, 2.71, 4.08 fold) and PBA (3.97 fold,$P \leq 0.05$, Table 4.1). ER stress aggravated lipid peroxidation (8.78 fold) and protein oxidation (6.67 fold) significantly ($P \leq 0.05$) compared with normal cells. While different doses of HCA (5, 10, and 20 µM) treatment reduced lipid peroxidation (1.62, 2.32, 4.34 fold respectively) and protein oxidation (1.26, 1.62, 2.76 fold) in dose dependent manner in ER stressed cells significantly ($P \leq 0.05$, Table 4.1). PBA-treated cells showed less oxidation of lipids (3.17 fold) and proteins (1.93 fold) compared to ER stress. GSH levels were lowered (3.40 fold) during ER stress and significantly elevated compared to stressed cells by HCA (1.26, 1.97, 3.03 fold) as well as PBA (2.94 fold). These results validate the potential effect of HCA on oxidative stress induced by ER stress.

	Control	Tunicamycin treated	Tunicamycin + 5 µM (-) hydroxycitric acid	Tunicamycin + 10 µM (-) hydroxycitric acid	Tunicamycin + 20 µM (-) hydroxycitric acid	Tunicamycin + 1mM sodium phenyl butyrate
Catalase (nM of H_2O_2 decomposed /min/mg protein)	6.07 ± 0.09	2.87 ± 0.22*	3.45 ± 0.03^{+}	4.015 ± 0.08^{+}	5.605 ± 0.10^{+}	4.94 ± 0.07^{+}
Total SOD (Unit/mg protein)	7.92 ± 0.28	3.89 ± 0.62*	4.83 ± 0.21^{+}	5.65 ± 0.30^{+}	6.53 ± 0.04^{+}	6.15 ± 0.23^{+}
GPx(Unit/mg protein)	35.2 ± 0.65	14.80 ± 0.26*	21.77 ± 0.63^{+}	32.10 ± 1.2^{+}	35.40 ± 0.24^{+}	32.00 ± 0.77^{+}
GR (Unit/mg protein)	7.55 ± 0.19	5.90 ± 0.50*	6.03 ± 0.12^{+}	6.55 ± 0.28^{+}	7.10 ± 0.21^{+}	6.47 ± 0.28^{+}
GSH (nM/mg protein)	10.00 ± 0.55	2.94 ± 0.16*	3.72 ± 0.03^{+}	5.81 ± 0.39^{+}	8.93 ± 0.06^{+}	8.67 ± 0.17^{+}
TBARs(nM MDA/mg protein)	2.57 ± 0.26	22.57 ± 1.05*	13.90 ± 1.14^{+}	9.71 ± 0.62^{+}	5.19 ± 0.21^{+}	7.10 ± 0.40^{+}
Protein carbonyls (nM/ml)	3.52 ± 0.11	23.52 ± 1.70*	18.52 ± 0.34^{+}	14.43 ± 0.79^{+}	8.52 ± 0.56^{+}	12.15 ± 0.34^{+}
Total antioxidant(nM of trolox equivalents)	0.22 ± 0.01	0.04 ± 0.00*	0.08 ± 0.00^{+}	0.12 ± 0.00^{+}	0.18 ± 0.00^{+}	0.18 ± 0.00^{+}

Table 4.1 Alterations in antioxidant status during endoplasmic reticulum stress in 3T3-L1 adipocytes. Values expressed as means ± SD (n = 6), represented by vertical bars.* indicates values are significantly different from the control cells and + indicates values are significantly different from the endoplasmic reticulum stressed group, significance accepted at $P \leq 0.05$.

4.4 Discussion

Endoplasmic reticulum is a dynamic organelle orchestrating several crucial pathways that decide cellular fate. It senses alterations in ER homeostasis and triggers UPR pathways with an aim to restore homeostasis by activating genes involved in protein folding and degrading machinery transcribed by factors like ATF6, XBP1, and ATF4. If unresolved, it initiates cell death pathways. Under such situations, UPR pathways trigger, affect, and integrate with multiple cellular signaling pathways. Neurodegenerative diseases, inflammatory diseases, cardiovascular diseases, diabetes mellitus, cancer, and several metabolic diseases have perturbed ER functions, which contribute to their pathogenesis. The existence of other complications like inflammation or oxidative stress is also to be considered. Recent findings have revealed interconnections between ER stress, inflammation, and oxidative stress pathways under pathological conditions.

In this chapter, the induction of UPR master regulators, as well as the downstream proteins was analyzed in context of ER stress in 3T3-L1 adipocytes. The results showed that, relative to the normal cells, ER stressed adipocytes exhibited increased activation of the UPR as indicated by increased expression of PERK, IRE1α and ATF6. These results are consistent with, and extend to the previously published data regarding obesity-associated UPR activation in tissues involved in the regulation of metabolism (Puri et al, 2008; Sharma et al, 2008). In the present study, we found evidence for the up-regulation of all 3 UPR-initiating pathways in the adipocytes during ER stress. Some earlier studies have reported less uniform activation of the 3 UPR branches in metabolically active tissues (Puri et al, 2008; Sharma et al, 2008). GRP78 normally binds to the N-termini of IRE1α, PERK, and ATF6, preventing their activation. Unfolded proteins in the ER cause GRP78 to release the UPR sensors. When GRP78 is released, IRE1α and PERK oligomerize in ER membranes. Oligomerized IRE1 binds TRAF2, leading to signaling of downstream kinases that activate NF-κB and c-Jun (AP-1), causing expression of genes linked with host defense. The intrinsic ribonuclease activity of IRE1 also results in production of XBP-1, a transcription factor that induces expression of genes involved in restoring protein folding or degrading unfolded proteins. Oligomerization of PERK activates its intrinsic kinase activity, resulting in phosphorylation of eIF2α and suppression of mRNA translation. Under these conditions, only selected mRNAs, including ATF4, are translated. ATF4 induces expression of genes involved in restoring ER homeostasis. Release of GRP78 from ATF6 allows this protein to translocate to

the Golgi apparatus for proteolytic processing to release active ATF6, which controls expression of UPR genes. The expression of PERK, IRE 1α, ATF6, XBP-1 and peIF2α which were found to be elevated in our study was significantly lowered by HCA treatment.

In our study nuclear translocation of phosphorylated Nrf2 was found to be increased. It is a substrate of PERK and it acts on antioxidant response genes including HO-1 and glutathione*S*-transferase (Cullinan et al, 2003). Under unstressed conditions, Nrf2 is constantly degraded via the ubiquitin–proteasome pathway in a Keap1-dependent manner. When oxidative stress inactivates Keap1, Nrf2 is stabilized and translocated into nuclei, where it heterodimerizes with small Maf proteins that activates target genes for cytoprotection through antioxidant response element (ARE). Therefore, activation of Nrf2 is critical for cellular rescue pathways against oxidative stress (Cho et al, 2006). In response to elevation of intracellular ROS above a critical threshold, Nrf2 stimulates expression of transcription Kruppel-like factor 9 (Klf9), resulting in further Klf9-dependent increases in ROS and subsequent cell death (Zucker et al, 2014). HO-1 is a stress-inducible enzyme that catalyses the degradation of heme to biliverdin, iron, and carbon monoxide (Foresti et al, 1997). HO-1 gene expression is also regulated by the Nrf2/ARE pathway, and induction of this enzyme protects cells against oxidative stress-induced cell death and tissue injury (Chapple et al, 2012; Jeong et al, 2006). HCA was found to reduce the Nrf2 translocation and the HO-1 activity, indicating a reduction in the ER stress response.

ROS generation is important in many physiological processes; meanwhile excessive ROS production indicates cellular stress. Present study showed an increased ROS generation as well as expression of ERO 1α and PDI. Reactive oxygen species are allied with obesity related chronic inflammation, adiponectin reduction, and other metabolic dysfunctions (Furukawa et al, 2004). In our study HCA could effectively reduce the oxidative stress generated during ER stress. The link between ER stress and ROS generation (Malhotra and Kaufman, 2007; Ozgur et al, 2014; Rutkowski and Kaufman, 2007), and the molecular mechanisms by which ROS are produced during UPR have been reported by many researchers (Santos et al, 2009). ER presents, an oxidative environment that helps the oxidation of cysteines and thereby, the formation of disulfide bonds through ER-resident oxidoreductases (Tu and Weissman, 2004). It has been shown that ERO1 is a major source of ROS in the ER and the cell (Haynes et al, 2004; Tu and Weissman, 2004). Oxidative protein folding in the ER takes place, in part, by the formation of disulfide bonds by PDI. To

introduce disulfides into the proteins, PDIs is maintained in an oxidized state, and ERO1 keeps PDI oxidized and active in the ER (Frand and Kaiser, 1999). ERO1 uses molecular oxygen as the final electron acceptor and thus, forms one molecule of H_2O_2 for every disulfide that it introduces (Tu and Weissman, 2004). Accumulation of unfolded proteins in the ER elicits Ca^{2+} leakage into the cytosol, increasing ROS production in the mitochondria (Malhotra and Kaufman, 2007). As protein folding and refolding in the ER are highly energy dependent processes, ATP depletion as a result of protein misfolding may also stimulate mitochondrial oxidative phosphorylation to increase ROS production.

Increased quantities of reactive oxygen species triggers lipid peroxidation in the cellular, mitochondrial and nuclear membranes along with protein oxidation (Dinu et al, 2011). Degree of lipid peroxidation in the cells or tissues can be estimated by quantifying TBARS level and it is the most commonly used method for measuring lipid peroxidation (Devasagayam et al, 2003). Protein carbonyls are used as a marker of protein oxidation as well as oxidative stress (Dalle-Donne et al, 2003; Halliwell, 1996). Increased level of TBARS and protein carbonyls along with reduced concentration of GSH in ER stress induced cells shows the oxidative damage during ER stress. In addition to this, ER stressed cells showed reduced activities of antioxidant enzymes. Intracellular antioxidant enzymes act as first line of defense against oxidative stress in the cell. Among the various antioxidant enzymes, SOD catalyzes the dismutation of superoxide anion to H_2O_2 and molecular oxygen. H_2O_2 is decomposed to H_2O by catalase and glutathione peroxidase. In the reaction catalyzed by GPx, GSH is oxidized to oxidized glutathione (GSSG), which can be subsequently reduced back to GSH by GR (Peng and Li, 2002). Decreased activities of GSH dependent enzymes like Gpx and GR in hypertrophied cells may be due to either free radical dependent inactivation of enzyme or depletion of GSH. GSH is one of the major non enzymatic antioxidant and a powerful nucleophile critical for cellular protection activities like detoxification of ROS and control of inflammatory cytokine cascade (Abhilash et al, 2012). Depletion of GSH leads to impairment of the cellular defense against reactive oxygen species and may lead to oxidative injury (Kent et al, 2003). GSH can also act as a cofactor for glutathione S Transferase.

The overall results show that HCA treatment reduced the activation of unfolded protein response, thereby reducing the expression of UPR sensors, as well as the downstream signaling molecules. The cells were protected from oxidative stress also. As the activation of UPR is a cell – life death decision, regulation of UPR activation and consequential

maintenance of redox status may prove beneficial for cell survival.

Chapter 5

Crosstalk between ER stress and mitochondrial function in 3T3-L1 adipocytes and possible amelioration with HCA

5.1 Introduction

Endoplasmic reticulum and mitochondria are vital organelles with significant role in cellular homeostasis, and dysfunction at either site has been linked to pathophysiological states, like metabolic diseases. Although the ER and mitochondria play distinct cellular functions, these organelles also physically communicates with each other at sites called mitochondria-associated ER membranes (MAMs). These interactions are essential for calcium, lipid and metabolite exchange. ER has been found linked with almost every cellular organelle in dynamic ways. Among all of the ER partners, mitochondria might be the most prominent with regard to its role in regulating metabolism and cell survival (Vance, 1990).

ER stress response in cells is mediated by three proximal sensors of the UPR: PERK, ATF6 and the IRE1 (Prell et al, 2013). When UPR fails to adapt to the stress, the prolonged UPR initiates apoptosis by the caspase pathways (Nakagawa et al, 2000). ER and mitochondria are functionally and morphologically connected by several pathways, hence ER stress can affect mitochondrial function (Vannuvel et al, 2013). The contact between ER and mitochondria is particularly crucial for co-ordination of the calcium transfer (Rowland and Voeltz, 2012).

The main function of mitochondria is the synthesis of ATP via oxidative phosphorylation. In this process ROS is generated in normal physiological condition. The morphology of mitochondria undergoes dynamic changes regulated by fusion and fission processes. Mitochondrial dynamics play a significant role on the management of mitochondrial activity and cell metabolism (Lee et al, 2004; Liesa et al, 2009; Zorzano, 2009). Mitochondrial fusion is the assembly of individual mitochondria that combine their membranes to form larger mitochondria. This process is controlled by MFN 1 and 2 and OPA1, a member of the dynamin family of mechanoenzymes. Mitochondrial fission involves the fragmentation of tubular interconnected mitochondria into several smaller individual organelles. The outer mitochondrial membrane protein FIS1 and the GTPase,

DRP-1 are the main elements of the mitochondrial fission machinery (Parra et al, 2011).

In this chapter, we evaluated the effect of ER stress on adipocyte mitochondria emphasising on, mitochondrial function and structural dynamics. The protective effect of HCA on mitochondria during tunicamycin induced ER stress was also analysed.

5.2 Methods

Cell culture and treatments were same as described in Chapter 2. Experimental groups are

B - Control

T - Tunicamycin treated groups

H1 - Tunicamycin + HCA 5 µM

H2 - Tunicamycin + HCA 10 µM

H3 - Tunicamycin + HCA 20 µM

P - Tunicamycin + PBA 1 mM

Following parameters were analysed to investigate the alterations in mitochondrial function during ER stress in 3T3-L1 adipocytes. Detailed procedures of all the experiments are given in Chapter 2

- Mitochondrial superoxide generation
- Alteration in mitochondrial transmembrane potential ($\Delta\Psi M$)
- Integrity of mitochondrial permeability transition pore (MPTP)
- Mitochondrial mass
- Activity of aconitase, Mn SOD and Cu Zn SOD
- Activities of mitochondrial respiratory complexes
    - NADH dehydrogenase(Complex I)
    - Succinate dehydrogenate(Complex II)
    - decylubiquinol cytochrome c oxidoreductase(Complex III)
    - Cytochrome oxidase(Complex IV)
- Oxygen consumption rate and ATP content
- Intracellular calcium overload
- Mitochondrial biogenesis markers
- Mitochondrial dynamics

5.3 Results

5.3.1 Superoxide radical production in mitochondria

The mitochondrial superoxide production was monitored in 3T3-L1 cells and significant increase was detected in superoxide production (4.91 fold) compared to normal cells. HCA (5, 10, 20 µM) treated group showed less fluorescence (1.29, 1.47, 1.81 fold respectively), suggesting protective effect of the same, against superoxide production in ER stressed cells. PBA also limited the superoxide production by 2.26 fold (Figure 5.1)

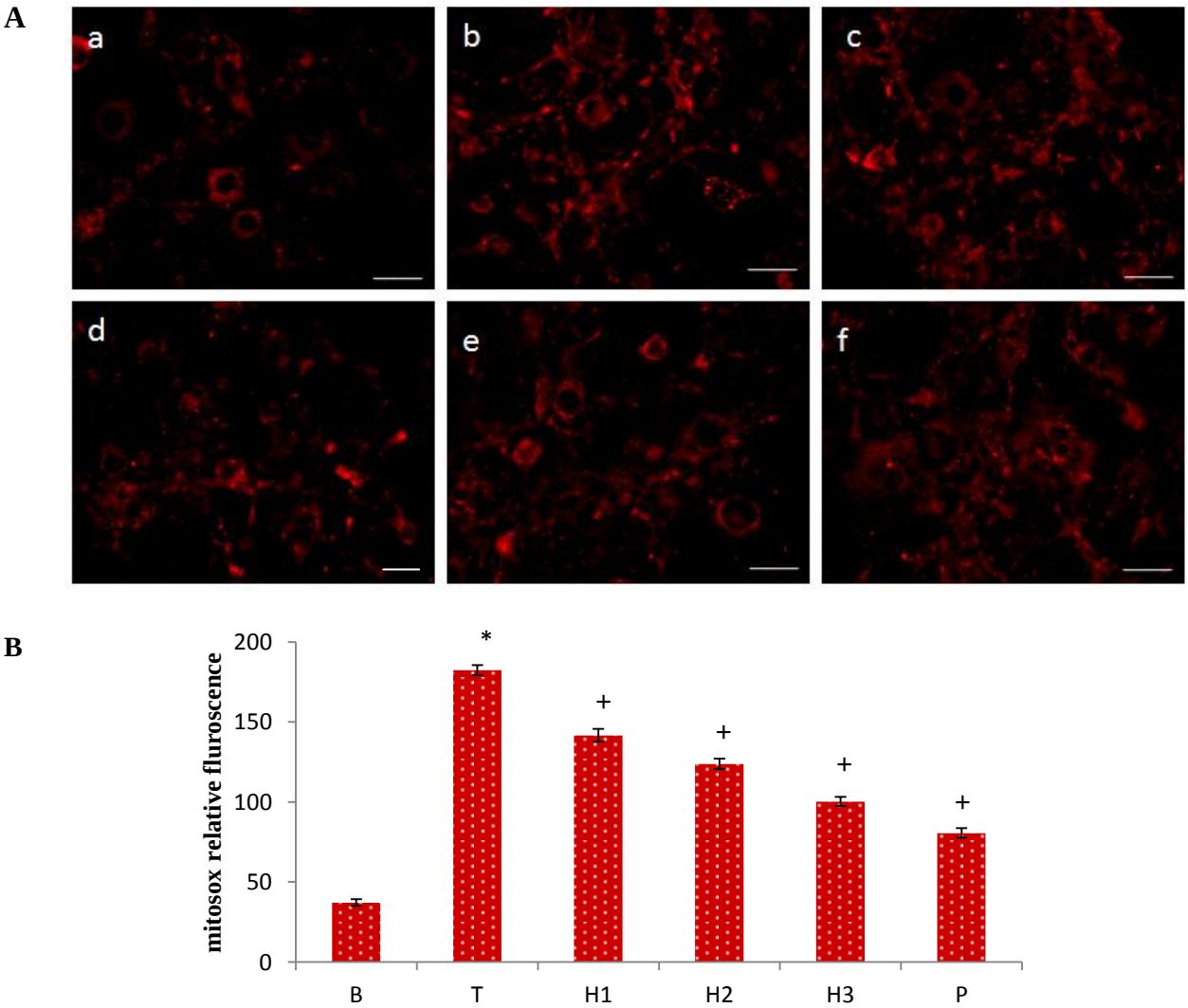

Figure 5.1 Mitochondrial superoxide production determined by mitoSOX^{TM}: A. Representative images of Mitosox fluorescence in 3T3-L1 cells (a) control, (b) tunicamycin treated, (c) tunicamycin + 5 µM (-) hydroxycitric acid, (d) tunicamycin + 10 µM (-) hydroxycitric acid, (e) tunicamycin + 20 µM (-) hydroxycitric acid, (f) tunicamycin + 1 mM PBA. Scale bar corresponds to 100 µm. B. Relative fluorescence shown by fluorimetric analysis. (B) control (T) tunicamycin, (H1) tunicamycin + 5 µM (-) hydroxycitric acid, (H2) tunicamycin + 10 µM (-) hydroxycitric acid, (H3) tunicamycin + 20 µM (-) hydroxycitric acid, (P) tunicamycin + 1 mM PBA. Values expressed as means ± SD (n = 6), represented by vertical bars.* indicates values are significantly different from the control cells and + indicates values are significantly different from the endoplasmic reticulum stressed group, significance accepted at $P \leq 0.05$.

5.3.2 Effect of HCA on activities of aconitase, Mn SOD, CuZn SOD

The activity of aconitase enzyme is sensitive to oxidative stress and superoxide radicals (Gardner et al, 1994; Gardner et al, 1995). Aconitase activity was significantly ($P \leq 0.05$) reduced in ER stressed cells (3.94 fold) when compared with control cells. HCA (5, 10, 20 µM) treatment dose dependently improved (1.49, 1.73, 2.59 fold) the activity significantly ($P \leq 0.05$) and brought back the activity near to normal. PBA also improved aconitase activity (2.39 fold, Table 5.1). Thus, inhibition of aconitase activity in ER stress indicates elevated level of mitochondria generated ROS.

MnSOD activity was reduced by 1.86 fold ($P \leq 0.05$) and Cu-ZnSOD by 2.18 fold, compared to controls. The activity of MnSOD was increased by 1.41, 1.53, 1.69 fold ($P \leq 0.05$) compared to tunicamycin treated cells on treatment with 5, 10 and 20 µM of HCA respectively(Table 5.2). Treatment with HCA (5, 10, 20 µM) increased Cu-ZnSOD activity by 1.11, 1.38 and 1.56 fold respectively relative to tunicamycin treatment (Table 5.1).

	Control	Tunicamycin	Tunicamycin + 5 µM (-) hydroxycitric acid	Tunicamycin + 10 µM (-) hydroxycitric acid	Tunicamycin + 20 µM (-) hydroxycitric acid	Tunicamycin + 1 mM PBA.
Aconitase (U/mg protein)	1.04 ± 0.05	0.26 ± 0.00*	0.39 ± 0.00^{+}	0.45 ± 0.02^{+}	0.68 ± 0.50^{+}	0.63 ± 0.05^{+}
MnSOD (U/mg protein)	3.12 ± 0.09	1.67 ± 0.02*	2.36 ± 0.20^{+}	2.57 ± 0.01^{+}	2.83 ± 0.02^{+}	2.67 ± 0.03^{+}
CuZnSOD (U/mg protein)	4.8 ± 0.30	2.22 ± 0.24*	2.47 ± 0.31^{+}	3.08 ± 0.14^{+}	3.70 ± 0.3^{+}	3.48 ± 0.11^{+}

Table 5.1 Activities of aconitase, MnSOD, CuZnSOD. Values expressed as means ± SD (n = 6).* indicates values are significantly different from the control cells and + indicates values are significantly different from the endoplasmic reticulum stressed group, significance accepted at $P \leq 0.05$.

5.3.3 Effect of HCA on mitochondrial content

Effect of HCA on mitochondrial content was determined using mitotracker red by fluorescence imaging. MitoTracker is a fluorescent dye that localizes to the mitochondrial matrix independent of the mitochondrial membrane potential and covalently binds to mitochondrial proteins by reacting with free thiol groups of cysteine residues. Fluorescence was considered relative to mitochondrial number. The decrease (2.95 fold) in the red fluorescence of mitotracker relative to control cells strongly suggests a substantial decrease in

total mitochondrial mass during ER stress (Figure 5.2). When the cells were co-treated with HCA and tunicamycin, mitochondrial mass was restored as shown by the increase in fluorescence compared to the stress induced cells. This indicates the protection of mitochondrial content by HCA during ER stress. HCA (5, 10, 20 µM) increased (1.43, 1.88, 2.74 fold) the mitochondrial mass in a dose dependent manner (Figure 5.2). PBA protected the cells from mitochondrial loss (2.72 fold).

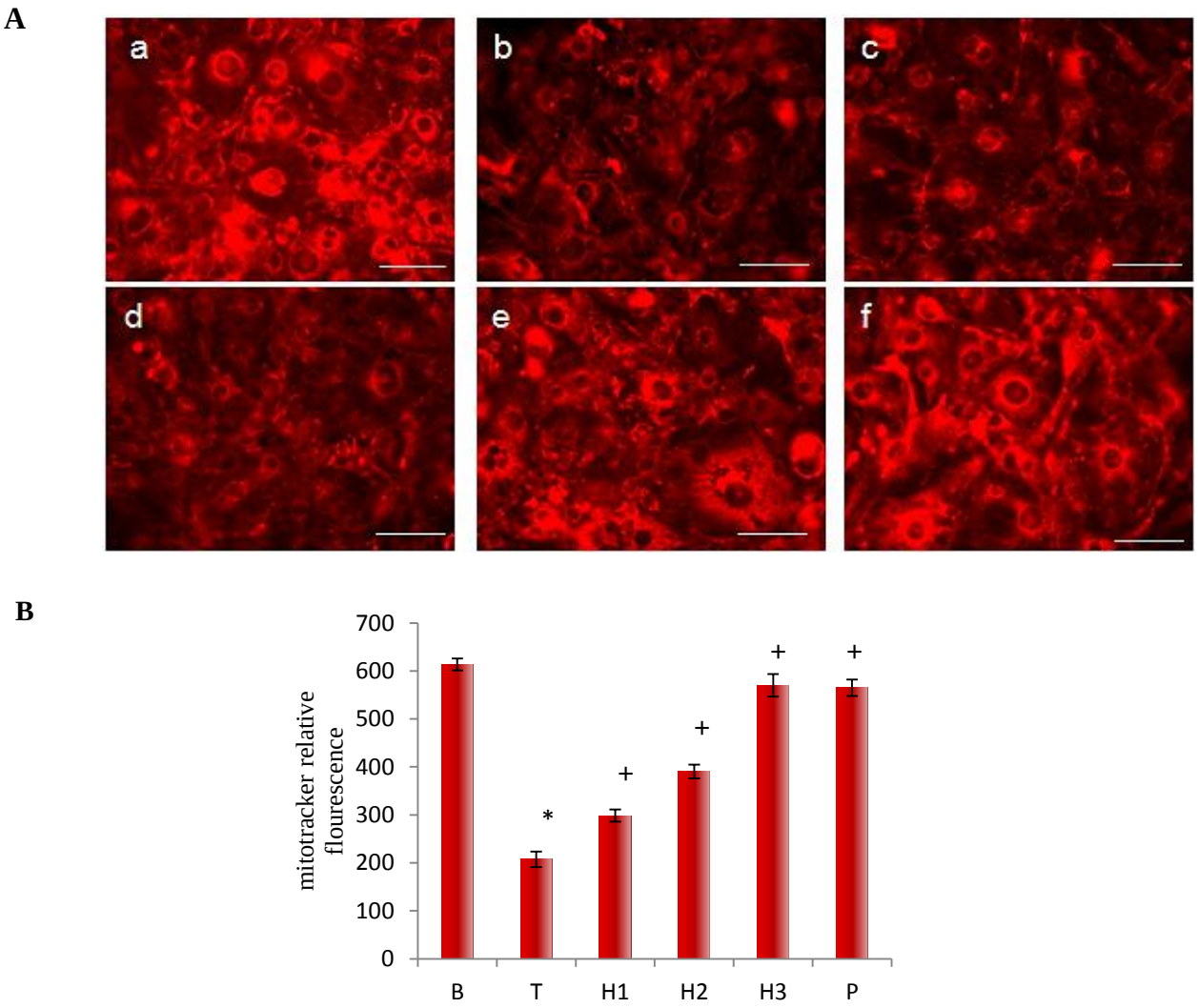

Figure 5.2 Effect of (-) hydroxycitric acid on mitochondrial mass in endoplasmic reticulum stress induced 3T3-L1 adipocytes. A. Representative images of 3T3-L1 stained with mitotracker. (a) control, (b) tunicamycin treated, (c) tunicamycin + 5 µM (-) hydroxycitric acid, (d) tunicamycin + 10 µM (-) hydroxycitric acid, (e) tunicamycin + 20 µM (-) hydroxycitric acid, (f) tunicamycin + 1 mM PBA. Scale bar corresponds to 100 µm. B. Relative fluorescence shown by fluorimetric analysis. (B) control, (T) tunicamycin, (H1) tunicamycin + 5 µM (-) hydroxycitric acid, (H2) tunicamycin + 10 µM (-) hydroxycitric acid, (H3) tunicamycin + 20 µM (-) hydroxycitric acid, (P) tunicamycin + 1 mM PBA. Values expressed as means ± SD (n = 6), represented by vertical bars.* indicates values are significantly different from the control cells and + indicates values are significantly different from the ER stressed group, significance accepted at $P \leq 0.05$.

5.3.4 Effect of HCA on ΔΨM

To understand the mechanisms involved in the ability of HCA to protect mitochondrial function in ER stressed cells, we analyzed the change in ΔΨM. Alteration in ΔΨM prevents the accumulation of JC-1 in mitochondria leading to a shift from red (JC-1 aggregates) to green fluorescence (JC-1 monomers) in ER stress induced cells. Tunicamycin decreased ($P \leq 0.05$) the red fluorescence by 4.84 fold indicative of ΔΨM dissipation, compared with vehicle treated cells (control). Treatment with 5, 10 or 20 μM of HCA resulted in a significant ($P \leq 0.05$) increase of relative red fluorescence of cells in a dose dependent manner (1.21, 2.08, 3.34 fold) compared to cells treated with tunicamycin alone, indicating that HCA prevents tunicamycin induced alteration of ΔΨM (Figure 5.3).

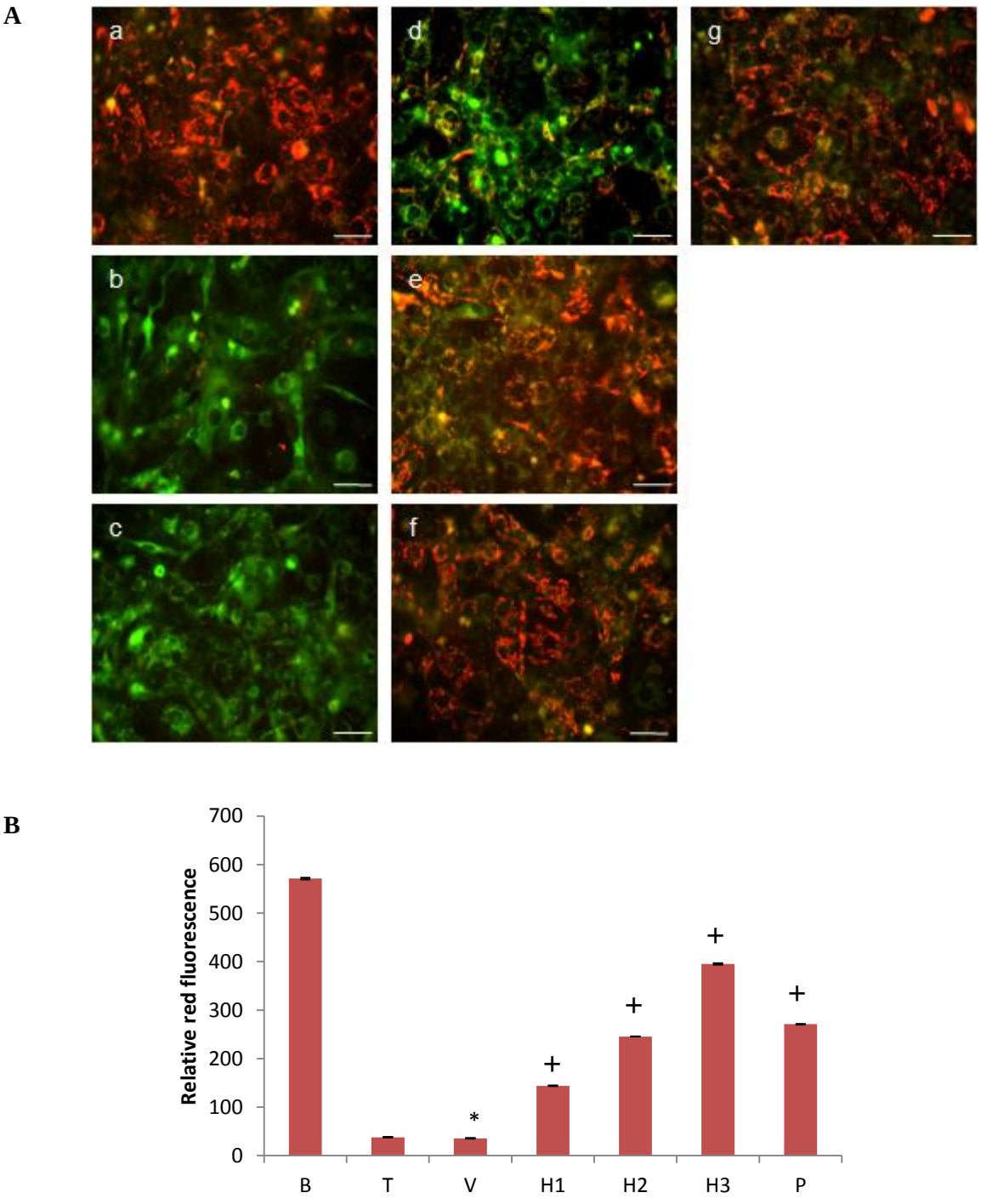

Figure 5.3 Effect of (-) hydroycitric acid on mitochondrial membrane potential in 3T3-L1 adipocytes during endoplasmic reticulum stress. A. Representative fluorescent images of 3T3-L1 adipocytes stained with JC-1, (a) control, (b) valinomycin treated (c) tunicamycin treated, (d) tunicamycin + 5 µM (-) hydroxycitric acid, (e) tunicamycin + 10 µM (-) hydroxycitric acid, (f) tunicamycin + 20 µM (-) hydroxycitric acid, (g) tunicamycin + 1 mM PBA . Scale bar corresponds to 100 µm. B. Relative red fluorescence shown by fluorimetric analysis. (B) control, (T) tunicamycin, (V) valinomycin, (H1) tunicamycin + 5 µM (-) hydroxycitric acid, (H2) tunicamycin + 10 µM (-) hydroxycitric acid, (H3) tunicamycin + 20 µM (-) hydroxycitric acid, (P) tunicamycin + 1mM PBA. Values expressed as means ± SD (n = 6), represented by vertical bars.* indicates values are significantly different from the control cells and + indicates values are significantly different from the endoplasmic reticulum stressed group, significance accepted at $P \leq 0.05$.

5.3.5 Effect of HCA on mitochondria permeability transition pore opening

The fluorescence from cytosolic calcein is quenched by the addition of $CoCl_2$, while the fluorescence from the mitochondrial calcein is maintained. This reveals a punctate pattern of mitochondrial calcein fluorescence in control cells. During ER stress, entry of excess calcium into the cells triggers mitochondrial pore activation and subsequent loss of mitochondrial calcein fluorescence. This was observed as a change in the fluorescence pattern from a mitochondrial punctuate pattern in control cells to a decreased and diffused fluorescence in stress induced cells. Treatment with HCA prevented the MPTP opening and maintained the integrity of MPTP (Figure.5.4).

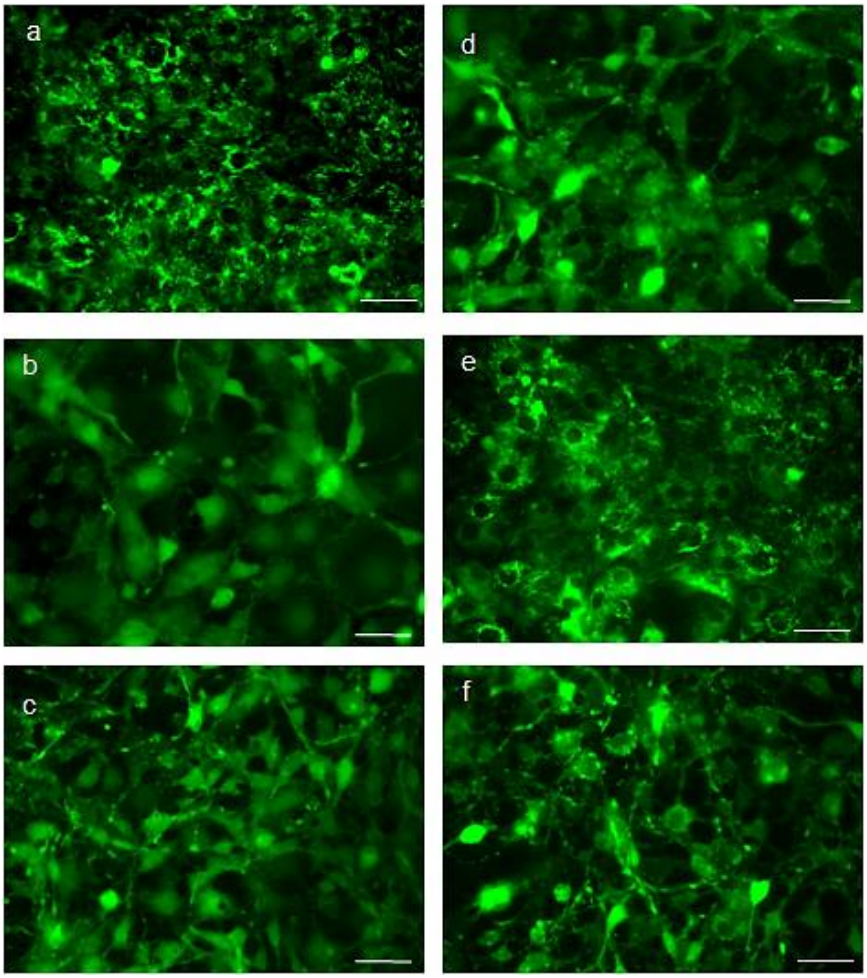

Figure 5.4 Effect of (-) hydroxycitric acid on mitochondrial permeability transition pore opening. Representative fluorescent images of 3T3-L1 stained with Calcein-$CoCl_2$. (a) control, (b) tunicamycin treated, (c) tunicamycin + 5 µM (-) hydroxycitric acid (d) tunicamycin + 10 µM (-) hydroxycitric acid, (e) tunicamycin + 20 µM (-) hydroxycitric acid, (f) tunicamycin + 1 mM PBA. Scale bar corresponds to 100 µm.

HCA on cytosolic calcium level

Calcium levels were quantified using calcium assay kit. ER stress significantly increased the cytoplasmic calcium (1.77 fold) while the cells treated with HCA (5, 10, 20 µM) showed a decrease (1.35, 1.51, 1.52 fold respectively) in calcium levels. PBA also reduced the calcium overload by 1.58 fold. These results were supported by confocal imaging data using Fura-2AM fluorescence (Figure 5.5)

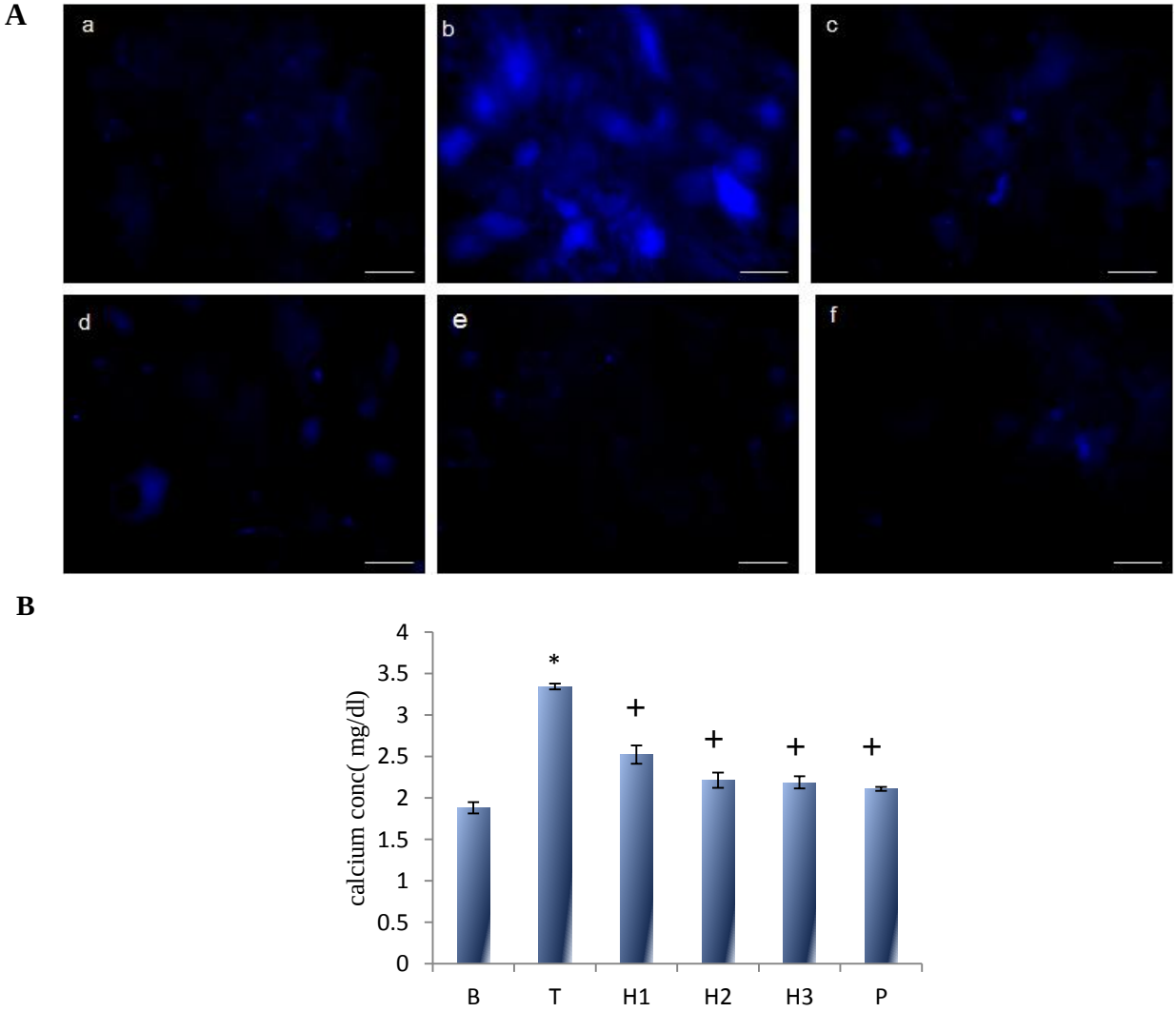

Figure 5.5 Effect of (-) hydroxycitric acid on calcium release in 3T3-L1 adipocytes during endoplasmic reticulum stress. A. Representative fluorescent images of 3T3-L1 cells stained with Fura-2 AM. (a) control, (b) tunicamycin treated, (c) tunicamycin + 5 µM (-) hydroxycitric acid (d) tunicamycin + 10 µM (-) hydroxycitric acid, (e) tunicamycin + 20 µM (-) hydroxycitric acid, (f) tunicamycin + 1 mM PBA. Scale bar corresponds to 100 µm. B. Quantification of calcium concentration. (B) control, (T) tunicamycin, (H1) tunicamycin + 5 µM (-) hydroxycitric acid, (H2) tunicamycin + 10 µM (-) hydroxycitric acid, (H3) tunicamycin + 20 µM (-) hydroxycitric acid, (P) tunicamycin + 1 mM PBA. Values expressed as means ± SD (n = 6), represented by vertical bars.* indicates values are significantly different from the control cells and + indicates values are significantly different from the endoplasmic reticulum stressed group, significance accepted at $P \leq 0.05$.

5.3.7 Effect of HCA on mitochondrial biogenesis

The mitobiogenesis in cell ELISA assay measures the specific activities of two

mitochondrial proteins, the subunit I of complex IV (cytochrome c oxidase- 1, COX-1), which is mtDNA encoded, and a subunit of complex II (succinate dehydrogenase-A, SDH-A), which is nuclear DNA-encoded. The specific activity of mtDNA encoded COX-1 was significantly ($P \leq 0.05$) depleted (1.42 fold) in ER stress group compared with control indicating, loss of mitochondrial biogenesis. The treatment with HCA (5, 10, 20 µM) significantly ($P \leq 0.05$) restored COX-1 activity (1.11, 1.21, 1.30 fold, Figure. 5.6) in a dose dependent manner, showing protection from loss of mitochondrial biogenesis. PBA restored the mitochondrial biogenesis by 1.38 fold. But there was no significant change in the activity of SDH-A, the nuclear DNA encoded protein. These results strongly support ER stress induced mitochondrial dysfunctions in adipocytes.

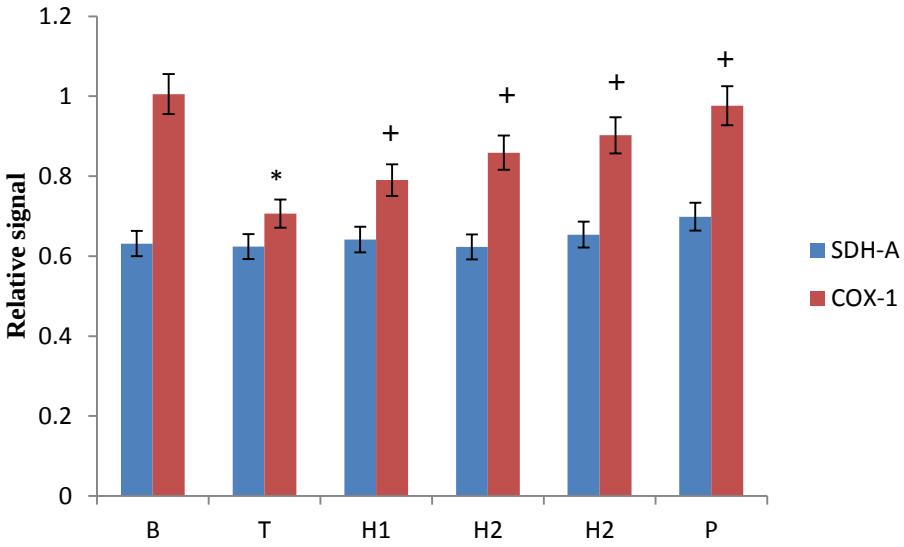

Figure 5.6 Effect of (-) hydroxycitric acid on mitochondrial biogenesis in 3T3-L1 adipocytes indicated by the expression of SDH-A and COX-1. (B) control, (T) tunicamycin, (H1) tunicamycin + 5 µM (-) hydroxycitric acid, (H2) tunicamycin + 10 µM (-) hydroxycitric acid, (H3) tunicamycin + 20 µM (-) hydroxycitric acid, (P) tunicamycin + 1 mM PBA. Values expressed as means ± SD (n = 6), represented by vertical bars.* indicates values are significantly different from the control cells and + indicates values are significantly different from the endoplasmic reticulum stressed group, significance accepted at $P \leq 0.05$.

5.3.8 Effect of HCA on mitochondrial biogenesis marker genes and mtDNA

We examined the mRNA level expression of the mitochondrial biogenesis related factors, *Pgc1a*, *Nrf1*, *mtTFA* and *Cyt b* in normal and ER stressed adipocytes. The results showed that the gene level expression of *Pgc1a*, *Nrf1*, *mtTFA* and *Cyt b* were lowered significantly ($P \leq 0.05$) in ER stress with respect to control (Figure. 5.7). Similarly qRT PCR analysis of mtDNA copy number also was found to be significantly decreased in ER stress (Figure 5.7). The treatment with HCA (5, 10, 20 µM) and PBA (1 mM) significantly ($P \leq 0.05$) restored mitochondrial biogenesis related proteins and mtDNA copy number almost

into normal level in ER stressed groups.

A

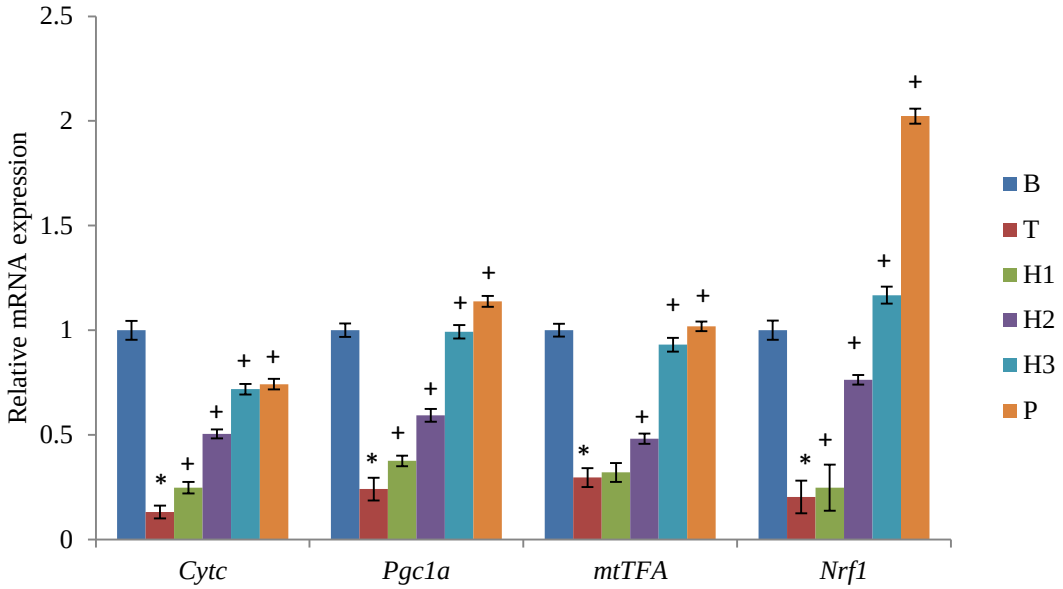

B

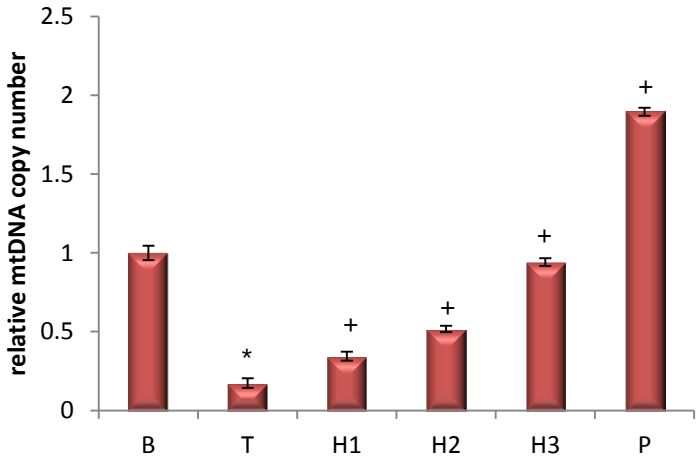

Figure 5.7 Effect of (-) hydroxycitric acid on genes involved in mitochondrial biogenesis in 3T3-L1 adipocytes during endoplasmic reticulum stress. A. mRNA expression of *Cytc*, *Pgc1α*, *mtTFA*, and *Nrf1*. B Mitochondrial DNA copy number quantified by RT PCR. (B) control, (T) tunicamycin, (H1) tunicamycin + 5 µM (-) hydroxycitric acid, (H2) tunicamycin + 10 µM (-) hydroxycitric acid, (H3) tunicamycin + 20 µM (-) hydroxycitric acid, (P) tunicamycin + 1 mM PBA. Values expressed as means ± SD (n = 6), represented by vertical bars.* indicates values are significantly different from the control cells and + indicates values are significantly different from the endoplasmic reticulum stressed group, significance accepted at $P \leq 0.05$.

5.3.9 Effect of HCA on expression of proteins involved in mitochondrial fission and fusion

An important factor mediating mitochondrial function is mitochondrial dynamics. An appropriate balance in mitochondrial fusion and fission is essential for cells to maintain normal function. We therefore investigated the expression of the fusion proteins, MFN2 and

OPA1, and fission proteins, DRP1 and FIS1 in ER stress and control cells by immunoblot analysis. The results showed a significant ($P \leq 0.05$) decrease in MFN2 and OPA1 (fusion proteins) expression and significant increase in DRP1 and FIS1 (fission proteins) in ER stressed adipocytes indicating impaired mitochondrial function. The treatment with HCA (5, 10, 20 µM) and PBA (1 mM) restored the fusion and fission proteins in normal range (Figure 5.8).

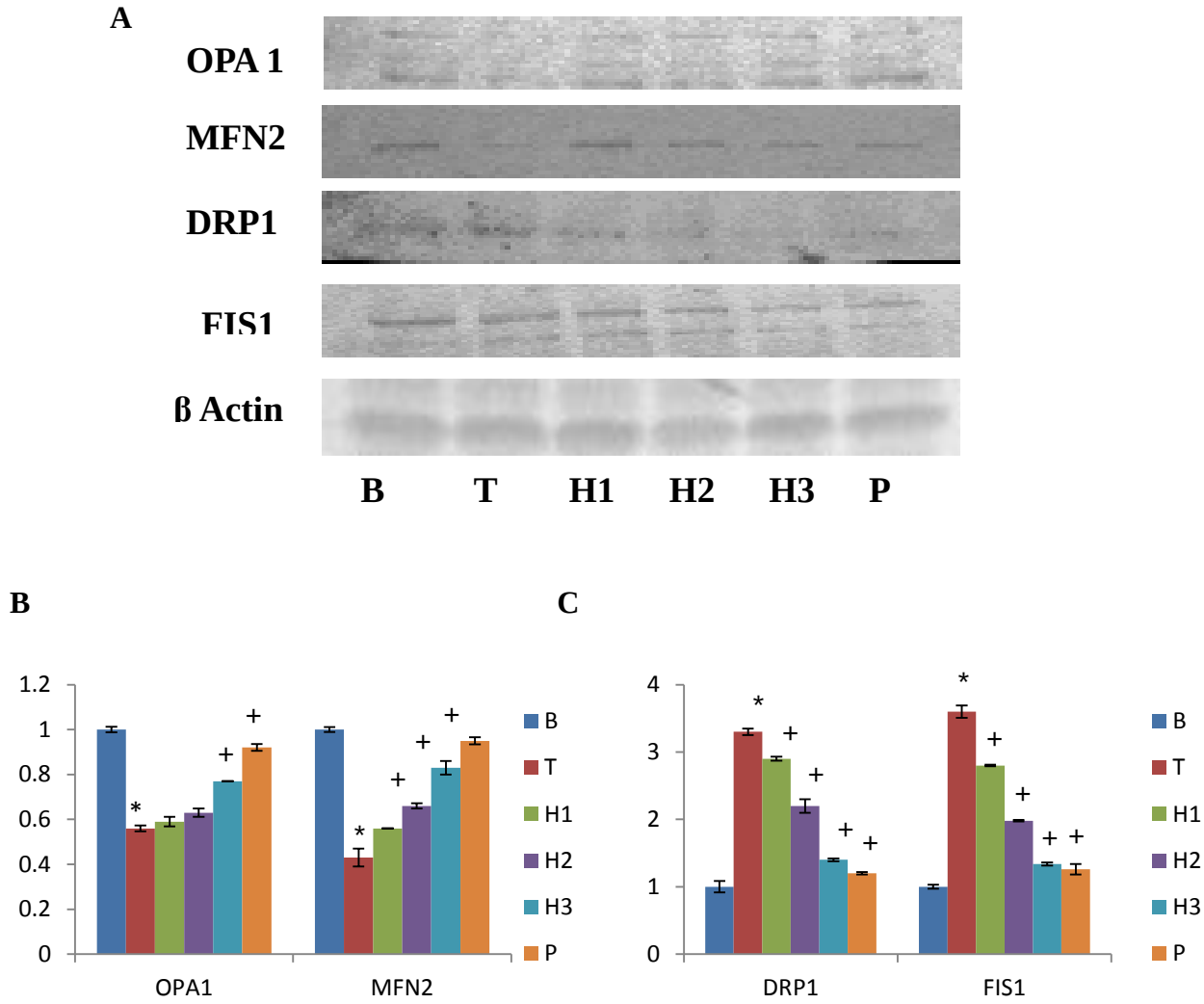

Figure 5.8 Effect of (-) hydroxycitric acid on mitochondrial dynamics in 3T3-L1 adipocytes during endoplasmic reticulum stress. A. Representative immunoblots of MFN2, OPA1, DRP1 and FIS1. B. Densitometric quantification of MFN2 and OPA1 normalised to β Actin. C. Densitometric quantification of DRP1 and FIS1 normalised to β Actin. (B) control, (T) tunicamycin, (H1) tunicamycin + 5 µM (-) hydroxycitric acid, (H2) tunicamycin + 10 µM (-) hydroxycitric acid, (H3) tunicamycin + 20 µM (-) hydroxycitric acid, (P) tunicamycin + 1 mM PBA. Values expressed as means ± SD (n = 6), represented by vertical bars.* indicates values are significantly different from the control cells and + indicates values are significantly different from the endoplasmic reticulum stressed group, significance accepted at $P \leq 0.05$.

5.3.10 Effect of HCA on oxygen consumption rate

The oxygen consumption rate (OCR) of cells is an important indicator of normal cellular function. Adipocytes under ER stress showed a decreased oxygen consumption rate

(2.9 fold) compared to the control cells (Figure 5.9). However, co-treatment of HCA dose dependently promoted oxygen consumption in cells under ER stress. In details, 5, 10, and 20 µM of HCA accelerated oxygen consumption by 1.49, 1.88, and 2.66 fold compared to the stress induced cells indicating significant ($P \leq 0.05$) protection against the defect in oxygen consumption. PBA was used as a positive control and it exhibited 3.19 fold more consumption compared to the stressed cells. Antimycin was used as a negative control.

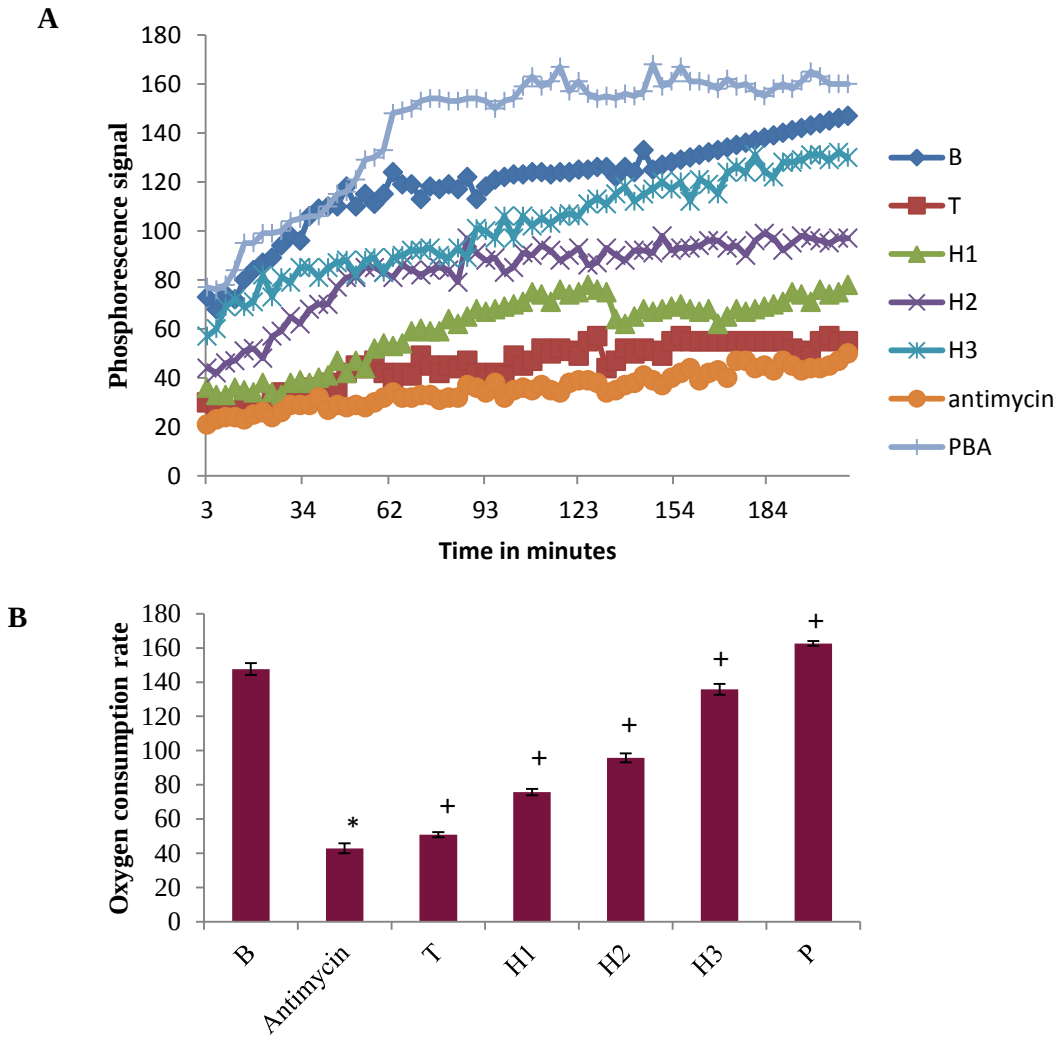

Figure 5.9 Effect of (-) hydroxycitric acid on oxygen consumption rate in 3T3-L1 adipocytes during endoplasmic reticulum stress A. Phosphorescence signal plotted against time. B. Rate of oxygen consumption calculated from the change in phosphorescence signal. (B) control, (T) tunicamycin, (H1) tunicamycin + 5 µM (-) hydroxycitric acid, (H2) tunicamycin + 10 µM (-) hydroxycitric acid, (H3) tunicamycin + 20 µM (-) hydroxycitric acid, (P) tunicamycin + 1 mM PBA. Values expressed as means ± SD (n = 6), represented by vertical bars.* indicates values are significantly different from the control cells and + indicates values are significantly different from the endoplasmic reticulum stressed group, significance accepted at $P \leq 0.05$.

5.3.11 Effect of HCA on ATP production

ATP production was significantly lowered by 3.64 fold during ER stress when compared to the normal adipocytes. On treatment with HCA (5, 10, 20 µM) ATP content was increased by 1.52, 2.6, 3.51 fold indicating significantly increased mitochondrial function. PBA also improved ATP production by 3.34 fold (Figure 5.10)

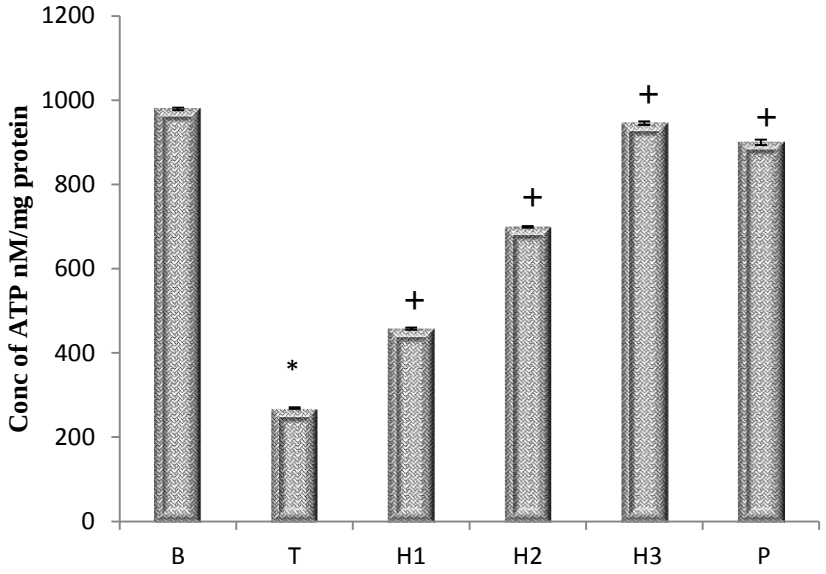

Figure 5.10 Effect of (-) hydroxycitric acid on ATP content in 3T3-L1 adipocytes during endoplasmic reticulum stress. (B) control, (T) tunicamycin, (H1) tunicamycin + 5 µM (-) hydroxycitric acid, (H2) tunicamycin + 10 µM (-) hydroxycitric acid, (H3) tunicamycin + 20 µM (-) hydroxycitric acid, (P) tunicamycin + 1 mM PBA. Values expressed as means ± SD (n = 6), represented by vertical bars.* indicates values are significantly different from the control cells and + indicates values are significantly different from the endoplasmic reticulum stressed group, significance accepted at $P \leq 0.05$.

5.3.12 Effect of HCA on electron transport chain complexes

Table.5.1 shows the activities of mitochondrial respiratory complexes in control and ER stress groups. The activities of respiratory chain complexes such as NADH dehydrogenase (Complex I), Succinate dehydrogenate (Complex II), decylubiquinol cytochrome oxidoreductase (Complex III), Cytochrome oxidase (Complex IV) were significantly decreased (1.34, 1.13, 2.42, 1.95 fold respectively) during ER stress in adipocytes ($P \leq 0.05$) compared to normal cells. PBA (1 mM) treatment prevented the reduction (1.08, 1.29, 2.10, 1.82 fold respectively) of respiratory chain complexes activities in ER stressed 3T3-L1 adipocytes ($P \leq 0.05$). HCA (5, 10, 20 µM) increased complex I activity by 1.09, 1.22, 1.24 fold, complex II activity by 1.07, 1.11, 1.12 fold, increased complex III activity by 1.21, 1.46,and 1.96 fold and complex IV activity was elevated by 1.23, 1.41, 1.76 fold.

	Complex I (NADH:ubiquinone oxidoreductase) (nm of NADH oidised/min/mg protein)	Complex II (Succinate-CoQ reductase) (nm of succinate reduced/min/mg protein)	Complex III (Cytochrome c reductase) (µM of ferricytochrome C reduced/min/mg protein)	Complex IV (Cytochrome c oxidase) (µM of ferrocytochrome C oxidized/min/mg protein)
B	71.11 ± 2.10	6.46 ± 0.84	6.43 ± 0.34	7.61 ± 0.18
T	53.06 ± 2.89*	5.70 ± 1.2*	2.65 ± 0.57*	3.90 ± 0.25*
H1	57.91 ± 1.98+	6.14 ± 0.4+	3.22 ± 0.42+	4.81 ± 0.29+
H2	64.87 ± 4.32+	6.21 ± 1.01+	3.89 ± 0.18+	5.52 ± 0.61+
H3	66.11 ± 1.45+	6.36 ± 0.59+	5.2 ± 0.46+	6.88 ± 0.41+
P	68.52 ± 5.1+	6.44 ± 0.66+	5.59 ± 0.22+	7.1 ± 0.67+

Table 5.2 Activities of mitochondrial complex enzymes. (B) control, (T) tunicamycin, (H1) tunicamycin + 5 µM (-) hydroxycitric acid, (H2) tunicamycin + 10 µM (-) hydroxycitric acid, (H3) tunicamycin + 20 µM (-) hydroxycitric acid, (P) tunicamycin + 1 mM PBA. Values expressed as means ± SD (n = 6), represented by vertical bars.* indicates values are significantly different from the control cells and + indicates values are significantly different from the endoplasmic reticulum stressed group, significance accepted at $P \leq 0.05$.

5.4 Discussion

ER and mitochondria are closely associated and play a major role in the energy homeostasis as well as critical biological functions. (Hock and Kralli, 2009). TCA cycle and β-oxidation take place in the mitochondria and chemical energy is converted into ATP and hence mitochondria are considered as "powerhouse" of the cell (Goldenthal and Marin-Garcia, 2004). The mitochondrial content in white adipose tissue is significantly less compared with brown adipose tissue. But more than 95% of cellular ATP required by adipocytes for triglyceride and adipokines synthesis and secretion, is produced by mitochondria. They also play indispensable role in many different pathways in the adipocyte physiology, including differentiation and maturation (De Pauw et al, 2009). So any alterations in mitochondrial activity may lead to malfunctions in adipocytes (Keijer and van Schothorst, 2008). Mitochondrial dysfunction is rising as a causative factor to pathogenesis of obesity.

The major contributors of mitochondrial dysfunction in obesity are ROS, ER stress, inflammation and hypoxia. The ER stress in adipocytes, is significant due to its importance in the etiology of metabolic syndrome (Vannuvel et al, 2013). The alterations in mitochondrial parameters have far-reaching consequences in the physiology of cell and this may amplify the pathologies due to ER stress (Vannuvel et al, 2013). During severe dysfunction, electron transport chain is disrupted, leading to complete depletion of ATP, resulting in cellular necrosis. Hence cell survival is highly dependent on the normal functioning of mitochondria (Bouchier-Hayes et al, 2005). In this study, the mitochondrial function parameters like mitochondrial mass, mitochondrial membrane potential, transition pore opening, oxygen consumption rate, and biogenesis markers have been evaluated during tunicamycin induced ER stress. As expected, there were significant alterations in various parameters of mitochondria. There are similar reports of altered mitochondrial functions in various cells and disease models from other laboratories (Koh et al, 2007; McInnes, 2013; Nicolson,2007) but a detailed study on mitochondria in ER stress induced 3T3-L1 adipocytes is very limited.

ER stress leads to an increased generation of ROS. As mitochondria represents the most important intracellular source of ROS, the generation of ROS during ER stress may be due to the mitochondrial dysfunction that follows. In both mitochondria and cytosol, enzymatic and non-enzymatic systems are available which serve to decrease the ROS steady state concentration. Mitochondrial superoxide levels were found to be elevated in our study. There was also a decrease in the activity of MnSOD and aconitase enzymes. Mitochondria contribute to many physiological and pathological responses by its increased superoxide production.

In the mitochondria, oxidative phosphorylation by proton translocation occurs from complexes I to II, III and IV across the inner membrane to the intermembrane space (Duchen et al, 2003). This proton gradient which drives the production of ATP by complex V (ATP synthetase) is expressed as mitochondrial membrane potential (Chen, 1988). The transfer of electrons from ubisemiquinone through the mitochondrial respiratory chain is more than 98% efficient, however, 1.5 to 2 % of electrons leak out to form superoxide anion ($O_2^{\cdot -}$) mainly at complex I (NADH coenzymeQ reductase) and III (ubiquinol cytochrome *c* reductase) (Forman, 1999). The superoxide anion is converted to H_2O_2 in mitochondria by superoxide dismutase. MnSOD is localized in the mitochondrial matrix (Weisiger and Fridovich, 1973) and CuZnSOD is found primarily in the cytosol (McCord and Fridovich, 1969). Overexpression of MnSOD protects the cells from mitochondrial

dysfunction, permeability transition and apoptosis induced by oxidative stress during various disease conditions (Kanwar et al, 2007; Klivenyi et al, 1998; Kowluru et al, 2006; Silva et al, 2005).

Metabolic homeostasis is highly depended on mitochondrial function (Nisoli et al, 2007). Although knowledge of the exact mechanism is absent, changes in ΔΨM are highly elemental to cell life-death transition. In normal cells mitochondria have a highly negative ΔΨM, approximately, -180 mV, due to the chemiosmotic gradient of protons across the mitochondrial membrane. The energy of this proton pump is used for ATP synthesis, in the respiratory chain. ΔΨM is an important measure of mitochondrial energetic state and cell viability (Chen, 1988). ΔΨM is coupled with oxidative phosphorylation to drive ATP synthesis (Liberman et al, 1969; Senior, 1988). In our study the alteration in ΔΨM was reported and HCA was shown to improve the ΔΨM. In stress conditions, an imbalance between mitochondrial calcium load and the buffer concentration of the matrix is induced. Such an imbalance causes prolonged mitochondrial calcium accumulation and opening of MPTP (Halestrap et al, 2004). Induction of ER stress in 3T3-L1 adipocytes lead to MPTP opening as shown by our results. HCA treatment showed a protective effect on the MPTP opening. During myocardial reperfusion injury, opening of the MPTP collapses ΔΨM and uncouples oxidative phosphorylation, resulting in ATP depletion and apoptosis (Beltran et al, 2000; Hausenloy and Yellon, 2003). The formation of mitochondrial ROS is dependent on ΔΨM (Korshunov et al, 1997), and increases exponentially as ΔΨM is increased or hyperpolarized above -140 mV (Lee et al, 2002).

Taking into account, the structural communication between mitochondria and ER, cellular homeostasis depends upon the functional relationship between them. In addition, ATP is required for ER to function properly, which may make it susceptible to metabolic stress. Dissemination of calcium signaling from ER to mitochondria occurs during ATP production as well as cell death (Szabadkai and Duchen, 2008). A number of studies have shown that ER stress induces mitochondrial dysfunction, thus direct to disruption of various physiological responses in the cells (Park et al, 2011). The presence of cytoplasmic calcium was increased in the ER stress condition and HCA reduced the calcium overload. Prolonged ER stress leads to release of calcium from the ER lumen, which then, causes mitochondria to uptake increased calcium into the mitochondrial matrix. Elevated calcium uptake induces an imbalance between mitochondrial calcium load and the buffering capacity of the matrix, by

which a prolonged episode of massive mitochondrial calcium accumulation occurs. Chronic calcium accumulation triggers opening of the mitochondrial permeability transition pore, resulting in swelling of the organelle, rupture of the outer mitochondrial membrane, and release of proapoptotic proteins into the cytosol (Deniaud et al, 2008). ROS are also thought to act as local messengers between the ER and mitochondria (Csordás and Hajnóczky, 2009). Many ROS sources and targets are localized to the ER and mitochondria. Elevated ROS levels inactivate the sarco-endoplasmic reticulum calcium ATPase (SERCA) and activate IP3R via oxidation. Modulation of calcium channel activity by ROS increases the level of calcium on the cytosolic face of the ER and also promotes calcium uptake into the mitochondrial matrix. Therefore, ROS production in ER provides an additional mechanism by which ER stress can induce mitochondrial dysfunction.

A reduction in mitochondrial oxygen consumption rate as well as intracellular ATP content after ER stress induction in 3T3-L1 adipocytes had been observed. ER stress is known to be associated with disturbances of ATP synthesis resulting from depressed functions of electron transport and oxidative phosphorylation in the respiratory chain (Malhotra and Kaufman, 2007). The mitochondrial membrane potential provides the driving force for ATP synthesis. In this study we found a dissipation of $\Delta\Psi M$ which ultimately might lead to disruption of ETC, ATP synthesis and oxygen consumption.

ER stress initiated mitochondrial depolarization and MPTP opening and these were followed by the loss of mitochondrial mass (Lin et al, 2012; Wang et al, 2011). Mitochondrial mass was observed to be reduced in our study also. And HCA had a protective effect on the loss of mitochondria. Decreased mitochondrial mass, activity and mtDNA copy number have been reported in murine ob/ob, db/db, and diet induced obesity models (Choo et al, 2006; Rong et al, 2007). Negative correlation between degree/severity of obesity and expression and activity of mitochondrial oxidative phosphorylation components have also been observed in human subjects (Kaaman et al, 2007). Studies have shown that improvement in mitochondrial function can protect mice against diet induced obesity (Vernochet et al, 2012).

Defect in mitochondrial function and biogenesis in subcutaneous adipose tissue have been reported in type 2 diabetes (Bogacka et al, 2005), obesity (Semple et al, 2004) and IR (Hammarstedt et al, 2003). In our study we analysed, how ER stress affects the major factors involved in mitochondrial biogenesis. Adipose mitochondrial biogenesis was significantly

lowered in both mouse models of diabetes/obesity and globally induced by rosiglitazone. (Rong et al, 2007). Our results demonstrated that ER stress reduced the level of biogenesis markers and HCA enhanced the expression of *Pgc-1a*, a master regulator of the transcriptional network that regulates mitochondrial biogenesis, its downstream molecules Nrf1, tfam, and mtDNA, in 3T3-L1 adipocytes. *Pgc-1a* activates the transcription of genes involved in oxidative phosphorylation and mtDNA replication. *Pgc-1a* also activates *Nrf-1* and *Nrf-2*, which are transcription factors acting on nuclear genes coding for proteins necessary for the mitochondrial respiratory chain or for mtDNA transcription and replication. *Pgc-1a* and *Nrf*s coactivate the expression of *Tfam*, which is vital for regulation and maintenance of mtDNA copy number (Hock et al, 2009; Lagouge et al, 2006; Scarpulla, 2008).

Mitochondria constantly fuse and divide, by processes known as fusion and fission, leading to dynamic networks of mitochondria. The occurrence of fusion and fission events is balanced to maintain the overall morphology of the mitochondrial population (Chan, 2006; Suen, 2008). A high fusion-to-fission ratio leads to elongated, tubular, interconnected mitochondrial networks, whereas a low ratio results in fragmented, discontinuous mitochondria. These two opposing processes are finely regulated by the mitochondrial fusion proteins MFN 1 and 2 and OPA 1 and by the mitochondrial fission proteins DRP1 and FIS1. Recent work has highlighted the importance of mitochondrial fusion and fission in cellular function and animal physiology (Detmer and Chan, 2007; Suen, 2008). During ER stress the fusion proteins decreased while fission proteins were increased.

Mitochondria are vital for cell function and survival, thus, it is not surprising that the loss of integrity of these organelles is associated with several pathological conditions. To date, great advances have been made to improve the knowledge of the link between mitochondrial dysfunction and metabolic diseases and different therapeutic approaches have been developed to reestablish normal function of the organelles and restore cellular homeostasis. Overall results of this chapter provide a new insight into ER stress induced impairment of mitochondrial function in 3T3-L1 adipocytes and possible recovery with HCA. Induction of ER stress significantly increased mitochondrial superoxide production. Excessive ROS production impaired mitochondrial membrane potential, led to transition pore opening, ER stress also reduced mitochondrial biogenesis, oxygen consumption, ATP synthesis, and proteins involved in oxidative phosphorylation. Mitochondrial fusion/fission

balance in adipocytes was also impaired during ER stress. Calcium signalling as well as ROS production connects mitochondria and ER function. HCA protected the 3T3-L1 adipocytes from the unfavourable effects of ER stress by enhancing mitochondrial biogenesis, mitochondrial functional performance and by controlling mitochondrial dynamics. In conclusion, ER stress impaired mitochondria functions in differentiated 3T3-L1 cells. Phytochemical treatment partially recovered the ER stress mediated mitochondrial dysfunction, suggesting that ER is an important cell organelle in the normal energy metabolism due to its strong link with mitochondrial function and natural products with potent property might be useful for treating metabolic syndrome.

Chapter 6

ER Stress induced inflammation and IR in 3T3-L1 and possible attenuation with HCA

6.1 Introduction

Obesity is associated with chronic, low grade, inflammatory responses in metabolically active sites, most notably, adipose tissue (Hotamisligil, 2006). This, increased chronic inflammatory status triggered by metabolic signals, which differs from the classic inflammation, is a critical link between obesity and other associated pathologies, such as IR and T2DM (Wellen et al, 2005; Wellen et al, 2007). The inflammatory role of adipocytes is related to its expansion, ie, hyperplasia and hypertrophy. This involves a variety of cellular stresses like ER stress, mitochondrial dysfunction, oxidative stress etc.

ER stress induced inflammation exacerbates conditions such as diabetes, obesity, atherosclerosis, and cancer. When activated, all three sensors of the UPR, PERK, IRE1, and ATF6, participate in upregulating inflammatory processes by activating NFkb. Furthermore, activation of the JNK–AP-1 and NFkB–Ik-B pathways plays a central role in obesity induced inflammation and metabolic abnormalities, including abnormal insulin action. Ozcan et al demonstrated that obesity causes ER stress leading to suppression of insulin receptor signaling through hyperactivation of JNK and subsequent serine phosphorylation of IRS-1(Ozcan et al, 2004).

Adipokines act locally as well as systemically regulating carbohydrate and lipid metabolism, immune function etc. Leptin, adiponectin, and resistin, are among the common adipokines but in fat-overloading, adipocytes secrete additional inflammatory cytokines and free fatty acids (Kershaw and Flier, 2004). They attract more macrophages (Weisberg et al, 2003), which get embedded into adipose tissues. Thus, cluster of macrophages with adipocytes form crown-like structures (CLSs) which are more inflammatory. The adipocyte hypertrophy behaves as source and target of inflammatory signals. It induces expression of TNF-α, IL-6, IL-1β, PG-E2, etc (Apovian et al, 2008).

In this chapter, we mainly discuss on the crosstalk between ER stress induced inflammation, and IR in 3T3-L1 adipocytes and possible reversal with HCA.

6.2 Methods

Cell culture and treatments were same as described in Chapter 2. Experimental groups are

B - Control

T - Tunicamycin treated groups

H1 - Tunicamycin + HCA 5μM

H2 - Tunicamycin + HCA 10μM,

H3 - Tunicamycin + HCA 20μM,

P - Tunicamycin + PBA 1mM.

Following parameters were analysed to investigate the effect of HCA on ER stress induced inflammation and IR in 3T3-L1 adipocytes. Detailed procedures of all the experiments are given in Chapter 2

- Secretion of adiponectin, leptin
- Expression of resistin
- Secretion of inflammatory cytokines
- Glucose uptake
- Intermediates of inflammatory and insulin signaling pathways
- TG content
- Lipolysis

6.3 Results

6.3.1 Effect of HCA on secretion and expression of adiponectin

Adipocytes behave as a rich source of adipokines, which may be the link between obesity and its complications. Endoplasmic reticulum stress in adipocytes can modulate adipokines secretion. Adiponectin, leptin, resistin etc are some of the important adipokines with significant physiological functions. Adiponectin levels in the culture medium were quantified using ELISA method. ER stress reduced the secretion of adiponectin by about 2.5 fold ($P \leq 0.05$) compared to control. HCA (5, 10, 20 μM) increased the adiponectin secretion by 1.89, 2.10, 2.24 fold respectively ($P \leq 0.05$) relative to stress induced cells in a dose dependent manner (Figure 6.1A). The protein level (Figure 6.1B) and mRNA (Figure 6.1C) expression studies also gave confirming results.

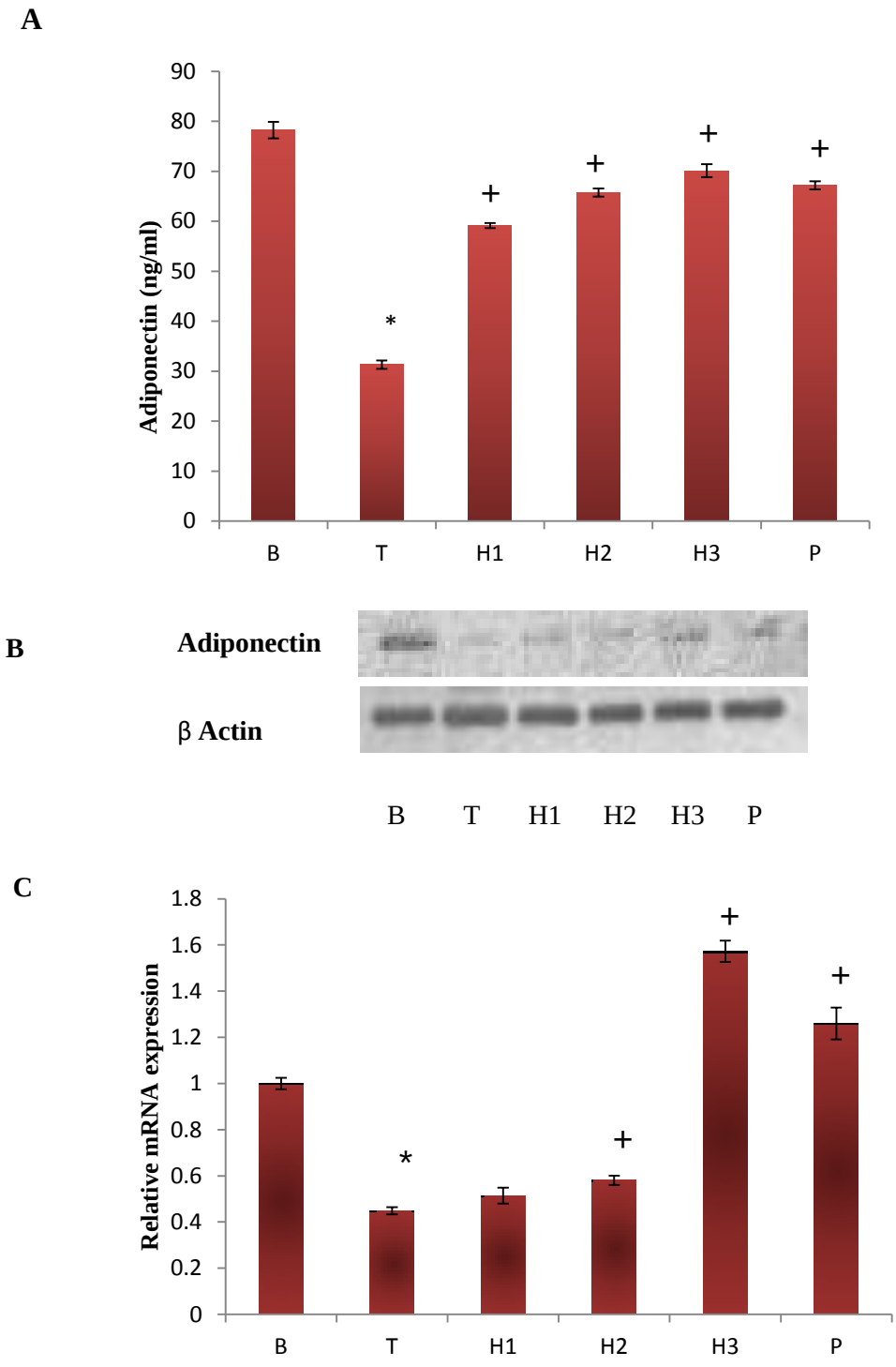

Figure 6.1 Adiponectin secretion and expression in 3T3-L1 adipocytes during endoplasmic reticulum stress. A. Quantification of adiponectin secretion by ELISA. B. Representative immunoblot of adiponectin. C. mRNA quantification normalised to β Actin. (B) control, (T) tunicamycin, (H1) tunicamycin + 5 µM (-) hydroxycitric acid, (H2) tunicamycin + 10 µM (-) hydroxycitric acid, (H3) tunicamycin + 20 µM (-) hydroxycitric acid, (P) tunicamycin + 1 mM PBA. Values expressed as means ± SD (n = 6), represented by vertical bars.* indicates values are significantly different from the control cells and + indicates values are significantly different from the endoplasmic reticulum stressed group, significance accepted at $P \leq 0.05$.

6.3.2 Effect of HCA on expression of leptin and resistin

The amount of leptin secreted into the medium was increased (3.1 fold) significantly ($P \leq 0.05$) under ER stress relative to the control. Treatment with HCA (5, 10, 20 μM) lowered the leptin levels by 1.29, 2.3, 2.8 fold respectively in a dose dependent manner ($P \leq 0.05$) (Figure 6.2A) when compared with tunicamycin treated cells. mRNA expression of resistin was also assessed. ER stress caused a significant increase in resistin levels while HCA treatment reduced the mRNA expression in a significant manner (Figure 6.2B).

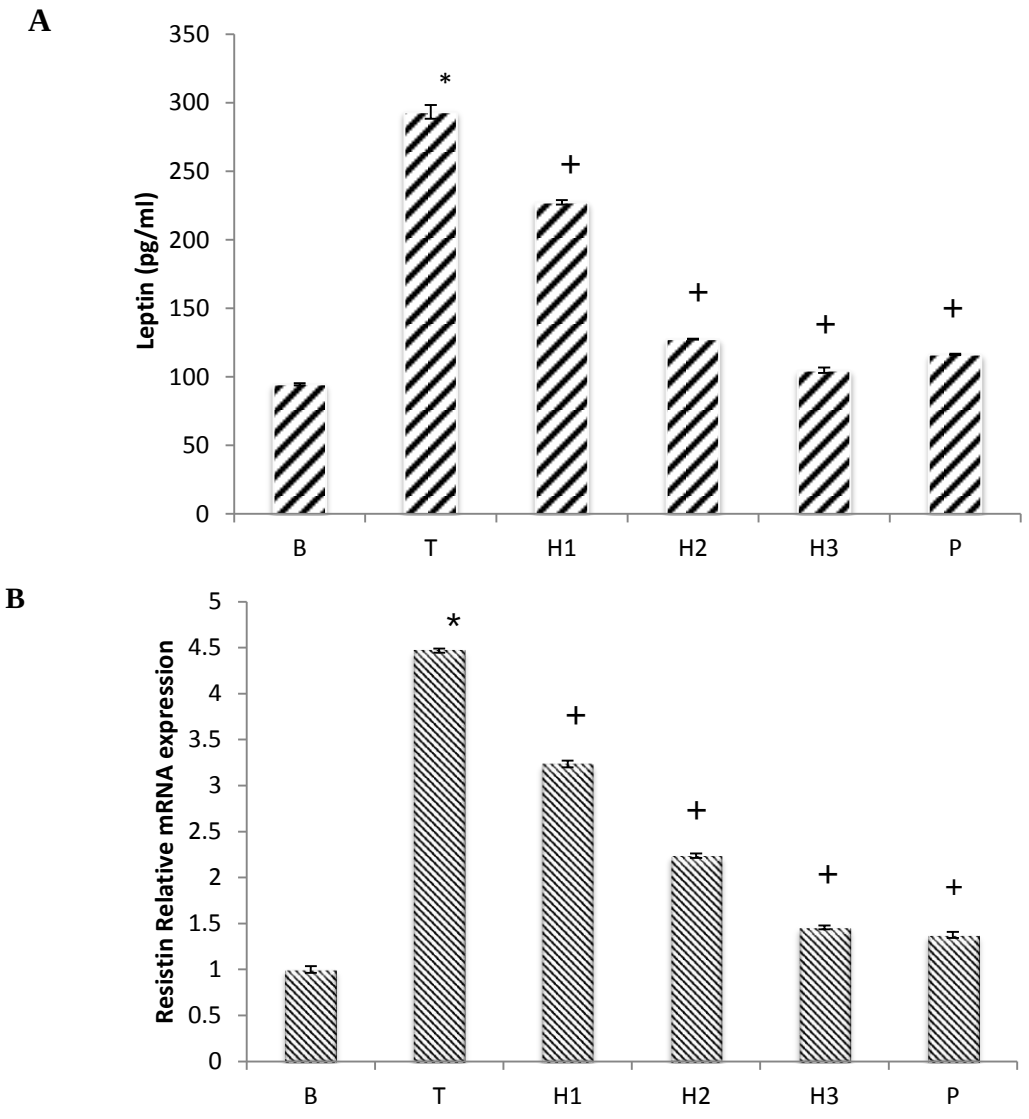

Figure 6.2 secretion of leptin and mRNA expression of resistin during endoplasmic reticulum stress in 3T3-L1 adipocytes. A. Quantification of leptin secretion by ELISA. B. mRNA expression of resistin normalised to β Actin (B) control, (T) tunicamycin, (H1) tunicamycin + 5 μM (-) hydroxycitric acid, (H2) tunicamycin + 10 μM (-) hydroxycitric acid, (H3) tunicamycin + 20 μM (-) hydroxycitric acid, (P) tunicamycin + 1 mM PBA. Values expressed as means ± SD (n = 6), represented by vertical bars.* indicates values are significantly different from the control cells and + indicates values are significantly different from the endoplasmic reticulum stressed group, significance accepted at $P \leq 0.05$.

6.3.3 Effect of HCA on inflammatory response during ER stress

Adipocytes over secrete inflammatory cytokines in response to stress conditions. ER stress caused significant increase in the level of inflammatory cytokines TNF-α, MCP-1, IL-10, IFNγ, IL-1 β, and IL-6 (Table 6.1) when compared with control cells. HCA (5, 10, 20 μM) was found to reduce the inflammatory markers in the stressed cells in a dose dependent manner compared to the stress induced cells (Table 6.1). TNF-α was increased significantly ($P \leq 0.05$) by 6.55 fold and reduced by 1.94, 4.02 and 6.25 fold respectively on treatment with HCA. The level of MCP-1 was increased significantly ($P \leq 0.05$) by 2.86 fold, which was reduced by 1.33, 1.91 and 2.13 fold respectively (Table 6.1). The secretion of IL-10 was increased by 1.87 fold ($P \leq 0.05$) and was decreased by 1.02, 1.10, and 1.25 fold on treatment with various concentration of HCA (Table 6.1). There was 4.18 fold increase in IFNγ while treatment with HCA (5, 10, 20μM) lowered the levels significantly ($P \leq 0.05$) by 2.08, 2.64, 2.76 fold respectively (Table 6.1). IL-1 β was elevated significantly ($P \leq 0.05$) by 2.033 fold and was reduced by 1.5, 1.81 and 1.92 fold on treatment with HCA (5, 10, 20 μM, Table 6.1). IL-6 was increased by 2.97 fold in stress induced cells and HCA treatment caused a significant ($P \leq 0.05$) decrease by 1.86, 2.11, 2.22 fold with 5, 10, 20 μM doses respectively (Table 6.1).

	Control	Tunicamycin	Tunicamycin + 5 µM (-) hydroxycitric acid,	Tunicamycin + 10 µM (-) hydroxycitric acid,	Tunicamycin + 20 µM (-) hydroxycitric acid,	Tunicamycin+1mM PBA.
TNFα (pg/100µl)	33.46 ± 0.56	219.40 ± 0.59*	112.54 ± 1.06^{+}	54.46 ± 0.49^{+}	35.06 ± 0.07^{+}	36.07 ± 0.55^{+}
MCP-1 (pg/100µl)	396.54 ± 1.16	1134.63 ± 2.8*	852.45 ± 02.5^{+}	591.15 ± 1.3^{+}	530.54 ± 1.7^{+}	565 ± 0.33^{+}
IL-10 (pg/100µl)	19.28 ± 0.177	36.12 ± 0.93*	35.40 ± 1.6^{+}	32.57 ± 0.33^{+}	28.79 ± 0.85^{+}	22.46 ± 0.63^{+}
IFN-γ (pg/100µl)	24.46 ± 0.212	102.32 ± 0.56*	49.10 ± 1.38^{+}	38.75 ± 0.50^{+}	36.96 ± 0.48^{+}	32.67 ± 1.41^{+}
IL-1β (pg/100µl)	753.50 ± 1.16	1582.50 ± 2.82*	1024.00 ± 2.54^{+}	840.9 ± 1.37^{+}	795.95 ± 1.7^{+}	927 ± 0.63^{+}
IL-6 (pg/100µl)	312.12 ± 1.5	928.37 ± 1.96*	498.37 ± 0.49^{+}	439.62 ± 1.11^{+}	417.12 ± 0.69^{+}	322.15 ± 0.63^{+}

Table 6.1 Quantification of inflammatory cytokines secreted by 3T3-L1 adipocytes during endoplasmic reticulum stress. Values expressed as means ± SD (n = 6), represented by vertical bars.* indicates values are significantly different from the control cells and # indicates values are significantly different from the ER stressed group, significance accepted at $P \leq 0.05$.

6.3.4 Effect of HCA on nitrite levels

Nitrite levels were significantly increased (2.79 fold, $P \leq 0.05$) in ER stressed cells compared to the control cells. HCA treatment effectively reduced the nitrite levels by 1.54, 2.07 and 4.16 fold respectively with 5, 10, 20 µM concentrations. PBA also reduced the nitrite levels by 3.2 fold (Figure 6.3).

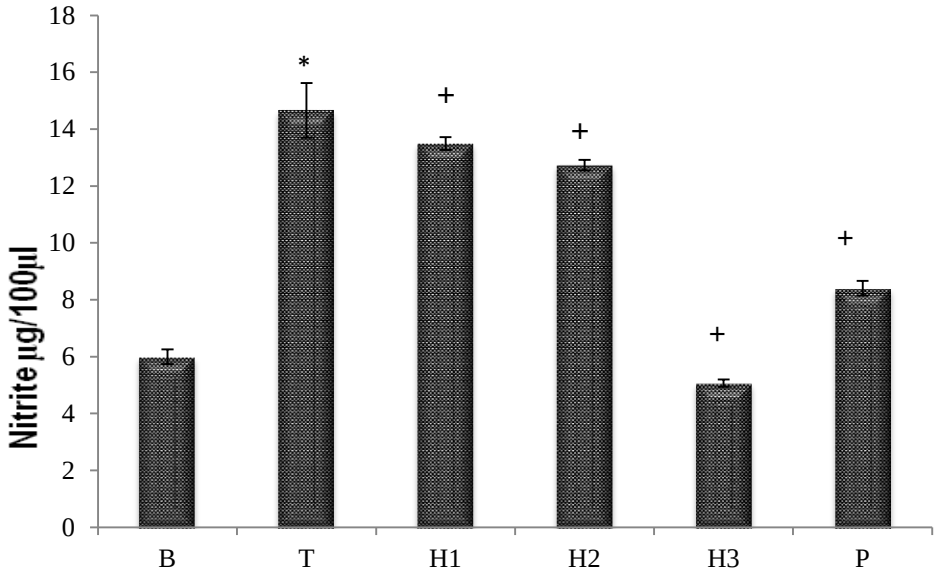

Figure 6.3 Quantification of nitrite levels secreted by 3T3-L1 adipocytes during endoplasmic reticulum stress. (B) control, (T) tunicamycin, (H1) tunicamycin + 5 µM (-) hydroxycitric acid, (H2) tunicamycin + 10 µM (-) hydroxycitric acid, (H3) tunicamycin + 20 µM (-) hydroxycitric acid, (P) tunicamycin + 1 mM PBA. Values expressed as means ± SD (n = 6), represented by vertical bars.* indicates values are significantly different from the control cells and + indicates values are significantly different from the endoplasmic reticulum stressed group, significance accepted at $P \leq 0.05$.

6.3.5 Effect of HCA on nuclear translocation of NF kB-p65

NF κB p65- translocation to the nucleus was examined by performing ELISA assay of the cytosolic and nuclear fractions of normal and ER stress induced cells. Induction of ER stress caused significant ($P \leq 0.05$) increase (1.5 fold) in nuclear fraction of p65 subunit compared to control group (Fig.6.4). The treatment with HCA (5, 10 and 20 µM)) significantly ($P \leq 0.05$) prevented (1.03, 1.12, 1.29 fold respectively) the ER stress induced nuclear translocation of p65 subunit in adipocytes (Figure. 6.4). PBA also reduced the nuclear translocation by 1.53 fold (Figure 6.4).

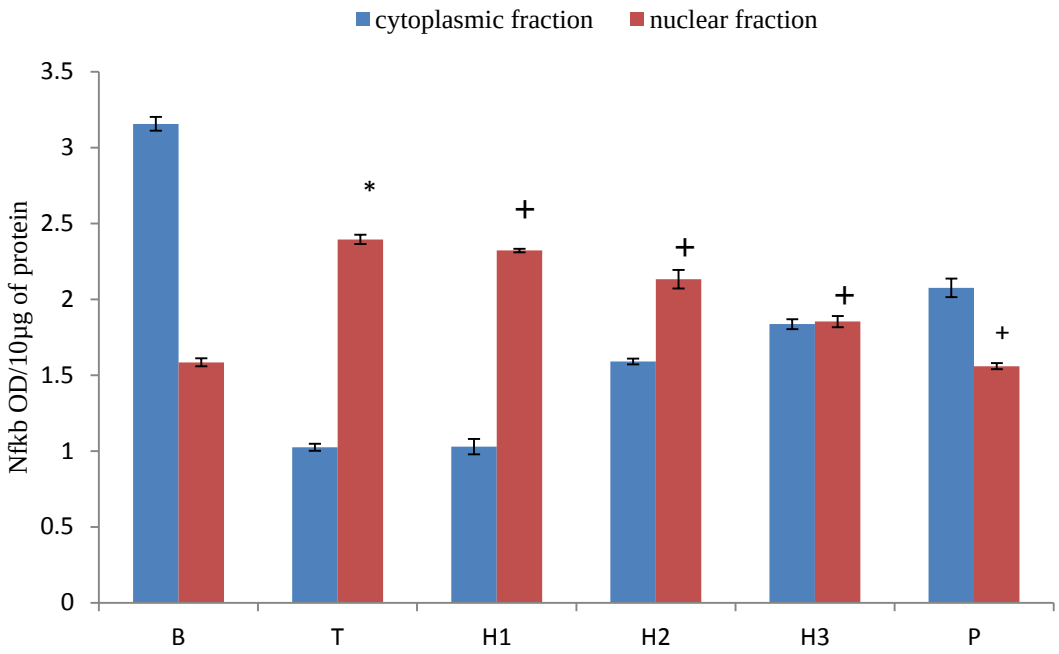

Figure 6.4 Nuclear translocation of NF kB p65 in 3T3-L1 adipocytes during endoplasmic reticulum stress. (B) control, (T) tunicamycin, (H1) tunicamycin + 5 µM (-) hydroxycitric acid, (H2) tunicamycin + 10 µM (-) hydroxycitric acid, (H3) tunicamycin + 20 µM (-) hydroxycitric acid, (P) tunicamycin + 1 mM PBA. Values expressed as means ± SD (n = 6), represented by vertical bars.* indicates values are significantly different from the control cells and + indicates values are significantly different from the endoplasmic reticulum stressed group, significance accepted at $P \leq 0.05$.

6.3.6 Effect of HCA on glucose uptake in ER stress

Flow cytometry was performed to examine glucose uptake in ER stress and control adipocytes by detecting the fluorescence of 2-NBDG within the cells. The results indicated that ER stress significantly ($P \leq 0.05$) decreased insulin dependent glucose uptake in adipocytes (Figure 6.5). In the 2-NBDG uptake assay, glucose uptake was found to be reduced by 1.54 fold in ER stressed adipocytes. Treatment with HCA and PBA resulted in an increased insulin dependent glucose uptake in ER stressed adipocytes. 20 µM of HCA and PBA elevated the glucose uptake by 1.21 fold and 1.28 fold respectively ($P \leq 0.05$, Figure. 6.5B).

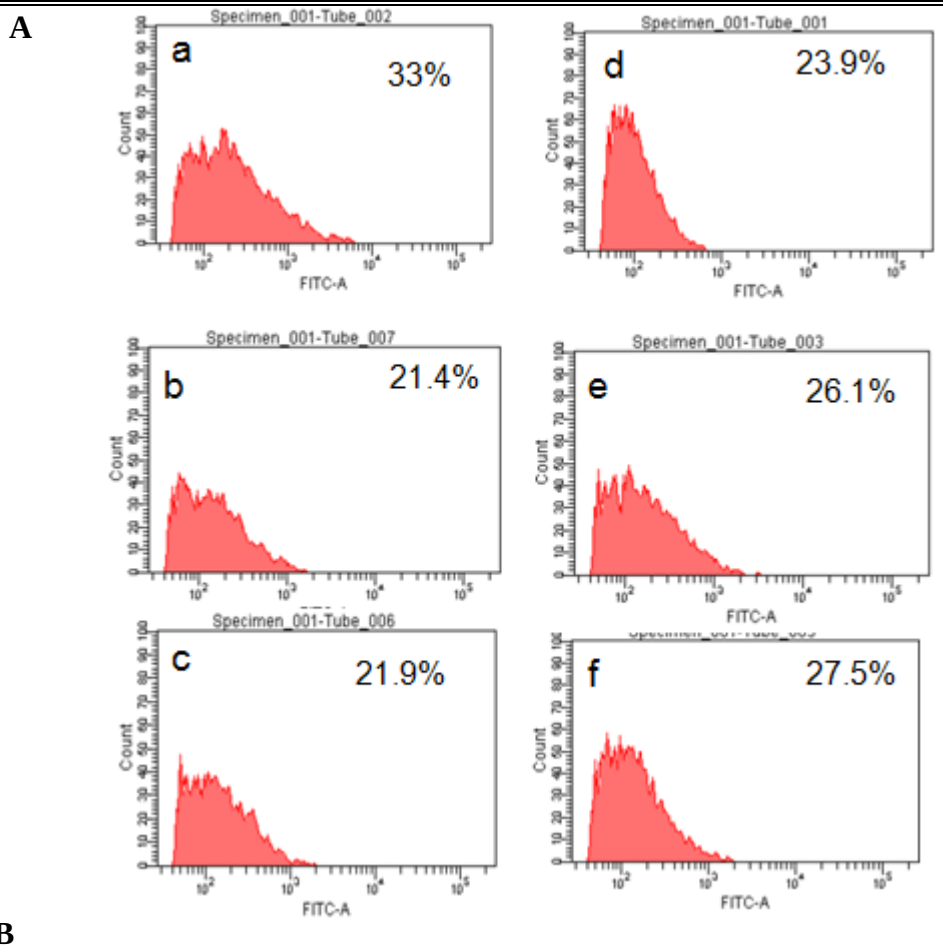

Figure 6.5 Glucose uptake in 3T3-L1 adipocytes during endoplasmic reticulum stress quantified using NBDG by flow cytometry. A. Representative histograms of glucose uptake quantified using flow cytometry (a) control, (b) tunicamycin treated, (c) tunicamycin + 5 µM (-) hydroxycitric acid, (d) tunicamycin + 10 µM (-) hydroxycitric acid, (e) tunicamycin + 20 µM (-) hydroxycitric acid, (f) tunicamycin + 1 mM PBA. B. Percentage population of cells showing NBDG fluorescence (B) control, (T) tunicamycin, (H1) tunicamycin + 5 µM (-) hydroxycitric acid, (H2) tunicamycin + 10 µM (-) hydroxycitric acid, (H3) tunicamycin + 20 µM (-) hydroxycitric acid, (P) tunicamycin + 1 mM PBA. Values expressed as means ± SD (n = 6), represented by vertical bars.* indicates values are significantly different from the control cells and + indicates values are significantly different from the endoplasmic reticulum stressed group, significance accepted at $P \leq 0.05$.

6.3.7 Effect of HCA on lactate release

Lactate levels in the culture media were quantified. Induction of ER stress significantly reduced the amount of lactate released into the media (3.05 fold, $P \leq 0.05$). On treatment with HCA (5, 10, 20 µM) the lactate levels were increased by 1.33, 1.74 and 2.99 fold respectively ($P \leq 0.05$). PBA, which was used as a positive control also showed a lactate lowering effect by 2.22 fold (Figure 6.6).

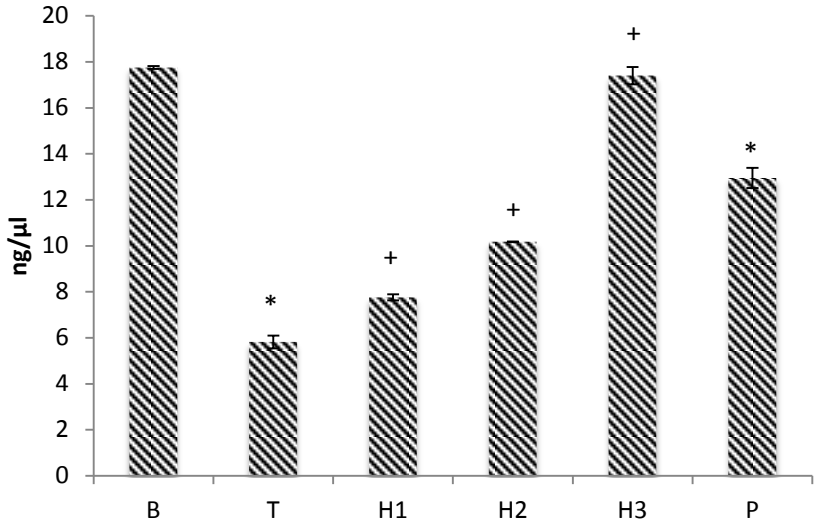

Figure 6.6 Lactate release by adipocytes during endoplasmic reticulum stress. (B) control, (T) tunicamycin, (H1) tunicamycin + 5 µM (-) hydroxycitric acid, (H2) tunicamycin + 10 µM (-) hydroxycitric acid, (H3) tunicamycin + 20 µM (-) hydroxycitric acid, (P) tunicamycin + 1 mM PBA. Values expressed as means ± SD (n = 6), represented by vertical bars.* indicates values are significantly different from the control cells and + indicates values are significantly different from the endoplasmic reticulum stressed group, significance accepted at $P \leq 0.05$.

6.3.8 Effect of HCA on expression of glucose transporters

We further analysed the expression of glucose transporters, GLUT1 and GLUT4 in control and ER stressed groups. GLUT4 and GLUT1 expression at protein level (Figure. 6.7A) and mRNA level (Figure. 6.7B) was significantly ($P \leq 0.05$) downregulated in ER stressed adipocytes compared with normal cells. HCA treatment significantly ($P \leq 0.05$) increased the expression (Figure. 6.7A and 6.7B)

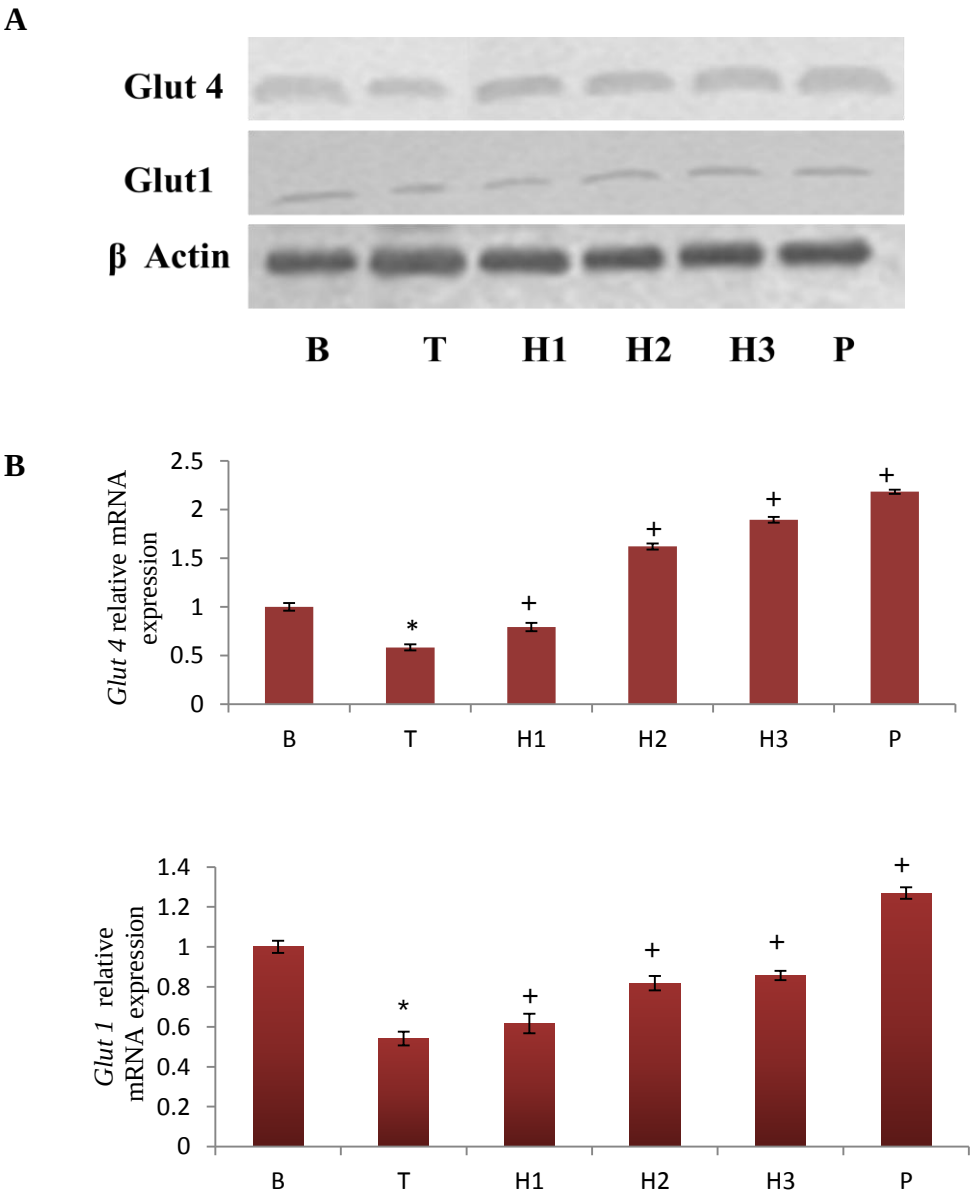

Figure 6.7 Protein and mRNA expression of GLUT 1 and GLUT4 during endoplasmic reticulum stress in 3T3-L1 adipocytes. A. Representative immunoblots of GLUT1 and GLUT4. B. Quantification of *Glut1* and *Glut 4* mRNA normalised to β Actin. (B) control, (T) tunicamycin, (H1) tunicamycin + 5 µM (-) hydroxycitric acid, (H2) tunicamycin + 10 µM (-) hydroxycitric acid, (H3) tunicamycin + 20 µM (-) hydroxycitric acid, (P) tunicamycin + 1 mM PBA. Values expressed as means ± SD (n = 6), represented by vertical bars.* indicates values are significantly different from the control cells and + indicates values are significantly different from the endoplasmic reticulum stressed group, significance accepted at $P \leq 0.05$.

6.3.9 Effect of HCA on JNK activation and insulin receptors

Immunoblot studies showed increased ($P \leq 0.05$) phosphorylation and subsequent activation of JNK, in ER stressed group compared with normal cells (Fig. 6.8A and B). We further investigated the effects of JNK and NF κB activation on insulin signaling receptors. Western blot analysis showed increased ($P \leq 0.05$) serine 307 phosphorylation of IRS-1 and

decreased expression of IRS-2 in ER stressed group showing ER stress induced impairment in insulin signaling (Figure 6.8). But treatment with HCA (5,10, 20 µM) and PBA (1 mM) significantly ($P \leq 0.05$) lowered phosphorylation of JNK, and serine phosphorylation of IRS-1, and also increased the expression of IRS2 showing protection from ER stress induced impairment in insulin signaling pathway (Fig.6.8). mRNA expression of *IRS-1* and *Irs2* were also increased by HCA treatment.

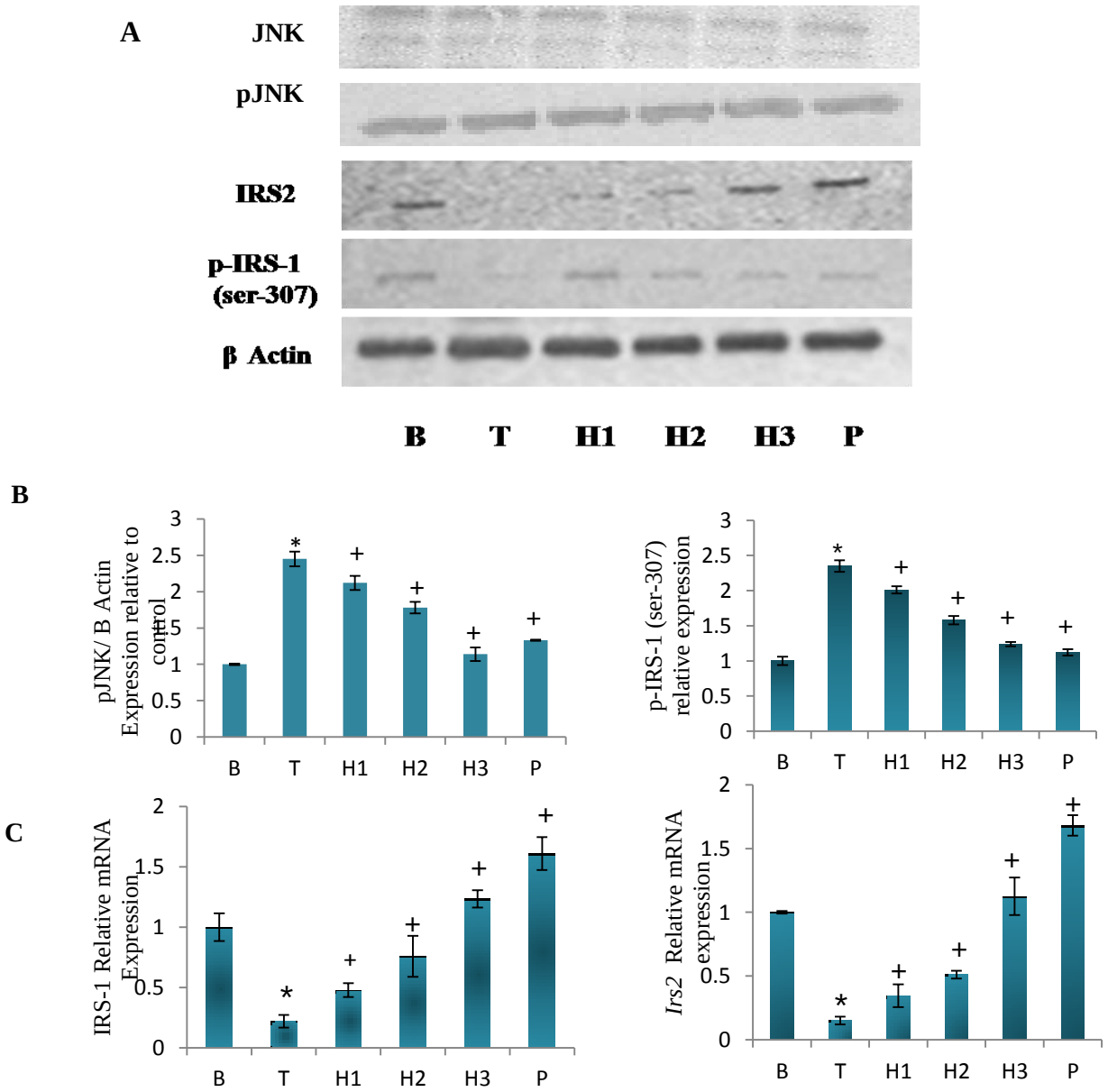

Figure 6.8 JNK activation and insulin receptors during endoplasmic reticulum stress. A. Representative immunoblots of JNK and insulin receptors. B. Densitometric quantification of the protein expression normalised to β Actin. C. mRNA expression of *IRS-1* and *Irs2* normalised to control (B) control, (T) tunicamycin, (H1) tunicamycin + 5 µM (-) hydroxycitric acid, (H2) tunicamycin + 10 µM (-) hydroxycitric acid, (H3) tunicamycin + 20 µM (-) hydroxycitric acid, (P) tunicamycin + 1mM PBA. Values expressed as means ± SD (n = 6), represented by vertical bars.* indicates values are significantly different from the control cells and + indicates values are significantly different from the endoplasmic reticulum stressed group, significance accepted at $P \leq 0.05$.

6.3.10 Effect of HCA on PPARγ expression

ER stress significantly ($P \leq 0.05$) downregulated PPARγ expression at mRNA and protein level in adipocytes. HCA and PBA significantly increased its expression in ER stressed adipocytes (Figure 6.9).

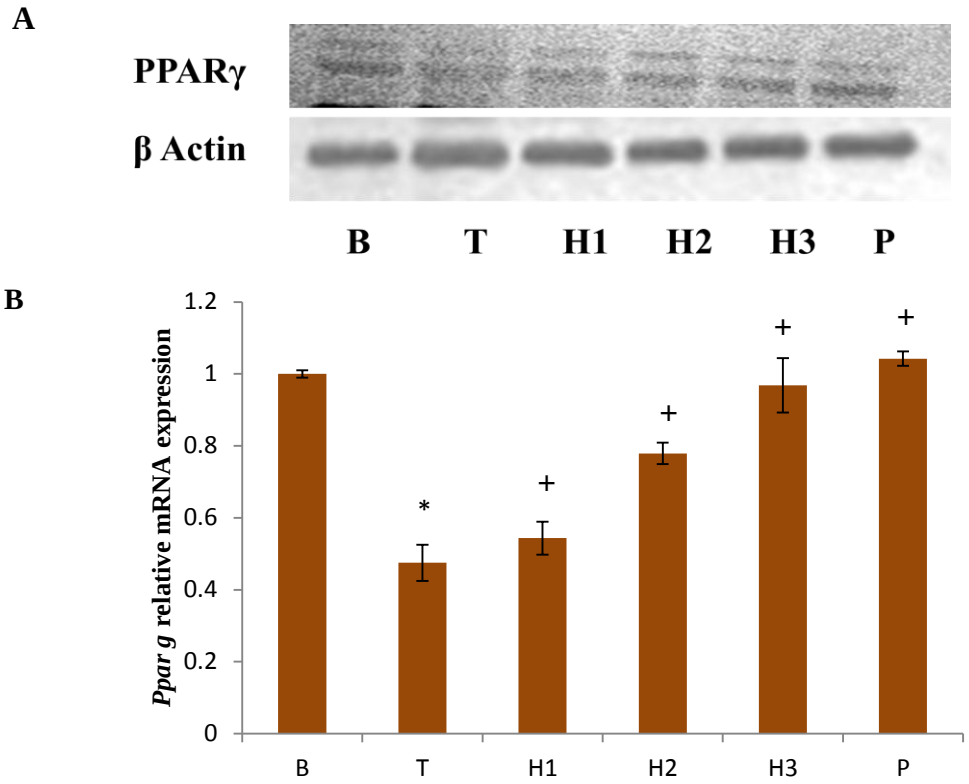

Figure 6.9 Expression of PPARγ in 3T3-L1 adipocytes during endoplasmic reticulum stress. A. Representative immunoblot of PPARγ. B. Quantification of mRNA levels of *Ppar g* normalised to β Actin. (B) control, (T) tunicamycin, (H1) tunicamycin + 5 µM (-) hydroxycitric acid, (H2) tunicamycin + 10 µM (-) hydroxycitric acid, (H3) tunicamycin + 20 µM (-) hydroxycitric acid, (P) tunicamycin + 1 mM PBA. Values expressed as means ± SD (n = 6), represented by vertical bars.* indicates values are significantly different from the control cells and + indicates values are significantly different from the endoplasmic reticulum stressed group, significance accepted at $P \leq 0.05$.

6.3.11 Effect of HCA on expression of PI3K, pAKT, PTP1B

Immunoblot studies showed decreased ($P \leq 0.05$) expression of PI3K and phosphorylation of AKT, in ER stressed group compared with normal cells (Figure. 6.10). Treatment with HCA (5, 10, 20 µM) and PBA (1 mM) significantly ($P \leq 0.05$) increased the phosphorylation of AKT, and expression of PI3K. Expression of PTP1B was also assessed, expression of which was found to be elevated and HCA significantly reduced its levels. PBA also had a similar effect on PBA (Figure 6.10).

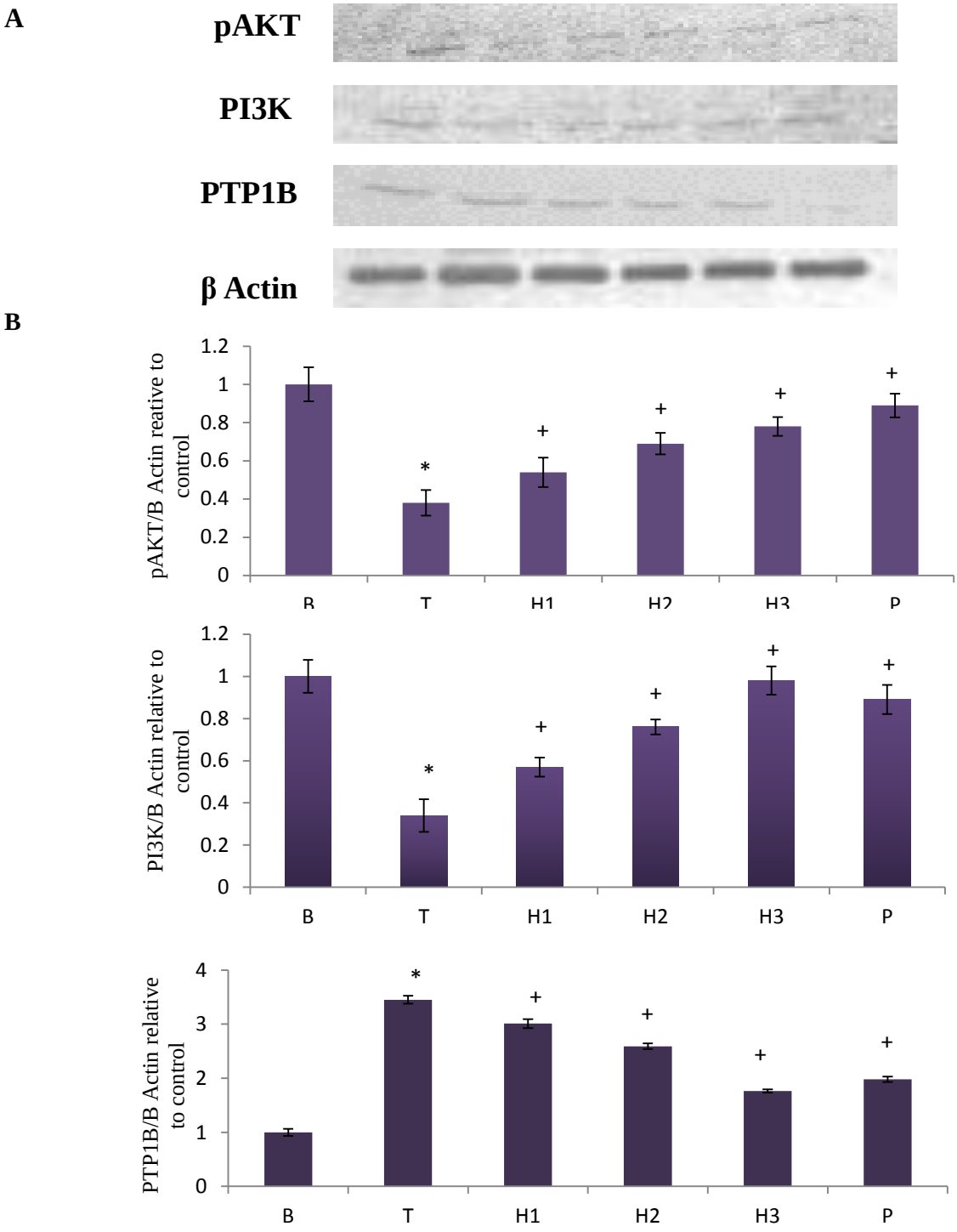

Figure 6.10 Expression of PI3K, pAKT and PTP1B in 3T3-L1 adipocytes during endoplasmic reticulum stress. A. Representative immunoblots of PI3K, pAKT and PTP1B. B. Densitometric quantification of protein levels normalised to β Actin. (B) control, (T) tunicamycin, (H1) tunicamycin + 5 µM(-) hydroxycitric acid, (H2) tunicamycin + 10 µM (-) hydroxycitric acid, (H3) tunicamycin + 20 µM (-) hydroxycitric acid, (P) tunicamycin + 1 mM PBA. Values expressed as means ± SD (n = 6), represented by vertical bars.* indicates values are significantly different from the control cells and + indicates values are significantly different from the endoplasmic reticulum stressed group, significance accepted at $P \leq 0.05$.

6.3.12 Effect of HCA on triglyceride content

The lipid droplets within the adipocytes were examined by confocal microscopy. In control cells, the average size of the lipid droplets was much bigger than from the group of ER stress. After induction of ER stress with tunicamycin the size of the lipid droplets decreased (Figure 6.11). HCA as well as PBA treatment showed bigger and more lipid droplets compared to the stressed cells. A representative image of lipid droplets within 3T3-L1 adipocytes is shown in Figure 6.11. This result was confirmed by the quantification of triglyceride content. Triglyceride content was found to be significantly lowered during ER stress (2.39 fold). HCA treatment increased the lipid contents by 1.26, 1.48 and 2.18 fold respectively. PBA induced a reduction of 2.28 fold in the triglyceride content.

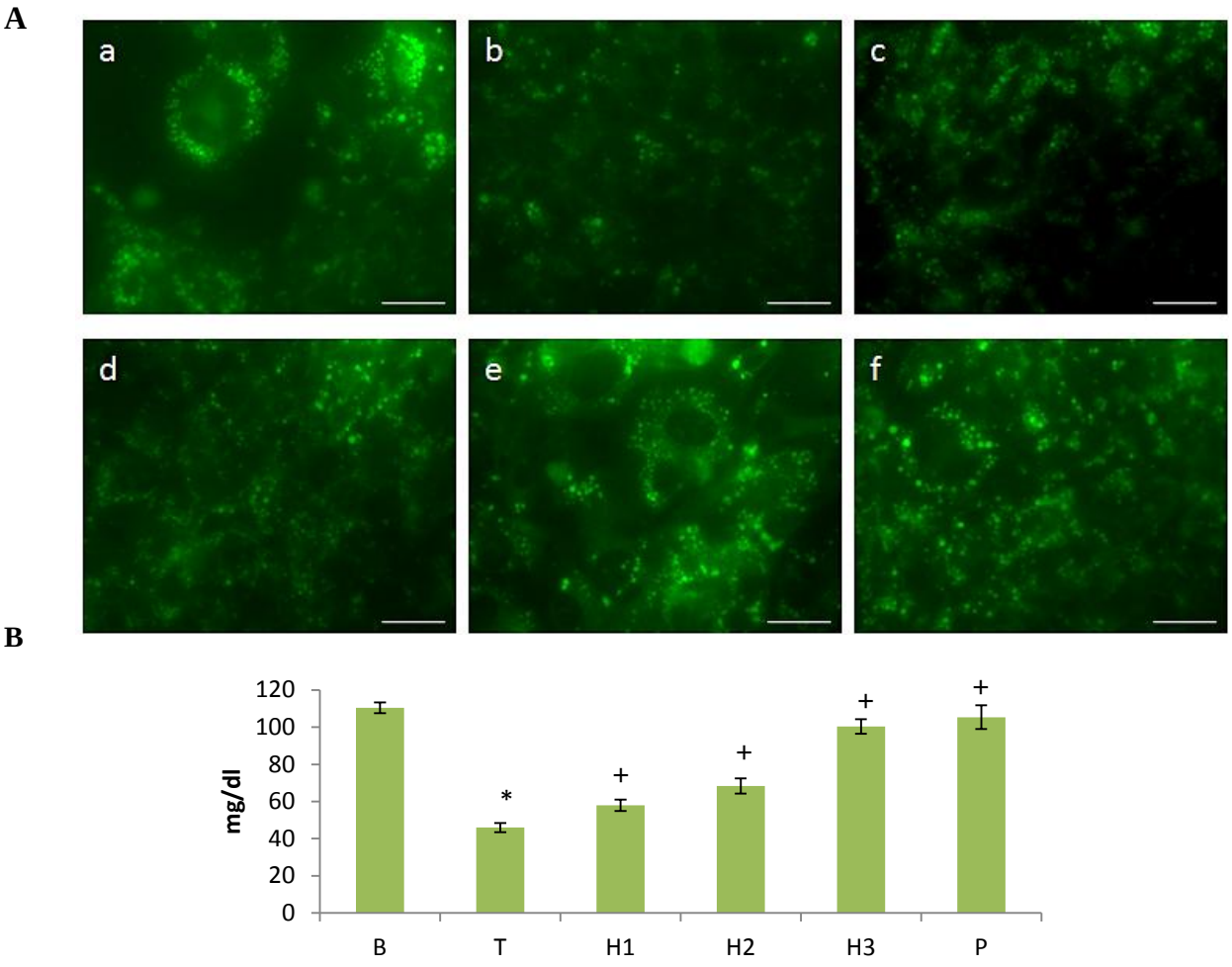

Figure 6.11 Triglyceride content in 3T3-L1 adipocytes during endoplasmic reticulum stress. A. Representative images of lipid droplets stained by Nile red. (a) control, (b) tunicamycin treated, (c) tunicamycin + 5 µM (-) hydroxycitric acid, (d) tunicamycin + 10 µM (-) hydroxycitric acid, (e) tunicamycin + 20 µM (-) hydroxycitric acid, (f) tunicamycin + 1 mM PBA. Scale bar corresponds to 100 µm. B. Quantification of triglyceride content. (B) control, (T) tunicamycin, (H1) tunicamycin + 5 µM (-) hydroxycitric acid, (H2) tunicamycin + 10 µM (-) hydroxycitric acid, (H3) tunicamycin + 20 µM (-) hydroxycitric acid, (P) tunicamycin + 1 mM PBA. Values expressed as means ± SD (n = 6), represented by vertical bars.* indicates values are significantly different from

the control cells and + indicates values are significantly different from the endoplasmic reticulum stressed group, significance accepted at $P \leq 0.05$.

6.3.13 Effect of HCA on lipolysis

The glycerol release from 3T3-L1 adipocytes during ER stress and normal condition were examined. It was significantly increased (1.61 fold) in stressed cell compared with normal cells. HCA (5, 10, and 20 μM) and PBA (1 mM) significantly ($P \leq 0.05$) prevented the glycerol release (1.01, 1.37, 1.61fold respectively, Figure. 6.12). PBA reduced the glycerol release by 1.46 fold. Increased glycerol release is an indication of increased lipolysis and free fatty acid release.

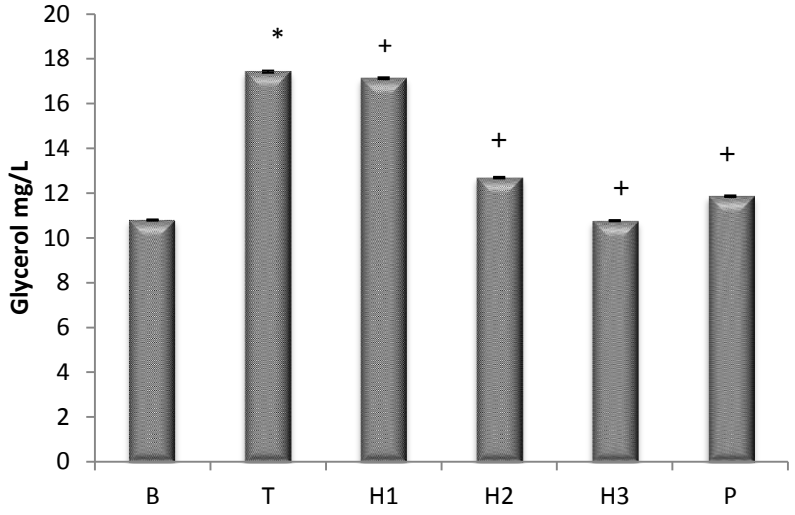

Figure 6.12 Quantification of glycerol released by 3T3-L1 adipocytes during endoplasmic reticulum stress. (B) control, (T) tunicamycin, (H1) tunicamycin + 5 μM (-) hydroxycitric acid, (H2) tunicamycin + 10 μM (-) hydroxycitric acid, (H3) tunicamycin + 20 μM (-) hydroxycitric acid, (P) tunicamycin + 1 mM PBA. Values expressed as means ± SD (n = 6), represented by vertical bars.* indicates values are significantly different from the control cells and + indicates values are significantly different from the endoplasmic reticulum stressed group, significance accepted at $P \leq 0.05$.

6.3.14 Effect of HCA on expression of *Tlr4* receptor

ER stress increased ($P \leq 0.05$) mRNA levels (8.8 fold) of *Tlr4* receptors, the key mediator of the activation of NF-κB and JNK pathway. The treatment with HCA (5, 10, 20 μM) and PBA (1 mM) significantly reduced (3.27, 3.4, 2.8 and 3.29 fold respectively, $P \leq 0.05$) mRNA level expression of *Tlr4* receptors in ER stressed adipocytes (Figure 6.13).

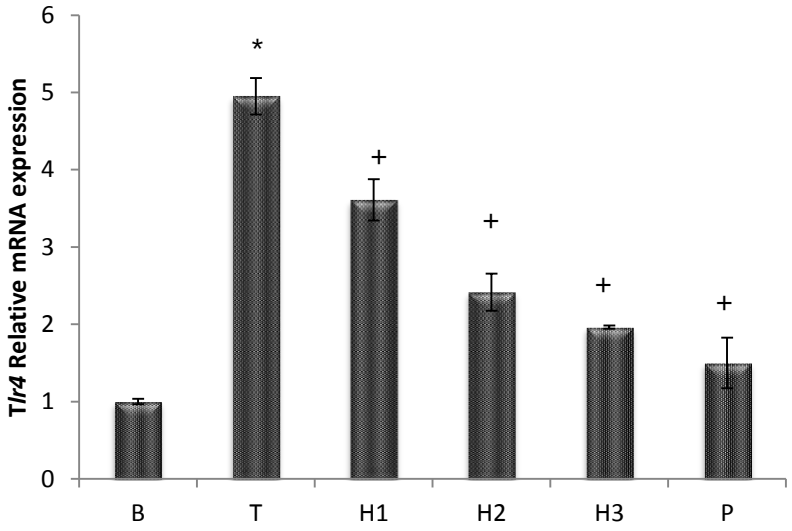

Figure 6.13 Quantification of mRNA expression of *Tlr4* in 3T3-L1 adipocytes during endoplasmic reticulum stress. (B) control, (T) tunicamycin, (H1) tunicamycin + 5 µM (-) hydroxycitric acid, (H2) tunicamycin + 10 µM (-) hydroxycitric acid, (H3) tunicamycin + 20 µM (-) hydroxycitric acid, (P) tunicamycin + 1 mM PBA. Values expressed as means ± SD (n = 6), represented by vertical bars.* indicates values are significantly different from the control cells and + indicates values are significantly different from the endoplasmic reticulum stressed group, significance accepted at $P \leq 0.05$.

6.4 Discussion

ER stress and inflammation are linked so clos10ely that ER function and metabolic homeostasis are integrated. Inflammation plays a critical role in the development and progression of obesity, IR, T2DM, and many other clustering metabolic disorders (Hotamisligil, 2006). Particularly, chronic inflammation of adipose tissue (and recruitment of professional immune cells to this site) (Alexaki et al, 2009; Feuerer et al, 2009; Liu et al, 2009; Nishimura et al, 2009; Winer et al, 2009), whether triggered metabolically or through injury or death of adipocytes, can trigger a diverse set of stress responses emerging from the ER. In the present study, we investigated the link between ER stress induced inflammation and IR in adipocytes. Our study also demonstrates the protective role of HCA against ER stress induced inflammation and other complications.

Adipocytes showed severe inflammation characterized by increased expression of inflammatory cytokines. TNF-α, IL-6, MCP-1, IFN-γ, IL-1β, leptin, resistin and adiponectin are some of the adipokines strongly associated with obesity-induced inflammation, IR and other obesity-related pathologies. TNFα is involved in lipid metabolism, insulin signaling, and secretion of inflammatory cytokines like IL-6, TNF-α and adiponectin. It also promotes IR and apoptosis in adipocytes. IL-6 plays a major role in whole body energy homeostasis by controlling food intake and appetite, and suppressing the lipoprotein lipase activity

(Emanuela et al, 2012). IL-10 is reported to increase insulin sensitivity, protects skeletal muscle from obesity-associated macrophage infiltration, increase in inflammatory cytokines, and their effects on insulin signaling and glucose metabolism (Hong et al, 2009). Elevated level of IL-1β leads to impaired insulin secretion, decreased cell proliferation, and apoptosis (Emanuela et al, 2012). IFNγ have differential effects on the metabolism of lipoprotein immune complexes (Morganelli et al, 2000)

All the three canonical UPR signaling pathways mediated by PERK, IRE1, and ATF6 that are activated by ER stress are identified to stimulate the expression of inflammatory cytokines in several cell types (Hotamisligil, 2010). NF-κB, a transcriptional regulator that plays a central role in mediating the inflammatory responses is activated by PERK signaling. The PERK arm mediates inhibition of protein translation via phosphorylation of eIF2α. Phosphorylation of eIF2α is reported to inhibit the translation of IκBα, the main negative regulator of NF-κB (Deng et al, 2004). Decreased translation of IκBα causes removal of inhibition of NF-κB activity and promotes the nuclear translocation of NF-κB from the cytoplasm. Down-regulation of this inhibitory control leads to induction of its downstream inflammatory genes. ATF6 also regulates the NF-κB pathway (Yamazaki et al, 2009). Precise mechanism by which ATF6 signaling pathway activates NF-κB is not known. ATF6 might be up-regulating the transcription of genes, which activate the NF-κB pathway. The third arm of the UPR is the IRE1 signaling pathway. IRE1 signaling pathway is reported to directly activate the JNK (Hu et al, 2006; Urano et al, 2000). JNK is an important inflammatory signaling mediator which up-regulates the expression of inflammatory cytokines by activating the AP-1 transcription factor complex. In the present study, we demonstrated that, induction of ER stress markedly up-regulated the inflammatory response and was successfully suppressed by HCA treatment in 3T3-L1 adipocytes. Inflammation in adipose tissue of high-fat diet-induced obese mice was reported to be caused by the activation of UPR signaling pathways via ER stress.

Numerous studies in rodents and humans have found a link between IR and ER stress in adipose tissue, as well as increased lipolysis and altered adipokine production (Boden et al, 2008; Gregor et al, 2009; Ozcan, 2004; Sharma et al, 2008; Xu et al, 2010). Xu et al reported a decrease in leptin and adiponectin secretion and an increase in IL-6 secretion in ER stress-associated conditions, including obesity (Xu et al, 2010). Studies have shown that adiponectin folding and multimerization are impaired in obese states due to a decreased

expression of ER disulfide-bond A oxidoreductase-like protein (DsbA-L), which leads to ER stress (Liu et al, 2008; Zhou et al, 2010). Resistin transcription and secretion in adipocytes is impaired by CHOP which is upregulated under ER stress (Lefterova et al, 2009). ER stress has been reported to decrease high-molecular-weight fractions as well as total adiponectin in human adipocytes, which may have role in insulin sensitivity and metabolic syndrome (Kern et al, 2003; Lara-Castro et al, 2006). Decreased levels of adiponectin are observed in conditions associated with excessive nutrient intake, including obesity. A decreased expression of the cytokine adiponectin may promote IR in obesity (Berg et al, 2002; Hu et al, 1996; Menzaghi et al, 2002). Adiponectin signaling affects AMPK, which is a negative regulator of mTOR. High levels of mTOR in turn cause serine phosphorylation of IRS-1. Hence low adiponectin levels leads to inhibition of IRS-1 causing IR through the activation of the mTOR signaling pathway. A study in which tunicamycin and thapsigargin was used to induce ER stress in human adipocytes showed that ER stress decreased adiponectin, increased TNF-α mRNA expression, lowered IκB protein (Mondal et al, 2012).

Couillard et al reported an increased leptin levels on feeding and decreased by fasting. A positive correlation exists between leptin levels and adiposity (Couillard et al, 2000). Insulin signaling was impaired by leptin in adipocytes and IR was triggered (Denroche et al, 2012). Resistin is an adipokine secreted by preadipocytes of human adipose tissue (Kaser et al, 2003) and has been associated with IR in obese individuals with a positive correlation (Silha et al, 2003). In a study, ER stress has been found to reduce resistin mRNA expression in 3T3-L1 adipocytes in a time and dose dependent manner (Lefterova et al, 2009).

IR is one of the most common physiological consequences of obesity. Cellular glucose uptake was found to be lowered during ER stress in correlation with the low expression of GLUT1 and GLUT4 in our study. We found an increased phosphorylation of JNK1 and IRS-1 at Ser307 in ER stressed adipocytes. A reduction in the expression of IRS2 was also noted. IRS2 expression is lowered in the livers of obese model mice (Shimomura et al, 2000), and disruption of hepatic IRS2 leads to IR (Kubota et al, 2000), suggesting that IRS-1 as well as IRS2 are critical for the pathogenesis of systemic IR.

Ozcan et al showed that the IRE1–JNK signaling pathway directly inhibits cytoplasmic insulin signaling in ob/ob mice by activating phosphorylation of IRS-1 at Ser307 by JNK (Ozcan et al, 2004). It is possible that activation of IRE1 during ER stress in adipocytes could disrupt insulin signaling. Our findings showed that alleviation of ER stress

improved insulin signaling via down-regulation of phosphorylation of IRS-1 at Ser307 in adipocytes. JNK pathways can be activated by the inflammatory cytokines secreted from adipocytes and macrophages in obese adipose tissue (Kyriakis, 2001). Inflammatory cytokines can disrupt insulin signaling by interfering directly with IRS-1 insulin receptor binding and promoting IRS-1 degradation (Shoelson, 2006). The link between ER stress and insulin signaling require further studies to elucidate the detailed mechanisms underlying the development of IR in obese adipose tissue. ROS is reported as another factor promoting IR and inflammation. ER stress is a major source of reactive oxygen species produced by the activation of PDI (Schroder and Kaufman, 2005; Zhang et al, 2008).

Treatment with TUDCA, a conjugated bile acid derivative that inhibits ER stress-induced apoptosis, increased insulin sensitivity in patients with IR (Kars et al, 2010). In addition, treatment with chaperones, like PBA, trimethylamine N-oxide dihydrate, dimethyl sulfoxide and 150 kDa oxygen-regulated protein, which protect cells from ER stress by stabilizing protein conformation and improving ER folding capacity, increased insulin sensitivity in obese diabetic mice (Nakatani et al, 2005; Ozcan, 2006). These data show that ER stress in adipocytes, hepatocytes and β-cells may initiate IR, as well as intensify pre-existing IR, particularly in the context of obesity. ER stress interferes with insulin receptor signaling through multiple ways.

Activation of insulin receptor phosphorylates the downstream docking protein IRS, which then activates the PI3K and AKT pathway leads to the translocation of GLUT4 vesicles to the cell surface resulting in cellular glucose uptake (Herman et al, 2006). PTP1B, a hydrolase that targets the tyrosine-phosphorylated insulin receptor β and IRS-1, has been reported as a negative regulator of insulin signalling (Dadke et al, 2000; Kenner et al, 1996). Deletion of PTP1B resulted in improved insulin sensitivity and glucose tolerance (Bence, 2010; Elchebly et al, 1999; Klaman et al, 2000). Several PTP1B inhibitors have been projected for the management of diabetes mellitus (Thareja et al, 2012). In mammalian cells, PTP1B is tethered to the ER via its C-terminal targeting sequence (Frangioni et al, 1992). PTP1B appears to be closely associated with the ER, in terms of both cellular localisation and function. In the present study we examined the effect of the ER stress inducer tunicamycin on PTP1B levels and insulin sensitivity in adipocytes. Studies have confirmed the negative effect of ER stress on PI-3K/AKT signaling followed by inhibition of glucose uptake and bioenergetic responses (Lin et al, 2011; Pfaffenbach et al, 2010; Qin et al, 2010).

The basal lipolysis in adipocytes was determined in ER stressed adipocytes by glycerol release and triglyceride content. An increased release of glycerol and reduced triglyceride content was found in this study indicating increased release of free fatty acids. Augmented lipolysis could be due to the close relationship between the ER and lipid droplet (Brasaemle et al, 2012; Gregor et al, 2007). The final steps of triglyceride synthesis occur at the ER and it has been suggested that the lipid droplet formation also takes place at the ER (Fujimoto et al, 2011; Ohsaki et al, 2014). White adipocytes contain a massive lipid droplet that occupies >90% of the adipocyte cell volume (Cushman et al, 1970). As the primary function of adipocytes is lipid storage and the ER and lipid droplet are closely associated, it is possible that ER stress or disturbances in ER function would cause alterations in lipolysis/lipogenesis. Deng *et al*. demonstrated that the ER stress inducer thapsigargin stimulated lipolysis *via* activation of the PKA signalling pathway and increased phosphorylation of HSL in cultured rat adipocytes, (Deng et al, 2012). Zhou et al showed that chronic ER stress in 3T3-L1 adipocytes led to decreases in perilipin levels (Zhou et al, 2009). Given the complex interaction between the ER and lipid droplet it is difficult to identify a precise mechanism of how ER stress or ER dysfunction would lead to augmented lipolysis.

Overall results showed that ER stress induced inflammation and IR in adipocytes as indicated by increased levels of inflammatory cytokines and alterations in the insulin signaling pathway. HCA ameliorated the inflammation and IR induced by ER stress revealing its potential as nutraceutical against metabolic syndrome.

Chapter 7

Summary and conclusion

ER stress is stimulated by multiple pathological factors like metabolic disorders, reactive oxygen species, altered ER Ca^{2+}, insufficient ER chaperones and foldases, xenobiotics, as well as increased demand for protein folding. Among these, metabolic syndrome is a state with increased protein folding demand, ROS accumulation and altered ER Ca^{2+} flux. Obesity is one of the major risk factors leading to metabolic syndrome which includes lipid metabolism disorders, hypertension, arteriosclerosis, and ischemic heart disease, IR and T2DM. The worldwide prevalence of obesity has increased to epidemic proportions. Even after lots of studies, current pharmacotherapeutic options for treating obesity and metabolic syndrome remains inadequate. Hence, understanding the molecular mechanisms involved during the onset and progression of obesity and related complications is crucial. Our results coincide with the earlier studies that ER stress and its stress responses in adipose tissue is a key factor in the aggravation of obesity related problems. This poses ER stress as a future therapeutic target for the treatment of metabolic syndrome. The etiology of ER stress in adipose tissue may be attributed to nutrient over-load, along with increased demand for protein synthesis for its metabolism, local glucose deprivation due to IR, and decreased vascularization. There occurs accumulation of unfolded or misfolded proteins, eliciting a cellular response known as the UPR. The UPR operates through three ER stress sensors which are activated, namely PERK, IRE1α, and ATF6, along with their downstream effecter molecules. Recent preclinical and clinical evidence supports the notion that pharmacological modulators of ER stress have therapeutic potential as novel treatments of metabolic disorders. Small molecule chemical chaperones have already demonstrated therapeutic efficacy in animal and human studies. The emergence of compounds that target specific UPR signaling pathways will provide more options for this purpose. Although the findings are promising, more studies are needed to elucidate the efficacy and side effects of these small molecules for future use in humans.

The ER is a vital eukaryotic organelle that is the site for protein synthesis, folding and trafficking, calcium homoeostasis and lipid and steroid synthesis. Secretory as well as, plasma membrane and organelle proteins are synthesized and folded in the ER. Disturbances in the ER homeostasis such as the accumulation of unfolded or misfolded proteins lead to ER

stress. ER stress triggers an evolutionarily conserved signaling cascade called UPR to alleviate this stress. As an initial response, the UPR aims at adapting and restoring ER function by translational attenuation, upregulation of ER chaperones and degradation of unfolded proteins. But, excessive or prolonged exposure to ER stress activates the cellular signals leading to cell death. ER stress negatively affects the metabolic homeostasis by triggering the inflammatory network. One of the most common physiological consequences of obesity is the development of IR. All the 3 branches of the UPR, namely PERK, IRE-1 and ATF6 activate JNK and/or NF-κB signaling pathways. This leads to subsequent inhibition of insulin action via IRS-1 phosphorylation, although other mechanisms are also possible. Moreover, increased JNK and NF-κB signaling is expected to induce other inflammatory mediators that are associated with metabolic disease. .

Mitochondria and the ER are structurally and functionally connected with each other through several pathways, hence any defect in one translates into other. Structural communication between mitochondria and the ER is also modulated by fission and fusion of mitochondria. Mitochondria are well known to be the power stations within cells, as one of their major functions is production of ATP. Mitochondria also play essential roles in intracellular ROS production, regulation of apoptosis, and Ca^{2+} storage. Disturbances in mitochondrial Ca^{2+} homeostasis causes apoptotic cell death during ER stress.

The prevalence of obesity and associated metabolic disorders has increased over the last decade, and current measures have not been able to stop this. A wide variety of weight management strategies are presently available, and some involve the use of dietary supplements marketed as slimming aids. One such slimming aid is *Garcinia* extract, containing HCA. HCA is a derivative of citric acid, found in plants like *Garcinia cambogia, Garcinia indica,* and *Garcinia atroviridis*. HCA causes weight loss by competitively inhibiting the enzyme adenosine triphosphatase-citrate-lyase. HCA also increases the release or availability of serotonin in the brain, thereby leading to appetite suppression. Other postulated weight loss mechanisms include inhibition of pancreatic alpha amylase and intestinal alpha glucosidase, thereby leading to a reduction in carbohydrate metabolism. HCA supplementation in obese Zucker rats reduced food-intake, body weight gain, and also attenuated the increases in inflammation, oxidative stress, and IR observed in untreated animals. Therefore, HCA may be used as an intervention to overcome obesity related complications, including inflammation, oxidative stress, and IR. Animal studies have

suggested that HCA causes weight loss, and human trials involving the use of HCA as a weight loss supplement have been carried out.

The present study uncovers the possibility that inhibition of ER stress may be an effective approach to reduce the risk of obesity and its metabolic complications. In other words, ER stress and its stress response (UPR) offer novel drug targets for obesity. ER stress is known to have various physiologic roles, including escape from apoptosis in cells with unfolded protein in the ER, regulation of secretory cell differentiation or maturation, and maintenance of cellular homeostasis. Complete elimination of ER stress by agents that prevent ER stress could be of disadvantage for living cells and biological regulation. To develop the agents targeting ER stress in clinical, more studies are needed to characterize the functional changes in cells during ER stress.

In the present study we established the protective effect of HCA against ER stress induced dysfunctions in 3T3-L1 adipocytes emphasizing on oxidative stress, mitochondrial dysfunctions, inflammation, and IR. ER stress was induced in differentiated 3T3-L1 adipocytes on 9th day by incubating with 2 µM of tunicamycin for 18 hours. The cells were treated with different concentrations of HCA (5, 10 and 20 µM) during ER stress induction. Sodium phenyl butyrate (1 mM), a chemical chaperone was used as positive control.

The induction of ER stress was confirmed by evaluating the expression of ER stress markers like GRP78 and CHOP. Beforehand, cytotoxicity of HCA and tunicamycin and ROS production was determined to fix the safe and effective concentrations.The treatment with HCA significantly reduced the gene and protein level expression of GRP78 and CHOP.

Among the various parameters we studied the ER stress induced oxidative stress in 3T3-L1 adipocytes. ER stress caused significant increase in oxidative stress compared with normal cells. HCA treatment reduced the intracellular ROS generation, lipid and protein oxidation in ER stressed adipocytes. The activities of endogenous antioxidant enzymes were elevated; showing protection from ER stress induced oxidative stress. In addition, HCA treatment showed a lowered Nrf2 mediated HO-1 expression indicating protection of adipocytes from oxidative stress. ER stress activated the UPR, up regulating the master sensors, as well as the downstream signaling molecules (ERO1-α, PDI, PERK, IRE-1α, ATF-6, *Xbp1*, peIF2α) in 3T3-L1 adipocytes compared to normal cells. HCA reduced the UPR and protected 3T3-L1 adipocytes from ER stress induced cell death.

Mitochondria act as major source of ROS production. So mitochondria are emerging as one of the important targets in the management adipose tissue ER stress and other associated complications. In this background, we designed further studies to evaluate the protective potential of HCA against mitochondrial dysfunction during ER stress in 3T3-L1 adipocytes. ER stress substantially increased mitochondrial superoxide production. Surplus ROS impaired mitochondrial membrane potential and integrity of permeability transition pore. ER stress also reduced mitochondrial biogenesis, oxygen consumption, ATP synthesis, and proteins involved in oxidative phosphorylation. ER stress also impaired fusion/fission balance in adipocytes. HCA protected the 3T3-L1 adipocytes from adverse effects of ER stress by enhancing mitochondrial biogenesis, mitochondrial functional performance and by controlling mitochondrial dynamics.

Chronic inflammation and reduced adiponectin in the white adipose tissue contribute to pathogenesis of IR. ER stress is considered as a potential risk factor for chronic inflammation. In obesity, oxygen species enhance ER stress, which worsen the inflammatory pathways. Here we studied the molecular mechanism underlying ER stress induced inflammation, and IR in 3T3-L1 adipocytes and possible reversal with HCA. ER stress significantly increased the release of TNF- α, IL-6, IL-10, MCP-1 and IFNγ. Leptin and resistin are the adipokines that induce inflammation and IR in adipocytes. But the secretion of adiponectin, a beneficial antidiabetic adipokine was significantly reduced in ER stressed adipocytes. ER stress also showed an increased mRNA expression of TLR4 receptors. Enhanced TLR4 with increased glycerol release activated inflammatory pathways, NFkB and JNK signaling in ER stress group. Activation of NFkB and JNK signaling pathways by ER stress and subsequent higher expression of cytokines impaired insulin signaling cascade by mediating serine phosphorylation of IRS-1 and by down regulating the expression of IRS-2. We observed a reduced glucose uptake in ER stress in response to reduced GLUT1, GLUT 4 expression. HCA ameliorated ER stress induced inflammation in 3T3-L1 adipocytes and improved insulin signaling.

From overall results of this study, we concluded that ER stress altered all vital parameters of adipocytes. ER stress lead to oxidative stress and mitochondrial dysfunction in adipocytes, insulin signaling cascade was impaired by the inflammatory response triggered by ER stress. The treatment with HCA protected adipocytes from ER stress induced dysfunctions. This establishes ER stress as an emerging area for extensive research on

metabolic syndromes and associated complications.Thus; further understanding of the molecular mechanisms in these interconnecting pathways occurring in numerous diseases may lead to discovery of novel therapeutic targets. However, comprehensive research is demanded to aim UPR in diseases, wherein side effects, efficacy, and safety are major concerns. Focused research and in depth investigations on ER stress are needed for a new therapeutic strategy.

References

Abhilash PA, Harikrishnan R, Indira M (2012) Ascorbic acid supplementation causes faster restoration of reduced glutathione content in the regression of alcohol-induced hepatotoxicity in male guinea pigs. Redox Rep 17:72-79.

Adachi T, Weisbrod RM, Pimentel DR, Ying J, Sharov VS, Schöneich C, Cohen RA (2004) S-Glutathiolation by peroxynitrite activates SERCA during arterial relaxation by nitric oxide. Nat Med 10:1200-1207.

Adachi Y, Yamamoto K, Okada T, Yoshida H, Harada A, Mori K (2008) ATF6 is a transcription factor specializing in the regulation of quality control proteins in the endoplasmic reticulum. Cell Struct Funct 33:75-89.

Alexaki VI, Notas G, Pelekanou V, Kampa M, Valkanou M, Theodoropoulos P, Stathopoulos EN, Tsapis A, Castanas E (2009) Adipocytes as immune cells: differential expression of TWEAK, BAFF, and APRIL and their receptors (Fn14, BAFF-R, TACI, and BCMA) at different stages of normal and pathological adipose tissue development. J Immunol 183:5948-5956.

Anderson PJ, Critchley JAJH, Chan JCN, Cockram CS, Lee ZSK, Thomas GN, Tomilnson B (2001) Factor analysis of the metabolic syndrome: obesity vs insulin resistance as the central abnormality. Int J Obesity 25:1782-1788.

Apovian CM, Bigornia S, Mott M, Meyers MR, Ulloor J, Gagua M, McDonnell M, Hess D, Joseph L, Gokce N (2008) Adipose macrophage infiltration is associated with insulin resistance and vascular endothelial dysfunction in obese subjects. Arterioscler Thromb Vasc Biol 28:1654-1659.

Arap MA, Lahdenranta J, Mintz PJ, Hajitou A, Sarkis ÁS, Arap W, Pasqualini R (2004) Cell surface expression of the stress response chaperone GRP78 enables tumor targeting by circulating ligands Cancer Cell 6:275-284.

Arita Y, Kihara S, Ouchi N, Takahashi M, Maeda K, Miyagawa J, Hotta K, Shimomura I, Nakamura T, Miyaoka K, Kuriyama H, Nishida M, Yamashita S, Okubo K, Matsubara K, Muraguchi M, Ohmoto Y, Funahashi T, Matsuzawa Y (1999) Biochem Biophys Res Commun. 257:79-83.

Arkan MC, Hevener AL, Greten FR, Maeda S, Li Z, Long JM, Wynshaw-Boris A, Poli G, Olefsky J, Karin M (2005) IKK-β links inflammation to obesity-induced insulin resistance. Nat Med 11:191-198.

Asada R, Saito A, Kawasaki N, Kanemoto S, Iwamoto H, Oki M, Miyagi H, Izumi S, Imaizumi K (2012) The endoplasmic reticulum stress transducer OASIS is involved in the terminal differentiation of goblet cells in the large intestine. J Biol Chem 287:8144-8153.

Asghar M, Monjok E, Kouamou G, Ohia SE, Bagchi D, Lokhandwala MF (2007) Super CitriMax (HCA-SX) attenuates increases in oxidative stress, inflammation, insulin resistance, and body weight in developing obese Zucker rats. Mol Cell Biochem 304:93-99.

Basseri S, Lhotak S, Sharma AM, Austin RC (2009) The chemical chaperone 4-phenylbutyrate inhibits adipogenesis by modulating the unfolded protein response. J Lipid Res 50:2486-2501.

Bastard J, Jardel C, Bruckert E, Blondy P, Capeau J, Laville M, Vidal H, Hainque B (2000) Elevated Levels of Interleukin 6 Are Reduced in Serum and Subcutaneous Adipose Tissue of Obese Women after Weight Loss. J. Clin. Endocrinol. Metab. 1 85:3338-3342.

Beltran B, Mathur A, Duchen MR, Erusalimsky JD, Moncada S (2000) The effect of nitric oxide on cell respiration: A key to understanding its role in cell survival or death. Proc Natl Acad Sci U S A 97:14602-14607.

Bence KK (2010) Hepatic PTP1B Deficiency: The Promise of a Treatment for Metabolic Syndrome?. J Clin Metab Diabetes 1:27-33.

Berg AH, Combs TP, Scherer PE (2002) ACRP30/adiponectin: an adipokine regulating glucose and lipid metabolism. Trends Endocrinol Metab 13:84-89.

Bhandary B, Marahatta A, Kim H, Chae H (2012) An involvement of oxidative stress in endoplasmic reticulum stress and its associated diseases. Int J Mol Sci. 14:434-456.

Boden G, Duan X, Homko C, Molina EJ, Song W, Perez O, Cheung P, Merali S (2008) Increase in endoplasmic reticulum stress-related proteins and genes in adipose tissue of obese, insulin-resistant individuals. Diabetes 57:2438-2444.

Boden G, Merali S (2011) Measurement of the increase in endoplasmic reticulum stress-related proteins and genes in adipose tissue of obese, insulin-resistant individuals. Methods Enzymol 489:67-82.

Bogacka I, Xie H, Bray GA, Smith SR (2005) Pioglitazone induces mitochondrial biogenesis in human subcutaneous adipose tissue in vivo. Diabetes 54:1392-1399.

Bonora E, Kiechl S, Willeit J, Oberhollenzer F, Egger G, Targher G, Alberiche M, Bonadonna RC, Muggeo M (1998) Prevalence of insulin resistance in metabolic disorders: the Bruneck Study. Diabetes 47:1643-1649.

Bouchier-Hayes L, Lartigue L, Newmeyer DD (2005) Mitochondria: pharmacological manipulation of cell death. J Clin Invest 115:2640-2647.

Boyce M, Yuan J (2006) Cellular response to endoplasmic reticulum stress: a matter of life or death. Cell Death Differ 13:363-373.

Braakman I, Bulleid NJ (2011) Protein folding and modification in the mammalian endoplasmic reticulum. Annu Rev Biochem 80:71-99.

Brasaemle DL, Wolins NE (2012) Packaging of fat: an evolving model of lipid droplet assembly and expansion. J Biol Chem 287:2273-2279.

Bravo R, Vicencio JM, Parra V, Troncoso R, Munoz JP, Bui M, Quiroga C, Rodriguez AE, Verdejo HE, Ferreira J, Iglewski M, Chiong M, Simmen T, Zorzano A, Hill JA, Rothermel

BA, Szabadkai G, Lavandero S (2011) Increased ER-mitochondrial coupling promotes mitochondrial respiration and bioenergetics during early phases of ER stress. J Cell Sci 124:2143-2152.

Bukau B, Weissman J, Horwich A (2006) Molecular chaperones and protein quality control. Cell 125:443-451.

Cao SS, Kaufman RJ (2013) Targeting endoplasmic reticulum stress in metabolic disease. Expert Opin Ther Targets 17:437-448.

Chan DC (2006) Mitochondrial fusion and fission in mammals. Annu Rev Cell Dev Biol 22:79-99.

Chang HC, Tang YC, Hayer-Hartl M, Hartl FU (2007) SnapShot: molecular chaperones, Part I. Cell 128:212.

Chapple SJ, Siow RC, Mann GE (2012) Crosstalk between Nrf2 and the proteasome: therapeutic potential of Nrf2 inducers in vascular disease and aging. Int J Biochem Cell Biol 44:1315-1320.

Chaudhari N, Talwar P, Parimisetty A, Lefebvre d'Hellencourt C, Ravanan P (2014) A molecular web: endoplasmic reticulum stress, inflammation, and oxidative stress. Front Cell Neurosci 8:213.

Chen G, Chen Z, Hu Y, Huang P (2011) Inhibition of mitochondrial respiration and rapid depletion of mitochondrial glutathione by β-phenethyl isothiocyanate: mechanisms for anti-leukemia activity. Antioxid Redox Signal 15:2911-2921.

Chen LB (1988) Mitochondrial-Membrane Potential in Living Cells. Annu. Rev. Cell Dev. Biol4:155–181.

Chen Y, Lewis W, Diwan A, Cheng EH, Matkovich SJ, Dorn GW,2nd (2010) Dual autonomous mitochondrial cell death pathways are activated by Nix/BNip3L and induce cardiomyopathy. Proc Natl Acad Sci U S A 107:9035-9042.

Cho H, Reddy SP, Kleeberger SR (2006) Nrf2 defends the lung from oxidative stress. Antioxid Redox Signal 8:76-87.

Choi EH, Chang H, Cho JY, Chun HS (2007) Cytoprotective effect of anthocyanins against doxorubicin-induced toxicity in H9c2 cardiomyocytes in relation to their antioxidant activities. Food Chem Toxicol 45:1873-1881.

Choo H, Kim J, Kwon O, Lee C, Mun J, Han SS, Yoon Y, Yoon G, Choi K, Ko Y (2006) Mitochondria are impaired in the adipocytes of type 2 diabetic mice. Diabetologia 49:784-791.

Chuang C, McIntosh MK (2011) Potential mechanisms by which polyphenol-rich grapes prevent obesity-mediated inflammation and metabolic diseases. Annu Rev Nutr 31:155-176.

Clouatre DL (2013). (-)-Hydroxycitric Acid for Controlling Inflammation. U.S. Patent Number 8394856

Cohen G, Dembiec D, Marcus J (1970) Measurement of catalase activity in tissue extracts. Anal Biochem 34:30-38.

Couillard C, Mauriege P, Imbeault P, Prud'homme D, Nadeau A, Tremblay A, Bouchard C, Despres J (2000) Hyperleptinemia is more closely associated with adipose cell hypertrophy than with adipose tissue hyperplasia. Int J Obes 24:782-788.

Csordás G, Hajnóczky G (2009) SR/ER–mitochondrial local communication: Calcium and ROS. Biochim Biophys Acta 1787:1352-1362.

Csordas G, Renken C, Varnai P, Walter L, Weaver D, Buttle KF, Balla T, Mannella CA, Hajnoczky G (2006) Structural and functional features and significance of the physical linkage between ER and mitochondria. J Cell Biol 174:915-921.

Cullinan SB, Diehl JA (2006) Coordination of ER and oxidative stress signaling: the PERK/Nrf2 signaling pathway. Int J Biochem Cell Biol 38:317-332.

Cullinan SB, Zhang D, Hannink M, Arvisais E, Kaufman RJ, Diehl JA (2003) Nrf2 is a direct PERK substrate and effector of PERK-dependent cell survival. Mol Cell Biol 23:7198-7209.

Cushman SW (1970) Structure-function relationships in the adipose cell. I. Ultrastructure of the isolated adipose cell. J Cell Biol 46:326-341.

Dadke S, Kusari J, Chernoff J(2000) Down-regulation of insulin signaling by protein-tyrosine phosphatase 1B is mediated by an N-terminal binding region. J Biol Chem. 275:23642–23647.

Dalle-Donne I, Rossi R, Giustarini D, Milzani A, Colombo R (2003) Protein carbonyl groups as biomarkers of oxidative stress. Clinica chimica acta 329:23-38.

David M, Richard JS (1983) In: Methods of enzymatic analysis, Bergmeyer, J and Grab M. (Eds), Verlag Chemie Wenhein Deer Field, Beach Floride, Pp 358.

Day CP (2006) From fat to inflammation. Gastroenterology 130:207-210.

de Brito OM, Scorrano L (2008) Mitofusin 2 tethers endoplasmic reticulum to mitochondria. Nature 456:605-610.

de Ferranti S, Mozaffarian D (2008) The perfect storm: obesity, adipocyte dysfunction, and metabolic consequences. Clin Chem 54:945-955.

De Pauw A, Tejerina S, Raes M, Keijer J, Arnould T (2009) Mitochondrial (dys) function in adipocyte (de) differentiation and systemic metabolic alterations. Am *J* Pathol 175:927-939.

Deng J, Liu S, Zou L, Xu C, Geng B, Xu G (2012) Lipolysis response to endoplasmic reticulum stress in adipose cells. J Biol Chem 287:6240-6249.

Deng J, Lu PD, Zhang Y, Scheuner D, Kaufman RJ, Sonenberg N, Harding HP, Ron D (2004) Translational repression mediates activation of nuclear factor kappa B by phosphorylated translation initiation factor 2. Mol Cell Biol 24:10161-10168.

Deng WG, Ruan KH, Du M, Saunders MA, Wu KK (2001) Aspirin and salicylate bind to immunoglobulin heavy chain binding protein (BiP) and inhibit its ATPase activity in human fibroblasts. FASEB J 15:2463-2470.

Deniaud A, Maillier E, Poncet D, Kroemer G, Lemaire C, Brenner C (2008) Endoplasmic reticulum stress induces calcium-dependent permeability transition, mitochondrial outer membrane permeabilization and apoptosis. Oncogene 27:285-299.

Denroche HC, Huynh FK, Kieffer TJ (2012) The role of leptin in glucose homeostasis. J Diabetes Invest 3:115-129.

Detmer SA, Chan DC (2007) Functions and dysfunctions of mitochondrial dynamics. Nat. Rev. Mol. Cell Biol. 8: 870–879.

Devasagayam T, Boloor K, Ramasarma T (2003) Methods for estimating lipid peroxidation: an analysis of merits and demerits. Indian J Biochem Biophys 40:300-308.

Dhanasekaran DN, Reddy EP (2008) JNK signaling in apoptosis. Oncogene 27:6245-6251.

Dillon LM, Rebelo AP, Moraes CT (2012) The role of PGC-1 coactivators in aging skeletal muscle and heart. IUBMB Life 64:231-241.

Dinu D, Bodea GO, Ceapa CD, Munteanu MC, Roming FI, Serban AI, Hermenean A, Costache M, Zarnescu O, Dinischiotu A (2011) Adapted response of the antioxidant defense system to oxidative stress induced by deoxynivalenol in Hek-293 cells. Toxicon 57:1023-1032.

Diwan A, Matkovich SJ, Yuan Q, Zhao W, Yatani A, Brown JH, Molkentin JD, Kranias EG, Dorn GW,2nd (2009) Endoplasmic reticulum-mitochondria crosstalk in NIX-mediated murine cell death. J Clin Invest 119:203-212.

Downs BW, Bagchi M, Subbaraju GV, Shara MA, Preuss HG, Bagchi D (2005) Bioefficacy of a novel calcium–potassium salt of (−)-hydroxycitric acid. Mutat Res.579:149-162.

Duchen MR, Surin A, Jacobson J (2003) Imaging mitochondrial function in intact cells. Meth Enzymol 361:353-389.

Elchebly M, Payette P, Michaliszyn E, Cromlish W, Collins S, Loy AL, Normandin D, Cheng A, Himms-Hagen J, Chan CC, Ramachandran C, Gresser MJ, Tremblay ML, Kennedy BP (1999) Increased insulin sensitivity and obesity resistance in mice lacking the protein tyrosine phosphatase-1B gene. Science 283:1544-1548.

Emanuela F, Grazia M, Marco DR, Maria Paola L, Giorgio F, Marco B (2012) Inflammation as a link between obesity and metabolic syndrome. J nutr metab

Empana JP, Ducimetiere P, Charles MA, Jouven X (2004) Sagittal abdominal diameter and risk of sudden death in asymptomatic middle-aged men: the Paris Prospective Study I. Circulation 110:2781-2785.

Engin F, Hotamisligil G (2010) Restoring endoplasmic reticulum function by chemical chaperones: an emerging therapeutic approach for metabolic diseases. Diabetes Obes Metab 12:108-115.

Erbay E, Babaev VR, Mayers JR, Makowski L, Charles KN, Snitow ME, Fazio S, Wiest MM, Watkins SM, Linton MF (2009) Reducing endoplasmic reticulum stress through a macrophage lipid chaperone alleviates atherosclerosis. Nat Med 15:1383-1391.

Ermakova SP, Kang BS, Choi BY, Choi HS, Schuster TF, Ma WY, Bode AM, Dong Z (2006) (-)-Epigallocatechin gallate overcomes resistance to etoposide-induced cell death by targeting the molecular chaperone glucose-regulated protein . Cancer Res 66:9260-9269.

Fawcett DW, Fawcett D (1981) The cell: its organelles and inclusions: an atlas of fine structure.

Feissner RF, Skalska J, Gaum WE, Sheu SS (2009) Crosstalk signaling between mitochondrial Ca2+ and ROS. Front Biosci 14:1197-1218.

Fels DR, Koumenis C (2006) The PERK/eIF2α/ATF4 module of the UPR in hypoxia resistance and tumor growth. Cancer Biol Ther. 5:723-728.

Feuerer M, Herrero L, Cipolletta D, Naaz A, Wong J, Nayer A, Lee J, Goldfine AB, Benoist C, Shoelson S (2009) Lean, but not obese, fat is enriched for a unique population of regulatory T cells that affect metabolic parameters. Nat Med 15:930-939.

Flegal KM, Graubard BI, Williamson DF, Gail MH (2005) Excess deaths associated with underweight, overweight, and obesity. JAMA 293:1861-1867.

Foresti R, Clark JE, Green CJ, Motterlini R (1997) Thiol compounds interact with nitric oxide in regulating heme oxygenase-1 induction in endothelial cells Involvement of superoxide and peroxynitrite anions. J Biol Chem 272:18411-18417.

Forman HJ, Azzi A(1999) Production of reactive oxygen species in mitochondria and age-associated pathophysiology: a reality check. In: Cadenas LPE, editor. Understanding the process of aging : The roles of mitochondria, Free radicals and Antioxidants. New York, Basel: Marcel Dekker Inc:73–94.

Fornace AJ,Jr, Nebert DW, Hollander MC, Luethy JD, Papathanasiou M, Fargnoli J, Holbrook NJ (1989) Mammalian genes coordinately regulated by growth arrest signals and DNA-damaging agents. Mol Cell Biol 9:4196-4203.

Frand AR, Kaiser CA (1999) Ero1p oxidizes protein disulfide isomerase in a pathway for disulfide bond formation in the endoplasmic reticulum. Mol Cell 4:469-477.

Frangioni JV, Beahm PH, Shifrin V, Jost CA, Neel BG (1992) The nontransmembrane tyrosine phosphatase PTP-1B localizes to the endoplasmic reticulum via its 35 amino acid C-terminal sequence. Cell 68:545-560.

Fujimoto T, Parton RG (2011) Not just fat: the structure and function of the lipid droplet. Cold Spring Harb Perspect Biol 3:10.1101/cshperspect.a004838.

Furukawa S, Fujita T, Shimabukuro M, Iwaki M, Yamada Y, Nakajima Y, Nakayama O, Makishima M, Matsuda M, Shimomura I (2004) Increased oxidative stress in obesity and its impact on metabolic syndrome. J Clin Invest 114:1752-1761.

Gesta S, Tseng Y, Kahn CR (2007) Developmental origin of fat: tracking obesity to its source. Cell 131:242-256.

Giorgi C, De Stefani D, Bononi A, Rizzuto R, Pinton P (2009) Structural and functional link between the mitochondrial network and the endoplasmic reticulum. Int J Biochem Cell Biol 41:1817-1827.

Goldenthal MJ, Marín-García J (2004) Mitochondrial signaling pathways: a receiver/integrator organelle. Mol Cell Biochem 262:1-16.

Görlach A, Klappa P, Kietzmann DT (2006) The endoplasmic reticulum: folding, calcium homeostasis, signaling, and redox control. Antioxid Redox Signal. 8:1391-1418.

Gotoh T, Mori M (2006) Nitric oxide and endoplasmic reticulum stress. Arterioscler Thromb Vasc Biol 26:1439-1446.

Grattagliano I, de Bari O, Bernardo TC, Oliveira PJ, Wang DQ, Portincasa P (2012) Role of mitochondria in nonalcoholic fatty liver disease-from origin to propagation. Clin Biochem 45:610-618.

Gregor MF, Hotamisligil GS (2007) Thematic review series: Adipocyte Biology. Adipocyte stress: the endoplasmic reticulum and metabolic disease. J Lipid Res 48:1905-1914.

Gregor MF, Hotamisligil GS (2011) Inflammatory mechanisms in obesity. Annu Rev Immunol 29:415-445.

Gregor MF, Yang L, Fabbrini E, Mohammed BS, Eagon JC, Hotamisligil GS, Klein S (2009) Endoplasmic reticulum stress is reduced in tissues of obese subjects after weight loss. Diabetes 58:693-700.

Gross E, Kastner DB, Kaiser CA, Fass D (2004) Structure of Ero1p, source of disulfide bonds for oxidative protein folding in the cell. Cell 117:601-610.

Gross LS, Li L, Ford ES, Liu S (2004) Increased consumption of refined carbohydrates and the epidemic of type 2 diabetes in the United States: an ecologic assessment. Am J Clin Nutr 79:774-779.

Gual P, Le Marchand-Brustel Y, Tanti J (2005) Positive and negative regulation of insulin signaling through IRS-1 phosphorylation. Biochimie 87:99-109.

Günzler W, Kremers H, Flohé L (1974) An improved coupled test procedure for glutathione peroxidase (EC 1.11. 1.9.) in blood. Clin. Chem. Lab. Med 12:444-448.

Halestrap AP, Clarke SJ, Javadov SA (2004) Mitochondrial permeability transition pore opening during myocardial reperfusion--a target for cardioprotection. Cardiovasc Res 61:372-385.

Halliwell B (1996) Antioxidants in human health and disease. Annu Rev Nutr 16:33-50.

Hammarstedt A, Jansson P, Wesslau C, Yang X, Smith U (2003) Reduced expression of PGC-1 and insulin-signaling molecules in adipose tissue is associated with insulin resistance. Biochem Biophys Res Commun 301:578-582.

Harding HP, Novoa I, Zhang Y, Zeng H, Wek R, Schapira M, Ron D (2000) Regulated translation initiation controls stress-induced gene expression in mammalian cells. Mol Cell 6:1099-1108.

Hausenloy DJ, Yellon DM (2003) The mitochondrial permeability transition pore: its fundamental role in mediating cell death during ischaemia and reperfusion. J Mol Cell Cardiol 35:339-341.

Hayamizu K, Ishii Y, Kaneko I, Shen M, Okuhara Y, Shigematsu N, Tomi H, Furuse M, Yoshino G, Shimasaki H (2003) Effects of Garcinia cambogia (Hydroxycitric Acid) on visceral fat accumulation: a double-blind, randomized, placebo-controlled trial. Curr Ther Res Clin Exp 64:551-567.

Hayashi T, Rizzuto R, Hajnoczky G, Su T (2009) MAM: more than just a housekeeper. Trends Cell Biol 19:81-88.

Hayashi T, Su T (2007) Sigma-1 receptor chaperones at the ER-mitochondrion interface regulate Ca 2 signaling and cell survival. Cell 131:596-610.

Haynes CM, Titus EA, Cooper AA (2004) Degradation of misfolded proteins prevents ER-derived oxidative stress and cell death. Mol Cell 15:767-776.

Haze K, Yoshida H, Yanagi H, Yura T, Mori K (1999) Mammalian transcription factor ATF6 is synthesized as a transmembrane protein and activated by proteolysis in response to endoplasmic reticulum stress. Mol Biol Cell 10:3787-3799.

Healy SJ, Gorman AM, Mousavi-Shafaei P, Gupta S, Samali A (2009) Targeting the endoplasmic reticulum-stress response as an anticancer strategy. Eur J Pharmacol 625:234-246.

Heilbronn LK, Gan SK, Turner N, Campbell LV, Chisholm DJ (2007) Markers of mitochondrial biogenesis and metabolism are lower in overweight and obese insulin-resistant subjects. J. Clin. Endocrinol. Metab. 92:1467-1473.

Hendershot LM (2004) The ER function BiP is a master regulator of ER function. Mt Sinai J Med 71:289-297.

Herman MA, Kahn BB (2006) Glucose transport and sensing in the maintenance of glucose homeostasis and metabolic harmony. J Clin Invest 116:1767-1775.

Heymsfield SB, Allison DB, Vasselli JR, Pietrobelli A, Greenfield D, Nunez C (1998) Garcinia cambogia (hydroxycitric acid) as a potential antiobesity agent: a randomized controlled trial. J Am Med Assoc 280:1596–1600.

Higa A, Chevet E (2012) Redox signaling loops in the unfolded protein response. Cell Signal 24:1548-1555.

Hiramatsu N, Joseph VT, Lin JH (2011) Monitoring and manipulating mammalian unfolded protein response. Methods Enzymo l 491:183-198.

Hirosumi J, Tuncman G, Chang L, Görgün CZ, Uysal KT, Maeda K, Karin M, Hotamisligil GS (2002) A central role for JNK in obesity and insulin resistance. Nature 420:333-336.

Hitomi J, Katayama T, Eguchi Y, Kudo T, Taniguchi M, Koyama Y, Manabe T, Yamagishi S, Bando Y, Imaizumi K, Tsujimoto Y, Tohyama M (2004) Involvement of caspase-4 in endoplasmic reticulum stress-induced apoptosis and Abeta-induced cell death. J Cell Biol 165:347-356.

Hock MB, Kralli A (2009) Transcriptional control of mitochondrial biogenesis and function. Annu Rev Physio l 71:177-203.

Hodgson EK, Fridovich I (1975) Interaction of bovine erythrocyte superoxide dismutase with hydrogen peroxide. Inactivation of the enzyme. Biochemistry 14:5294-5299.

Hong EG, Ko HJ, Cho YR, Kim HJ, Ma Z, Yu TY, Friedline RH, Kurt-Jones E, Finberg R, Fischer MA, Granger EL, Norbury CC, Hauschka SD, Philbrick WM, Lee CG, Elias JA, Kim JK (2009) Interleukin-10 prevents diet-induced insulin resistance by attenuating macrophage and cytokine response in skeletal muscle. Diabetes 58:2525-2535.

Hosoi T, Ozawa K (2009) Endoplasmic reticulum stress in disease: mechanisms and therapeutic opportunities. Clin Sci 118:19-29.

Hotamisligil GS (2006) Inflammation and metabolic disorders. Nature 444:860-867.

Hotamisligil GS (2010) Endoplasmic reticulum stress and the inflammatory basis of metabolic disease. Cell 140:900-917.

Hotamisligil GS, Peraldi P, Budavari A, Ellis R, White MF, Spiegelman BM (1996) IRS-1-mediated inhibition of insulin receptor tyrosine kinase activity in TNF-alpha- and obesity-induced insulin resistance. Science 271:665-668.

Hu E, Liang P, Spiegelman BM (1996) AdipoQ is a novel adipose-specific gene dysregulated in obesity. J Biol Chem 271:10697-10703.

Hu FB (2003) Sedentary lifestyle and risk of obesity and type 2 diabetes. Lipids 38:103-108.

Hu P, Han Z, Couvillon AD, Kaufman RJ, Exton JH (2006) Autocrine tumor necrosis factor alpha links endoplasmic reticulum stress to the membrane death receptor pathway through IRE1alpha-mediated NF-kappaB activation and down-regulation of TRAF2 expression. Mol Cell Biol 26:3071-3084.

Hu WK, Liu R, Pei H, Li B (2012) Endoplasmic reticulum stress-related factors protect against diabetic retinopathy. Exp Diabetes Res 2012:507986.

Hummasti S, Hotamisligil GS (2010) Endoplasmic reticulum stress and inflammation in obesity and diabetes. Circ Res 107:579-591.

Irie Y, Yamagata K, Gan Y, Miyamoto K, Do E, Kuo C, Taira E, Miki N (2000) Molecular cloning and characterization of Amida, a novel protein which interacts with a neuron-specific immediate early gene product arc, contains novel nuclear localization signals, and causes cell death in cultured cells. J Biol Chem 275:2647-2653.

Itani SI, Ruderman NB, Schmieder F, Boden G (2002) Lipid-induced insulin resistance in human muscle is associated with changes in diacylglycerol, protein kinase C, and IkappaB-alpha. Diabetes 51:2005-2011.

Iwakoshi NN, Lee A, Vallabhajosyula P, Otipoby KL, Rajewsky K, Glimcher LH (2003) Plasma cell differentiation and the unfolded protein response intersect at the transcription factor XBP-1. Nat Immunol 4:321-329.

Iwawaki T, Oikawa D (2013) The role of the unfolded protein response in diabetes mellitus. Semin Immunopathol 35:333-350.

Jager J, Grémeaux T, Cormont M, Le Marchand-Brustel Y, Tanti J (2007) Interleukin-1β-induced insulin resistance in adipocytes through down-regulation of insulin receptor substrate-1 expression. Endocrinology 148:241-251.

Jamaluddin MS, Weakley SM, Yao Q, Chen C (2012) Resistin: functional roles and therapeutic considerations for cardiovascular disease. Br J Pharmacol 165:622-632.

Javadov S, Baetz D, Rajapurohitam V, Zeidan A, Kirshenbaum LA, Karmazyn M (2006) Antihypertrophic effect of Na+/H+ exchanger isoform 1 inhibition is mediated by reduced mitogen-activated protein kinase activation secondary to improved mitochondrial integrity and decreased generation of mitochondrial-derived reactive oxygen species. J Pharmacol Exp Ther 317:1036-1043.

Jekabsone A, Ivanoviene L, Brown GC, Borutaite V (2003) Nitric oxide and calcium together inactivate mitochondrial complex I and induce cytochrome c release. J Mol Cell Cardiol 35:803-809.

Jena B, Jayaprakasha G, Singh R, Sakariah K (2002) Chemistry and biochemistry of (-)-hydroxycitric acid from Garcinia. J Agric Food Chem 50:10-22.

Jeong G, Oh G, Pae H, Jeong S, Kim Y, Shin M, Seo BY, Han SY, Lee HS, Jeong J (2006) Comparative effects of curcuminoids on endothelial heme oxygenase-1 expression: ortho-

methoxy groups are essential to enhance heme oxygenase activity and protection. Exp Mol Med 38:393-400.

Kaaman M, Sparks L, Van Harmelen V, Smith S, Sjölin E, Dahlman I, Arner P (2007) Strong association between mitochondrial DNA copy number and lipogenesis in human white adipose tissue. Diabetologia 50:2526-2533.

Kakkar P, Das B, Viswanathan P (1984) A modified spectrophotometric assay of superoxide dismutase. Indian J Biochem Biophys 21:130-132.

Kanwar M, Chan P, Kern TS, Kowluru RA (2007) Oxidative damage in the retinal mitochondria of diabetic mice: possible protection by superoxide dismutase. Invest Ophthalmol Vis Sci 48:3805-3811.

Karalis KP, Giannogonas P, Kodela E, Koutmani Y, Zoumakis M, Teli T (2009) Mechanisms of obesity and related pathology: linking immune responses to metabolic stress. FEBS journal 276:5747-5754.

Karin M, Ben-Neriah Y (2000) Phosphorylation meets ubiquitination: the control of NF-κB activity. Annu Rev Immunol 18:621-663.

Kars M, Yang L, Gregor MF, Mohammed BS, Pietka TA, Finck BN, Patterson BW, Horton JD, Mittendorfer B, Hotamisligil GS, Klein S (2010) Tauroursodeoxycholic Acid may improve liver and muscle but not adipose tissue insulin sensitivity in obese men and women. Diabetes 59:1899-1905.

Kaser S, Kaser A, Sandhofer A, Ebenbichler C, Tilg H, Patsch J (2003) Resistin messenger-RNA expression is increased by proinflammatory cytokines in vitro. Biochem Biophys Res Commun 309:286-290.

Kaufman RJ (2002) Orchestrating the unfolded protein response in health and disease. J Clin Invest 110:1389-1398.

Kawasaki N, Asada R, Saito A, Kanemoto S, Imaizumi K (2012) Obesity-induced endoplasmic reticulum stress causes chronic inflammation in adipose tissue. Sci Rep 2 799: doi:10.1038/srep00799

Keijer J, van Schothorst EM (2008) Adipose tissue failure and mitochondria as a possible target for improvement by bioactive food components. Curr Opin Lipidol 19:4-10.

Keller RK, Boon DY, Crum FC (1979) N-Acetylglucosamine-1-phosphate transferase from hen oviduct: solubilization, characterization, and inhibition by tunicamycin. Biochemistry 18:3946-3952.

Kenner KA, Anyanwu E, Olefsky JM, Kusari J (1996) Protein-tyrosine phosphatase 1B is a negative regulator of insulin-and insulin-like growth factor-I-stimulated signaling. J Biol Chem 271:19810-19816.

Kent K, Harper W, Bomser J (2003) Effect of whey protein isolate on intracellular glutathione and oxidant-induced cell death in human prostate epithelial cells. Toxicol In Vitro 17:27-33.

Kern PA, Di Gregorio GB, Lu T, Rassouli N, Ranganathan G (2003) Adiponectin expression from human adipose tissue: relation to obesity, insulin resistance, and tumor necrosis factor-alpha expression. Diabetes 52:1779-1785.

Kershaw EE, Flier JS (2004) Adipose tissue as an endocrine organ. J Clin Endocrinol Metab 89:2548-2556.

Kim I, Xu W, Reed JC (2008) Cell death and endoplasmic reticulum stress: disease relevance and therapeutic opportunities. Nat Rev Drug Discov 7:1013-1030.

Kim R, Emi M, Tanabe K, Murakami S (2006) Role of the unfolded protein response in cell death. Apoptosis 11:5-13.

Klaman LD, Boss O, Peroni OD, Kim JK, Martino JL, Zabolotny JM, Moghal N, Lubkin M, Kim YB, Sharpe AH, Stricker-Krongrad A, Shulman GI, Neel BG, Kahn BB (2000) Increased energy expenditure, decreased adiposity, and tissue-specific insulin sensitivity in protein-tyrosine phosphatase 1B-deficient mice. Mol Cell Biol 20:5479-5489.

Klivenyi P, Clair DS, Wermer M, Yen H, Oberley T, Yang L, Beal MF (1998) Manganese superoxide dismutase overexpression attenuates MPTP toxicity. Neurobiol Dis 5:253-258.

Koh EH, Park JY, Park HS, Jeon MJ, Ryu JW, Kim M, Kim SY, Kim MS, Kim SW, Park IS, Youn JH, Lee KU (2007) Essential role of mitochondrial function in adiponectin synthesis in adipocytes. Diabetes 56:2973-2981.

Kohno K (2010) Stress-sensing mechanisms in the unfolded protein response: similarities and differences between yeast and mammals. J Biochem 147:27-33.

Kojima E, Takeuchi A, Haneda M, Yagi A, Hasegawa T, Yamaki K, Takeda K, Akira S, Shimokata K, Isobe K (2003) The function of GADD34 is a recovery from a shutoff of protein synthesis induced by ER stress: elucidation by GADD34-deficient mice. FASEB J 17:1573-1575.

Kondo S, Saito A, Asada R, Kanemoto S, Imaizumi K (2011) Physiological unfolded protein response regulated by OASIS family members, transmembrane bZIP transcription factors. IUBMB Life 63:233-239.

Korshunov SS, Skulachev VP, Starkov AA (1997) High protonic potential actuates a mechanism of production of reactive oxygen species in mitochondria. FEBS Lett 416:15-18.

Kovacs E, Westerterp-Plantenga M, Saris W (2001) The effects of 2-week ingestion of (-)-hydroxycitrate and (-)-hydroxycitrate combined with medium-chain triglycerides on satiety, fat oxidation, energy expenditure and body weight. Int J Obes Relat Metab Disord 25: 1087-1094.

Kowluru RA, Kowluru V, Xiong Y, Ho Y (2006) Overexpression of mitochondrial superoxide dismutase in mice protects the retina from diabetes-induced oxidative stress. Free Radic Biol Med 41:1191-1196.

Kozutsumi Y, Segal M, Normington K, Gething MJ, Sambrook J (1988) The presence of malfolded proteins in the endoplasmic reticulum signals the induction of glucose-regulated proteins. Nature 332:462-464.

Kriketos A, Thompson H, Greene H, Hill J (1999) (-)-Hydroxycitric acid does not affect energy expenditure and substrate oxidation in adult males in a post-absorptive state. Int J Obes Relat Metab Disord 23:867-73.

Kubota N, Tobe K, Terauchi Y, Eto K, Yamauchi T, Suzuki R, Tsubamoto Y, Komeda K, Nakano R, Miki H, Satoh S, Sekihara H, Sciacchitano S, Lesniak M, Aizawa S, Nagai R, Kimura S, Akanuma Y, Taylor SI, Kadowaki T (2000) Disruption of insulin receptor substrate 2 causes type 2 diabetes because of liver insulin resistance and lack of compensatory beta-cell hyperplasia. Diabetes 49:1880-1889.

Kyriakis JM, Avruch J (2001) Mammalian mitogen-activated protein kinase signal transduction pathways activated by stress and inflammation. Physiol Rev 81:807-869.

Lago F, Dieguez C, Gómez-Reino J, Gualillo O (2007) Adipokines as emerging mediators of immune response and inflammation. Nat Clin Pract Rheumatol 3:716-724.

Lagouge M, Argmann C, Gerhart-Hines Z, Meziane H, Lerin C, Daussin F, Messadeq N, Milne J, Lambert P, Elliott P (2006) Resveratrol improves mitochondrial function and protects against metabolic disease by activating SIRT1 and PGC-1α. Cell 127:1109-1122.

Lane N (2006) Mitochondrial disease: powerhouse of disease. Nature 440:600-602.

Lara-Castro C, Luo N, Wallace P, Klein RL, Garvey WT (2006) Adiponectin multimeric complexes and the metabolic syndrome trait cluster. Diabetes 55:249-259.

Lee A, Glimcher LH (2009) Intersection of the unfolded protein response and hepatic lipid metabolism. Cell Mol Life Sci.66:2835-2850.

Lee AS (2001) The glucose-regulated proteins: stress induction and clinical applications. Trends Biochem Sci 26:504-510.

Lee AS, Delegeane A, Scharff D (1981) Highly conserved glucose-regulated protein in hamster and chicken cells: preliminary characterization of its cDNA clone. Proc Natl Acad Sci U S A 78:4922-4925.

Lee G, Bhandary B, Lee E, Park J, Jeong K, Kim I, Kim H, Chae H (2011) The roles of ER stress and P450 2E1 in CCl 4-induced steatosis. Int J Biochem Cell Biol 43:1469-1482.

Lee GH, Kim HK, Chae SW, Kim DS, Ha KC, Cuddy M, Kress C, Reed JC, Kim HR, Chae HJ (2007) Bax inhibitor-1 regulates endoplasmic reticulum stress-associated reactive oxygen species and heme oxygenase-1 expression. J Biol Chem 282:21618-21628.

Lee I, Bender E, Kadenbach B (2002) Control of mitochondrial membrane potential and ROS formation by reversible phosphorylation of cytochrome c oxidase. In: Anonymous Oxygen/Nitrogen Radicals: Cell Injury and Disease. Mol Cell Biochem 63-70.

Lee YJ, Jeong SY, Karbowski M, Smith CL, Youle RJ (2004) Roles of the mammalian mitochondrial fission and fusion mediators Fis1, Drp1, and Opa1 in apoptosis. Mol Biol Cell 15:5001-5011.

Lefterova MI, Mullican SE, Tomaru T, Qatanani M, Schupp M, Lazar MA (2009) Endoplasmic reticulum stress regulates adipocyte resistin expression. Diabetes 58:1879-1886.

Li G, Mongillo M, Chin KT, Harding H, Ron D, Marks AR, Tabas I (2009) Role of ERO1-alpha-mediated stimulation of inositol 1,4,5-triphosphate receptor activity in endoplasmic reticulum stress-induced apoptosis. J Cell Biol 186:783-792.

Li M, Baumeister P, Roy B, Phan T, Foti D, Luo S, Lee AS (2000) ATF6 as a transcription activator of the endoplasmic reticulum stress element: thapsigargin stress-induced changes and synergistic interactions with NF-Y and YY1. Mol Cell Biol 20:5096-5106.

Liberman E, Topaly V, Tsofina L, Jasaitis A, Skulachev V (1969) Mechanism of coupling of oxidative phosphorylation and the membrane potential of mitochondria.

Liesa M, Palacin M, Zorzano A (2009) Mitochondrial dynamics in mammalian health and disease. Physiol Rev 89:799-845.

Lim EJ, Heo J, Kim Y (2015) Tunicamycin promotes apoptosis in leukemia cells through ROS generation and downregulation of survivin expression. Apoptosis 20:1087-1098.

Lin C, Lee C, Shih Y, Lin C, Wang S, Chen T, Shih C (2012) Inhibition of mitochondria-and endoplasmic reticulum stress-mediated autophagy augments temozolomide-induced apoptosis in glioma cells. PLoS One 7:e38706 doi: 10.1371/journal.pone.0038706.

Lin Y, Wang Z, Liu L, Chen L (2011) Akt is the downstream target of GRP78 in mediating cisplatin resistance in ER stress-tolerant human lung cancer cells. Lung Cancer 71:291-297.

Lindholm D, Wootz H, Korhonen L (2006) ER stress and neurodegenerative diseases. Cell Death Differ 13:385-392.

Lisa S, Domingo B, Martinez J, Gilch S, Llopis JF, Schatzl HM, Gasset M (2012) Failure of prion protein oxidative folding guides the formation of toxic transmembrane forms. J Biol Chem 287:36693-36701.

Liu J, Divoux A, Sun J, Zhang J, Clément K, Glickman JN, Sukhova GK, Wolters PJ, Du J, Gorgun CZ (2009) Genetic deficiency and pharmacological stabilization of mast cells reduce diet-induced obesity and diabetes in mice. Nat Med 15:940-945.

Liu L, Wise DR, Diehl JA, Simon MC (2008) Hypoxic reactive oxygen species regulate the integrated stress response and cell survival. J Biol Chem 283:31153-31162.

Liu M, Zhou L, Xu A, Lam KS, Wetzel MD, Xiang R, Zhang J, Xin X, Dong LQ, Liu F (2008) A disulfide-bond A oxidoreductase-like protein (DsbA-L) regulates adiponectin multimerization. Proc Natl Acad Sci U S A 105:18302-18307.

Luo B, Lee AS (2013) The critical roles of endoplasmic reticulum chaperones and unfolded protein response in tumorigenesis and anticancer therapies. Oncogene 32:805-818.

Luo C, Long J, Liu J (2008) An improved spectrophotometric method for a more specific and accurate assay of mitochondrial complex III activity. Clin Chim Acta 395:38-41.

Mackeen MM, Ali AM, Lajis NH, Kawazu K, Kikuzaki H, Nakatani N (2002) Antifungal garcinia acid esters from the fruits of Garcinia atroviridis. Z Naturforsch C 57:291-295.

Maeda S (2010) NF-kappaB, JNK, and TLR Signaling Pathways in Hepatocarcinogenesis. Gastroenterol Res Pract 2010:367694.

Mahendran P, Vanisree A, Devi S (2002) The antiulcer activity of Garcinia cambogia extract against indomethacin-induced gastric ulcer in rats. Phytotherapy Research 16:80-83.

Majeed M, Badmaev V, Rajendran R (1998) Potassium hydroxycitrate for the suppression of appetite and induction of weight loss. Assignee: Sabinsa Corporation (Piscataway, NJ). US Patent# 5,783,603. March 31, 1997.

Malhi H, Kaufman RJ (2011) Endoplasmic reticulum stress in liver disease. J Hepatol 54:795-809.

Malhotra JD, Kaufman RJ (2007) Endoplasmic reticulum stress and oxidative stress: a vicious cycle or a double-edged sword? Antioxid Redox Signal 9:2277-2294.

Malhotra JD, Kaufman RJ (2007) The endoplasmic reticulum and the unfolded protein response. Semin Cell Dev Biol 18:716-731.

Malik VS, Popkin BM, Bray GA, Despres JP, Willett WC, Hu FB (2010) Sugar-sweetened beverages and risk of metabolic syndrome and type 2 diabetes: a meta-analysis. Diabetes Care 33:2477-2483.

Marciniak SJ, Ron D (2006) Endoplasmic reticulum stress signaling in disease. Physiol Rev 86:1133-1149.

Marciniak SJ, Yun CY, Oyadomari S, Novoa I, Zhang Y, Jungreis R, Nagata K, Harding HP, Ron D (2004) CHOP induces death by promoting protein synthesis and oxidation in the stressed endoplasmic reticulum. Genes Dev 18:3066-3077.

Marshall S, Garvey WT, Traxinger RR (1991) New insights into the metabolic regulation of insulin action and insulin resistance: role of glucose and amino acids. FASEB J 5:3031-3036.

Matsumoto A, Hanawalt PC (2000) Histone H3 and heat shock protein GRP78 are selectively cross-linked to DNA by photoactivated gilvocarcin V in human fibroblasts. Cancer Res 60:3921-3926.

Mattes RD, Bormann L (2000) Effects of (−)-hydroxycitric acid on appetitive variables. Physiol Behav 71:87-94.

Mayer M, Bukau B (2005) Hsp70 chaperones: cellular functions and molecular mechanism. Cell Mol Life Sci 62:670-684.

McCord JM, Fridovich I (1969) Superoxide dismutase. An enzymic function for erythrocuprein (hemocuprein). J Biol Chem 244:6049-6055.

McCullough KD, Martindale JL, Klotz LO, Aw TY, Holbrook NJ (2001) Gadd153 sensitizes cells to endoplasmic reticulum stress by down-regulating Bcl2 and perturbing the cellular redox state. Mol Cell Biol 21:1249-1259.

McInnes J (2013) Insights on altered mitochondrial function and dynamics in the pathogenesis of neurodegeneration. Transl Neurodegener 2: doi: 10.1186/2047-9158-2-12.

Meares GP, Hughes KJ, Naatz A, Papa FR, Urano F, Hansen PA, Benveniste EN, Corbett JA (2011) IRE1-dependent activation of AMPK in response to nitric oxide. Mol Cell Biol 31:4286-4297.

Menzaghi C, Ercolino T, Di Paola R, Berg AH, Warram JH, Scherer PE, Trischitta V, Doria A (2002) A haplotype at the adiponectin locus is associated with obesity and other features of the insulin resistance syndrome. Diabetes 51:2306-2312.

Minamino T, Komuro I, Kitakaze M (2010) Endoplasmic reticulum stress as a therapeutic target in cardiovascular disease. Circ Res 107:1071-1082.

Minokoshi Y, Kim Y, Peroni OD, Fryer LG, Müller C, Carling D, Kahn BB (2002) Leptin stimulates fatty-acid oxidation by activating AMP-activated protein kinase. Nature 415:339-343.

Misra UK, Deedwania R, Pizzo SV (2006) Activation and cross-talk between Akt, NF-kappaB, and unfolded protein response signaling in 1-LN prostate cancer cells consequent to ligation of cell surface-associated GRP78. J Biol Chem 281:13694-13707.

Mohamed-Ali V, Pinkney J, Coppack S (1998) Adipose tissue as an endocrine and paracrine organ. Int J Obes 22:1145-1158.

Mondal AK, Das SK, Varma V, Nolen GT, McGehee RE, Elbein SC, Wei JY, Ranganathan G (2012) Effect of endoplasmic reticulum stress on inflammation and adiponectin regulation in human adipocytes. Metab Syndr Relat Disord 10:297-306.

Morganelli PM, Kennedy SM, Mitchell TI (2000) Differential effects of interferon-gamma on metabolism of lipoprotein immune complexes mediated by specific human macrophage Fcgamma receptors. J Lipid Res 41:405-415.

Moserova I, Kralova J (2012) Role of ER stress response in photodynamic therapy: ROS generated in different subcellular compartments trigger diverse cell death pathways. PLoS One. 7:e32972 doi: 10.1371/journal.pone.0032972.

Mozdy AD, Shaw JM (2003) A fuzzy mitochondrial fusion apparatus comes into focus. Nat Rev Mol Cell Biol 4:468-478.

Mukhopadhyay P, Rajesh M, Yoshihiro K, Haskó G, Pacher P (2007) Simple quantitative detection of mitochondrial superoxide production in live cells. Biochem Biophys Res Commun 358:203-208.

Mulhern ML, Madson CJ, Danford A, Ikesugi K, Kador PF, Shinohara T (2006) The unfolded protein response in lens epithelial cells from galactosemic rat lenses. Invest Ophthalmol Vis Sci 47:3951-3959.

Murakami T, Saito A, Hino S, Kondo S, Kanemoto S, Chihara K, Sekiya H, Tsumagari K, Ochiai K, Yoshinaga K (2009) Signalling mediated by the endoplasmic reticulum stress transducer OASIS is involved in bone formation. Nat Cell Biol 11:1205-1211.

Murphy MP (2009) How mitochondria produce reactive oxygen species. Biochem J 417:1-13.

Nakagawa T, Zhu H, Morishima N, Li E, Xu J, Yankner BA, Yuan J (2000) Caspase-12 mediates endoplasmic-reticulum-specific apoptosis and cytotoxicity by amyloid-β. Nature 403:98-103.

Nakamura T, Furuhashi M, Li P, Cao H, Tuncman G, Sonenberg N, Gorgun CZ, Hotamisligil GS (2010) Double-stranded RNA-dependent protein kinase links pathogen sensing with stress and metabolic homeostasis. Cell 140:338-348.

Nakamura T, Tokunaga K, Shimomura I, Nishida M, Yoshida S, Kotani K, Islam AW, Keno Y, Kobatake T, Nagai Y (1994) Contribution of visceral fat accumulation to the development of coronary artery disease in non-obese men. Atherosclerosis 107:239-246.

Nakano Y, Tobe T, Choi-Miura NH, Mazda T, Tomita M (1996) Isolation and characterization of GBP28, a novel gelatin-binding protein purified from human plasma. J Biochem 120:803-812.

Nakatani Y, Kaneto H, Kawamori D, Yoshiuchi K, Hatazaki M, Matsuoka TA, Ozawa K, Ogawa S, Hori M, Yamasaki Y, Matsuhisa M (2005) Involvement of endoplasmic reticulum stress in insulin resistance and diabetes. J Biol Chem 280:847-851.

Nandi A, Chatterjee I (1988) Assay of superoxide dismutase activity in animal tissues. J Biosci 13:305-315.

Negi P, Jayaprakasha G (2004) Control of Foodborne Pathogenic and Spoilage Bacteria by Garcinol and Garcinia indicaextracts, and their Antioxidant Activity. J Food Sci 69:FMS61-FMS65.

Nesto RW (2003) The relation of insulin resistance syndromes to risk of cardiovascular disease. Rev Cardiovasc Med 4:S11-S18.

Ng DT, Spear ED, Walter P (2000) The unfolded protein response regulates multiple aspects of secretory and membrane protein biogenesis and endoplasmic reticulum quality control. J Cell Biol 150:77-88.

Ni M, Zhang Y, Lee AS (2011) Beyond the endoplasmic reticulum: atypical GRP78 in cell viability, signalling and therapeutic targeting. Biochem J 434:181-188.

Ni M, Zhou H, Wey S, Baumeister P, Lee AS (2009) Regulation of PERK signaling and leukemic cell survival by a novel cytosolic isoform of the UPR regulator GRP78/BiP Plosone 4:e6868.

Nicolson GL (2007) Metabolic syndrome and mitochondrial function: molecular replacement and antioxidant supplements to prevent membrane peroxidation and restore mitochondrial function. J Cell Biochem 100:1352-1369.

Nishimura S, Manabe I, Nagai R (2009) Adipose tissue inflammation in obesity and metabolic syndrome.

Nishimura S, Manabe I, Nagasaki M, Eto K, Yamashita H, Ohsugi M, Otsu M, Hara K, Ueki K, Sugiura S (2009) CD8 effector T cells contribute to macrophage recruitment and adipose tissue inflammation in obesity. Nat Med 15:914-920

Nishitoh H (2012) CHOP is a multifunctional transcription factor in the ER stress response. J Biochem 151:217-219.

Nisoli E, Clementi E, Carruba MO, Moncada S (2007) Defective mitochondrial biogenesis: a hallmark of the high cardiovascular risk in the metabolic syndrome?. Circ Res 100:795-806.

Novoa I, Zeng H, Harding HP, Ron D (2001) Feedback inhibition of the unfolded protein response by GADD34-mediated dephosphorylation of eIF2alpha. J Cell Biol 153:1011-1022.

Odegaard JI, Chawla A (2013) Pleiotropic actions of insulin resistance and inflammation in metabolic homeostasis. Science 339:172-177.

Ohia SE, Opere CA, LeDay AM, Bagchi M, Bagchi D, Stohs SJ (2002) Safety and mechanism of appetite suppression by a novel hydroxycitric acid extract (HCA-SX). Mol Cell Biochem 238:89-103.

Ohsaki Y, Suzuki M, Fujimoto T (2014) Open questions in lipid droplet biology. Chem Biol 21:86-96.

Ong JM, Kern PA (1989) The role of glucose and glycosylation in the regulation of lipoprotein lipase synthesis and secretion in rat adipocytes. J Biol Chem 264:3177-3182.

Ouchi N, Kihara S, Funahashi T, Matsuzawa Y, Walsh K (2003) Obesity, adiponectin and vascular inflammatory disease. Curr Opin Lipidol 14:561-566.

Ouchi N, Parker JL, Lugus JJ, Walsh K (2011) Adipokines in inflammation and metabolic disease. Nat Rev Immunol 11:85-97.

Ozcan L, Tabas I (2012) Role of Endoplasmic Reticulum Stress in Metabolic Disease and Other Disorders. Annu Rev Med. 63: 317–328.

Ozcan U, Cao Q, Yilmaz E, Lee AH, Iwakoshi NN, Ozdelen E, Tuncman G, Gorgun C, Glimcher LH, Hotamisligil GS (2004) Endoplasmic reticulum stress links obesity, insulin action, and type 2 diabetes. Science 306:457-461.

Ozcan U, Yilmaz E, Ozcan L, Furuhashi M, Vaillancourt E, Smith RO, Gorgun CZ, Hotamisligil GS (2006) Chemical chaperones reduce ER stress and restore glucose homeostasis in a mouse model of type 2 diabetes. Science 313:1137-1140.

Ozgur R, Turkan I, Uzilday B, Sekmen AH. (2014) Endoplasmic reticulum stress triggers ROS signalling, changes the redox state, and regulates the antioxidant defence of Arabidopsis thaliana. J Exp Bot 65: 1377–1390

Pagliassotti MJ (2012) Endoplasmic reticulum stress in nonalcoholic fatty liver disease. Annu Rev Nutr 32:17-33.

Park L, Min D, Kim H, Chung H, Lee C, Park I, Kim Y, Park Y (2011) Tat-enhanced delivery of metallothionein can partially prevent the development of diabetes. Free Radic Biol Med 51:1666-1674.

Park S, Ahn IS, Kim JH, Lee MR, Kim JS, Kim HJ (2010) Glyceollins, one of the phytoalexins derived from soybeans under fungal stress, enhance insulin sensitivity and exert insulinotropic actions. J Agric Food Chem 58:1551-1557.

Parmar V, Schroder M (2012) Sensing endoplasmic reticulum stress. Adv Exp Med Biol, 738:153–168

Parra V, Verdejo H, Del Campo A, Pennanen C, Kuzmicic J, Iglewski M, Hill JA, Rothermel BA, Lavandero S (2011) The complex interplay between mitochondrial dynamics and cardiac metabolism. J Bioenerg Biomembr 43:47-51.

Patil C, Walter P (2001) Intracellular signaling from the endoplasmic reticulum to the nucleus: the unfolded protein response in yeast and mammals. Curr Opin Cell Biol 13:349-355.

Paul MK, Kumar R, Mukhopadhyay AK (2008) Dithiothreitol abrogates the effect of arsenic trioxide on normal rat liver mitochondria and human hepatocellular carcinoma cells. Toxicol Appl Pharmacol 226:140-152.

Pedruzzi E, Guichard C, Ollivier V, Driss F, Fay M, Prunet C, Marie JC, Pouzet C, Samadi M, Elbim C, O'dowd Y, Bens M, Vandewalle A, Gougerot-Pocidalo MA, Lizard G, Ogier-Denis E (2004) NAD(P)H oxidase Nox-4 mediates 7-ketocholesterol-induced endoplasmic reticulum stress and apoptosis in human aortic smooth muscle cells. Mol Cell Biol 24:10703-10717.

Peng X, Li Y (2002) Induction of cellular glutathione-linked enzymes and catalase by the unique chemoprotective agent, 3H-1, 2-dithiole-3-thione in rat cardiomyocytes affords protection against oxidative cell injury. Pharmacol Res 45:491-497.

Perjes A, Kubin A, Konyi A, Szabados S, Cziraki A, Skoumal R, Ruskoaho H, Szokodi I (2012) Physiological regulation of cardiac contractility by endogenous reactive oxygen species. Acta physiologica 205:26- 40.

Petronilli V, Miotto G, Canton M, Brini M, Colonna R, Bernardi P, Di Lisa F (1999) Transient and long-lasting openings of the mitochondrial permeability transition pore can be monitored directly in intact cells by changes in mitochondrial calcein fluorescence. Biophys J 76:725-734.

Pfaffenbach KT, Gentile CL, Nivala AM, Wang D, Wei Y, Pagliassotti MJ (2010) Linking endoplasmic reticulum stress to cell death in hepatocytes: roles of C/EBP homologous protein and chemical chaperones in palmitate-mediated cell death. Am J Physiol Endocrinol Metab 298:E1027-35.

Pickett C, Montisano D, Eisner D, Cascarano J (1980) The physical association between rat liver mitochondria and rough endoplasmic reticulum: I. Isolation, electron microscopic examination and sedimentation equilibrium centrifugation analyses of rough endoplasmic reticulum-mitochondrial complexes. Exp Cell Res 128:343-352.

Pincus D, Chevalier MW, Aragón T, Van Anken E, Vidal SE, El-Samad H, Walter P (2010) BiP binding to the ER-stress sensor Ire1 tunes the homeostatic behavior of the unfolded protein response. Plos Biol 8: e1000415.

Pinton P, Giorgi C, Siviero R, Zecchini E, Rizzuto R (2008) Calcium and apoptosis: ER-mitochondria Ca2+ transfer in the control of apoptosis. Oncogene 27: 6407- 6418.

Poirier P, Giles TD, Bray GA, Hong Y, Stern JS, Pi-Sunyer FX, Eckel RH (2006) Obesity and cardiovascular disease: pathophysiology, evaluation, and effect of weight loss. Arterioscler Thromb Vasc Biol 26:968-976.

Pollack A (2013) AMA recognizes obesity as a disease. The New York Times 18:18

Prasad S, Ravindran J, Sung B, Pandey MK, Aggarwal BB (2010) Garcinol potentiates TRAIL-induced apoptosis through modulation of death receptors and antiapoptotic proteins. Mol Cancer Ther 9:856-868.

Prell T, Lautenschläger J, Grosskreutz J (2013) Calcium-dependent protein folding in amyotrophic lateral sclerosis. Cell Calcium 54:132-143.

Preuss H, Bagchi D, Bagchi M, Rao CS, Dey D, Satyanarayana S (2004) Effects of a natural extract of (–)-hydroxycitric acid (HCA-SX) and a combination of HCA-SX plus niacin-bound chromium and Gymnema sylvestre extract on weight loss. Diabetes Obes Metab 6:171-180.

Preuss HG, Bagchi D, Bagchi M, Rao CS, Satyanarayana S, Dey DK (2004) Efficacy of a novel, natural extract of (–)-hydroxycitric acid (HCA-SX) and a combination of HCA-SX, niacin-bound chromium and Gymnema sylvestre extract in weight management in human volunteers: A pilot study. Nutr Res 24:45-58.

Price BD, Calderwood SK (1992) Gadd45 and Gadd153 messenger RNA levels are increased during hypoxia and after exposure of cells to agents which elevate the levels of the glucose-regulated proteins. Cancer Res 52:3814-3817.

Puri P, Mirshahi F, Cheung O, Natarajan R, Maher JW, Kellum JM, Sanyal AJ (2008) Activation and dysregulation of the unfolded protein response in nonalcoholic fatty liver disease. Gastroenterology 134:568-576.

Puthalakath H, O'Reilly LA, Gunn P, Lee L, Kelly PN, Huntington ND, Hughes PD, Michalak EM, McKimm-Breschkin J, Motoyama N (2007) ER stress triggers apoptosis by activating BH3-only protein Bim. Cell 129:1337-1349.

Qin L, Wang Z, Tao L, Wang Y (2010) ER stress negatively regulates AKT/TSC/mTOR pathway to enhance autophagy. Autophagy 6:239-247.

Radermacher KA, Wingler K, Langhauser F, Altenhöfer S, Kleikers P, Hermans JR, Hrabě de Angelis M, Kleinschnitz C, Schmidt HH (2013) Neuroprotection after stroke by targeting NOX4 as a source of oxidative stress. Antioxid Redox Signal 18:1418-1427.

Rizzuto R, Pinton P, Carrington W, Fay FS, Fogarty KE, Lifshitz LM, Tuft RA, Pozzan T (1998) Close contacts with the endoplasmic reticulum as determinants of mitochondrial Ca2+ responses. Science 280:1763-1766.

Robinson JA, Jenkins NS, Holman NA, Roberts-Thomson SJ, Monteith GR (2004) Ratiometric and nonratiometric Ca 2 indicators for the assessment of intracellular free Ca 2 in a breast cancer cell line using a fluorescence microplate reader. J Biochem Biophys Methods 58:227-237.

Ron D (2002) Translational control in the endoplasmic reticulum stress response. J Clin Invest 110:1383-1388.

Ron D, Hubbard SR (2008) How IRE1 reacts to ER stress. Cell 132:24-26.

Ron D, Walter P (2007) Signal integration in the endoplasmic reticulum unfolded protein response. Nat Rev Mol Cell Biol 8:519-529.

Rong JX, Qiu Y, Hansen MK, Zhu L, Zhang V, Xie M, Okamoto Y, Mattie MD, Higashiyama H, Asano S, Strum JC, Ryan TE (2007) Adipose mitochondrial biogenesis is suppressed in db/db and high-fat diet-fed mice and improved by rosiglitazone. Diabetes 56:1751-1760.

Ronti T, Lupattelli G, Mannarino E (2006) The endocrine function of adipose tissue: an update. Clin Endocrinol 64:355-365.

Roongpisuthipong C, Kantawan R, Roongpisuthipong W (2007) Reduction of adipose tissue and body weight: effect of water soluble calcium hydroxycitrate in Garcinia atroviridis on the short term treatment of obese women in Thailand. Asia Pac J Clin Nutr 16:25.

Rowland AA, Voeltz GK (2012) Endoplasmic reticulum–mitochondria contacts: function of the junction. Nat Rev Mol Cell Biol 13:607-625.

Roy S, RINK C, KHANNA S, PHILLIPS C, BAGCHI D, BAGCHI M, SEN CK (2003) Body weight and abdominal fat gene expression profile in response to a novel hydroxycitric acid-based dietary supplement. Gene Expr 11:251-262.

Ruan H, Pownall HJ, Lodish HF (2003) Troglitazone antagonizes tumor necrosis factor-alpha-induced reprogramming of adipocyte gene expression by inhibiting the transcriptional regulatory functions of NF-kappaB. J Biol Chem 278:28181-28192.

Rudich A, Kanety H, Bashan N (2007) Adipose stress-sensing kinases: linking obesity to malfunction. Trends Endocrinol Metab 18:291-299.

Rutkowski DT, Arnold SM, Miller CN, Wu J, Li J, Gunnison KM, Mori K, Akha AAS, Raden D, Kaufman RJ (2006) Adaptation to ER stress is mediated by differential stabilities of pro-survival and pro-apoptotic mRNAs and proteins. Plos biol 4:e374.

Rutkowski DT, Hegde RS (2010) Regulation of basal cellular physiology by the homeostatic unfolded protein response. J Cell Biol 189:783-794.

Rutkowski DT, Kaufman RJ (2007) That which does not kill me makes me stronger: adapting to chronic ER stress. Trends Biochem Sci 32: 469–476

Rutkowski DT, Kaufman RJ (2007) That which does not kill me makes me stronger: adapting to chronic ER stress. Trends Biochem Sci 32: 469–476

Saad MF, Lillioja S, Nyomba BL, Castillo C, Ferraro R, De Gregorio M, Ravussin E, Knowler WC, Bennett PH, Howard BV (1991) Racial differences in the relation between blood pressure and insulin resistance. N Engl J Med 324:733-739.

Sacks FM, Bray GA., Carey VJ, Smith SR, Ryan DH, Anton SD, McManus K, Champagne CM, Bishop LM, Laranjo N, Leboff MS, Rood JC, Jonge L, Greenway FL, Loria CM, Obarzanek E, Williamson DA, (2010) Comparison of Weight-Loss Diets with Different Compositions of Fat, Protein, and Carbohydrates. N Engl J Med 360: 859-873.

Samuel VT, Shulman GI (2012) Mechanisms for insulin resistance: common threads and missing links. Cell 148:852-871.

Santos CX, Tanaka LY, Wosniak Jr J, Laurindo FR (2009) Mechanisms and implications of reactive oxygen species generation during the unfolded protein response: roles of endoplasmic reticulum oxidoreductases, mitochondrial electron transport, and NADPH oxidase. Antioxidants & Redox Signaling 11:2409-2427.

Sanz A, Scialo F, Mallikarjun V, Stefanatos R (2012) Regulation of lifespan by the mitochondrial electron transport chain: ROS-dependent and ROS-independent mechanisms. Antioxid Redox Signal 19:1953-1969.

Scarpulla RC (2008) Transcriptional paradigms in mammalian mitochondrial biogenesis and function. Physiol Rev 88:611-638.

Schröder M, Kaufman RJ (2005) ER stress and the unfolded protein response. Mutat Res 569 : 29-63.

Schröder M, Kaufman RJ (2005) The mammalian unfolded protein response. Annu Rev Biochem 74:739-789.

Sell H, Eckel J (2010) Adipose tissue inflammation: novel insight into the role of macrophages and lymphocytes. Curr Opin Clin Nutr Metab Care 13:366-370.

Semple R, Crowley V, Sewter C, Laudes M, Christodoulides C, Considine R, Vidal-Puig A, O'Rahilly S (2004) Expression of the thermogenic nuclear hormone receptor coactivator PGC-1α is reduced in the adipose tissue of morbidly obese subjects. Int J Obes 28:176-179.

Senior AE (1988) ATP synthesis by oxidative phosphorylation. Physiol Rev 68:177-231.

Shaffer A, Shapiro-Shelef M, Iwakoshi NN, Lee A, Qian S, Zhao H, Yu X, Yang L, Tan BK, Rosenwald A (2004) XBP1, downstream of Blimp-1, expands the secretory apparatus and other organelles, and increases protein synthesis in plasma cell differentiation. Immunity 21:81-93.

Shani G, Fischer WH, Justice NJ, Kelber JA, Vale W, Gray PC (2008) GRP78 and Cripto form a complex at the cell surface and collaborate to inhibit transforming growth factor beta signaling and enhance cell growth. Mol Cell Biol 28:666-677.

Sharma NK, Das SK, Mondal AK, Hackney OG, Chu WS, Kern PA, Rasouli N, Spencer HJ, Yao-Borengasser A, Elbein SC (2008) Endoplasmic reticulum stress markers are associated with obesity in nondiabetic subjects. J Clin Endocrinol Metab 93:4532-4541.

Shi H, Tzameli I, Bjorbaek C, Flier JS (2004) Suppressor of cytokine signaling 3 is a physiological regulator of adipocyte insulin signaling. J Biol Chem 279:34733-34740.

Shimomura I, Matsuda M, Hammer RE, Bashmakov Y, Brown MS, Goldstein JL (2000) Decreased IRS-2 and increased SREBP-1c lead to mixed insulin resistance and sensitivity in livers of lipodystrophic and ob/ob mice. Mol Cell 6:77-86.

Shoelson SE, Lee J, Goldfine AB (2006) Inflammation and insulin resistance. J Clin Invest 116:1793-1801.

Shore GC, Tata JR (1977) Two fractions of rough endoplasmic reticulum from rat liver. I. Recovery of rapidly sedimenting endoplasmic reticulum in association with mitochondria. J Cell Biol 72:714-725.

Sideraki V, Gilbert HF (2000) Mechanism of the antichaperone activity of protein disulfide isomerase: facilitated assembly of large, insoluble aggregates of denatured lysozyme and PDI. Biochemistry 39:1180-1188.

Silha JV, Krsek M, Skrha JV, Sucharda P, Nyomba BL, Murphy LJ (2003) Plasma resistin, adiponectin and leptin levels in lean and obese subjects: correlations with insulin resistance. Eur J Endocrinol 149:331-335.

Silva JP, Shabalina IG, Dufour E, Petrovic N, Backlund EC, Hultenby K, Wibom R, Nedergaard J, Cannon B, Larsson NG (2005) SOD2 overexpression: enhanced mitochondrial tolerance but absence of effect on UCP activity. EMBO J 24:4061-4070.

Simmen T, Aslan JE, Blagoveshchenskaya AD, Thomas L, Wan L, Xiang Y, Feliciangeli SF, Hung CH, Crump CM, Thomas G (2005) PACS-2 controls endoplasmic reticulum-mitochondria communication and Bid-mediated apoptosis. EMBO J 24:717-729.

Simmen T, Lynes EM, Gesson K, Thomas G (2010) Oxidative protein folding in the endoplasmic reticulum: tight links to the mitochondria-associated membrane (MAM). Biochim Biophys Acta 1798:1465-1473.

Sommer T, Jarosch E (2002) BiP binding keeps ATF6 at bay. Dev Cell 3:1-2.

Spiegelman BM (1998) PPAR-gamma: adipogenic regulator and thiazolidinedione receptor. Diabetes 47:507-514.

Suen DF, Norris KL, Youle RJ (2008) Mitochondrial dynamics and apoptosis. Genes Dev 22:1577-1590.

Suganami T, Ogawa Y (2010) Adipose tissue macrophages: their role in adipose tissue remodeling. J Leukoc Biol 88:33-39.

Sun FC, Wei S, Li CW, Chang YS, Chao CC, Lai YK (2006) Localization of GRP78 to mitochondria under the unfolded protein response. Biochem J 396:31-39.

Suzuki T, Lu J, Zahed M, Kita K, Suzuki N (2007) Reduction of GRP78 expression with siRNA activates unfolded protein response leading to apoptosis in HeLa cells. Arch Biochem Biophys 468:1-14.

Szabadkai G, Bianchi K, Varnai P, De Stefani D, Wieckowski MR, Cavagna D, Nagy AI, Balla T, Rizzuto R (2006) Chaperone-mediated coupling of endoplasmic reticulum and mitochondrial Ca2+ channels. J Cell Biol 175:901-911.

Szabadkai G, Duchen MR (2008) Mitochondria: the hub of cellular Ca2+ signaling. Physiology 23:84-94.

Tabas I, Ron D (2011) Integrating the mechanisms of apoptosis induced by endoplasmic reticulum stress. Nat Cell Biol 13:184-190.

Tabata Y, Takano K, Ito T, Iinuma M, Yoshimoto T, Miura H, Kitao Y, Ogawa S, Hori O (2007) Vaticanol B, a resveratrol tetramer, regulates endoplasmic reticulum stress and inflammation. Am J Physiol Cell Physiol 293: C411-418.

Takatsuki A, TAMURA G (1971) Effect of tunicamycin on the synthesis of macromolecules in cultures of chick embryo fibroblasts infected with Newcastle disease virus. J Antibiot 24:785-794.

Tavender TJ, Bulleid NJ (2010) Molecular mechanisms regulating oxidative activity of the Ero1 family in the endoplasmic reticulum. Antioxid Redox Signal 13:1177-1187.

Thareja S, Aggarwal S, Bhardwaj T, Kumar M (2012) Protein tyrosine phosphatase 1B inhibitors: a molecular level legitimate approach for the management of diabetes mellitus. Med Res Rev 32:459-517.

Toromanyan E, Aslanyan G, Amroyan E, Gabrielyan E, Panossian A (2007) Efficacy of Slim339® in reducing body weight of overweight and obese human subjects. Phytother Res 21:1177-1181.

Travers KJ, Patil CK, Wodicka L, Lockhart DJ, Weissman JS, Walter P (2000) Functional and genomic analyses reveal an essential coordination between the unfolded protein response and ER-associated degradation. Cell 101:249-258.

Tsang KY, Chan D, Cheslett D, Chan WC, So CL, Melhado IG, Chan TW, Kwan KM, Hunziker EB, Yamada Y (2007) Surviving endoplasmic reticulum stress is coupled to altered chondrocyte differentiation and function. PLoS Biol 5:e44 doi: 10.1371/journal.pbio.0050044.

Tu BP, Weissman JS (2002) The FAD-and O 2-dependent reaction cycle of Ero1-mediated oxidative protein folding in the endoplasmic reticulum. Mol Cell 10:983-994.

Ullman E, Fan Y, Stawowczyk M, Chen HM, Yue Z, Zong WX (2008) Autophagy promotes necrosis in apoptosis-deficient cells in response to ER stress. Cell Death Differ 15:422-425.

Urano F, Wang X, Bertolotti A, Zhang Y, Chung P, Harding HP, Ron D (2000) Coupling of stress in the ER to activation of JNK protein kinases by transmembrane protein kinase IRE1. Science 287:664-666.

van der Kallen, Carla JH, van Greevenbroek MM, Stehouwer CD, Schalkwijk CG (2009) Endoplasmic reticulum stress-induced apoptosis in the development of diabetes: is there a role for adipose tissue and liver?. Apoptosis 14:1424-1434.

van der Vlies D, Makkinje M, Jansens A, Braakman I, Verkleij AJ, Wirtz KW, Post JA (2003) Oxidation of ER resident proteins upon oxidative stress: effects of altering cellular redox/antioxidant status and implications for protein maturation. Antioxid Redox Signal 5:381-387.

Vance JE (1990) Phospholipid synthesis in a membrane fraction associated with mitochondria. J Biol Chem 265:7248-7256.

Vannuvel K, Renard P, Raes M, Arnould T (2013) Functional and morphological impact of ER stress on mitochondria. J Cell Physiol 228:1802-1818.

Vaughan D (2005) PAI-1 and atherothrombosis. J Thromb Haemost 3:1879-1883.

Vecchi C, Montosi G, Zhang K, Lamberti I, Duncan SA, Kaufman RJ, Pietrangelo A (2009) ER stress controls iron metabolism through induction of hepcidin. Science 325:877-880.

Vernochet C, Mourier A, Bezy O, Macotela Y, Boucher J, Rardin MJ, An D, Lee KY, Ilkayeva OR, Zingaretti CM (2012) Adipose-specific deletion of TFAM increases mitochondrial oxidation and protects mice against obesity and insulin resistance. Cell Metab 16:765-776.

Virbasius JV, Scarpulla RC (1994) Activation of the human mitochondrial transcription factor A gene by nuclear respiratory factors: a potential regulatory link between nuclear and

mitochondrial gene expression in organelle biogenesis. Proc Natl Acad Sci U S A 91:1309-1313.

Waki H, Tontonoz P (2007) Endocrine functions of adipose tissue. Annu Rev Pathol 2:31-56.

Wang H, Joseph JA (1999) Quantifying cellular oxidative stress by dichlorofluorescein assay using microplate reader. Free Radic Biol Med 27:612-616.

Wang X, Eno CO, Altman BJ, Zhu Y, Zhao G, Olberding KE, Rathmell JC, Li C (2011) ER stress modulates cellular metabolism. Biochem J 435:285-296.

Weinstock M (2013) The Facts About Obesity.

Weisberg SP, McCann D, Desai M, Rosenbaum M, Leibel RL, Ferrante AW,Jr (2003) Obesity is associated with macrophage accumulation in adipose tissue. J Clin Invest 112:1796-1808.

Weisiger RA, Fridovich I (1973) Mitochondrial superoxide simutase. Site of synthesis and intramitochondrial localization. J Biol Chem 248:4793- 4796.

Wellen KE, Fucho R, Gregor MF, Furuhashi M, Morgan C, Lindstad T, Vaillancourt E, Gorgun CZ, Saatcioglu F, Hotamisligil GS (2007) Coordinated regulation of nutrient and inflammatory responses by STAMP2 is essential for metabolic homeostasis. Cell 129:537-548.

Wellen KE, Hotamisligil GS (2005) Inflammation, stress, and diabetes. J Clin Invest 115:1111-1119.

Westermann B (2010) Mitochondrial fusion and fission in cell life and death. Nat Rev Mol Cell Biol 11:872-884.

Wielinga PY, Wachters-Hagedoorn RE, Bouter B, van Dijk TH, Stellaard F, Nieuwenhuizen AG, Verkade HJ, Scheurink AJ (2005) Hydroxycitric acid delays intestinal glucose absorption in rats. Am J Physiol Gastrointest Liver Physiol 288:G1144-1149.

Willis MS, Townley-Tilson WH, Kang EY, Homeister JW, Patterson C (2010) Sent to destroy: the ubiquitin proteasome system regulates cell signaling and protein quality control in cardiovascular development and disease. Circ Res 106:463-478.

Winer S, Chan Y, Paltser G, Truong D, Tsui H, Bahrami J, Dorfman R, Wang Y, Zielenski J, Mastronardi F (2009) Normalization of obesity-associated insulin resistance through immunotherapy. Nat Med 15:921-929.

Xu L, Spinas GA, Niessen M (2010) ER stress in adipocytes inhibits insulin signaling, represses lipolysis, and alters the secretion of adipokines without inhibiting glucose transport. Horm Metab Res 42:643-651.

Xu W, Liu L, Charles IG, Moncada S (2004) Nitric oxide induces coupling of mitochondrial signalling with the endoplasmic reticulum stress response. Nat Cell Biol 6:1129-1134.

Yamada T, Hida H, Yamada Y (2007) Chemistry, physiological properties, and microbial production of hydroxycitric acid. Appl Microbiol Biotechnol 75:977-982.

Yamaguchi H, Wang HG (2004) CHOP is involved in endoplasmic reticulum stress-induced apoptosis by enhancing DR5 expression in human carcinoma cells. J Biol Chem 279:45495-45502.

Yamamoto K, Sato T, Matsui T, Sato M, Okada T, Yoshida H, Harada A, Mori K (2007) Transcriptional induction of mammalian ER quality control proteins is mediated by single or combined action of ATF6α and XBP1. Dev Cell 13:365-376.

Yamazaki H, Hiramatsu N, Hayakawa K, Tagawa Y, Okamura M, Ogata R, Huang T, Nakajima S, Yao J, Paton AW, Paton JC, Kitamura M (2009) Activation of the Akt-NF-kappaB pathway by subtilase cytotoxin through the ATF6 branch of the unfolded protein response. J Immunol 183:1480-1487.

Yao S, Sang H, Song G, Yang N, Liu Q, Zhang Y, Jiao P, Zong C, Qin S (2012) Quercetin protects macrophages from oxidized low-density lipoprotein-induced apoptosis by inhibiting the endoplasmic reticulum stress-C/EBP homologous protein pathway. Exp Biol Med 237:822-831.

Ye J (2009) Emerging role of adipose tissue hypoxia in obesity and insulin resistance. Int J Obes 33:54-66.

Ye J, Keller JN (2010) Regulation of energy metabolism by inflammation: a feedback response in obesity and calorie restriction. Aging 2:361-368.

Ye J, Rawson RB, Komuro R, Chen X, Dave UP, Prywes R, Brown MS, Goldstein JL(2000) ER stress induces cleavage of membrane-bound ATF6 by the same proteases that process SREBPs. Mol Cell 6:1355–1364.

Yoon H, Kim D, Lee G, Kim K, Kim H, Chae H (2011) Apoptosis induced by manganese on neuronal SK-N-MC cell line: endoplasmic reticulum (ER) stress and mitochondria dysfunction Environ Health Toxicol 26:e2011017 doi: 10.5620/eht.2011.26.e2011017.

Yoshida H (2007) ER stress and diseases. FEBS J 274:630-658.

Yoshida H, Haze K, Yanagi H, Yura T, Mori K (1998) Identification of the cis-acting endoplasmic reticulum stress response element responsible for transcriptional induction of mammalian glucose-regulated proteins. Involvement of basic leucine zipper transcription factors. J Biol Chem 273:33741-33749.

Yoshida H, Matsui T, Yamamoto A, Okada T, Mori K (2001) XBP1 mRNA is induced by ATF6 and spliced by IRE1 in response to ER stress to produce a highly active transcription factor. Cell 107:881-891.

Yoshida H, Matsui T, Yamamoto A, Okada T, Mori K (2001) XBP1 mRNA is induced by ATF6 and spliced by IRE1 in response to ER stress to produce a highly active transcription factor. Cell 107:881-891.

Yoshida H, Okada T, Haze K, Yanagi H, Yura T, Negishi M, Mori K (2001) Endoplasmic reticulum stress-induced formation of transcription factor complex ERSF including NF-Y (CBF) and activating transcription factors 6alpha and 6beta that activates the mammalian unfolded protein response. Mol Cell Biol 21:1239-1248.

Yoshiuchi K, Kaneto H, Matsuoka T, Kasami R, Kohno K, Iwawaki T, Nakatani Y, Yamasaki Y, Shimomura I, Matsuhisa M (2009) Pioglitazone reduces ER stress in the liver: direct monitoring of in vivo ER stress using ER stress-activated indicator transgenic mice. Endocr J 56:1103-1111.

Yuan M, Konstantopoulos N, Lee J, Hansen L, Li ZW, Karin M, Shoelson SE (2001) Reversal of obesity- and diet-induced insulin resistance with salicylates or targeted disruption of Ikkbeta. Science 293:1673-1677.

Zeyda M, Stulnig TM (2009) Obesity, inflammation, and insulin resistance - a mini-review. Gerontology 55: 379-386.

Zhang K, Kaufman R (2006) The unfolded protein response: a stress signaling pathway critical for health and disease Neurology 66:S102-S109.

Zhang K, Kaufman RJ (2008) From endoplasmic-reticulum stress to the inflammatory response. Nature 454:455-462.

Zhang L, Zhang X (2010) Roles of GRP78 in physiology and cancer. J Cell Biochem 110:1299-1305.

Zhang X, Zhang G, Zhang H, Karin M, Bai H, Cai D (2008) Hypothalamic IKKβ/NF-κB and ER stress link overnutrition to energy imbalance and obesity. Cell 135:61-73.

Zhang Y, Liu R, Ni M, Gill P, Lee AS (2010) Cell surface relocalization of the endoplasmic reticulum chaperone and unfolded protein response regulator GRP78/BiP. J Biol Chem 285:15065-15075.

Zhao H, Liao Y, Minamino T, Asano Y, Asakura M, Kim J, Asanuma H, Takashima S, Hori M, Kitakaze M (2008) Inhibition of cardiac remodeling by pravastatin is associated with amelioration of endoplasmic reticulum stress. Hypertens Res 31:1977.

Zhong J (2013) Endoplasmic Reticulum (ER) Stress in the Pathogenesis of Type 1 Diabetes. INTECH Open Access Publisher.

Zhou L, Liu M, Zhang J, Chen H, Dong LQ, Liu F (2010) DsbA-L alleviates endoplasmic reticulum stress-induced adiponectin downregulation. Diabetes 59:2809-2816.

Zhou QG, Zhou M, Hou FF, Peng X. Asymmetrical dimethylarginine triggers lipolysis and inflammatory response *via* induction of endoplasmic reticulum stress in cultured adipocytes. Am J Physiol Endocrinol Metab. 2009;296:E869–78

Zhou Y, Lee AS (1998) Mechanism for the suppression of the mammalian stress response by genistein, an anticancer phytoestrogen from soy. J Natl Cancer Inst 90:381-388.

Zingg J, Hasan ST, Meydani M (2013) Molecular mechanisms of hypolipidemic effects of curcumin. Biofactors 39:101-121.

Zinszner H, Kuroda M, Wang X, Batchvarova N, Lightfoot RT, Remotti H, Stevens JL, Ron D (1998) CHOP is implicated in programmed cell death in response to impaired function of the endoplasmic reticulum. Genes Dev 12:982-995.

Zorzano A, Liesa M, Palacín M (2009) Role of mitochondrial dynamics proteins in the pathophysiology of obesity and type 2 diabetes. Int J Biochem Cell Biol 41:1846-1854.

Zucker SN, Fink EE, Bagati A, Mannava S, Bianchi-Smiraglia A, Bogner PN, Wawrzyniak JA, Foley C, Leonova KI, Grimm MJ (2014) Nrf2 amplifies oxidative stress via induction of Klf9. Mol Cell 53:916-928.

List of Publications

- Nisha VM, Priyanka A, Anusree SS, Raghu KG (2014). (-)-Hydroxycitric acid attenuates endoplasmic reticulum stress-mediated alterations in 3T3-L1 adipocytes by protecting mitochondria and downregulating inflammatory markers. Free Radic Res, 48: 1386-1396.

- Nisha VM, Anusree SS, Priyanka A, Raghu KG (2014). Apigenin and quercetin ameliorate mitochondrial alterations by tunicamycin-induced ER stress in 3T3-L1 adipocytes. Appl Biochem Biotechnol, 174: 1365-1375.

- Anusree SS, Nisha VM, Priyanka A, Raghu KG (2015). Insulin resistance by TNF-α is associated with mitochondrial dysfunction in 3T3-L1 adipocytes and is ameliorated by punicic acid, a PPARγ agonist. Mol Cell Endocrinol, 413: 120-128.

- Anusree SS, Priyanka A, Nisha VM, Arya A Das, Raghu KG (2014). An in vitro study reveals nutraceutical potential of punicic acid relevant to diabetes via enhanced GLUT4 expression and adiponectin secretion. Food Funct, 5: 2590-2601.

- Priyanka A, Nisha VM, Anusree SS, Raghu KG (2014). Bilobalide attenuates hypoxia induced oxidative stress, inflammation, and mitochondrial dysfunctions in 3T3 L1 adipocytes via its antioxidant potential, Free radical research, 48: 1206-1217.

- Priyanka A, Anusree SS, Nisha VM, Raghu KG (2014). Curcumin improves hypoxia induced dysfunctions in 3T3-L1 adipocytes by downregulating oxidative stress, inflammation, and mitochondrial alterations. J. Biofactors, 40: 513-523.

- Dhanya R , Arun K B, Nisha VM, Syama HP, Nisha P, Santhosh Kumar TR, Jayamurthy P (2015). Preconditioning L6 Muscle cells with naringin ameliorates oxidative stress and increases glucose uptake. PLoS One. 6,10(7):e0132429. doi: 10.1371/journal.pone.013242

- Lekshmi PC, Ranjith A, Nisha VM, Menon AN, Raghu KG (2013). In vitro antidiabetic and inhibitory potential of turmeric (Curcuma longa L) rhizome against cellular and LDL oxidation and angiotensin converting enzyme. J Food Sci Technol, DOI 10.1007/s13197-013-0953-7

- Prathapan A, Mahesh SK, Nisha VM, Sundaresan A, Raghu KG (2012). Polyphenol rich fruit pulp of Aegle marmelos (L.) Correa exhibits nutraceutical properties to down regulate diabetic complications — An in vitro study. Food Research International, 48: 690-695.
- Indu Sasidharan, Sundaresan A, Nisha VM, Mahesh SK, Raghu KG, Jayamurthi P(2012). Inhibitory effect of Terminalia chebula Retz. fruit extracts on digestive enzyme related to diabetes and oxidative stress. J Enzyme Inhib Med Chem, 27, 578-586.
- Priya rani M, K. Padmakumari P, Sankarikutty B, Lijo Cherian O, Nisha VM, Raghu KG. (2011). Inhibitory potential of ginger extracts against enzymes linked to type 2 diabetes, inflammation and induced oxidative stress. International Journal of Food Sciences and Nutrition. 62(2):106-110.

List of presentations in scientific conferences

- Poster presentation on "Endoplasmic reticulum stress-potential therapeutic target for metabolic syndrome is modulated bioactive-hydrocitric acid from Garcinia sps." at Indian Academy of Biomedical Sciences, 9^{th} - 11^{th}, January, 2015, Hyderabad.
- Oral presentation on "An investigation on the role of an investigation on the role of endoplasmic reticulm stress in adipocyte function and effect of quercetin and apigenin" at International conference on "Phytochemicals in Health and Disease: Challenges and Future Opportunities (ICPHD-2013), JAN 23-25, Annamalai University.
- Participated at International conference on Genomics and Proteomics (ICGP-2012) held at NIT Calicut, 14-16 July 2012.
- Oral presentation on Fruit polyphenols protect adipocytes from er stress: an in vitro study on energy homeostasis. 12^{th} International Congress of Ethnopharmacology, February 17-19, 2012 , Kolkata